N. Janardhana Raju
Wolfgang Gossel
M. Sudhakar *Editors*

Management of Natural Resources in a Changing Environment

Springer

Management of Natural Resources in a Changing Environment

N. Janardhana Raju • Wolfgang Gossel
M. Sudhakar
Editors

Management of Natural Resources in a Changing Environment

Springer

Editors
N. Janardhana Raju
Jawaharlal Nehru University
New Delhi, India

Wolfgang Gossel
Martin Luther University
Halle, Germany

M. Sudhakar
Ministry of Earth Sciences
New Delhi, India

Co-published by Springer International Publishing, Cham, Switzerland, with Capital Publishing Company, New Delhi, India.

Sold and distributed in North, Central and South America by Springer, 233 Spring Street, New York 10013, USA.

In all other countries, except SAARC countries—Afghanistan, Bangladesh, Bhutan, India, Maldives, Nepal, Pakistan and Sri Lanka—sold and distributed by Springer, Haberstrasse 7, D-69126 Heidelberg, Germany.

In SAARC countries—Afghanistan, Bangladesh, Bhutan, India, Maldives, Nepal, Pakistan and Sri Lanka—printed book sold and distributed by Capital Publishing Company, 7/28, Mahaveer Street, Ansari Road, Daryaganj, New Delhi, 110 002, India.

ISBN 978-3-319-12558-9 ISBN 978-3-319-12559-6 (eBook)
DOI 10.1007/978-3-319-12559-6
Springer Cham Heidelberg New York Dordrecht London

Library of Congress Control Number: 2014957126

© Capital Publishing Company 2015
This work is subject to copyright. All rights are reserved by Capital Publishing Company, whether the whole or part of the material is concerned, specifically the rights of translation, reprinting, reuse of illustrations, recitation, broadcasting, reproduction on microfilms or in any other physical way, and transmission or information storage and retrieval, electronic adaptation, computer software, or by similar or dissimilar methodology now known or hereafter developed. Exempted from this legal reservation are brief excerpts in connection with reviews or scholarly analysis or material supplied specifically for the purpose of being entered and executed on a computer system, for exclusive use by the purchaser of the work. Duplication of this publication or parts thereof is permitted only under the provisions of the Copyright Law of the Publisher's location, in its current version, and permission for use must always be obtained from Capital Publishing Company. Permissions for use may be obtained through Capital Publishing Company. Violations are liable to prosecution under the respective Copyright Law.
The use of general descriptive names, registered names, trademarks, service marks, etc. in this publication does not imply, even in the absence of a specific statement, that such names are exempt from the relevant protective laws and regulations and therefore free for general use.
While the advice and information in this book are believed to be true and accurate at the date of publication, neither the authors nor the editors nor the publisher can accept any legal responsibility for any errors or omissions that may be made. The publishers make no warranty, express or implied, with respect to the material contained herein.

Printed on acid-free paper

Springer is part of Springer Science+Business Media (www.springer.com)

Message from Alexander von Humboldt Foundation

Alexander von Humboldt
Stiftung/Foundation

Maintaining a dynamic exchange of ideas and gaining new insights – this deep interest makes us human beings. Fostering and supporting people's scientific curiosity has been the Alexander von Humboldt Foundation's mission for 60 years now. Since its establishment in 1953, the Alexander von Humboldt Foundation sponsors top-level scientists and scholars from abroad who come to Germany within the scope of our fellowships and awards to work here in close cooperation with German colleagues. The fellowships and awards of the Alexander von Humboldt Foundation have earned a considerable reputation worldwide. We aim to support excellence and to create an expanding global network of cultural and scientific dialogue on highest levels. Until today, the Alexander von Humboldt Foundation has sponsored more than 26,000 scientists and scholars from all over the world embracing over 130 countries and including 49 Nobel Prize winners. We never set any quota for countries of origin nor fields of research in the selection of future Humboldt fellows. Our only criterion is scientific excellence. So far, the Alexander von Humboldt Foundation has granted well above 5100 research fellowships and awards to excellent scientists and scholars from Asia, amongst them 1781 from India. Today, roundabout 1200 Humboldt Alumni live in India. They form one of the largest regional Alumni networks in the world having established 16 active, self-organized Humboldt Alumni Associations in the country. The Humboldt fellows on the Indian sub-continent are vividly and enthusiastically participating in national and international Alumni activities.

"Once an Humboldtian, always an Humboldtian" – from the very beginning this was the hallmark of the Alexander von Humboldt Foundation. Humboldt sponsorship

is enduring: the foundation is a lifetime partner, maintaining connections on a long-term basis through its alumni sponsorship programmes. Moreover, the foundation encourages its Alumni to undertake their own initiatives and collaborations across disciplinary and national borders. As a result, many Humboldtians make use of the foundation's extensive Alumni sponsorship offers. It was in this context that the Humboldt Kolleg "Management of Water, Energy and Bio-resources in Changing Climate Regime" took place in Delhi in February 2013. The Humboldt Kolleg was hosted by Humboldt Alumnus Professor Dr. Nandimandalam Janardhana Raju from the School of Environmental Sciences at the Jawaharlal Nehru University choosing a topic of major importance to the development in Asia for the conference. The Humboldt Kolleg served as a forum for scientific exchange and networking between Humboldtians and other young and experienced researchers from various disciplines. In total, 231 researchers participated in the conference, amongst them 35 Humboldt Alumni, 135 young academics, seven scholars from Germany and 54 other experienced researchers. A total of 135 presentations were given; another 63 scholars introduced the audience to their fields of research interest during a scientific poster session.

Dealing with the changes of our earth climate and its impacts on natural resources and the environment is one of the biggest challenges for mankind in this century. Worldwide, experts call for action against climate change and its negative environmental, fiscal, social, and cultural effects. As the organizers and presenters during the Humboldt Kolleg pointed out correctly, fragile and conflict-ridden societies will be especially prone to climate change and its impacts, as diminishing resources like groundwater and increasingly unequal distribution will tighten competition and will potentially evolve violent consequences.

On behalf of the Alexander von Humboldt Foundation I would like to thank Professor Dr. Janardhana Raju and the organizing committee at Jawaharlal Nehru University for their dedication and the initiative to conduct the Humboldt Kolleg whose outcome is published in the proceedings of this conference. The Alexander von Humboldt Foundation is most grateful to its Humboldtians, who support our aims and goals of fostering academic cooperation across borders and bringing forward the next generations of top-class international researchers. I wish all participants in the Humboldt Kolleg and the authors of this conference volume success and the best of luck for their future plans.

Dpt. Secretary General — Dr. Thomas Hesse
Alexander von Humboldt Foundation
Bonn, Germany
August 2013

Foreword

This volume titled *Management of Natural Resources in a Changing Environment* contains papers presented during the International Alexander von Humboldt Kolleg that was held at Jawaharlal Nehru University, New Delhi (India), on February 8–9, 2013. The meeting, convened by Dr. N. Janardhana Raju, School of Environmental Sciences, brought together about 200 scientists from different parts of India and overseas including Germany, USA, Brazil, Croatia, Taiwan, Tajikistan, Bangladesh, Iran, Ethiopia, Nepal and Sri Lanka. This edited volume brings out various aspects of natural resources management in the changing environment addressed during the meeting and is divided into three sections—(i) Management of Water Resources: Challenges for Sustainability; (ii) Bio-remediation for Resource Enrichment; and (iii) Environmental Pollution: Issues and Strategies. The themes and topics covered thoroughly show the broad spectrum of multidisciplinary scientific activities. Most of the papers are written by eminent scholars and young scientists in their fields which consist of lot of edifying data/methods with suggestions for improvement and conservation of natural resources management. Environmental sciences require a broad knowledge that goes beyond the boundary of any single discipline and covers multiple objectives of researchers from various subjects. Knowledge of different aspects of geosciences can greatly assist in coping with mechanisms for sustainable development and management of natural resources in the changing environment. Water shortages are caused mainly by increasing population, waste and pollution resulting in negative impacts on the environmental, socio-cultural, political and economic spheres of society. Water contamination can be one of the critical challenges adversely affecting natural ecosystems, agriculture and human health.

Overall this book addresses water resources management, biomass productivity and environmental pollution/hazards which must be the important objectives of all governmental policies and strategies in their course of action. Future water shortages which challenge human health and the environment and their remediation methods are also discussed in different sections. The book holds interest for all those who are keen to know about the management of natural resources such as water, bio-resources and environmental pollution and should make an important

contribution to a better understanding of natural resources management in the environment. I trust that this book will serve those concerned to acquire additional scientific information, knowledge and experience required for ensuring quality and quantity aspects of nature to protect natural resources from indiscriminate exploitation and consequent environmental degradation.

I complement all the contributors of this book which will stimulate future work for sustainable development and management of natural resources. I also congratulate the editorial team for their tremendous effort in bringing out this edited book. I trust the volume will serve for many years as a scientific information base for future planning of the management of natural resources and synergy among academicians, researchers, stakeholders and policy makers for documentation and dissemination of knowledge in natural resources management.

Hydro- & Environmental Geology Peter Wycisk
Martin Luther University Halle-Wittenberg,
Halle, Germany

Preface

The natural resource management incorporates the understanding of the scientific and technical aspects of water, energy and bio-resources distribution and ecological systems which helps in supporting the healthy survival of life on the planet 'Earth'. These natural resources are the most fundamental resources for the sustenance of any civilization. Demand for these resources is ever increasing at an alarming rate post war and are moving towards unsustainable levels. Degradation and erosion of natural resources, namely, land, water, forest, biodiversity (plant, animal and microbial genetic resources), livestock and air—those parts of the natural world that are used to produce food and other valued goods and services that are essential for our survival and prosperity—are also the root causes of the agrarian crisis in the world. Diminishing water resources and their unequal distribution in the changing scenarios will increase competition for water which may turn potentially to violent events/wars in future. The majority of the populations are looking forward for energy efficient system to enhance the judicial conservation of water and bio-resources of our environment. The human pressure and their anthropogenic activities are slowly but steadily deteriorating these resource management capacities in the changing environment. This edited contribution contains papers of multidisciplinary views of authors for managing the natural resources which will be useful guideline for better management of such resources in changing climate scenarios in the world. It is aimed to hold interest for all those who are keen to know about the management of natural resources. The biggest contribution has been, of course, from all the renowned authors. The papers are contributed from distinguished scientists and academicians from reputed universities and institutions from all over the world including India who are contemporary workers in this field of natural resource management. We are very much appreciative of all the contributors who have responded to our call and submitted their papers timely to bring out this book.

The present edited book is the outcome of the International Humboldt Kolleg (IHK2013) held from 8 to 9 February, 2013, in Jawaharlal Nehru University (JNU), New Delhi, India, on the theme of Management of Water, Energy and Bio-resources in Changing Climate Regime: Emerging Issues and Environmental Challenges.

It contains 22 chapters which are grouped under three sections such as (i) Management of Water Resources: Challenges for Sustainability; (ii) Bio-remediation for Resource Enrichment; and (iii) Environmental Pollution: Issues and Strategies. This volume presents case studies and examples in the context of changing environment scenarios and their management. The case studies presented thus provide an insight into present day issues, challenges, opportunities and new approaches that need to be considered in future for efficient and effective natural resources management. These papers give an insight into the present and past issues and their interrelationships in judicial management of these natural resources. Each chapter demonstrates the need for managing each of the demanding resources due to change in climate, land use, industrialization and the need for each country's managers to take initiatives and commit themselves to manage these resources in a sustainable way.

We would like to thank all the contributors for expressing their individual views and also acknowledge our colleagues for their untiring efforts to timely review of manuscripts. The author's commitment and the reviewers' efforts with high quality review of the manuscripts contributed significantly to keep the high scientific contents of the book. One of the editors (N. Janardhana Raju) would particularly like to thank his collaborators and research scholars for supporting his research activities over two decades which helped him in the process of bringing out this contribution. The generous financial support extended by the Alexander von Humboldt Foundation, Germany, in organizing International Humboldt Kolleg at JNU is gratefully acknowledged. We hope this book will be very useful for managers, environmentalists, hydrologists, water resource and energy managers, and for governmental and other regulatory bodies dealing with water, energy and bio-resources issues by providing an opportunity to acquire pertinent scientific information. Finally, we thank the publishers for taking this effort to bring out this volume with due diligence and in a timely manner.

New Delhi, India — N. Janardhana Raju
Halle, Germany — Wolfgang Gossel
New Delhi, India — M. Sudhakar

Contents

Part I Management of Water Resources: Challenges for Sustainability

Hydro-geochemical Investigation and Quality Assessment of Groundwater for Drinking and Agricultural Use in Jawaharlal Nehru University (JNU), New Delhi, India 3
N. Janardhana Raju, Anurag Chaudhary, Sadaf Nazneen, Shubhra Singh, and Ankur Goyal

Comparison of Relationship Between the Concentrations of Water Isotopes in Precipitation in the Cities of Tehran (Iran) and New Delhi (India)..... 29
Maryam Mosaffa, Farzin Nasiri Saleh, and Yousef Khalaj Amirhosseini

Geophysical Expression for Groundwater Quality in Part of Chittoor District, Andhra Pradesh, India 39
S.Md. Farooq Basha

Geospatial Analysis of Fluoride Contamination in Groundwater of Southeastern Part of Anantapur District, Andhra Pradesh 61
B. Muralidhara Reddy, V. Sunitha, and M. Ramakrishna Reddy

Identification of Surface Water Harvesting Sites for Water Stressed Area Using GIS: A Case Study of Ausgram Block, Burdwan District, West Bengal, India..... 75
C. Prakasam

Forecasting Groundwater Level Using Hybrid Modelling Technique 93
Sumant Kumar and Surjeet Singh

Alterations in Physico-chemical Parameters of Water and Aquatic Diversity at Maneri-Bhali Phase I Dam Site on River Ganges in District Uttarkashi, Uttarakhand..... 99
Madhu Thapliyal, Poonam Tiwari, and Ashish Thapliyal

Part II Bio-remediation for Resource Enrichment

Effective Removal of Heavy Metals and Dyes from Drinking Water Utilizing Bio-compatible Magnetic Nanoparticle 115
Dwiptirtha Chattopadhyay and Keka Sarkar

UASBR: An Effective Wastewater Treatment Option to Curb Greenhouse Gas Emissions 125
Rajesh Singh and C.K. Jain

Biogas Upgrading and Bottling Technology for Vehicular and Cooking Applications 135
Virendra Kumar Vijay, Rimika Kapoor, Abhinav Trivedi, and Pradip Narale

Use of Indigenous Bacteria from Arsenic Contaminated Soil for Arsenic Bioremediation 155
Ivy Mallick, Sk Tofajjen Hossain, Sangram Sinha, and Samir Kumar Mukherjee

Adsorption of Arsenite and Fluoride on Untreated and Treated Bamboo Dust 167
Sanjoy Kumar Nath and Krishna G. Bhattacharyya

Reducing the Toxicity of Carbon Nanotubes and Fullerenes Using Surface Modification Strategy 181
Jyoti Chawla and Arun Kumar

Phytoremediation Study and Effect of pH on Biomass Productivity of *Eichhornia crassipes* 193
Ajay Kumar, Neetu Singh, Shilpa Gupta, Pallavi Joshi, Sukirti Tiwari, and Kavita Swaroop

Regeneration of White Oak (*Quercus leucotrichophora*) in Two Pine Invaded Forests in Indian Central Himalaya 205
Satish Chandra Garkoti

Part III Environmental Pollution: Issues and Strategies

Human Health Risk Assessment of Heavy Metals from Bhalaswa Landfill, New Delhi, India 215
Balsher Singh Sidhu, Dikshant Sharma, Tushar Tuteja, Smit Gupta, and Arun Kumar

Transport of Trace Metals by the Rainwater Runoff in the Urban Catchment of Guwahati, India 225
Upama Devi and Krishna G. Bhattacharyya

Analysis of Leachate Characteristics to Study Coal Ash Usability 241
Pooja Vishnoi and M. Shambhavi Kamath

Air Pollution Mapping and Quality Assessment Study at an Urban Area Tirupati Using GIS 249
M. Praveen Kumar, S. Venkata Mohan, and S. Jayarama Reddy

Environmental Hazards and Conservation Approach to the Biodiversity and Ecosystem of the St. Martin's Island in Bangladesh 259
Nurul Hoque Upal

Uranium Toxicity in the State of Punjab in North-Western India 271
Alok Srivastava, Friedhart Knolle, Frieder Hoyler, Ulrich W. Scherer, and Ewald Schnug

Fluoride Toxicity in the Fluoride Endemic Villages of Gaya District, Bihar, India 277
Shahla Yasmin and Suneet Ranjan

Index 289

About the Editors

Dr. Nandimandalam Janardhana Raju did M.Sc. in Geology and Ph.D. in Hydrogeology from Sri Venkateswara University, Tirupati, India, and is currently Associate Professor at the School of Environmental Sciences, Jawaharlal Nehru University, New Delhi, India. He has vast experience in hydrogeology and environmental geosciences and is engaged with research on hydrogeochemistry, rainwater harvesting systems and groundwater quality (arsenic and fluoride) in collaboration with a number of universities in India and overseas. His teaching and research career spans over 28 years – as Visiting Scientist at Ruprecht Karl University, Heidelberg, Germany; Asmara University, Eritrea; Federal University of Fluminense, Rio di Janeiro, Brazil; and Martin Luther University, Halle, Germany. He has received prestigious academic awards such as: Alexander von Humboldt Fellowship (Ruprecht Kral University), Germany; INSA-Brazil Fellowship (UFF), Brazil; Guest Professorship (Martin Luther University), Germany; and Dr Sudarshan Pani – Dr (Smt) Rama Dwivedy Medal, India, for his pioneering contributions to teaching and scientific research. He has guided few PhDs in the hydrogeology and groundwater quality aspects and published more than 55 research papers in refereed journals. He has edited a book on *Management of Water, Energy and Bio-resources in the Era of Climate Change: Emerging Issues and Challenges* published by Springer and Capital Publishing Company and also published one chapter in the book entitled *Geochemical Processes: Conceptual Models for Reactive Transport in Soil and Groundwater*. He has travelled widely (Germany, Japan, Eritrea, Egypt, Brazil, Thailand) participating in around 30 national and international conferences/workshops. He is a member of The National Academy of Sciences India (NASI); International Association for Mathematical Geosciences (IAMG); Geological Society of India (GSI); International Association of Hydrogeologists (IAH); and International Association of Hydrological Sciences (IAHS). He has served as referee for many national and international journals.

Dr. Wolfgang Gossel holds a Ph.D. (1999) degree from the Freie University, Berlin, Germany, and completed Habilitation (2008) from the Martin Luther University, Halle, and is presently working as Senior Scientist, Hydrogeology and Environmental Geology, in the same university. He has contributed more than 20 research papers in refereed journals and has published a book Interfaces in Coupling of Hydrogeological Modeling Systems. He has travelled widely participating in national and international conferences/workshops and also conducted training programmes in Egypt and India, and International Training Courses in Germany on GIS and Hydrogeological Flow and Transport Modeling. Dr. Gossel has completed major research projects pertinent to groundwater flow modeling and salt water intrusion in Egypt, Mexico and Germany. He is a member of the International Association for Mathematical Geosciences (IAMG) and International Association of Hydrogeologists (IAH). He has served as referee and associate editor for many national and international journals.

Dr. M. Sudhakar did his Ph.D. in Applied Geology from Indian School of Mines, Dhanbad, and M.Sc. in Law of the Sea and Marine Policy (1990) from London School of Economics and Political Science, UK. He worked in two premier institutions of the country i.e., National Institute of Oceanography (NIO) and National Centre for Antarctic and Ocean Research (NCAOR), Goa, for 27 years in research and development, survey, planning, teaching and administration in the field of oceanography/offshore surveys/polar science/marine technology. Currently he is an Advisor to the Government of India, Ministry of Earth Sciences (MoES), New Delhi, and heads the Outreach and Awareness, Research Vessels Programmes of the MoES. He has been the project leader of various major programmes and has led several oceanographic expeditions to the Indian and Southern Oceans and Antarctica. Dr. Sudhakar is an elected member of the International Seabed Authority (ISA) in Legal and Technical Commission from 2007 till 2016 and represents India in ISA. He is associated with many professional bodies and has published 50 research papers in refereed international/national journals and conference proceeding volumes and in seminar/symposia. He has been serving in the National Standing and Technical Committees of the Government of India.

Part I
Management of Water Resources: Challenges for Sustainability

Hydro-geochemical Investigation and Quality Assessment of Groundwater for Drinking and Agricultural Use in Jawaharlal Nehru University (JNU), New Delhi, India

N. Janardhana Raju, Anurag Chaudhary, Sadaf Nazneen, Shubhra Singh, and Ankur Goyal

Introduction

Water is an essential and vital component for the life support system. Since most of the human sufferings are directly related to water, man is always fascinated to explore and understand the chemical content of water. Water never exists in its purest form; as soon as it enters the atmosphere through precipitation it gathers gases, few elements and organic material before touching the earth's surface. During its course of flow on surface and in subsurface, the water gets dissolved with ample number of ions, most of which are essential for the living organisms and some are harmful if present in high concentrations. The subsurface water, most of which originates from rainfall or surface water bodies, gains minerals during its transport and residency period of earth's crust (Kruawal et al. 2005; Raju 2007; Wang 2013; Alam et al. 2013). During last decades, it is observed that the intensive use of natural resource and increased human activities are posing great threat to groundwater quality (Foster 1995; Mor et al. 2006).

Each groundwater system in the area has a unique chemistry, acquired as a result of chemical alteration of meteoric water recharging the system (Back 1966; Drever 1982). The chemical alteration of the rain water depends on several factors such as soil-water interaction, dissolution of mineral species and anthropogenic activites (Faure 1998). Many of the major and minor elements in limited quantities are essential for the human metabolism but if present in undesirable level they prove very harmful and the same water turns into a disease causing commodity. The water containing inorganic constituents beyond the permissible limits cause different types of ailments (Raju 2012a). Hence, it is imperative to regularly assess the water chemistry to initiate preventive measures and guide people from

N.J. Raju (✉) • A. Chaudhary • S. Nazneen • S. Singh • A. Goyal
Hydrogeology and Environmental Geology Laboratory, School of Environmental Sciences, Jawaharlal Nehru University, New Delhi 110067, India
e-mail: rajunj7@gmail.com

© Capital Publishing Company 2015

N.J. Raju et al. (eds.), *Management of Natural Resources in a Changing Environment*, DOI 10.1007/978-3-319-12559-6_1

time to time on the consumption of such waters by improving its quality. Groundwater by virtue of its disposition gets dissolved with many elements and in due course some elements reach the harmful stage. Some of the common disease causing elements are F, Ca, NO_3, Fe and As, which if present in more than maximum permissible limits may inflict long lasting damage to human beings. For the purpose of groundwater management, there is a requirement for improved understanding of the controlling processes and the natural geologically controlled baseline chemistry (Raju et al. 2011).

In Delhi, drinking water supply is not from a single source; 70 % of the population is getting supply from water of Yamuna river. Groundwater source like tube wells, hand pumps and borings are the other sources of water supply in capital city. The routine monitoring of groundwater can assure the population that the quality of their drinking water is adequate. It can also be beneficial in detecting deterioration in the quality of drinking water and facilitate appropriate timely corrective actions with minimal negative impacts on population health (Hook 2005; Kruawal et al. 2005). The study of groundwater from a given area offers clues to various possible trends of chemical alteration which the meteoric water undergoes before acquiring distinct chemical characteristics and attaining a chemical steady state in the aquifer. These identified trends in turn may be related to natural and anthropogenic causative factors (Raju 2012b). An attempt is made in this paper to evaluate the hydrogeochemical constituents of groundwater with respect to its suitability for domestic and irrigation uses, referring to several aspects of chemical data interpretation in both the pre- and post-monsoon seasons.

Geology and Area of Study

The National Capital Territory (NCT) of Delhi is part of the Indo-Gangetic alluvial plains. The river Yamuna, a tributary of the Ganga, flows through the eastern part of the territory, and a Quartzite Ridge, rising between up to 91 m above the surrounding plains, acts as a groundwater divide between the western and eastern parts of Delhi. The alluvial formations overlying the quartzitic bedrock have different nature on either side of the ridge. The geological units that influence and control the groundwater occurrence and movement are: alluvial plains on eastern and western sides of the ridge, Yamuna flood plain deposits, isolated and nearly closed Chattarpur alluvial basin and NE-SW trending Quartzitic Ridge. Rapid urbanization, increased agricultural activity and population explosion are attributed as the major cause of water crisis in Delhi (Lorenzen et al. 2010). The situation becomes grimmer during dry seasons and large numbers of residents have to depend on groundwater to augment the municipal water supply.

Jawaharlal Nehru University (JNU) campus, New Delhi (Fig. 1) is a part of Aravali-Delhi-Hardwar ridge, consists of NS to NE-SW trending structural ridges, inselberges and composed of folded and jointed quartzites. Since the campus is situated in the Aravali quartzite rock, the groundwater supply depends on secondary porosity

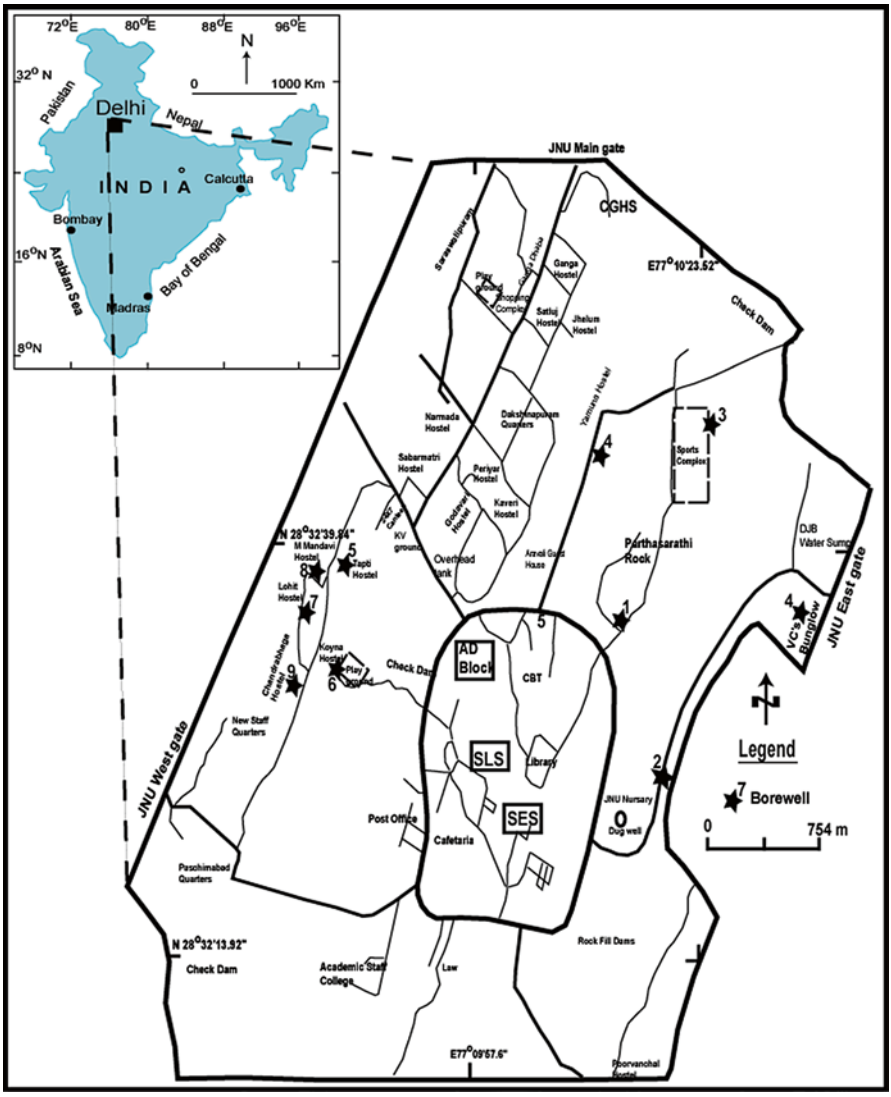

Fig. 1 Map of the study area showing the different sampling locations. *1*. Parthsarathi rock, *2*. JNU nursery, *3*. Tennis court, *4*. VC bungalow, *5*. Tapti enquiry, *6*. Koyna lawn, *7*. Lohit hostel, *8*. Mahi Mandvi lawn and *9*. Chandrabhaga hostel

conditions only. The total area of JNU campus is 405 ha (~16 km^2) and lies in between north latitudes 28°31′37″–28°33′12″ and east longitudes 77°09′08″–77°10′46″. Within this small campus area, few bore wells were drilled in the quartzite rocks in order to supply groundwater to the various institutions and hostels. There has been a widespread drop in the groundwater table in southern part of Delhi (in which JNU campus is situated) especially the area is underlain by Aravali quartzites. Lack of

regulation related to private and individual extraction of groundwater aggravates this situation in general in the capital city. The availability of the groundwater resources from the bore wells situated in the campus is inadequate in the summer season in addition to the water quality problems. Hence, major water supply for the campus domestic and gardening needs depends on Delhi Jal Board water supply and meagre amount of groundwater from the existing bore wells. The maximum and minimum temperature of study area is 46 °C and 4 °C, respectively. The average annual rainfall in Delhi is 765 mm, three fourths of which falls in July, August and September.

Materials and Methods

In order to understand the water quality of the available water source within the campus, nine groundwater samples were collected in pre- (May 2011) and post-monsoon (November 2011) seasons to assess the groundwater quality from available bore wells. The locations of the sampling sites, recorded using global positioning system (GPS, Garmin), are shown in Fig. 1. At each site, water samples were collected in clean polypropylene bottles, rinsed two times with groundwater to be sampled. The physico-chemical parameters were determined by the following standard protocol (APHA 2005). pH and EC were measured using respective electrodes. Alkalinity, bicarbonate and chloride were determined by titration method. Total hardness and calcium were estimated by EDTA titration method, and magnesium estimated by the difference of the hardness and calcium. Sodium and potassium were estimated by flame photometer (Elico Model CL-378). Sulphate and nitrate estimations were done by the UV-spectrophotometer (Lab India Model UV 3000). Fluoride was measured using an ion analyzer (Orion Model 4 star) with an ion selective electrode. The analytical precision for the measurement was determined by calculating the ionic balance error, which is generally found to be within ±5 %. The changes in saturation state has been used to distinguish different stages of hydrochemical evolution and to identify which geochemical reactions are important in controlling water chemistry (Koetsiers and Walraevens 2006). Aqueous speciation computed with WATEQ4F program (Ball and Nordstrom 1992) was used to better define the possible chemical reactions in the aquifer system to assess the state of equilibrium between groundwater and minerals present in terms of saturation index (SI) using the following equation:

$$\mathrm{SI} = \log\left(IAP / K_t\right)$$

where SI is saturation index of a mineral, IAP is ion activity product of the dissociated mineral, and K_t is equilibrium solubility at mineral temperature. $\mathrm{SI} < 0$ indicates that the groundwater is under-saturated with respect to a particular mineral (mineral dissolution condition). $\mathrm{SI} > 0$ reflects whether the groundwater is oversaturated with respect to a particular mineral (mineral precipitation condition). $\mathrm{SI} = 0$ is equilibrium state.

Results and Discussion

Chemical Quality of Groundwater

Understanding the groundwater quality is important as it is the major factor determining its suitability for drinking, domestic, agricultural and industrial purposes. In order to know the chemical quality of groundwater, nine water samples have been collected from the bore wells situated in the JNU institutional area. The summarized results of chemical analysis of major ions are presented in Table 1. Overall, the groundwater of the study area is slightly alkaline in nature in pre-monsoon (6.9–7.5) and post-monsoon (6.7–7.7) seasons. The EC ranges are 481–2,430 µS/cm (mean: 1,113 µS/cm) in pre-monsoon and 589–2,220 µS/cm (mean: 1,052 µS/cm) in post-monsoon season. TDS varies from 207 to 1,002 mg/l (mean: 509 mg/l) in pre-monsoon and 260–965 mg/l (mean: 462 mg/l) in post-monsoon. Groundwater samples in pre- and post-monsoon contain freshwater, since the TDS values are <1,000 mg/l, except one location in pre-monsoon (Davis and De Wiest 1966), and all groundwater evaluated is therefore suitable for drinking and irrigation purposes (Table 2).

The low TDS content observed could be either a result of the slow decomposition of metamorphic rocks, since the terrain is underlain by mostly quartzite rocks, or due to the short residence time of the groundwater. Seasonal variation in the TDS, EC and ionic concentrations in the groundwater may be attributed to geochemical processes and anthropogenic activities (Raju et al. 2011). Among the cationic concentrations in pre- and post-monsoon seasons: Na^+ is the dominating ion with mean values of 125.44 and 106.65 mg/l, respectively, followed by Ca^{2+} (means: 63.46 and 64.08 mg/l), Mg^{2+} (means: 8.95 and 12.84 mg/l), and K^+ (means: 2.54 and 2.18 mg/l) (Table 1). In this groundwater system, in both the seasons, there is no dominant cation that exceeds the threshold of dominance (i.e. meq/l > 50 %) except sample number 2 where Na^+ is dominating cation. Since overall no one cation constitutes as much as 50 % of totals in the pre- and post-monsoon seasons, the water is recognized as a mixed cation type except sample number 2. The hydrochemistry of cationic dominance pattern is in the order of $Na^+ > Ca^{2+} > Mg^{2+} > K^+$ in pre- and post-monsoon seasons. In general, weathering, dissolution and base-exchange processes control the levels of cationic concentrations in groundwater.

Among the anionic concentrations in pre- and post-monsoon seasons: HCO_3^- is the dominating ion, ranging from 176 to 420 mg/l (mean: 307 mg/l) and 224–376 mg/l (mean: 288 mg/l), respectively, followed by Cl^- (means: 130.27 and 118.55 mg/l), SO_4^{2-} (means: 47.57 and 47 mg/l), F^- (means: 0.90 and 1.08 mg/l) and PO_4^{3-} (means: 0.30 and 0.04 mg/l) (Table 1). The concentration of fluoride in the groundwater of the area varies from 0.4 to 2.0 mg/l and 0.7 to 2.0 mg/l in pre- and post-monsoon seasons, respectively. Two groundwater samples (i.e. Koyana Lawn and Mahi Mandvi Lawn) out of nine samples analyzed in the study area exceed the maximum permissible limits of fluoride (1.5 mg/l) set by WHO (Table 1). The weathering activity characterized by alternate wet and dry conditions is responsible for leaching fluoride from the micasious minerals present in the soils and rocks (Jal Nigam Report 2006). Easy accessibility of circulating water to the weathered

Table 1 Range of chemical parameters in groundwater of Jawaharlal Nehru University campus

Parameters	Concentrations (mg/l)				Maximum permissible limits of WHO (1993) (mg/l)	Sample number exceeding permissible limits of WHO (1993)		Undesirable effect
	Pre-monsoon		Post-monsoon			Pre-monsoon	Post-monsoon	
	Range	Mean	Range	Mean				
pH	6.9–7.5	7.2	6.7–7.7	7.2	9.2	–	–	Taste
TDS	207–1002	526	260–965	489	1500	–	–	–
Ca^{2+}	29.03–112	63.46	39.36–93.3	64.08	200	–	–	Scale formation
Mg^{2+}	7.26–13.25	8.95	6.77–20.22	12.84	150	–	–	–
Na^{+}	36.20–281	125.44	39.40–249	106.65	200	**2**	**2**	High blood pressure
K^{+}	0.10–6.90	2.54	0.10–5.90	2.18	12	–	–	Bitter taste
Fe	0.02–0.44	0.12	0.02–0.17	0.09	0.3	6	–	Promotes iron bacteria
HCO_3^{-}	176–420	307	224–376	288	800	–	–	–
SO_4^{2-}	24.4–68.11	47.57	28.58–61.35	47.00	400	–	–	Laxative effect
Cl^{-}	1–462	130.27	2.0–452	118.55	600	–	–	Salty taste
F^{-}	0.40–2.0	0.90	0.70–2.00	1.08	1.5	**6,8**	**6,8**	Dental and skeletal fluorosis
PO_4^{3-}	0.05–0.56	0.30	0.02–0.07	0.04	–	–	–	–
TH	119–334	208	73–224	172	500	–	–	Scale formation
pCO_2 (atm)	3.7×10^{-3}–7.4×10^{-2}	1.9×10^{-2}	6.8×10^{-3}–5.6×10^{-2}	2.2×10^{-2}	–	–	–	–

Table 2 Domestic and irrigation classification of groundwater using different methods

Water class	Range	Number of samples	
		Pre-monsoon	Post-monsoon
Total dissolved solids (TDS) classification (Davis and DeWiest 1996) (mg/l)			
Desirable for drinking	<500	05	06
Permissible for drinking	500–1,000	04	03
Useful for irrigation	1,000–3,000	–	–
Unfit for drinking and irrigation	>3,000	–	–
Total dissolved solids (TDS) classification (Freeze and Cherry 1979) (mg/l)			
Fresh water type	<1,000	08	09
Brackish water type	1,000–10,000	01	–
Saline water type	10,000–100,000	–	–
Brine water type	>100,000	–	–
Total hardness (TH) classification (Sawyer and McCarty 1967) (mg/l)			
Soft	<75	–	–
Moderately hard	75–150	01	–
Hard	150–300	07	09
Very hard water	>300	01	–
Electrical conductivity (EC) classification (Wilcox 1955) (µS/cm)			
Excellent	<250	–	–
Good	250–750	03	02
Fair/Medium	750–2,250	05	07
Poor/Bad	2,250–5,000	01	–
Sodium percent (% Na) classification (Wilcox 1955) (%)			
Excellent	0–20	–	–
Good	20–40	02	04
Permissible	40–60	05	03
Doubtful	60–80	02	02
Unsuitable	>80	–	–
Sodium adsorption ratio (SAR) classification (Richards 1954) (meq/l)			
Excellent	0–10	09	09
Good	10–18	–	–
Fair	18–26	–	–
Poor	>26	–	–
Residual sodium carbonate (RSC) classification (Richards 1954) (meq/l)			
Good	<1.25	05	09
Medium	1.25–2.5	04	–
Bad	>2.5	–	–
Chloride (Cl^-) classification (Stuyfzand 1989) (meq/l)			
<0.14	Extremely fresh	02	01
0.14–0.85	Very fresh	01	03
0.85–4.23	Fresh	04	03
4.23–8.46	Fresh brackish	01	01
8.46–28.21	Brackish brackish	01	01
28.21–564.13	Salt	–	–
>564.13	Hypersaline	–	–

product dissolves and leaches the micasious minerals which contribute F^- to the groundwater (Raju et al. 2012). The anionic dominance patterns is in the order of $HCO_3^- > Cl^- > SO_4^{2-} > F^- > PO_4^{3-}$ in pre-monsoon and $HCO_3^- > SO_4^{2-} > Cl^- > F^- > PO_4^{3-}$ in post-monsoon. For most wells, HCO_3^- is the only anion that exceeds the dominance level (meq/l > 50 %) except sample number 2 (Cl^- dominance) and sample number 9 (mixed type) in the study area.

Groundwater in the semi-arid regions is generally characterized by high ion concentrations and the dominant anion species of the water changes systematically from HCO_3^- to SO_4^{2-} to Cl^- as water flows from the recharge area to the discharge area (Ronit et al. 1997). Anthropogenic CO_2 gas should be considered as a potential source of bicarbonate in the study area. Potential sources of CO_2 gas are municipal wastes within unlined landfill sites, due to the oxidation of organic material leaked from old latrines and open sewage systems and dissolved HCO_3^- ion from sulphate reduction of organic materials in the aquifer (Clark and Fritz 1997). Few groundwaters of high bicarbonate concentrations are likely to be influenced by anthropogenic carbon dioxide. In order to obtain more detail on its source, pCO_2 in groundwater samples was calculated using WATEQ4F program (Ball and Nordstrom 1992). The computed pCO_2 values in the study area ranges from 3.7×10^{-3} to 7.4×10^{-2} atm with a mean of 1.9×10^{-2} atm and 6.8×10^{-3} to 5.6×10^{-2} atm with a mean of 2.2×10^{-2} atm in pre- and post-monsoon seasons, respectively (Table 1). The common range of CO_2 pressures of $10^{-1.5}$–$10^{-2.5}$ atm is found in open system soil layers (Appelo and Postma 1993). CO_2 is generated in soils by decay of organic material and by root respiration. In case of CO_2 pressure $<10^{-2.5}$ atm, CO_2 gas was consumed through mineral dissolution in a closed groundwater system.

Hydrochemical Facies and Processes

Hydrochemical facies are water masses that have different geochemical attributes and are helpful for comparing the origins and distribution of groundwater masses (Lloyd and Heathcote 1985; Raju 2012a, b). Hydrochemical facies are a function of the lithology, solution kinetics, and flow patterns of the aquifer. Based on the relative dominance of major cations and anions in terms of their reacting values, nine groundwater samples have been classified into three hydrochemical facies which are Ca^{2+}-Na^+-HCO_3^- (three in pre- and four in post-monsoon); Na^+-Ca^{2+}-HCO_3^- (four in pre- and three in post-monsoon) and Na^+-Ca^{2+}-Cl^- (two each in pre- and post-monsoon) (Table 3). Sodium dominated facies are most widely distributed in the study area. The average chemical composition and percent content of masses of different hydrochemical facies are presented in Table 3. Ca^{2+}-Na^+-HCO_3^-, Na^+-Ca^{2+}-HCO_3^- and Na^+-Ca^{2+}-Cl^- each represent 33 % in pre-monsoon and 45 % in post-monsoon; 45 % in pre-monsoon and 33 % in post-monsoon; 22 % in both the seasons of the total number of water samples analyzed, respectively. Na^+-Ca^{2+}-HCO_3^- type water is dominated in pre-monsoon whereas Ca^{2+}-Na^+-HCO_3^- type of water is dominated in post-monsoon season in most part of the studied area. In the Na^+-Ca^{2+}-HCO_3^- facies Na^+ values ranges from 1.57 to 5.83 meq/l (pre-) & 3.13 to 5.13 meq/l (post-), and Ca^{2+}

Table 3 Average chemical composition of different hydrochemical facies

Facies	TDS (mg/l)	Ca^{2+} (meq/l)	Mg^{2+} (meq/l)	Na^{+} (meq/l)	K^{+} (meq/l)	HCO_3^{-} (meq/l)	SO_4^{2-} (meq/l)	Cl^{-} (meq/l)	F^{-} (meq/l)	PO_4^{3-} (meq/l)	Sample number
Ca^{2+}-Na^{+}-HCO_3^{-} (Pre-monsoon season)											**1, 3, 4**
Minimum	303	2.75	0.59	2.42	0.03	4.26	0.78	0.03	0.03	0.01	
Maximum	343	3.35	0.63	2.74	0.10	4.98	0.91	0.98	0.03	0.01	
Average	327	3.02	0.61	2.55	0.07	4.64	0.85	0.49	0.02	0.01	
% content		48.12	9.93	40.77	1.18	77.28	14.22	7.96	0.44	0.10	
Ca^{2+}-Na^{+}-HCO_3^{-} (Post-monsoon season)											**1, 3, 4, 8**
Minimum	260	1.96	0.99	1.71	0.01	3.67	0.80	0.05	0.03	0.00	
Maximum	332	3.51	1.66	1.92	0.09	4.78	0.95	0.50	0.10	0.01	
Average	292	2.64	1.26	1.83	0.04	4.24	0.88	0.30	0.05	0.01	
% content		45.54	21.53	32.30	0.63	77.05	16.08	5.88	0.97	0.02	
Na^{+}-Ca^{2+}-HCO_3^{-} (Pre-monsoon season)											**5, 6, 7, 8**
Minimum	207	1.44	0.63	1.57	0.01	2.88	0.82	0.02	0.02	0.01	
Maximum	583	4.26	0.93	5.83	0.04	6.42	1.28	2.84	0.10	0.02	
Average	432	2.93	0.73	4.32	0.02	4.97	1.09	1.66	0.06	0.01	
% content		35.64	8.55	55.53	0.28	63.29	13.79	21.91	0.84	0.17	
Na^{+}-Ca^{2+}-HCO_3^{-} (Post-monsoon season)											**5, 6, 7**
Minimum	339	2.19	0.55	3.13	0.01	4.06	1.08	0.90	0.05	0.00	
Maximum	503	3.60	1.03	5.13	0.11	5.90	1.21	1.91	0.36	0.01	
Average	424	2.98	0.79	4.04	0.05	4.98	1.15	1.44	0.18	0.01	
% content		38.72	10.07	50.62	0.59	64.02	14.9	18.81	2.25	0.02	

(continued)

Table 3 (continued)

Facies	TDS (mg/l)	Ca^{2+} (meq/l)	Mg^{2+} (meq/l)	Na^{+} (meq/l)	K^{+} (meq/l)	HCO_3^{-} (meq/l)	SO_4^{2-} (meq/l)	Cl^{-} (meq/l)	F^{-} (meq/l)	PO_4^{3-} (meq/l)	Sample number
Na^{+}-Ca^{2+}-Cl^{-} (Pre-monsoon season)											**2, 9**
Minimum	785	3.73	0.61	7.80	0.04	4.19	0.50	5.78	0.02	0.00	
Maximum	1,002	5.58	1.08	12.23	0.17	6.88	1.41	13.03	0.02	0.01	
Average	894	4.66	0.85	10.02	0.11	5.53	0.96	9.40	0.02	0.01	
% content		29.79	5.45	64.05	0.71	34.76	6.04	59.02	0.15	0.03	
Na^{+}-Ca^{2+}-Cl^{-} (Post-monsoon season)											**2, 9**
Minimum	737	4.36	1.02	8.24	0.02	3.99	0.59	5.52	0.03	0.00	
Maximum	965	4.66	1.08	10.86	0.15	6.16	1.27	12.73	0.03	0.01	
Average	851	4.51	1.05	9.55	0.08	5.08	0.93	9.12	0.03	0.01	
% content		29.69	6.92	62.81	0.58	33.47	6.17	60.11	0.24	0.01	

values ranges from 1.44 to 4.26 meq/l (pre-) & 2.19 to 3.60 meq/l (post-) whereas in the Ca^{2+}-Na^{+}-HCO_3^{-} facies Ca^{2+} values ranges from 2.75 to 3.35 meq/l (pre-) & 1.96 to 3.51 meq/l (post-), and Na^{+} values ranges from 2.42 to 2.74 meq/l (pre-) & 1.71 to 1.92 meq/l (post-) (Table 3). Average TDS value for the Na^{+}-Ca^{2+}-Cl^{-} water type is 894 mg/l in pre- and 851 mg/l in post-monsoon. The Ca^{2+}-Na^{+}-HCO_3^{-} (average TDS = 327 mg/l in pre- and 292 mg/l in post-monsoon) and Na^{+}-Ca^{2+}-HCO_3^{-} (average TDS = 432 mg/l in pre- and 424 mg/l in post-monsoon) type waters are less mineralized than the other type of groundwaters. Hydrogeochemistry is modified primarily due to the sluggish movement of groundwater and dominant ion-exchange process in pre- and post-monsoon seasons in the study area.

Hydrochemical data was presented in various graphical plots to identify hydrogeochemical processes responsible for enhancement of salinity in the study area. Hydrochemical concepts can help to elucidate the mechanisms of flow and transport in groundwater systems, and unlock an archive of paleo-environmental information (Hem 1992; Pierre et al. 2005). The facies can be classified on the basis of dominant ions using the Piper's trilinear diagram. The concentrations of major ionic constituents of groundwater samples were plotted in the Piper trilinear diagram (Piper 1953) to determine the water type (Fig. 2). The classification for cation and anion facies, in terms of major ion percentages and water types, is according to the domain in which they occur on the diagram segments (Raju et al. 2009).

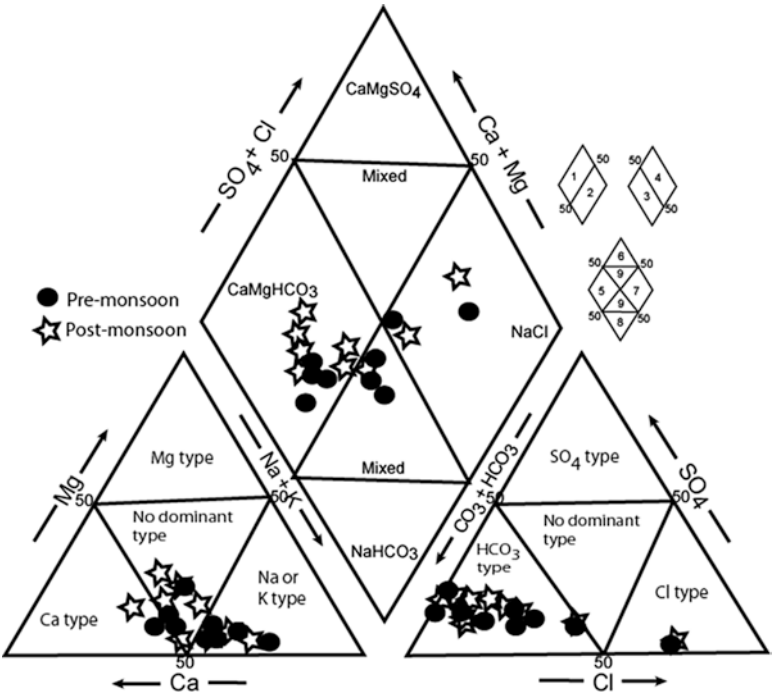

Fig. 2 Trilinear diagram showing the relative cation and anion composition of groundwater samples (After Piper 1953)

From the cationic and anionic triangular files of Piper diagram, it is observed that 56 %, 33 % and 11 % of groundwater samples fall into the Na^+, no-dominant and Ca^{2+} fields in cation facies of pre-monsoon, respectively whereas 56 %, 33 % and 11 % of groundwater samples fall into the no-dominant, Na^+ and Ca^{2+} fields in cation facies of post-monsoon, respectively. Conversely, 89 % and 11 % of groundwater samples fall into the HCO_3^- and Cl^- fields in anion facies for both pre- and post-monsoon, respectively. The diamond shaped field between the two triangles is used to represent the composition of water with respect to both cations and anions. The points of both the cations and anions are plotted on the appropriate triangle diagrams. The positions of the points are projected parallel to the magnesium and sulphate axes until they intersect in the centre field. The plot of chemical data on diamond shaped trilinear diagram (Fig. 2) reveals that majority of groundwater samples fall in the fields of 2, 3 and 5 suggesting that alkalies exceed alkaline earths, weak acids exceed strong acids and the ions representing carbonate hardness (secondary alkalinity) exceed 50 %, respectively in the pre-monsoon, whereas in the post-monsoon season majority of samples fall in the fields of 1, 3 and 5 suggesting that alkaline earths exceed alkalies, weak acids exceed strong acids and the ions representing carbonate hardness (secondary alkalinity) exceed 50 %, respectively.

From the data plots, it is apparent that the total hydrochemistry is dominated by equal sharing of alkalies and alkaline earths and weak acids in the pre-monsoon, and alkaline earths and weak acids in the post-monsoon season. However, some of the groundwater samples having high chloride concentration falls in 1 and 4 fields indicating alkaline earths exceed alkalies and strong acids exceed weak acids in pre-monsoon, whereas in the post-monsoon season samples fall in 2 and 4 fields indicating alkalies exceed alkaline earths and strong acids exceed weak acids. Some samples also fall in the field 9 indicating mixed water having no one cation-anion pair exceeding 50 %.

Ca^{2+}/Mg^{2+} ratio is used to know the source of Ca^{2+} in groundwater of the study area. If Ca^{2+}/Mg^{2+} ratio is unity, there would be dolomite dissolution releasing Ca^{2+} and Mg^{2+} ions in equal ratio. If ratio is towards higher side, calcite dissolution dominates over dolomite dissolution in releasing the calcium ion in groundwater. If ratio exceeds 2, then silicate weathering provides Ca^{2+} and Mg^{2+} in the aquifer system (Katz et al. 1998). The ratio varies between 1.55–6.76 with an average of 4.85 in pre- and 1.54–2.85 with an average of 2.11 in post-monsoon indicating silicate weathering as dominant source for the Ca^{2+} in the aquifer system of the study area. Correlation study shows that there is a poor positive correlation between Ca^{2+} and Mg^{2+} ($r=0.28$) in pre- and ($r=-0.32$) in post-monsoon (Table 4) indicating that the major source of Ca^{2+} and Mg^{2+} may not be from the carbonate weathering in ground waters. A good correlation between Ca^{2+}-HCO_3^- ($r=0.85$ in pre- and $r=0.52$ in post-monsoon) and Mg^{2+}-HCO_3^- ($r=0.14$ in pre- and $r=-0.27$ in post-monsoon) indicates silicate weathering. There could be also gypsum dissolution for Ca^{2+} availability in the groundwater. If gypsum is the major source of Ca^{2+} in groundwater it will dissociate Ca^{2+} and SO_4^{2-} in equal concentration. There is positive and good correlation between Ca^{2+}-SO_4^{2-} ($r=0.51$ in pre- and $r=0.02$ in post-monsoon) (Table 4) indicating gypsum dissolution as source of Ca in groundwater in pre-monsoon but not in the post-monsoon.

Table 4 Correlation matrix of various parameters analyzed in pre-monsoon and post-monsoon season

Parameter	Ca^{2+}	Mg^{2+}	Na^{+}	K^{+}	HCO_3^{-}	SO_4^{2-}	Cl^{-}	F^{-}	PO_4^{3-}	pH	TDS
Ca^{2+}	1.00										
Mg^{2+}	*0.28*	1.00									
	−0.32										
Na^{+}	*0.60*	*0.03*	1.00								
	0.83	**−0.22**									
K^{+}	*0.27*	*−0.38*	*0.59*	1.00							
	0.56	**−0.40**	**0.49**								
HCO_3^{-}	*0.85*	*0.14*	*0.33*	*−0.14*	1.00						
	0.52	**−0.27**	**0.31**	**−0.17**							
SO_4^{2-}	*0.51*	*0.39*	*−0.04*	*−0.58*	*0.77*	1.00					
	0.02	**−0.48**	**−0.08**	**−0.44**	**0.73**						
Cl^{-}	*0.49*	*0.04*	*0.96*	*0.72*	*0.11*	*−0.26*	1.00				
	0.79	**−0.10**	**0.95**	**0.63**	**0.05**	**−0.38**					
F^{-}	*−0.67*	*0.24*	*−0.32*	*−0.63*	*−0.45*	*0.09*	*−0.33*	1.00			
	−0.64	**0.00**	**−0.29**	**−0.55**	**−0.44**	**0.15**	**−0.32**				
PO_4^{3-}	*−0.29*	*0.10*	*−0.26*	*−0.59*	*0.06*	*0.53*	*−0.40*	*0.64*	1.00		
	0.14	**−0.27**	**0.01**	**0.21**	**0.34**	**0.48**	**−0.11**	**−0.30**			
pH	*−0.46*	*−0.02*	*0.22*	*0.07*	*−0.59*	*−0.29*	0.29	*0.56*	*0.27*	1.00	
	−0.33	**0.08**	**0.06**	**−0.29**	**−0.21**	**0.25**	**−0.02**	**0.65**	**0.36**		
TDS	*0.71*	*0.10*	*0.99*	*0.59*	*0.43*	*0.04*	*0.94*	*−0.42*	*−0.31*	*0.10*	1.00
	0.88	**−0.19**	**0.99**	**0.55**	**0.31**	**−0.14**	**0.96**	**−0.38**	**0.00**	**−0.03**	

Pre-monsoon values are in italics and post-monsoon values are in bold

Plotting of $Na^+ + K^+$ vs $Ca^{2+} + Mg^{2+}$ scatter plot (Fig. 3a) shows that majority of samples fall below 1:1 trend line in pre- and above in post-monsoon season indicating deficient $Ca^{2+} + Mg^{2+}$ in pre-monsoon and $Na^+ + K^+$ deficiency in post-monsoon which is due to cation exchange process (Jeevanandam et al. 2007). Molar ratio of Na^+/Ca^{2+} greater than 1 indicates Ca^{2+} deficiency may be due to precipitation of $CaCO_3$ or ion-exchange process. Na^+/Ca^{2+} ratio of the study area ranges from 0.305 to 1.367 with an average of 0.814 in pre- and from 0.429 to 2.049 with an average of 0.999 in post-monsoon indicating Ca^{2+} deficiency in some of the samples in both the seasons may be due to precipitation of $CaCO_3$. A high Na concentration is an indicator of ion-exchange in the groundwater. In the scatter plot of $(Ca^{2+} + Mg^{2+})$ vs $(HCO_3^- + SO_4^{2-})$, it is evident that samples which fall above the equiline (1:1) suggest that an excess of $(HCO_3^- + SO_4^{2-})$ in the water has been balanced by alkalies

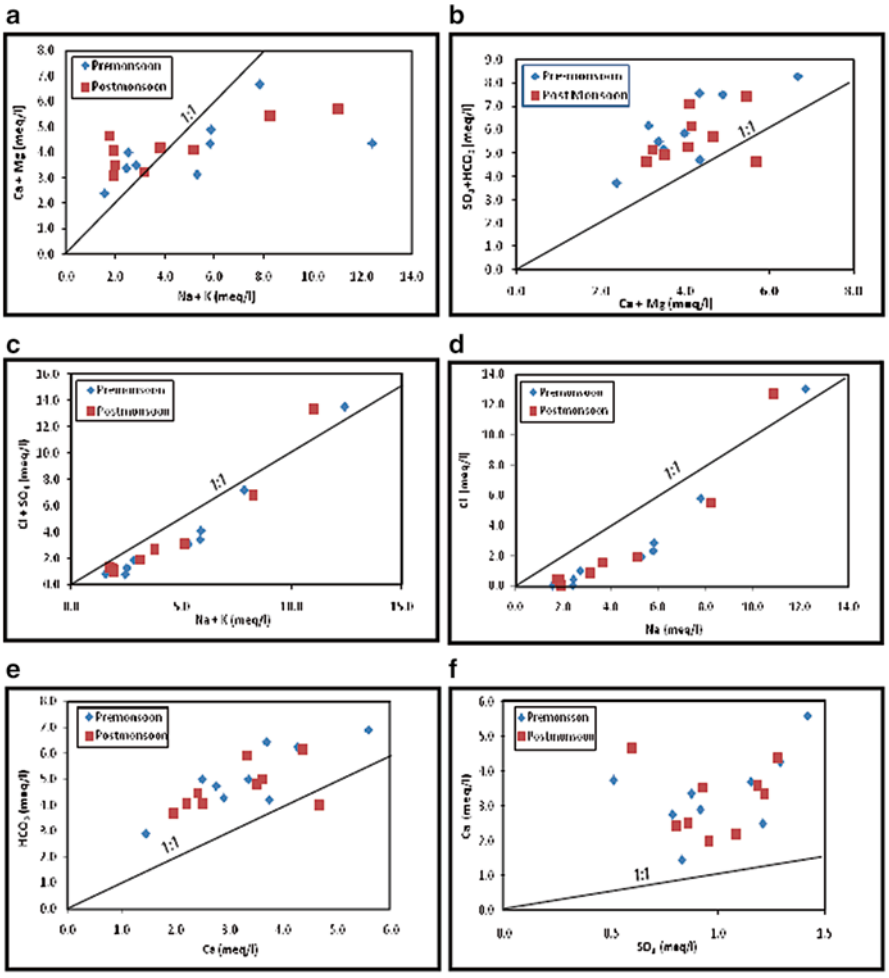

Fig. 3 (**a–f**) Ion scatter diagrams for groundwater in the study area

($Na^+ + K^+$) in pre- and post-monsoon seasons indicating that silicate weathering is the dominant process for cations (Fig. 3b).

Most of the samples of pre-monsoon and post-monsoon falling above the equiline due to excess $SO_4^{2-} + HCO_3^-$ over $Ca^{2+} + Mg^{2+}$ indicate ion exchange process dominance. Therefore, the excess positive charge of SO_4^{2-} and HCO_3^- must be balanced by alkalies ($Na^+ + K^+$). The plot of $Ca^{2+} + Mg^{2+}$ versus $SO_4^{2-} + HCO_3^-$ will be close to the 1:1 line if the dissolution of calcite, dolomite and gypsum are the dominant reactions in a system (Anupam et al. 2012). $Na^+ + K^+$ plotted against $Cl^- + SO_4^{2-}$ (Fig. 3c) shows that majority of samples fall below the 1:1 trend line indicating that these ions have a common source. Most of the groundwater samples fall towards $Na^+ + K^+$ indicating the release of Na^+ from rock weathering (Meybeck 1987). In arid regions, the $Na^+ - Cl^-$ relationship is generally used to determine the mechanism of salinity acquisition and saline intrusions (Ravikumar et al. 2010). The dissolution of halite is an important source for Na^+ and Cl^- in groundwater, along with soil salts, anthropogenic activities, poor drainage and agricultural activities (Raju 2012b). A good correlation exists between $Na^+ - Cl^-$ in pre-monsoon ($r = 0.96$) and in post-monsoon ($r = 0.95$) (Table 4). When the Na^+ concentration is plotted against that of Cl^-, most of the water samples lie slightly below the 1:1 trend line towards to Na^+ (Fig. 3d). The high Na^+/Cl^- ratios in the study area are probably due to silicate weathering, ion-exchange process or water-rock interactions (Adomako et al. 2011). High Na^+/Cl^- (>1) ratio is used to account for silicate weathering contribution of Na^+ (Meybeck 1987).

The dissolved Ca^{2+}-HCO_3^- in the water resulting from calcite weathering by carbonic acid would be 1:2 whereas from dolomite weathering by carbonic acid would be 1:4 (Stallard and Edmond 1983). The plot of Ca^{2+} versus HCO_3^- (Fig. 3e) shows that most of the data fall above the 1:1 line towards HCO_3^-. The low Ca^{2+}/HCO_3^- ratio (<1) of both the seasons in the study area may be due to either Ca depletion by cation exchange or HCO_3^- enrichment. In the study area the Ca^{2+}/HCO_3^- ratio varies between 0.50 and 0.89 with an average of 0.65 in pre- and 0.53–1.16 with an average of 0.68 in post-monsoon. If sulphuric acid is responsible for carbonate weathering then Ca^{2+}-SO_4^{2-} is almost 1:1 for calcite and 1:2 for dolomite (Stallard and Edmond 1983). The plot of SO_4^{2-} versus Ca shows that most of the data fall above the 1:1 line towards Ca^{2+} (Fig. 3f). This indicates carbonic acid contribution towards carbonate or silicate dissolution in the study area. Correlation study shows that good correlation exists between Ca^{2+} and HCO_3^- ($r = 0.85$) in pre- and ($r = 0.52$) in post-monsoon, which supports the carbonate and/or silicate weathering process for the contribution of Ca^{2+}. Ca^{2+} and Mg^{2+} has positive correlation ($r = 0.28$) in pre- but negative correlation ($r = -0.38$) in post-monsoon depicting that dolomite is providing Ca^{2+} and Mg^{2+} in groundwater in pre-monsoon but not in post-monsoon. If gypsum is the major source for Ca^{2+} in groundwater it will dissociate Ca^{2+} and SO_4^{2-} in equal concentration, there is positive and good correlation between Ca^{2+} and SO_4^{2-} ($r = 0.51$) in pre-monsoon and poor correlation ($r = 0.02$) in post-monsoon season, indicating gypsum dissolution as source for Ca^{2+} in groundwater in pre-monsoon season. It has been observed that Ca^{2+}, Na^+, K^+ and Cl^- contents exhibit mutual positive correlation and correlate strongly with TDS in both pre- and post-monsoon (Table 4).

Base Exchange Indices (r_1) and Meteoric Genesis Indices (r_2)

The changes in the chemical composition of groundwater during its travel in the subsurface must be understood (Sarin et al. 1989). Base Exchange Indices (r_1) and Meteoric Genesis Indices (r_2) are proposed to indicate the ion exchange between the groundwater and its host environment. Base Exchange Indices (r_1) is determined by using the equation which could be applied for the further classification of groundwater given as follows:

$$r_1 = \left(Na^+ - \mathrm{Cl}^-\right) / \mathrm{SO}_4^{2-} \left(where \text{ all ions in meq/l}\right)$$

The groundwater can be grouped as Na^+-HCO_3^- type if $r_1 > 1$ and Na^+-SO_4^{2-} type if $r_1 < 1$ (Soltan 1998). Majority of samples in both the seasons are of Na^+-HCO_3^- type. Based on Base Exchange Indices, 89 % and 11 % of samples are Na^+-HCO_3^- type and Na^+-SO_4^{2-} type waters in both the seasons, respectively (Fig. 4). The dissolution of gases and minerals, particularly CO_2 and CO_3^{2-} related compounds in the atmosphere and in the unsaturated zone during precipitation and infiltration, would impart the observed HCO_3^- water type (Shanyengana et al. 2004; Singh et al. 2006).

The groundwater sources can also be classified based on Meteoric Genesis Index and can be computed using following equation (Soltan 1999):

$$r_2 = \left\{\left(K^+ + \mathrm{Na}^+\right) - \mathrm{Cl}^-\right\} / SO_4^{2-} \left(where \text{ all ions in meq/l}\right)$$

The groundwater source is of deep meteoric water percolation type, if $r_2 < 1$ while $r_2 > 1$ indicates that it is of shallow meteoric water percolation type. No significant variations were noticed within this category. Based on r_2 indices, 89 % and 11 % of samples are shallow meteoric water and deep meteoric water type in both the seasons, respectively (Fig. 5). The groundwater samples are showing shallow meteoric waters due to less utilization of bore well waters as well as hard basement rock in the study area.

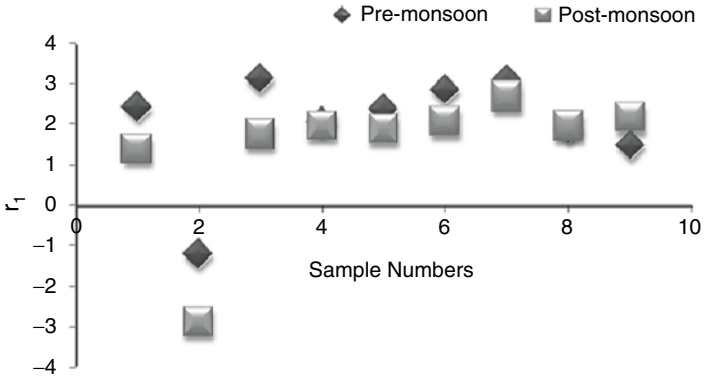

Fig. 4 Scatter plot of base-exchange indices

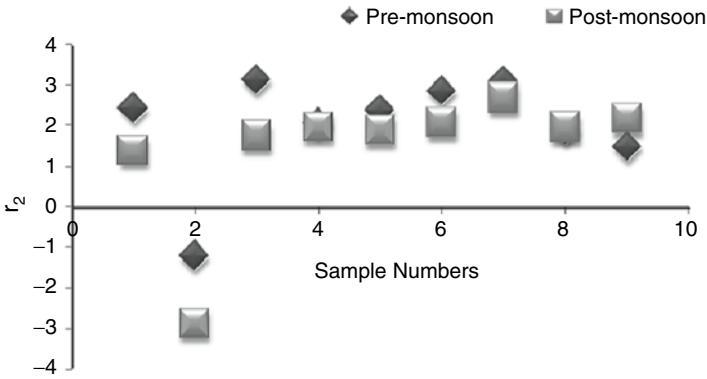

Fig. 5 Scatter plot of meteoric genesis indices

Saturation Index

The saturation indices (SI) describe the quantitative deviation of water from equilibrium with respect to dissolved minerals (Sandow et al. 2011; Raju 2012b). The variation in chemical composition of groundwater in an area is controlled by the evaporation, rainfall, climate, minerals present in geological formations and hydro-geochemical processes such as dissolution, precipitation, sorption and ion-exchange and anthropogenic activity (Raju et al. 2009, 2011). The changes in the saturation state can be used to distinguish the different hydrochemical evolution stages as well as to identify the pertinent geochemical reactions that determine the water chemistry (Stumm and Morgan 1981; Guler et al. 2002). By using the SI approach, the subsurface reactive mineralogy can be obtained from groundwater data without the need to collect solid-phase samples, and the mineralogy can be analyzed (Deutsch 1997).

The calculated SI values range for anhydrite −2.516 to −1.919 (mean: −2.226) and −2.382 to −2.044 (mean: −2.233); aragonite −0.413 to 0.136 (mean: −0.114) and −0.613 to 0.32 (mean: −0.196); calcite −0.269 to 0.28 (mean: 0.029) and −0.469 to 0.464 (mean: −0.053); dolomite −1.679 to −0.654 (mean: −1.015) and −1.844 to 1.357 (mean: −0.704); fluorapatite −1.549 to 3.483 (mean: 1.342) and −3.923 to 0.91 (mean: −1.342); goethite 2.224–5.025 (mean: 3.542) and 1.631–5.234 (mean: 3.405); gypsum −2.296 to −1.699 (mean: −2.006) and −2.162 to −1.824 (mean: −2.014); halite −8.826 to −5.499 (mean: −6.797) and −8.622 to −5.561 (mean: −7.158); magnesite −1.44 to −0.862 (mean: −1.076) and −1.406 to −0.523 (mean: −0.983); and siderite −1.785 to −0.685 (mean: −1.191) and −1.997 to −0.467 (mean: −1.265) for pre- and post-monsoon season, respectively. Variation of saturation index for different minerals of both pre- and post-monsoon is shown in Fig. 6. Study of saturation indices reveals that all groundwater samples are undersaturated with respect to anhydrite, gypsum, dolomite, halite, magnesite and siderite minerals, whereas supersaturated with goethite mineral in pre- and post-monsoon seasons. 56 %, 44 % and 22 % samples show undersaturation and 44 %, 56 % and 78 % samples show supersaturation in pre-monsoon, whereas 78 %, 67 % and 78 %

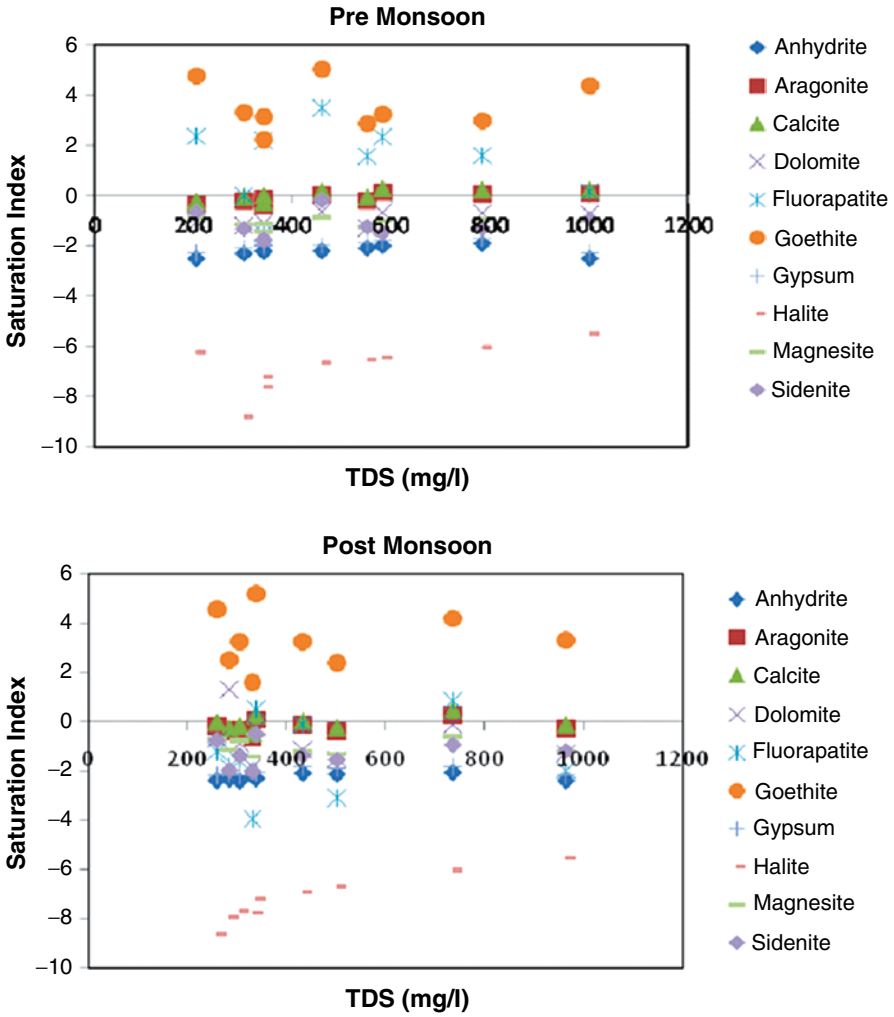

Fig. 6 Plots of saturation indices (SI) with respect to different minerals against total dissolved solids for pre-monsoon and post-monsoon

samples show undersaturation and 22 %, 33 % and 22 % samples show supersaturation with respect to aragonite, calcite and fluorapatite minerals in post-monsoon season, respectively (Fig. 6).

Water samples are undersaturated with respect to sulphur-bearing minerals (gypsum and anhydrite) in all groundwater samples both in pre- and post-monsoon; it suggests that dissolution of these minerals have contributed Ca^{2+}, Mg^{2+} and other ions into the groundwater. Dissolution of silicate minerals is generally a very slow process that does not produce significant variations in water chemistry (Condesso de Melo et al. 1999). Study of saturation indices reveals that all the samples of

carbonate minerals such as gypsum, anhydrite, dolomite and magnesite show undersaturation, whereas about 50 % of calcite and aragonite minerals show oversaturation in the groundwater samples of the study area. Water samples which are oversaturated with these carbonate minerals indicated that the excess input of Ca^{2+} and Mg^{2+} ions are mainly from carbonate weathering processes. Oversaturation of groundwater with carbonate minerals in some of the samples shows that these minerals calcite, dolomite and aragonite are already precipitated in the past and are not contributing much of Ca^{2+} and Mg^{2+} in the groundwater.

Classification of Groundwater for Domestic Use

The water used for drinking should be free from colour, turbidity and microorganisms (Karanth 1989). To ascertain the suitability of groundwater for drinking and public health use, hydrochemical parameters of the study area are compared (Table 2) with the guidelines recommended by World Health Organization (WHO 1993). From Table 1, it is evident that one groundwater sample for sodium ion, two samples for fluoride ion in pre- and post-monsoon season, and six groundwater samples for iron in pre-monsoon season are exceeding the permissible limits set by WHO. According to World Health Organization, a TDS of up to 500 mg/l is the optimum value, whereas a TDS of 1,500 mg/l is the maximum permissible concentration (Table 1) and all the groundwater samples of the study area are within the permissible limits. Water can be classified (Davis and De Wiest 1966) on the basis of total dissolved solids. It is observed that 56 % and 43 % in pre-monsoon and 66 % and 33 % in post-monsoon samples are within desirable limits for drinking and permissible limits for drinking respectively and all are useful for irrigation (Table 2). As per the Freeze and Cherry (1979) classification 89 %, 11 % in pre-monsoon and 100 % in post-monsoon season are within fresh water type and brackish water type, respectively. The groundwater classification based on total hardness (TH) (Sawyer and McCarty 1967) shows that 11 %, 78 %, 11 % in pre-monsoon fall in the moderately hard, hard and very hard water category, and 100 % in post-monsoon fall in the hard water category (Table 2). As per the WHO standards, TH for all samples is within the maximum permissible limit (500 mg/l) of groundwater (Table 1). Water with TH above 75 mg/l cannot be used for domestic purposes because it coagulates soap lather.

Classification of Groundwater for Irrigation Use

The development and maintenance of successful irrigation projects involve not only the supply of irrigation water to the land but also the control of salt and alkali in the soil (Haritash et al. 2008). The suitability of groundwater for agricultural uses is determined by parameters such as chloride (Cl^-), electrical conductivity (EC),

sodium adsorption ratio (SAR), percent sodium (%Na), and residual sodium carbonate (RSC) (Raju 2007; Raju et al. 2009). Stuyfzand (1989) classified water into seven divisions on the basis of the Cl^- concentration: 22 %, 11 %, 45 %, 11 % and 11 % in pre-monsoon and 11 %, 33 %, 34 %, 11 % and 11 % in post-monsoon season samples are extremely fresh, very fresh, fresh, fresh brackish and brackish-brackish category of waters, respectively (Table 2). EC is a measure of the degree in which water conducts electricity. Salty water conducts electricity more readily than pure water, hence is routinely used to measure salinity. The US Salinity Laboratory (Richards 1954) classified groundwater on the basis of the EC: 33 % and 56 % in pre-monsoon and 22 % and 78 % in post-monsoon are good and fair category waters, respectively (Table 2).

Sodium concentration is important in classifying irrigation water because sodium reacts with soil to reduce its permeability. Excess sodium in water produces undesirable effects of changing soil properties and reducing soil permeability (Kelley 1951). In all natural waters percent of sodium content is important parameter to evaluate its suitability for agricultural purposes (Wilcox 1955). The calculated values of percent sodium range from 36.86 to 73.98 with an average of 51.58 in pre-monsoon and 27.2 to 65.96 with an average of 44.18 in post-monsoon seasons. A maximum of 60 % sodium in groundwater is allowed for agricultural purposes (Ramakrishna 1998). The chemical quality of groundwater samples was studied from plots of percentage of sodium and electrical conductivity on the Wilcox diagram (Fig. 7). Wilcox diagram revealed that, out of nine groundwater samples in the study area, 34 % and 22 % samples belong to excellent to good category, 22 % and 56 % belong to good to permissible category, 33 % and 11 % belong to permissible to doubtful category, followed by 11 % and 11 % belonging to doubtful to unsuitable category in pre- and post-monsoon seasons, respectively (Fig. 7).

The agricultural crop yields are generally low in lands irrigated with waters belonging to doubtful to unsuitable category. This is probably due to the presence of excess sodium salts in groundwater, which causes osmotic effects on soil-plant system. When the concentration of sodium is high in irrigation water, sodium ions tend to be adsorbed by clay particles, displacing Mg and Ca ions. This exchange process of Na^+ in water for Ca^{2+} and Mg^{2+} in soil reduces the permeability and eventually results in soil with poor internal drainage (Raju 2007). Hence, air and water circulation is restricted during wet conditions and such soils are usually hard when dry (Collins and Jenkins 1996; Saleh et al. 1999).

Sodium adsorption ratio (SAR) is used to determine the relative concentrations of sodium, calcium and magnesium in irrigation water and to serve as an indicator of the potential damaging effects of these ions on soil structure and permeability (Raju et al. 2011). Typically, a SAR value below 3.0 is considered very safe for turf grasses. Over time, water with a SAR of 9.0 or above can cause significant structural damage to clay soils. Sandy soils are not susceptible to structural and permeability problems and can tolerate higher SAR values (~10) in most cases. The SAR value is most likely to be affected by irrigation water. The SAR values range from 1.45 to 8.28 with an average of 3.49 in pre-monsoon and 1.12 to 6.43 with an average of 2.82 in

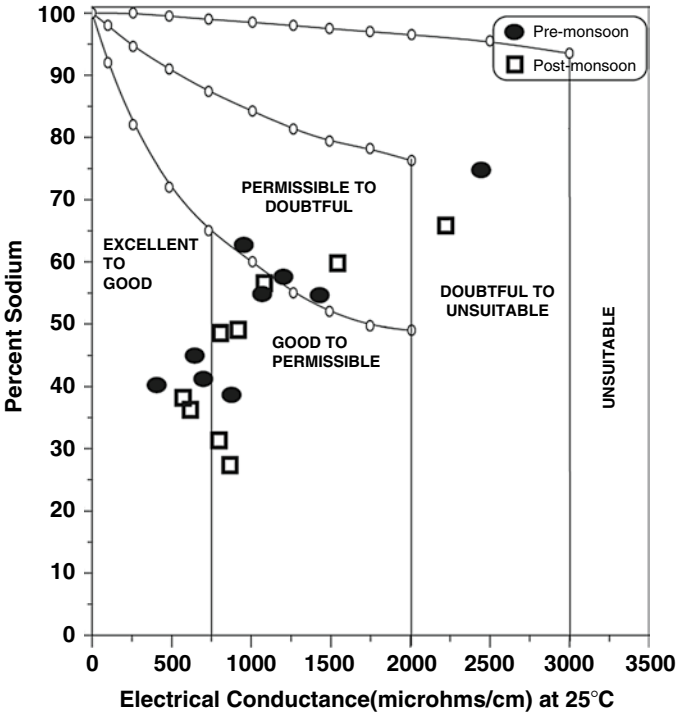

Fig. 7 Rating of groundwater samples on the basis of EC and % Na (After Wilcox 1955)

post-monsoon seasons. According to the Richards (1954) classification based on SAR values, all samples belong to the excellent category in the study area (Table 2). SAR can indicate the degree to which irrigation water tends to enter cation exchange reactions in soil.

Residual sodium carbonate (RSC) is commonly used to assess the sodium permeability hazard by considering the bicarbonate/carbonate and calcium/magnesium concentration in irrigation water. RSC is important because it mainly considers the relative concentrations of bicarbonate and carbonate as compared to those of calcium, magnesium and sodium instead of the absolute bicarbonate and carbonate concentrations. A positive RSC indicates that sodium buildup in the soil is possible. The classification of irrigation water according to the RSC value indicates that water with an RSC of above 2.5 meq/l is not suitable for irrigation, those with RSCs of 1.25–2.5 meq/l are considered doubtful, and those with RSCs below 1.25 meq/l are good for irrigation (Table 2). Based on this classification, 56 % and 44 % samples are good and doubtful category in pre-monsoon, whereas in post-monsoon 100 % groundwater samples are of good category.

Conclusions

Hydrochemical analysis shows that the groundwater in the study area is slightly alkaline in nature. Based on the total dissolved solids, groundwater samples for both the seasons are in the freshwater (<1,000 mg/l) category and all groundwater evaluated is therefore suitable for drinking and irrigation purposes. Majority of groundwater is hard in nature in both the seasons. Among the nine groundwater samples analyzed in the study area, 22 % of samples have high fluoride content than the maximum permissible limit (1.5 mg/l). The occurrence of the high fluoride concentration in some of the wells is attributed to the dissolution of micacious minerals that are associated with the mica schist formations. The hydrochemistry of cationic dominance pattern is in the order of $Na^+ > Ca^{2+} > Mg^{2+} > K^+$ in pre- and post-monsoon seasons. The anionic dominance patterns is in the order of $HCO_3^- > Cl^- > SO_4^{2-} > F^- > PO_4^{3-}$ in pre-monsoon and $HCO_3^- > SO_4^{2-} > Cl^- > F^- > PO_4^{3-}$ in post-monsoon. The hydrochemical types can be classified into three major groups such as Ca^{2+}-Na^+-HCO_3^- (average TDS value is around 310 mg/l), Na^+-Ca^{2+}-HCO_3^- (average TDS value is around 430 mg/l) and Na^+-Ca^{2+}-Cl^- types (average TDS value is around 870 mg/l). Ca^{2+}-Na^+-HCO_3^- type of water is dominated in post-monsoon, whereas Na^+-Ca^{2+}-HCO_3^- type water is dominated in pre-monsoon, it may be attributed to the ion-exchange process. Based on Base Exchange Indices, 89 % and 11 % of samples are Na^+-HCO_3^- type and Na^+-SO_4^{2-} type waters, respectively and majority of the groundwater samples are shallow meteoric genesis in both the seasons. Variation study of saturation indices reveals that all groundwater samples are undersaturated with respect to anhydrite, gypsum, dolomite, halite, magnesite and siderite minerals, and supersaturated with goethite mineral in both the seasons. As per the SAR and RSC classification, all samples belong to good to excellent category in post-monsoon, whereas 44 % in pre-monsoon (as per RSC) are doubtful category in the study area.

Acknowledgements The authors are thankful to the SES, Jawaharlal Nehru University for providing research facilities and University Engineering Department, JNU for providing groundwater samples and bore well information.

References

Adomako D, Osae S, Akiti TT (2011) Geochemical and isotopic studies of groundwater conditions in the Densu River basin of Ghana. Environ Earth Sci 62:1071–1084

Alam M, Rais S, Aslam M (2013) Hydrochemical investigation and quality assessment of groundwater in rural areas of Delhi, India. Environ Earth Sci. doi:10.1007/s12665-011-1210-x

Anupam S, Abhay KS, Kamlesh K (2012) Environmental geochemistry and quality assessment of surface and subsurface water of Mahi River basin, western India. Environ Earth Sci 65:1231–1250

APHA (2005) Standard methods for the examination of water and wastewater, 21st edn. American Public Health Association, Washington, DC

Appelo CAJ, Postma D (1993) Geochemistry, groundwater and pollution. A. A. Balkema, Rotterdam

Back, W. (1966). Hydrochemical facies and groundwater flow patterns in the northern part of the Atlantic Coastal Plain, USGS professional paper 498-A

Ball JW, Nordstrom DK (1992) User's manual for WATEQ4F with revised thermodynamic database and test cases for calculating speciation of minor, trace and redox elements in natural waters. U.S. Geol Surv Open File Rep 91:183–189

Clark I, Fritz P (1997) Environmental isotopes in hydrology. Lewis Boca Raton, New York

Collins R, Jenkins A (1996) The impact of agricultural land use on stream chemistry in the middle hills of the Himalayas. Nepal J Hydrol 185:71–86

Condesso de Melo MT, Marques da Silva MA, Edmunds WM (1999) Hydrochemistry and flow modeling of the Aveiro multilayer cretaceous aquifer. Phys Chem Earth Part B: Hydrol Oceans Atmos 4:331–336

Davis SN, De Wiest RJM (1966) Hydrogeology. Wiley, New York

Deutsch WJ (1997) Groundwater geochemistry: Fundamentals and application to contamination. CRC, Boca Raton

Drever JJ (1982) The geochemistry of natural waters. Prentice-Hall, Englewood Cliffs

Faure G (1998) Principles and applications of geochemistry, 2nd edn. Prentice-Hall, Englewood Cliffs

Foster SSD (1995) Groundwater for development – an overview of quality constraints. In: Nash H, McCall GJH (eds) Groundwater quality, 17th special report. Chapman and Hall, London

Freeze RA, Cherry JA (1979) Groundwater. Prentice-Hall, Englewood Cliffs

Guler C, Thyne GD, McCray JE, Turner AK (2002) Evaluation of graphical and multivariate statistical methods for classification of water chemistry data. Hydrogeol J 10:455–474

Haritash AK, Kaushik CP, Kaushik A, Kansal A, Yadav AK (2008) Suitability assessment of groundwater for drinking, irrigation and industrial use in some north Indian villages. Environ Monit Assess 145:397–406

Hem JD (1992) Study and interpretation of the chemical characteristics of natural water. U.S. Government Print Office, Washington

Hook Z (2005) An assessment of the water quality of drinking water in rural districts in Zimbabwe. The case of Gokwe South, Nkayi Lupane, and Mwenezi districts. Phys Chem Earth 30:859–866

Jal Nigam Report (2006) Strata chart and test report of constructed tube wells in the Jawaharlal Nehru University. Lucknow

Jeevanandam M, Kannan R, Srinivasalu S, Rammohan V (2007) Hydrogeochemistry and groundwater quality assessment of lower part of the Ponnaiyar River basin, Cuddalore district, south India. Environ Monit Assess 132:263–274

Karanth KR (1989) Groundwater assessment, development and management. Tata McGraw-Hill, New Delhi

Katz BG, Coplen TB, Bullen TD, Davis JH (1998) Use of chemical and isotopic tracers to characterize the interaction between groundwater and surface water in mantled karst. Groundwater 35(6):1014–1028

Kelley WP (1951) Alkali soils – their formation properties and reclamation. Reinold Publication Corporation, New York

Koetsiers M, Walraevens K (2006) Chemical characterization of the Neogen aquifer, Belgium. Hydrogeol J 14:1556–1568

Kruawal K, Sacher F, Werner K, Mqller J, Knepper TP (2005) Chemical water quality in Thailand and its impacts on the drinking water production in Thailand. Sci Total Environ 340:57–70

Lloyd JW, Heathcote JA (1985) Natural inorganic hydrochemistry in relation to groundwater. Clarendon Press, Oxford

Lorenzen G, Sprenger C, Taute T, Pekdeger A, Massmann G (2010) Assessment of the potential for bank filtration in a water stressed megacity (Delhi, India). Environ Earth Sci 61:1419–1434

Meybeck M (1987) Global chemical weathering of surficial rocks estimated from river dissolved loads. Am J Sci 287:401–428

Mor S, Ravindra K, Dahiya RP, Chandra A (2006) Leachate characterization and assessment of groundwater pollution near municipal solid waste landfill site. Environ Monit Assess 118:435–456

Pierre D, Glynn L, Plummer N (2005) Geochemistry and the understanding of groundwater systems. Hydrogeol J 13:263–287

Piper AM (1953) A graphic procedure in the geochemical interpretation of water analysis, USGS groundwater note, no. 12

Raju NJ (2007) Hydrogeochemical parameters for assessment of groundwater quality in the upper Gunjanaeru River basin, Cuddapah District, Andhra Pradesh, South India. Environ Geol 52:1067–1074

Raju NJ (2012a) Evaluation of hydrogeochemical processes in the Pleistocene aquifers of middle Ganga Plain, Uttar Pradesh, India. Environ Earth Sci 65:1291–1308

Raju NJ (2012b) Arsenic exposure through groundwater in the middle Ganga plain in the Varanasi environs, India: a future threat. J Geol Soc India 79:302–314

Raju NJ, Ram P, Dey S (2009) Groundwater quality in the lower Varuna River basin, Varanasi district, Uttar Pradesh, India. J Geol Soc India 73:178–192

Raju NJ, Shukla UK, Ram P (2011) Hydrogeochemistry for the assessment of groundwater quality in Varanasi: a fast urbanizing centre in Uttar Pradesh, India. Environ Monit Assess 173:279–300

Raju NJ, Dey S, Gossel W, Wycisk P (2012) Fluoride hazard and assessment of groundwater quality in the semi-arid upper Panda River basin, Sonbhadra District, Uttar Pradesh, India. Hydrol Sci J 57(7):1433–1452

Ramakrishna (1998) Groundwater. Handbook, India, 556 p

Ravikumar P, Venkatesharaju K, Somashekar RK (2010) Major ion chemistry and hydrochemical studies of groundwater of Bangalore South Taluk, India. Environ Monit Assess 163:643–653

Richard LA (1954) Diagnosis and improvement of saline and alkali soils, Handbook, no. 60. US Department of Agriculture, Washington, DC

Ronit N, Eilon A, Ofer D, Llan N (1997) Water salinization in arid regions: observations from the Negev Desert, Israel. J Hydrol 196(1–4):271–296

Saleh A, Al-Ruwaih F, Shehata M (1999) Hydrogeochemical processes operating within the main aquifers of Kuwait. J Arid Environ 42:195–209

Sandow MY, Banoeng-Yakubo B, Akabzaa T (2011) Characterization of the groundwater flow regime and hydrochemistry of groundwater from the Buem formation, Eastern Ghana. Hydrol Process 25:2288–2301

Sarin MM, Krishnaswamy S, Dilli K (1989) Major ion chemistry of the Ganga-Brahmaputra river system: weathering processes and fluxes to the Bay of Bengal. Geochemica et Cosmochimica Acta 53:997–1009

Sawyer CN, McCarty PL (1967) Chemistry for sanitary engineers, 2nd edn. McGraw-Hill, New York

Shanyengana MK, Seely MK, Sanderson RD (2004) Major ion chemistry and groundwater salinization in ephemeral floodplains in some arid regions of Namibia. J Arid Environ 57:71–83

Singh PK, Amrita M, Dinesh M, Vinod KS, Singh S (2006) Evaluation of groundwater quality in northern Indo-Gangetic alluvium region. Environ Monit Assess 112:211–230

Soltan ME (1998) Characterization, classification and evaluation of some groundwater samples in upper Egypt. Chemosphere 37:735–747

Soltan ME (1999) Evaluation of groundwater quality in Dakhla Oasis (Egyptian Western Desert). Environ Monit Assess 57:157–168

Stallard RF, Edmond JM (1983) Geochemistry of Amazon 2. The influence of geology and weathering environment on the dissolved load. J Geophys Res 88:9671–9688

Stumm W, Morgan JJ (1981) Aquatic chemistry. Wiley Interscience, New York

Stuyfzand PJ (1989) Nonpoint source of trace element in potable groundwater in Netherland. In: Proceedings of the 18th TWSA Water Working, Testing and Research Institute, KIWA, Nieuwegein

Wang S (2013) Groundwater quality and its suitability for drinking and agricultural use in the Yandi Basin of Xinjiang Province, Northwest China. Environ Monit Assess 185:7469–7484
WHO (1993) Guidelines for drinking water quality, vol 1, recommendations, 2nd edn. WHO, Geneva
Wilcox LV (1955) Classification and use of irrigation waters. US Dept of Agricul Cir 969. US Department of Agriculture, Washington, DC

Comparison of Relationship Between the Concentrations of Water Isotopes in Precipitation in the Cities of Tehran (Iran) and New Delhi (India)

Maryam Mosaffa, Farzin Nasiri Saleh, and Yousef Khalaj Amirhosseini

Introduction

The term 'Tracerhydrology' is used as a short expression for the use of tracers in hydrology. It is understood as an advanced method that allows for an integrative investigation of the hydrologic system (Leibundgut et al. 2009). Environmental and artificial tracer can be used for investigating the movement of water in the hydrological cycle. Artificial tracers are described as those elements deliberately injected into the hydrologic system (Luhua et al. 2010). By studying the motion of the injected particles, one may measure some physical processes of hydrologic system such as the escape of water from a reservoir (Evans 1983). There are more than 1,000 isotopes known for about 92 chemical elements. Most of these isotopes are called as environmental isotopes which are either stable or unstable (Leibundgut et al. 2009). The stable isotopes of hydrogen and oxygen are recognized as important traces in hydrological cycle. The heavy stable isotopic components of water, $HD^{16}O$ and H_2O^{18}, occur in natural waters in concentration of about 320 and 2,000 ppm, respectively (Evans 1983). The variation of isotopic concentration is due to fractionation caused by phase changes, evaporation, condensation, precipitation, and snow and ice formation (Chidambaram et al. 2009). Isotopic fraction is affected by meteorological factors such as temperature and altitude change (Leibundgut et al. 2009). The small variations of isotopic concentrations are usually

M. Mosaffa
Water Engineering, Tarbiat Modares University, Tehran, Iran

F.N. Saleh (✉)
Tarbiat Modares University, Tehran, Iran
e-mail: nasiri_f@modares.ac.ir

Y.K. Amirhosseini
Department of Hydraulics and Hydro-Environmental Engineering,
Water Research Institute, Tehran, Iran

© Capital Publishing Company 2015

N.J. Raju et al. (eds.), *Management of Natural Resources in a Changing Environment*, DOI 10.1007/978-3-319-12559-6_2

measured by mass spectrometry. In general, the isotopic abundance ratios are expressed as parts per mil of their deviations as given by (Vienna Standard Mean Ocean Water, VSMOW)

$$\delta = \frac{R_{\text{sample}} - R_{\text{SMOW}}}{R_{\text{SMOW}}} \times 100‰ \quad (1)$$

where R refers to the isotopic ratio (D/H) or ($^{18}O/^{16}O$) (Machavaram and Krishnamurthy 1995). In 1954, the International Atomic Energy Agency (IAEA), in co-operation with the World Meteorological Organization (WMO), conducted a worldwide survey of oxygen and hydrogen isotope content in precipitation. Since 1961, more than 780 meteorological stations in 101 countries have been monthly collecting precipitation samples. These samples are analyzed at the isotope hydrology laboratory (IAEA 2006).

Monitoring the variation of isotopic composition of precipitation requires to investigate $\delta^{18}O$ and δD values of precipitation. Many researchers such as Argiriou and Lykoudis (2006), Yu et al. (2008), Takeuchi et al. (2009), Van der Veer et al. (2009), Kumar et al. (2010a, b), Warrier and Babu (2011), and Vodila et al. (2011) have recently studied the variation of $\delta^{18}O$ and δD in precipitation for different parts of the world.

In this study, the effect of meteorological factors on precipitation isotopic data have been investigated in two stations of the Atomic Energy Agency, namely Tehran and New Delhi stations. The precipitation of Tehran is controlled by the Atlantic and the Eastern Mediterranean moisture sources, while in New Delhi it is controlled by Southwest monsoon rainfall that comes from the direction of Arabian Sea. The source of the moisture in the cities of Tehran and New Delhi are different. The most important aim of this study is to discuss the effects of these different sources of moisture on water isotopes' concentration in precipitation.

Materials and Methods

Sampling Stations

In this research, rainfall recorded at two GNIP stations (Tehran-New Delhi) are used to study the effect of the meteorological factor on the concentration of isotope composition.

Tehran situated in the north of Iran on the southern slopes of Alborz Mountains is located between 35°34′ and 35°50′N and 51°20′ and 51°36′E and encompasses an altitude range between 1,050 and 2,000 m above mean sea level (amsl). Tehran features a semi-arid and continental climate which is largely defined by its geographic

location with Alborz Mountains in its north and the central desert in the south. It can be generally described as mild in spring and autumn, hot and dry in the summer, and cold in the winter. As the city is large with significant differences in elevation for various zones, the weather is often cooler in the hilly north than in the flat southern part of Tehran. Average annual amount of precipitation recorded at the meteorological station is approximately 227 mm. Monthly rainfall is strongly influenced by season (month and moisture). The maximum and minimum recorded temperatures are approximately 39 °C in July and −1 °C in January. Tehran's main moisture source of precipitation is due to the Atlantic and the Eastern Mediterranean rainfalls. It has 12 meteorological stations, where measurements of meteorological data are available since 1951–2012.

New Delhi is located in the north of India (lat. 77°12′N; long. 28°36′E) with an average elevation of 216 m above msl. New Delhi's version of a humid subtropical climate is noticeably different from many other cities with this climate classification. In other words, it features long and very hot summers, relatively dry and cool winters, a monsoonal period, and dust storms. Summers are long, from early April to October, with the monsoon season in the middle of summer. Winter starts in November and peaks in January. New Delhi's highest temperature ever recorded is 47.2 °C, while the lowest recorded temperature is −0.6 °C. The average annual rainfall is approximately 714 mm, most of which occurs during the monsoons in July and August.

Data

In the Tehran and New Delhi stations, precipitation samples were collected to monitor oxygen, deuterium, and tritium isotopes in precipitation.

In Iran, precipitation samples were collected from 1960 to 1987 in Mehrabad station located at 35.41°N, 51.19°E and 1,200 m above msl. Tehran has 12 meteorological stations, among which Mehrabad meteorological station is the nearest one to Tehran GNIP station.

Since 1960, 40 meteorological stations in India are monthly collecting precipitation samples for the GNIP. The data has been derived from New Delhi station (N:28.58°, E:77.7° and 212 m above msl). The isotope and meteorological data have been recorded from 1960 to 2009 at New Delhi station.

This research contains two main initial objectives: firstly, the local meteoric water lines (LMWLs) were derived by using regression models of these cities and secondly, an investigation was conducted to examine the effects of variations in temperature on oxygen isotope value ($\delta^{18}O$). The time-series variation of the $\delta^{18}O$, δD and D-excess values of precipitation with the observed monthly amount of precipitation (mm) and temperature (°C), which were collected at the same time, are presented in Table 1 (IAEA 2012).

Table 1 The time-series variation of the $\delta^{18}O$, δD and deuterium excess (‰) values of precipitation with the observed monthly amount of precipitation (mm) and temperature (°C) (IAEA/WMO 2012)

	Tehran: N:51.32°, E:35.68°, 1,200 m amsl					New Delhi: N:28.58°, E:77.22°, 212 m amsl				
Sample date	δD	$\delta^{18}O$	D-excess	Precip.	Temp.	δD	$\delta^{18}O$	D-excess	Precip.	Temp.
Nov 1961	22.3	2.1	5.5	1	11.1	−45.9	−7.1	10.9	1	18.7
Dec 1961	−11.8	−4.3	22.6	19	7.8	−45.9	−6	2.1	9	12.8
Jan 1962	−26.1	−6.1	22.7	14	4.4	−16.2	−3.9	15	33	12.9
Feb 1962	−31	−5.7	14.6	108	7.2	15	1.6	2.2	13	17.7
Mar 1962	−12.4	−3.9	18.8	5	13.1	20.5	1.6	7.7	8	22.4
Sep 1962	−52.1	−7	3.9	2	23.1	−75.6	−11.5	16.4	183	28.3
Nov 1962	−11.8	−2	4.2	5	9.7	−76.9	−10.9	10.3	2	20
Dec 1962	−36.6	−4.6	0.2	15	6.7	12.5	2.9	−10.7	25	14.8
Feb 1963	−23	−3.6	5.8	12	8.5	13.1	3.9	−18.1	12	18.5
Jun 1963	−10	−1.8	4.4	1	27.1	27.3	6.2	−22.3	118	33.1
Aug 1963	−13	−2.4	6.2	12	29.1	−49.6	−7.7	12	298	28.9
Sep 1963	−2.5	−1.5	9.5	1	25.6	−120	−15.3	2.4	278	28.1
Nov 1963	−16.8	−2.6	4	19	11	−109	−14.2	4.6	1	21.7
Dec 1963	−53.3	−9.6	23.5	63	2.9	−19.2	−1.4	−8	27	15.2
Feb 1964	−85.5	−12.2	12.1	33	4.9	−9.4	−0.2	−7.8	1	16.7
Mar 1964	−39.7	−6.6	13.1	10	12.2	−8.7	0.4	−11.9	1	24.1
Apr 1964	−40.3	−5.4	2.9	17	13.9	−30.2	−3.6	−1.4	5	29.5
Dec 1964	−99	−14.5	17	25	1.9	−36	−4.3	−1.6	16	15.2
Jan 1965	−74.4	−11.2	15.2	117	0.2	38.5	4.8	0.1	9	15.6
Feb 1965	−18.6	−4.2	15	8	3.3	55.8	5.8	9.4	9	16.7
Apr 1965	21.8	3.3	−4.6	16	14.8	17.4	2.4	−1.8	14	26.3
May 1965	19.9	3.1	−4.9	7	25.6	19.3	3.6	−9.5	6	31.3
Jun 1965	22.4	4.2	−11.2	1	27.1	46.6	8.2	−19	3	35
Aug 1965	31.1	7.5	−28.9	1	29.2	−47.1	−7.4	12.1	185	29.5

Sep 1965	−19.9	−4.7	17.7	10	24.1	−48.3	−6.6	4.5	197	28.5
Jan 1966	−14.3	−3.1	10.5	14	8.7	31.5	2.6	10.7	3	14.8
Feb 1966	−28.2	−5.8	18.2	33	9	0.4	−0.4	3.6	25	19.1
Apr 1966	10.3	−1	18.3	11	16	36.8	4.3	2.4	1	28.9
May 1966	55.8	9.3	−18.6	16	21.7	21.7	1.7	8.1	59	32.3
Jun 1966	3	−1	11	2	28.5	7	0.01	6.92	163	32.5
Jul 1966	3	−0.6	7.8	1	29.6	−13.5	−2.8	8.9	89	32.2
Oct 1966	−1	0.2	−2.6	22	17.1	−52	−8.5	16	30	26.3
Mar 1967	−18.9	−2.7	2.7	7	9.8	−34.8	−6.23	15.04	50	21.3
Oct 1967	12.3	3.15	−12.9	8	19.3	−38.8	−6.38	12.24	25	25.5
Jun 1968	−3.2	−1.28	7.04	12	25.3	18.7	1.56	6.22	24	34.1
Feb 1969	−74.7	−9.48	1.14	23	2	−21.8	−2.96	1.88	9	17.5
Jul 1969	−34.1	−5.88	12.94	5	28.4	−33.5	−5.33	9.14	227	30.9
Sep 1969	2.9	2.53	−17.34	6	23.1	−82.3	−12.42	17.06	197	33.9
Jan 1973	−57.8	−9.08	14.84	19	−0.5	14.4	−0.05	14.8	29	14.3
Jun 1974	6.1	0.1	5.3	2	26.1	30.7	3.61	1.82	21	33.3
Jul 1974	35	5.2	−6.6	1	29.5	−30.3	−5.85	16.5	375	30.6
Dec 1974	−83.6	−12.48	16.24	27	4.9	8.9	−1.58	21.54	9	14.8
Jan 1975	−93.6	−14	18.4	52	2.6	−47.8	−6.81	6.68	23	13.5
Feb 1975	−52.1	−8.31	14.38	70	4.5	4.5	−0.51	8.58	6	15.9
Mar 1975	−33.9	−6.38	17.14	21	9.8	43.1	7.58	−17.54	11	22.4
Jan 1976	−36.2	−6.41	15.08	26	5.3	3.8	−0.32	6.36	1	15.5
Feb 1976	−23.5	−5.84	23.22	33	3	7.6	−0.8	14	23	17.4
Mar 1976	−58.3	−9.17	15.06	44	6.1	1.5	−0.77	7.66	13	21.7
Apr 1976	−36.2	−6.04	12.12	32	15.2	1.1	0	1.1	7	27.9
May 1976	−24.1	−4.24	9.82	22	20.8	6.8	0.17	5.44	73	31.8

(continued)

Table 1 (continued)

	Tehran: N:51.32°, E:35.68°, 1,200 m amsl					New Delhi: N:28.58°, E:77.22°, 212 m amsl				
Sample date	δD	$\delta^{18}O$	D-excess	Precip.	Temp.	δD	$\delta^{18}O$	D-excess	Precip.	Temp.
Feb 1979	−15.7	−5.09	25.02	23	5.2	17.8	0.38	14.76	45	16.3
Mar 1979	−24.8	−4.73	13.04	77	9.6	23.2	1.51	11.12	23	21
Apr 1979	27.5	2.67	6.14	11	18.8	2.8	−1.06	11.28	12	29.3
May 1979	−28.2	−3.98	3.64	28	20.3	24.5	3.59	−4.22	15	31.1
Jun 1979	6.4	0.36	3.52	15	26.2	9.4	−0.65	14.6	96	33.5
Dec 1979	−30.3	−6.22	19.46	44	5.5	7.6	−0.37	10.56	9	16.5
Jan 1980	−78.8	−11.84	15.92	48	1.8	−12.2	−2.17	5.16	5	14.2
Feb 1980	−83	−12.08	13.64	69	3.5	28.4	3.11	3.52	9	18.2
Mar 1980	−55.2	−7.61	5.68	43	10.7	−2.4	−1.8	12	26	21.6
May 1980	11.6	0.5	7.6	3	23.1	27.3	5.23	−14.54	12	34.7
Dec 1980	−51.9	−9.35	22.9	20	8.2	−3.4	−1.53	8.84	8	15.9
Jan 1981	−21.9	−4.92	17.46	44	5.2	0.8	−1.86	15.68	32	14.9
Feb 1981	−21.1	−5.07	19.46	32	7.3	24.5	2.07	7.94	16	17.9
Mar 1981	−20.7	−3.3	5.7	32	12.6	9.5	0.97	1.74	13	21.5
Nov 1981	−41.4	−6.5	10.6	7	11.7	−2.9	−1.31	7.58	27	21.5
Dec 1981	−114.2	−15.34	8.52	28	9	22.3	2.48	2.46	2	15.3
Dec 1985	−67.9	−9.68	9.54	–	–	−1.8	−0.39	1.32	35	16.7
Jan 1986	−64.7	−7.82	−2.14	–	–	−2.3	−1.26	7.78	27	13.9
Feb 1986	−46.7	−4.54	−10.38	–	–	−34.8	−5.07	5.76	41	16.2
Mar 1986	−38.9	−6.72	14.86	–	–	14.3	2.25	−3.7	12	22.5
Apr 1986	−19.7	−3.7	9.9	–	–	−2.6	1.14	−11.72	6	28.5
May 1986	40	8.35	−26.8	–	–	11.6	3.6	−17.2	23	30.6
Dec 1986	−77.7	−12.04	18.62	–	–	−7.5	−2.55	12.9	9	14.5
Feb 1987	−31.9	−4.55	4.5	–	–	23.2	1.68	9.76	20	18.7
Mar 1987	−10.8	−0.8	−4.4	–	–	−14.4	−2.75	7.6	20	23.2

Results and Discussion

The isotopic data in Tehran station shows a wide variability with $\delta^{18}O$, ranging from −15.34‰ to 9.3‰, while the δD values vary from −114.2‰ to 55.8‰, respectively. In New Delhi station, the $\delta^{18}O$ values vary from −15.3‰ to 8.2‰, and δD values range from −120‰ to 55.8‰. These changes are controlled by hydrological parameters. In general, values of isotope ratios are affected by different factors including temperature, precipitation, altitude, latitude and seasonal effect (Vodila 2011; Leibundgut et al. 2009; Kumar et al. 2010a). A seasonal oscillation of stable isotope ratios is often observed as a result of temperature (Leibundgut et al. 2009). In this paper, the effects of temperature on precipitation isotope data in the stations of Tehran and New Delhi have been investigated and compared.

Local Meteoric Water Line

In order to study the overall stable isotopic characteristic, the isotope concentration values for all seasons are plotted. In general, there is a linear relationship between $\delta^{18}O$ and δD, which in global precipitation, defines the global meteoric water line (GMWL) (Craig 1961). The GMWL was originally defined as $\delta D = 8 \times \delta^{18}O + 10$. In each area, the LMWL may be defined similar to GMWL. Figure 1 shows the δD and $\delta^{18}O$ values of the monthly precipitation samples collected in the stations of Tehran and New Delhi. The variation in the slope and intercept of LMWL line strongly depends on the weather condition in each area (Craig 1961).

By fitting a straight line on isotopic data collected in Tehran and New Delhi stations, LMWL equations are obtained from the present study as follows.

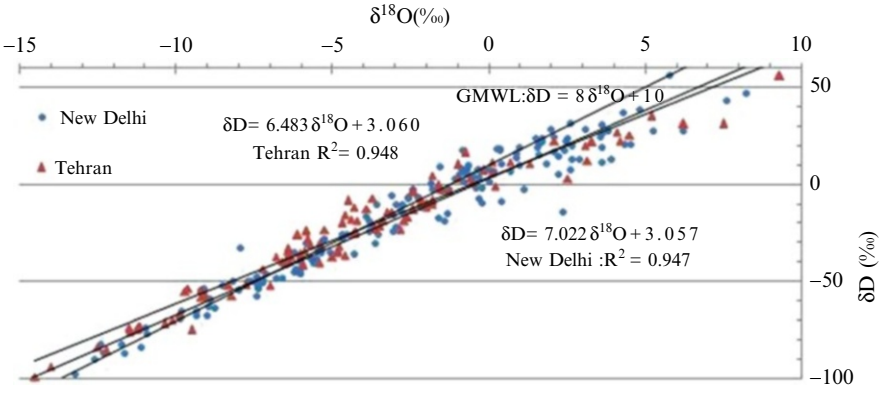

Fig. 1 The LMWL derived from the stable isotope composition in precipitation in the cities of Tehran and New Delhi

$$\text{Tehran}: \delta D = 6.483\delta^{18}O + 3.06 \ \left(R^2 = 0.95\right) \tag{2}$$

$$\text{New Delhi}: \ \delta D = 7.02\delta^{18}O + 3.06 \ \left(R^2 = 0.95\right) \tag{3}$$

By comparing the obtained LMWL equations with GMWL, it is observed that the slopes and intercepts of the LMWLs are less than the GMWL. Furthermore, Fig. 1 shows that most of the observed isotope values are below the GMWL. This phenomenon may be principally assigned to the effect of secondary evaporation during rainfall (Vodila 2011). Source of the moisture in the cities of Tehran and New Delhi are different, while the humidity is the same for both cities. Therefore, the intercepts of the fitted LMWL are the same. In addition, the obtained LMWL for New Delhi station in this study is nearly the same as the LMWL reported by Kumar B. et al. (2010a). They developed the LMWL for New Delhi station based on all seasons and monsoon data, respectively as

$$\delta D = 7.20 \ \left(\pm 0.10\right) \ \delta^{18}O + 4.60 \ \left(\pm 0.50\right) \ \left(R^2 = 0.95\right) \tag{4}$$

$$\delta D = 7.20 \ \left(\pm 0.10\right) \ \delta^{18}O + 2.70 \ \left(\pm 0.80\right) \ \left(R^2 = 0.97\right) \tag{5}$$

Effects of Temperature

As already discussed, the concentration of water's heavy stable isotopic components may change due to fraction process (Leibundgut et al. 2009). The variation in $\delta^{18}O$ corresponding to precipitation with temperature in the stations of Tehran and New Delhi are shown in Fig. 2. By investigation of data recorded in both stations (see Table 1), more negative values are generally occurred during the winter. As a

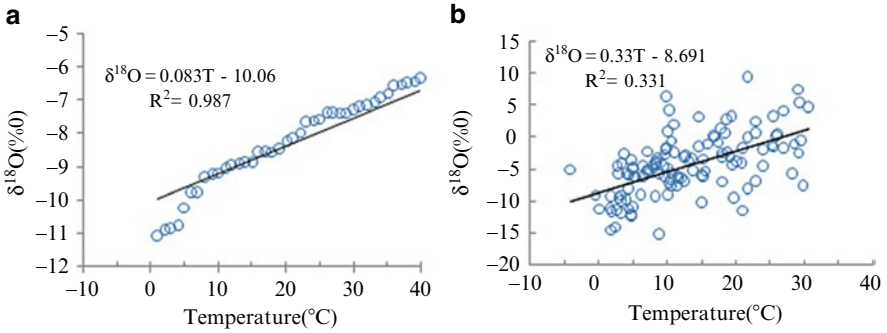

Fig. 2 Correlation between isotope values oxygen-18 and air temperature (T) at (**a**) New Delhi and (**b**) Tehran stations

result, the isotopic composition of precipitation in cold environments is more depleted compared to warm environments. It means that isotope concentration decreases with decreasing temperature as confirmed in Fig. 2. This figure also shows a good correlation between $\delta^{18}O$ and air temperature in the New Delhi station, while the corresponding correlation is relatively weak in the Tehran station.

Conclusions

In this study, time-series of oxygen and hydrogen stable isotope of the precipitation water collected monthly from 1961 to 1987 in the stations of Tehran and New Delhi were analyzed. The concentrations of water isotopes ($\delta^{18}O$, δD) vary spatially and temporally. These variations result from isotopic fractionation processes at each phase change of water during its atmospheric cycle. The changes in concentration of these isotopes are used to trace the movement of water in hydrological and meteorological processes. The slopes of the least-squares fitting lines range from 6.48 (Tehran) to 7.02 (New Delhi) in all seasons. The obtained LMWLs for these stations show significantly lower intercept and slope values than the GMWL. This result shows good agreement with the results reported in some recent works (Kumar et al. 2010a; Vodila et al. 2011). The source of the moisture in Tehran and New Delhi are different, however the humidity is the same in the both cities. Therefore, the intercepts of the fitted LMWL are the same. By plotting $\delta^{18}O$ values versus air temperature data of Tehran and New Delhi stations, a good correlation between $\delta^{18}O$ and air temperature in the New Delhi station ($R^2 = 0.987$) was obtained, while a relatively weak correlation was observed between $\delta^{18}O$ and air temperature in the Tehran station ($R^2 = 0.331$). The obtained results also showed that the maximum and minimum values of $\delta^{18}O$ are obtained during winter and summer, respectively. A linear relationship exists between monthly isotope data and meteorological parameters at each station. These results are consistent with the findings of Argiriou and Lykoudis (2006) in Greece.

References

Argiriou A, Lykoudis S (2006) Isotopic composition of precipitation in Greece. J Hydrol 327:486–495

Chidambaram S, Prasanna MV, Ramanathan AL, Vasu K, Hameed S, Warrier UK, Srinivasamoorthy K, Manivannan R, Tirumalesh K, Anandhan P, Johnsonbabu G (2009) A study on the factors affecting the stable isotopic composition in precipitation of Tamil Nadu, India. Hydrol Process 23:1792–1800

Craig M (1961) Isotopic variation in meteoric waters. Science 133:1702–1703

Evans GV (1983) Tracer techniques in hydrology. Int J Appl Radiat Isot 34:451–475

IAEA (2006) Statistical treatment of isotope data in precipitation. International Atomic Energy Agency, IAEA

IAEA (2012) http://nds121.iaea.org/wiser
IAEA/WMO (2012) Global network of isotopes in precipitation. The GNIP Database, www.naweb.iaea.org
Kumar B, Rai SP, Kumar US, Verma SK, Garg P, Kumar SVV, Jaiswal R, Purendra BK, Kumar SR, Pande NG (2010a) Isotopic characteristics of Indian precipitation. Water Resour Res 46. doi:10.1029/2009WR008532
Kumar US, Kumar B, Rai SP, Sharma S (2010b) Stable isotope ratios in precipitation and their relationship with meteorological conditions in the Kumaon Himalayas, India. J Hydrol 391:1–8
Leibundgut C, Maloszewski P, Kulls C (2009) Tracer in hydrology. Wiley, Chichester
Luhua X, Wei G, Deng W, Zhao X (2010) Daily $\delta^{18}O$ and δD of precipitations from 2007 to 2009 in Guangzhou, South China: implications for changes of moisture source. J Hydrol 400:477–489
Machavaram MV, Krishnamurthy RV (1995) Earth surface evaporative process: a case study from the Great Lakes region of the United States based on deuterium excess in precipitation. Geochemical et Cosmochimica Acta 59:4279–4283
Takeuchi A, Goodwin AJ, Moravec BG, Larson PB, Keller CK (2009) Isotopic evidence for temporal variation in proportion of seasonal precipitation since the last glacial time in the inland Pacific Northwest of the US. Quat Res 72:198–206
Van der Veer G, Voerkelius S, Lorentz G, Heiss G, Hoogewerff JA (2009) Spatial interpolation of the deuterium and oxygen-18 composition of global precipitation using temperature as ancillary variable. J Geochem Explor 101:175–184
Vodila G, Palcsu L, Futo I, Szanto Z (2011) A 9-year record of stable isotope ratios of precipitation in Eastern Hungary: implications on isotope hydrology and regional palaeoclimatology. J Hydrol 400:144–153
Warrier CU, Babu MP (2011) A comparative study on isotopic composition of precipitation in wet tropic and semi-arid stations across southern India. J Earth Syst Sci 120:1085–1094
Yu W, Yao T, Tian L, Ma Y, Ichiyanagi K, Wang Y, Sun W (2008) Relationships between $\delta^{18}O$ in precipitation and air temperature. Atmos Res 87:158–169

Geophysical Expression for Groundwater Quality in Part of Chittoor District, Andhra Pradesh, India

S.Md. Farooq Basha

Introduction

Water quality is a consequence of the natural, physical and chemical state of the water as well as any alterations that may have occurred as interference by human activity. The minerals contained in soils and rocks are also commonly responsible for the type of quality of ground water in a region. Quality of ground water has gained much importance as its quantity. Growing population, urbanization, industrialization, increased social and agricultural activities are increasing the demand of potable groundwater, as such making us to think of water in terms of quality.

Geophysical methods are widely used to locate aquifers in different lithological formations. These methods play a vital role in locating the groundwater tables and in reducing the infructuous amount of drilling expenditures by eliminating the non-feasible locations where the negative indications are recorded. In surface geophysical methods, certain physical properties and parameters of subsurface formations are measured by instruments located on the surface. The success of these methods depends on how best the physical parameters deduced are interpreted in terms of hydrogeological language. As the geophysical characteristic or its range is not unique to hydrogeological parameters, one or more alternatives arise from which a choice has to be made on the basis of knowledge of hydrogeology of the area. At times, a combination of two or more methods may have to be chosen (Karanth 1995). The Electrical Resistivity Method is one of the geophysical methods which are extensively used and play a vital role in the groundwater mapping and groundwater exploration. Water-bearing and water-barren formations are identifiable based on the contrast in the electrical resistivity (Zohdy 1974). In this paper an attempt is

S.Md.F. Basha (✉)
Civil Engineering, Muffakhamjha College of Engineering, Hyderabad 500034, India
e-mail: farooq_mjcet@gmail.com

© Capital Publishing Company 2015

N.J. Raju et al. (eds.), *Management of Natural Resources in a Changing Environment*, DOI 10.1007/978-3-319-12559-6_3

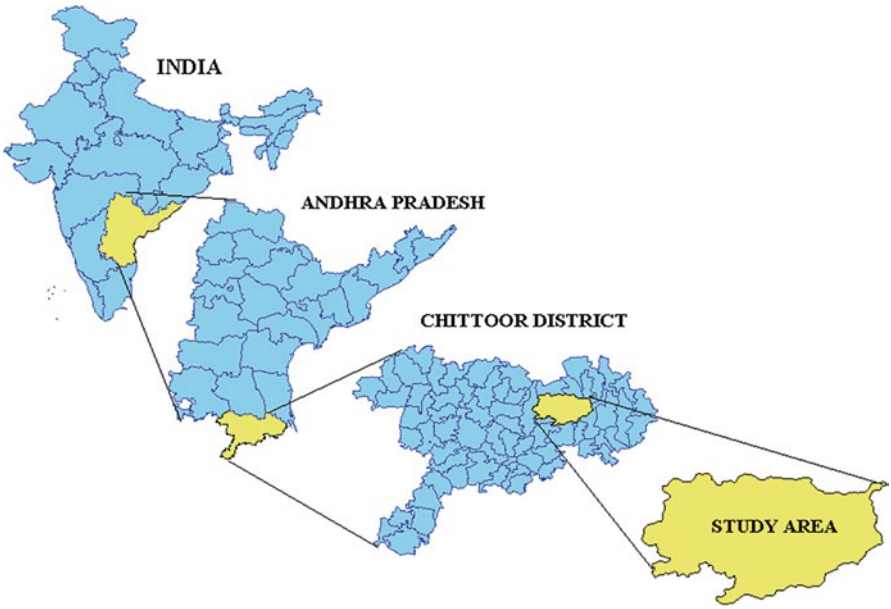

Fig. 1 Index map of study area

made to find a relation between the Dar-Zarrouk, parameter, longitudinal unit conductance (*S*) and primary hydrogeochemical parameters.

The study area shown in Fig. 1 falls in some parts of Chittoor district which is the southernmost district of Andhra Pradesh. It covers an area of 674 sq. km and lies between the geographical coordinates of north latitude 13° 27′ 48″ and 13° 41′ 10″ and east longitudes 79° 13′ 36″ and 79° 38′ 40″ covering the parts of topographical sheet numbers 57O/2, 57O/6, 57O/7, 57O/10 in Chittoor district of Andhra Pradesh. Swarnamukhi river flows in the study area. The river originates in Panapakam hill ranges and flows south-westerly through parts of Thottambedu Mandal of Chittoor district and finally joins the Bay of Bengal to the south of the Nellore town. The total area of the river basin is ~3,225 km^2. However, a part of the basin, an area of ~674 km^2 has been covered in the present study. The study area has hot and semi-arid climate, the mean annual temperature is 29 °C, average annual rainfall is recorded as 375–750 mm and the wind speed is in the range of 5–9 km/h.

Geophysical Expression for Groundwater Quality

The electrical resistivity method is widely used in locating the groundwater potential zones. Groundwater quality is being chemically analyzed in the laboratory to assess and recommend the same for drinking, industrial and agricultural purposes. This is the most accurate method. However for mapping groundwater quality for large

areas, the method is cumbersome, time-consuming and expensive. Quicker, cost-effective techniques of analysis of groundwater quality can be achieved by comparing and correlating primary hydrogeochemical parameters with an easily obtainable geophysical parameter. This study reveals the significant relationship between geophysical parameter and hydrogeochemical ions, i.e., longitudinal unit conductance (S) and Ca, Na, Cl, NO_3, SAR, EC, total hardness, TDS.

Methodology

Vertical electrical soundings carried out at 28 locations are shown in Fig. 2. The vertical electrical sounding data used in the present study are subjected to refinement of the interpretations through the use of the software package Resist 87. The computed values of apparent resistance ρ, layer thickness (h) and longitudinal unit conductance (S) are given in Table 1. The interpreted curves of few soundings are shown in Fig. 3. Longitudinal unit conductance (S) is the sum of the ratios of thickness (h) of different layers to their corresponding resistivities. In the present study, S is the sum of $S_1 + S_2$, where S_1 is ratio of thickness and resistivity of 1st layer, i.e. h_1/ρ_1, while $S_2 = h_2/\rho_2$ of 2nd layer.

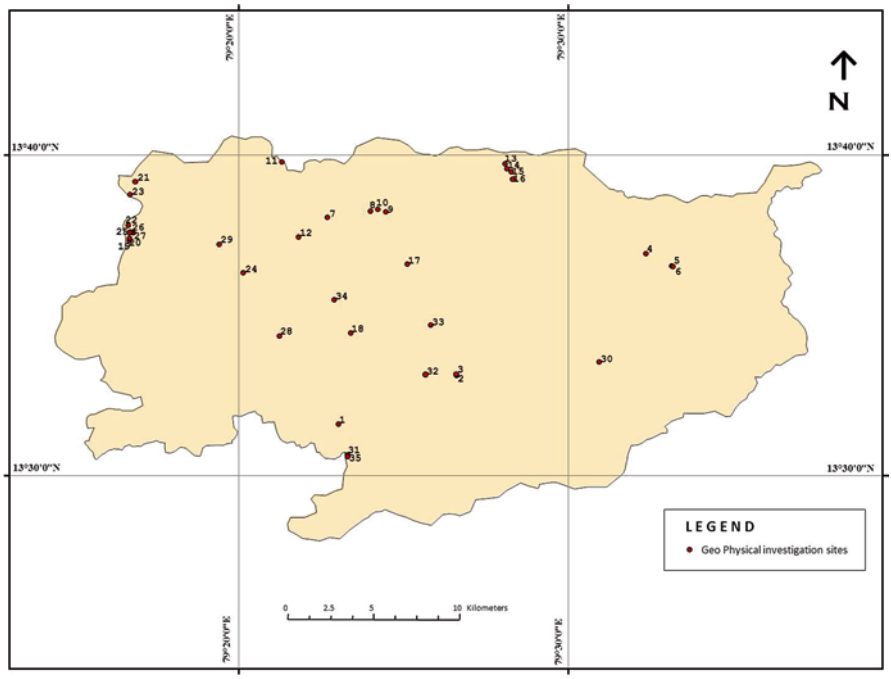

Fig. 2 Location of geophysical soundings

Table 1 VES data of different locations

VES No.	Village name	Interpreted layer parameters				
			Layers			Longitudinal unit conductance (S)
			I	II	III	
1	P.V. Puram	ρ	63.2	18.4	107.5	0.0346
		h	0.6	1.1	3.8	
2	Kamapally	ρ	23	13.6	426.4	0.3644
		h	0.7	9.5	–	
3	Kamapally	ρ	64.8	12.6	337.5	0.4895
		h	0.7	12.2	–	
4	Kura Kalva	ρ	180.3	9.1	59.4	0.8439
		h	1.2	15.3	–	
5	Jipalem	ρ	2.6	7.8	9898.6	0.8269
		h	2.7	4.8	–	
6	Jipalem	ρ	3.4	13.5	194.8	0.7876
		h	4.5	3.4	–	
7	Veterinary college	ρ	97.8	9.4	24.4	0.1036
		h	0.5	1.9	15.6	
8	Ladies hostel	ρ	214.9	6.6	10024.6	0.4629
		H	3.6	6	–	
9	Deputy warden	ρ	89.4	25.1	110.9	0.5832
		h	4.2	28.1	–	
10	SVU campus	ρ	64.1	17.2	10009.9	0.6954
		h	2.7	23.2	–	
11	Chellampuram	ρ	37.3	11.6	112	0.2872
		h	3.1	5.7	–	
12	Kothur	ρ	220.5	48.5	1223.4	0.2366
		h	1.6	22.6	–	
13	TUDA	ρ	2.5	139.8	9613.9	0.2582
		h	1	16.3	–	
14	TUDA	ρ	236.1	19	117.2	0.1185
		h	1.3	4.4	5.5	
15	TUDA	ρ	56.3	28.1	254.1	0.1121
		h	1.4	5.6	–	
16	TUDA	ρ	20	27.7	67.1	0.1361
		h	1.4	5.6	21	
17	Avulati	ρ	60.7	21.7	10208.3	0.3415
		h	0.9	14.5	–	
18	Durgasamudram	ρ	146.4	389.8	24.6	0.0071
		h	0.9	3.1	16.7	
19	A. Rangampeta	ρ	48.4	62.3	10.2	0.0258
		h	1.1	1.8	3	

(continued)

Table 1 (continued)

VES No.	Village name	Interpreted layer parameters				
			Layers			Longitudinal unit conductance (S)
			I	II	III	
20	Madigapalem	P	92.1	8.8	9866.6	0.3788
		h	0.7	6.6	–	
21	Nagapatla	ρ	207.1	68.3	9906.6	0.3582
		h	0.7	48.7	–	
22	Arepalli	ρ	29.1	348.6	42.2	0.0208
		h	0.9	3.7	15	
23	Nagapatla	ρ	24	25.1	49.5	0.3325
		h	2	14.6	19.9	
24	Thandawada	ρ	38.3	25.3	57.9	0.4116
		h	1.1	20.1	19.2	
25	Arepalli	ρ	42.9	13.8	10149.7	0.3422
		h	2	8.8	–	
26	Arepalli	ρ	136.9	26.4	10362	0.2286
		h	0.9	11.9	–	
27	Arepalli	ρ	94.1	65.87	177.2	0.2046
		h	0.7	33.1	13.8	
28	Kotta Sanabatla	ρ	129.9	33.6	167.2	0.2017
		h	0.6	13.4	14.9	
29	Kothur	ρ	169.9	21.2	450.3	0.1695
		h	1.5	7	–	
30	Kandiri Mangalam	ρ	99.9	45.6	539.1	0.1815
		h	1	16.1	–	
31	Rayala Cheruvu	ρ	184.6	32	224	0.0954
		h	0.6	6	39.6	
32	Nennuru	ρ	86.7	43.3	1506.4	0.5491
		h	1.7	46.7	–	
33	Kotha Kinda	p	114.6	55.2	943.8	0.2217
	Venkatapuram	h	1	24	–	
34	Gollapalle	ρ	9.4	10.4	10162	0.5788
		h	1.3	10.6	–	
35	Royal Cheruvu	ρ	117.3	41.3	177.4	0.1225
		h	0.9	9.8	51.4	

Groundwater samples collected at 28 locations were analyzed at sites where VES were conducted in the study area. A qualitative and quantitative correlation of hydrogeochemical parameters with a Dar-Zarrouk parameter, longitudinal unit conductance (*S*) parameters is derived and discussed in detail. Contour maps and graphs are prepared from groundwater quality data and Dar-Zarrouk parameter, longitudinal unit conductance (*S*) is compared to drive the relationship in between them.

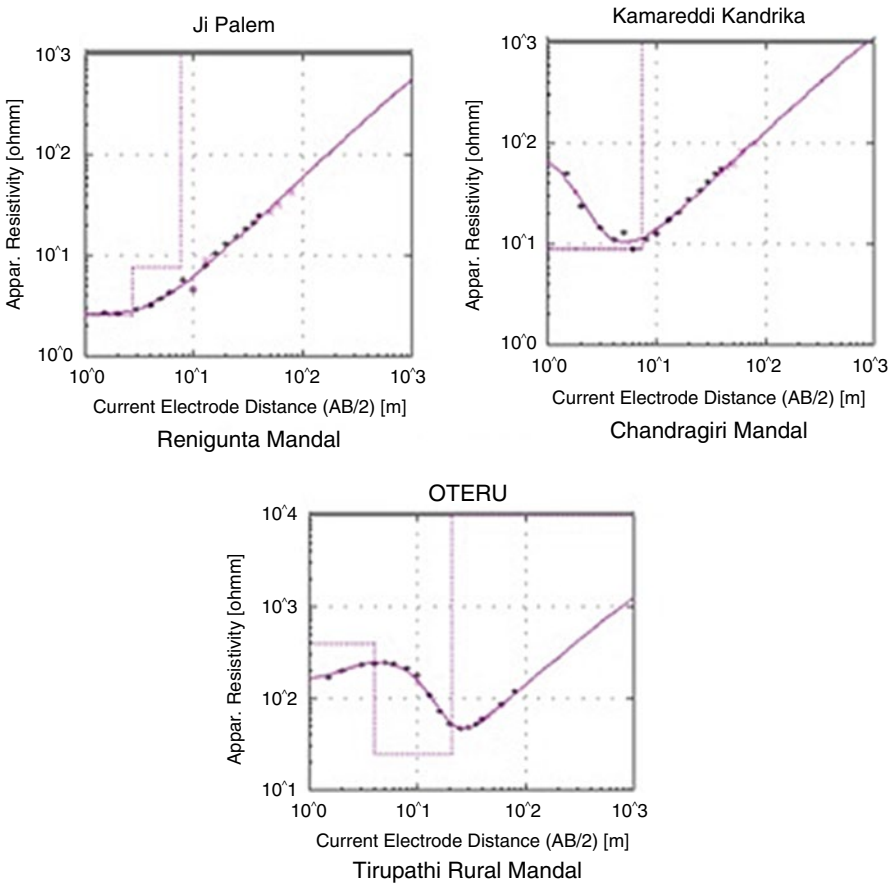

Fig. 3 Interpreted curves

Dar-Zarrouk Parameters

Maillet (1947) termed the Dar-Zarrouk parameters as D.Z. parameters. T is the resistance normal to the face, and S is the conductance parallel to the face for a unit cross-sectional area, which plays an important role in resistivity soundings. D.Z. parameters are sufficient to compute the distribution of surface potential and, therefore, an electrical resistivity graph. For example, in a cross section of the unit prism from a layer extending laterally, whose resistivity is ρ (in ohm-m) and thickness is h (in m), the resistance normal to the face of the prism is the transverse unit resistance (T measured in ohm-m^2). The conductance parallel to the face of the prism is the longitudinal unit conductance (S, measured in mho, or micro siemens) and are given by

$$T = h \times \rho \text{ and } S = \rho / h$$

If this prism consists of N parallel and isotropic layers of resistivities, $\rho_1, \rho_2, \rho_3, \ldots, \rho_N$ and thickness $h_1, h_2, h_3, \ldots, h_N$, when the current is flowing normal to the base, the total resistance of the prism is

$$T = h_1\rho_1 + h_2\rho_2 + h_3\rho_3 + \ldots + h_N\rho_N = \sum_{i=1}^{i=N} h_i/\rho_1$$

In the same way, when the current is flowing parallel to base

$$S = \rho_1/h_1 + \rho_2/h_2 + \rho_3/h_3 + \ldots + \rho_N/h_N = \sum_{i=1}^{i=N} \rho_i/h_i$$

$$\left(\text{Longitudinal conductance}\right)$$

$$R_t = T/h$$

Dar-Zarrouk parameters have been used earlier by some researchers. Zohdy (1965) developed a technique to interpret the vertical electrical sounding curves by using the Dar-Zarrouk parameters.

Sree Devi (1999) prepared a longitudinal conductance map, and noted that longitudinal conductance is reciprocal relation of resistance and conductance. If a geological formation is more conductive, it has less resistivity which indicates good aquifer. Hodlur et al. (2002, 2003, 2006) extensively worked on the Dar-Zarrouk parameters and used the parameters to develop a technique to improve and update the resolution of fresh and the saline water aquifers in coastal areas. They showed the existence of a relation between the Dar-Zarrouk parameters and the natural recharge. A relation between formation water resistivity (Rw) and the longitudinal unit conductance (S) was recognized.

Earlier researchers have not done extensive work to find a relation between the Dar-Zarrouk parameters and the groundwater quality. In this paper, a modest beginning is made to successfully unravel the relation between the longitudinal unit conductance (S) and the primary chemical water quality parameters like carbonate, bicarbonate, total hardness, total dissolved solids and some other parameters.

The qualitative and quantitative correlation of hydrogeochemical parameters with Dar-Zarrouk parameter, longitudinal unit conductance (S) parameters is shown in Fig. 4a–c to Fig. 7a–c respectively. Tables 2, 3, 4 and 5 show the longitudinal unit conductance (S), hydrogeological parameters such as total dissolved solids, electrical conductance, calcium, sodium, carbonate, chloride, total hardness, etc.

The contour pattern of longitudinal unit conductance (S) is compared with some hydrogeochemical parameters and a qualitative correlation in their behaviour has been recognized. Graphical comparison of geophysical and hydrogeochemical parameters clearly illustrates a qualitative relationship between the two parameters. Use of such qualitative relation in the field of groundwater exploration is explained in this paper.

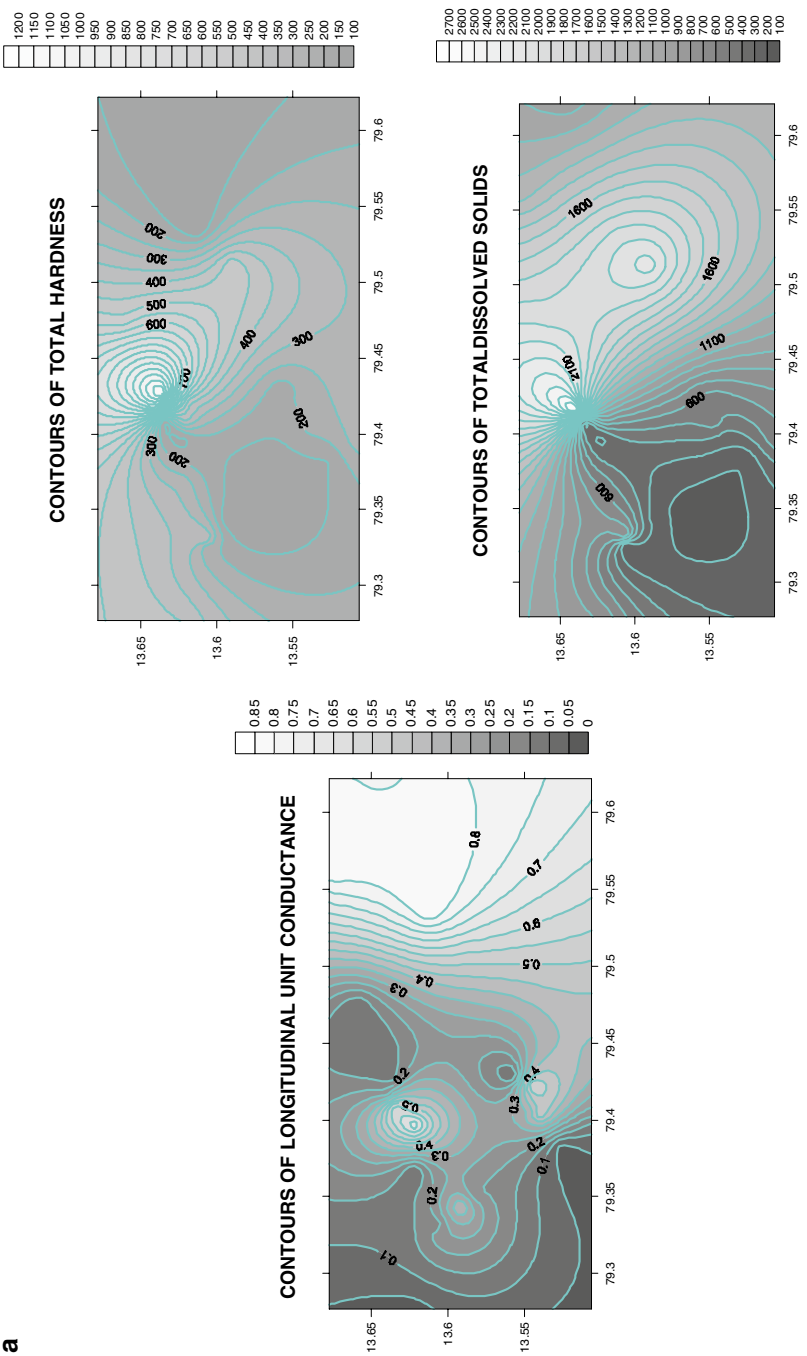
a
CONTOURS OF LONGITUDINAL UNIT CONDUCTANCE
CONTOURS OF TOTAL HARDNESS
CONTOURS OF TOTALDISSOLVED SOLIDS
13.65
13.6
13.55
79.3
79.35
79.4
79.45
79.5
79.55
79.6

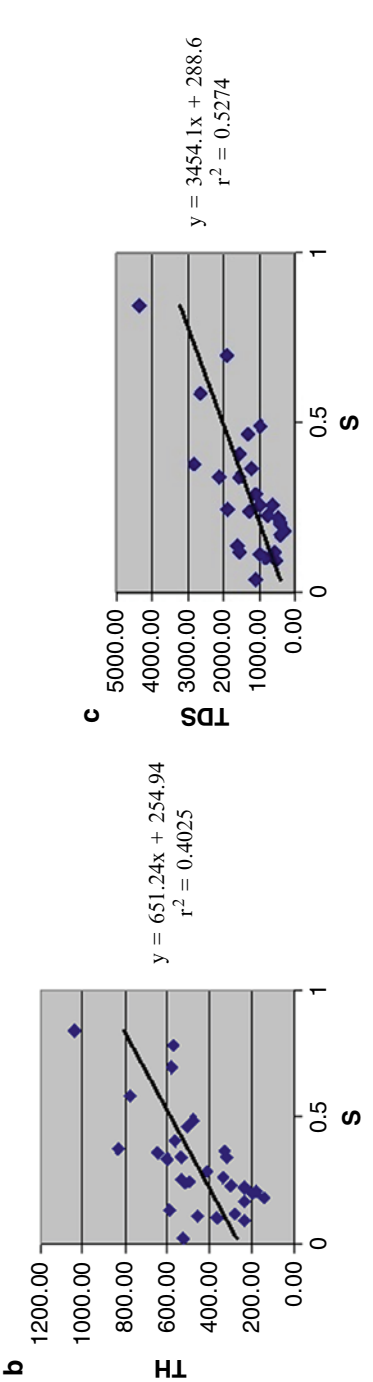

Fig. 4 (**a**) Relation between longitudinal unit conductance (*S*) and total hardness (TH) and total dissolved solids (TDS). (**b**) Quantitative relation between longitudinal unit conductance and total hardness (TH). (**c**) Quantitative relation between longitudinal unit conductance and TDS

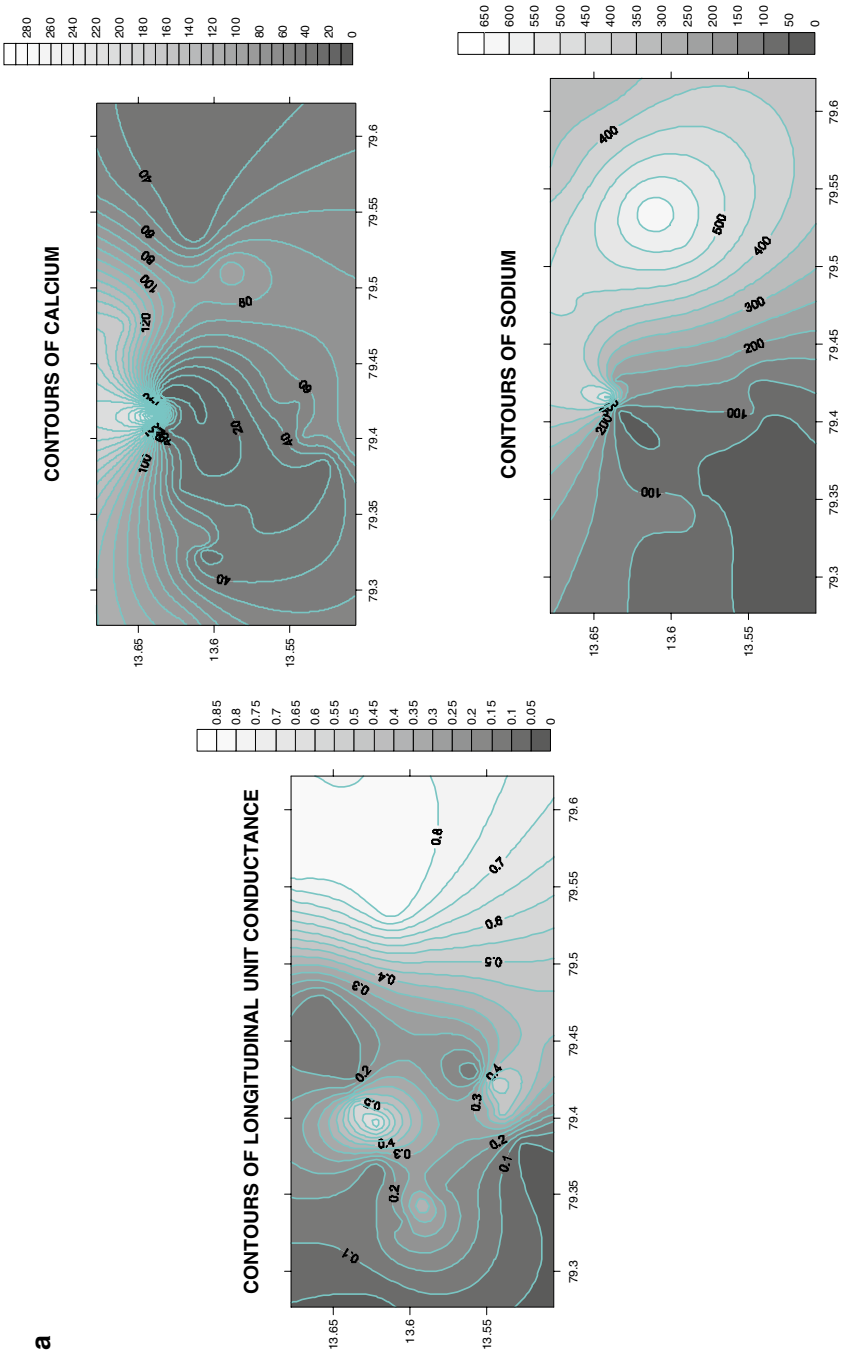
a
CONTOURS OF LONGITUDINAL UNIT CONDUCTANCE
CONTOURS OF CALCIUM
CONTOURS OF SODIUM

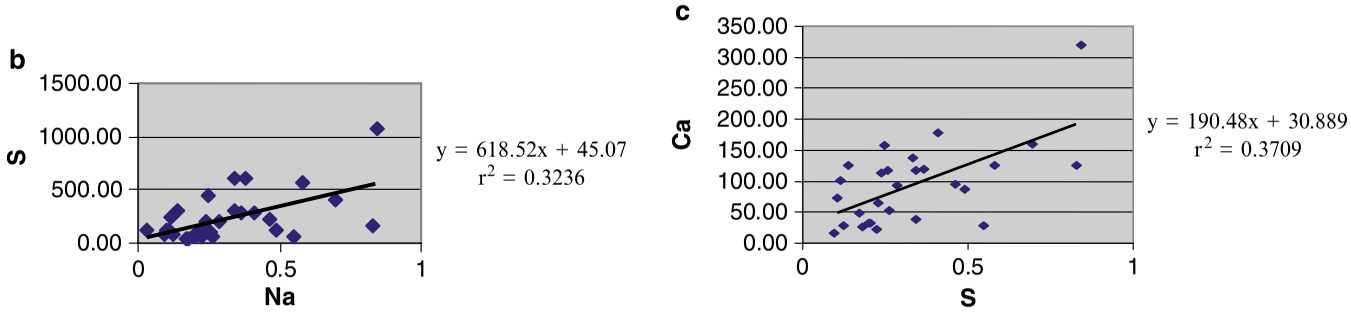

Fig. 5 (**a**) Relation between longitudinal unit conductance (S) and calcium (Ca) and sodium (Na). (**b**) Quantitative relation between longitudinal unit conductance and sodium. (**c**) Quantitative relation between longitudinal unit conductance and calcium

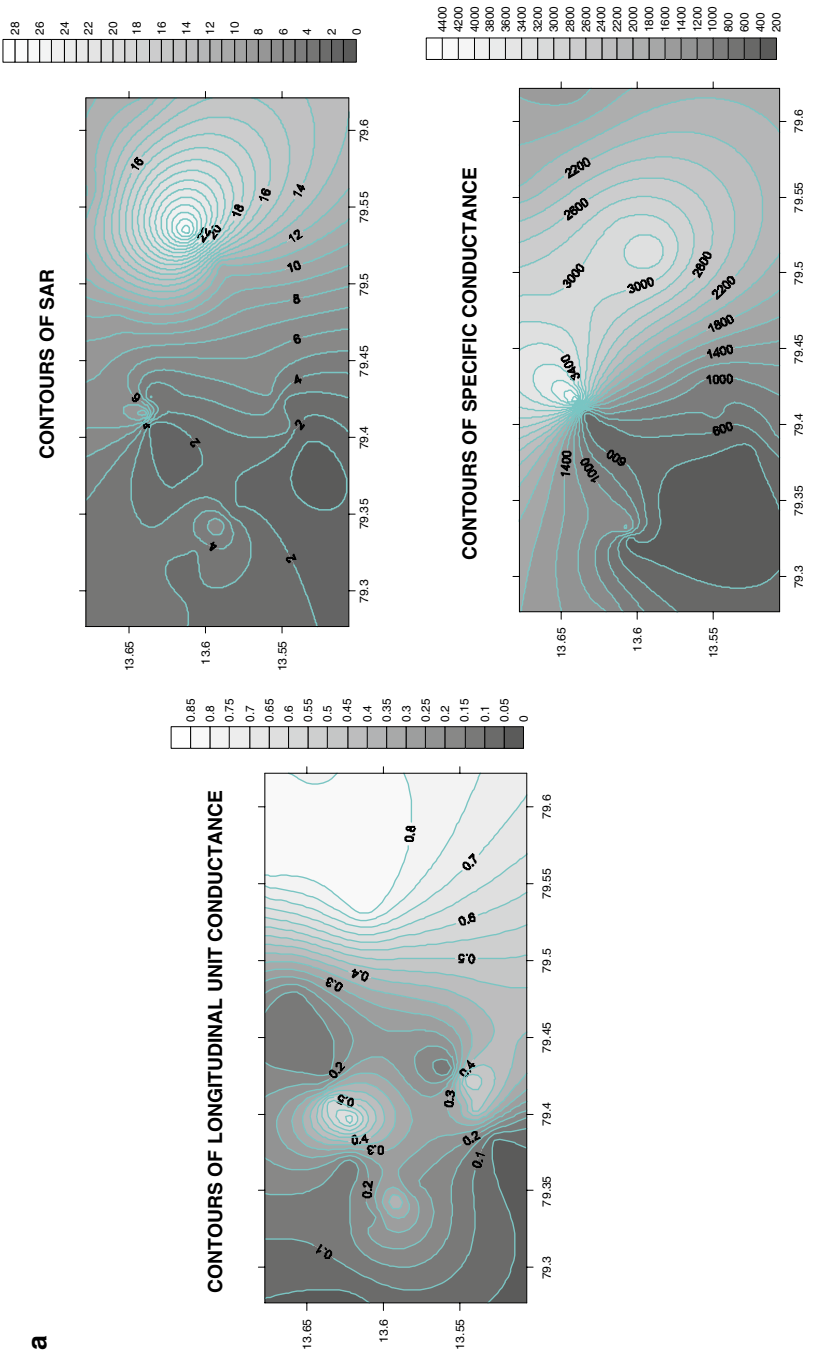
a
CONTOURS OF LONGITUDINAL UNIT CONDUCTANCE
CONTOURS OF SAR
CONTOURS OF SPECIFIC CONDUCTANCE

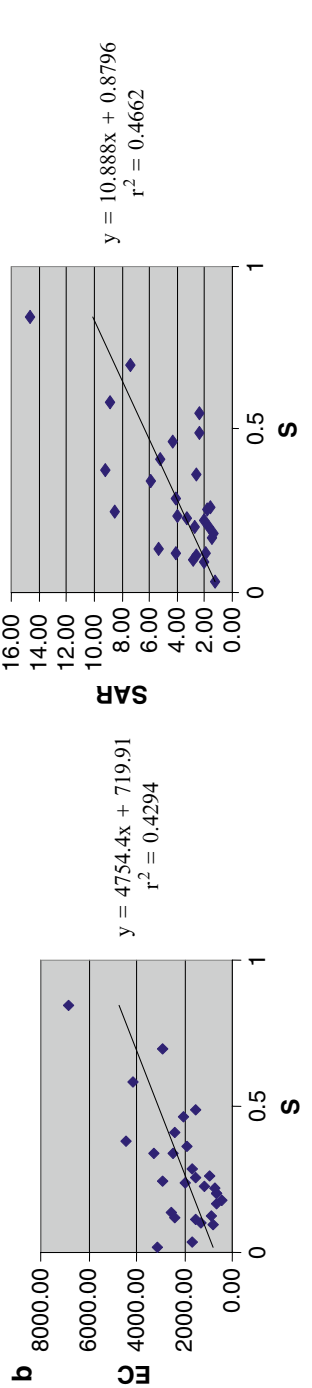

Fig. 6 (**a**) Relation between longitudinal unit conductance (*S*) and sodium adsorption ratio and electrical conductance. (**b**) Quantitative relation between longitudinal unit conductance (*S*) and electrical conductance (EC). (**c**) Quantitative relation between longitudinal unit conductance (*S*) and SAR

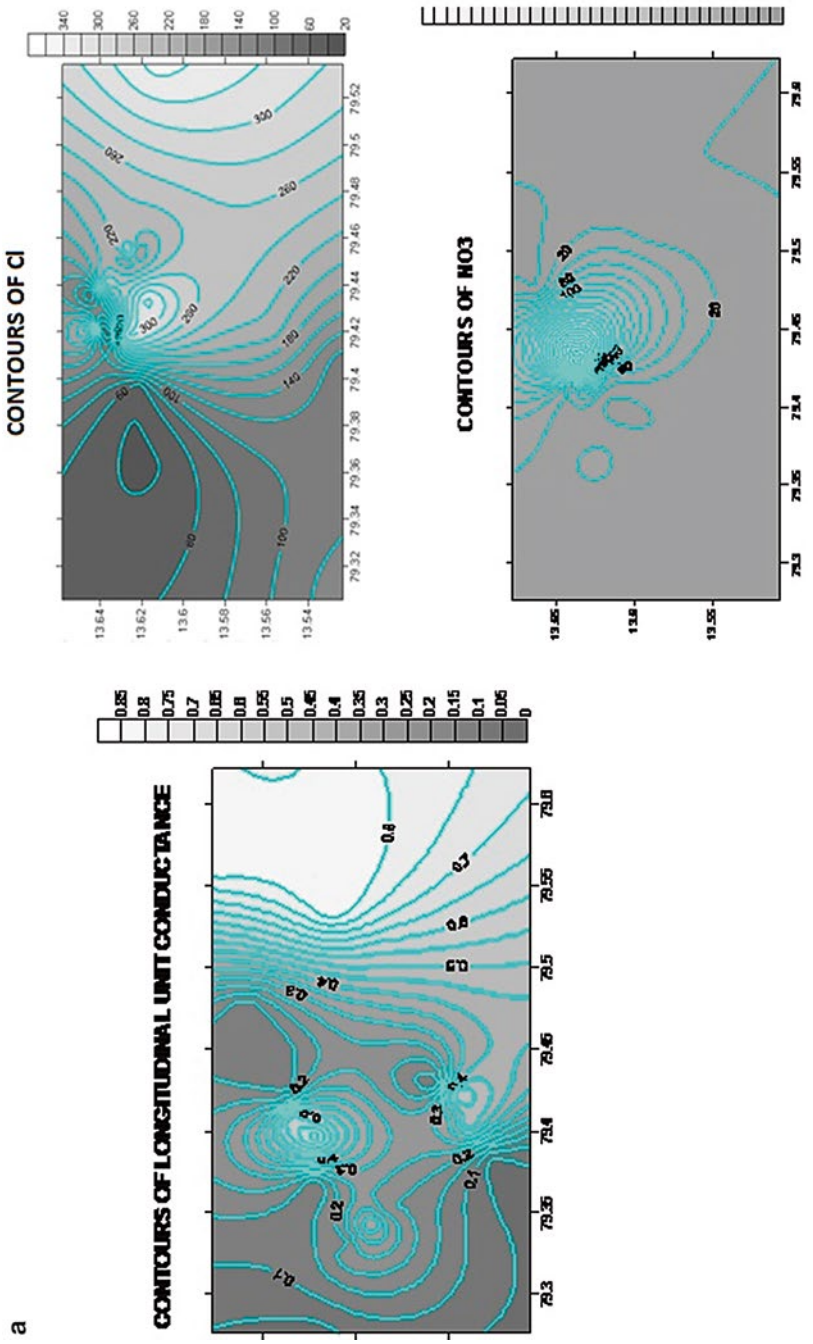
a
CONTOURS OF LONGITUDINAL UNIT CONDUCTANCE
CONTOURS OF Cl
CONTOURS OF NO3

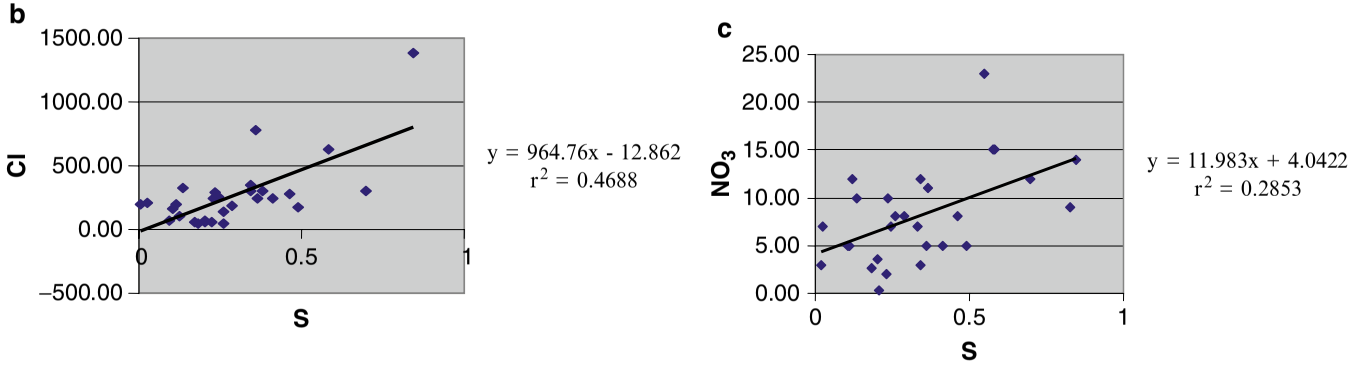

Fig. 7 (**a**) Relation between longitudinal unit conductance (*S*), chloride (Cl) and nitrate (NO_3). (**b**) Quantitative relation between longitudinal unit conductance (*S*) and chloride (Cl). (**c**) Quantitative relation between longitudinal unit conductance (*S*) and NO_3

Table 2 Values of longitudinal conductance (*S*), calcium and sodium

S	Ca	Na
0.364482097	120.00	283.00
0.489528219	86.00	122.00
0.843987128	320.00	1084.00
0.826923077	126.00	172.00
0.103620067	72.00	126.00
0.462921443	96.00	225.00
0.583250889	126.00	568.00
0.695479447	160.00	406.00
0.287244615	94.00	194.00
0.236617809	114.00	210.00
0.112077521	102.00	131.00
0.136083032	126.00	298.00
0.341514892	118.00	311.00
0.33250332	138.00	–
0.411593515	178.00	285.00
0.245320088	158.00	438.00
0.342150603	38.00	601.00
0.228665859	64.00	130.00
0.204625792	32.00	84.00
0.201714231	32.00	56.00
0.169508701	48.00	50.00
0.181540093	26.00	38.00
0.095375135	16.00	71.00
0.549064892	28.00	70.00
0.260247479	52.00	67.00
0.221754306	22.00	70.00
0.122480385	28.00	74.00

Table 3 Values of longitudinal conductance (*S*), Cl and NO_3

S	Cl	NO_3
0.364482097	245.00	11.00
0.489528219	172.00	5.00
0.843987128	380.00	14.00
0.103620067	165.00	9.00
0.462921443	278.00	5.00
0.583250889	630.00	8.00
0.695479447	300.00	15.00
0.287244615	185.00	12.00
0.236617809	285.00	8.00
0.258297568	136.00	10.00
0.112077521	194.00	8.00
0.136083032	328.00	12.00
0.341514892	350.00	5.00
0.007050169	198.00	10.00
0.025809864	210.00	12.00
0.378800217	300.00	7.00

Table 3 (continued)

S	Cl	NO_3
0.358205378	780.00	5.00
0.411593515	246.00	3.00
0.245320088	260.00	7.00
0.342150603	302.00	5.00
0.228665859	250.00	7.00
0.204625792	60.00	3.00
0.201714231	65.00	1.97
0.169508701	57.00	0.27
0.181540093	46.00	3.58
0.095375135	74.00	2.70
0.260247479	43.00	23.00
0.221754306	57.00	15.00
0.122480385	106.00	15.00

Table 4 Values of longitudinal conductance (*S*), SAR and EC

S	SAR	EC
0.03463814	1.25	1684.00
0.364482097	2.59	1914.00
0.489528219	2.43	1523.00
0.843987128	14.63	6836.00
0.103620067	2.87	1297.00
0.462921443	4.33	2055.00
0.583250889	8.82	4117.00
0.695479447	7.32	2945.00
0.287244615	4.14	1700.00
0.236617809	4.01	2000.00
0.258297568	1.80	1497.00
0.118542544	4.10	2434.00
0.112077521	2.65	1513.00
0.136083032	5.31	2544.00
0.341514892	5.85	2466.00
0.378800217	9.16	4441.00
0.411593515	5.25	3125.00
0.245320088	8.50	2409.00
0.228665859	3.26	2930.00
0.204625792	2.73	3278.00
0.201714231	1.72	1155.00
0.169508701	1.43	668.00
0.181540093	1.40	628.00
0.095375135	2.04	665.00
0.549064892	2.33	440.00
0.260247479	1.58	775.00
0.221754306	2.01	970.00
0.122480385	1.92	760.00

Table 5 Values of longitudinal conductance (*S*), TH and TDS

S	Total hardness	TDS
0.364482097	330.00	1224.96
0.489528219	478.00	974.72
0.843987128	1038.00	4375.04
0.787690632	570.00	–
0.103620067	365.00	830.08
0.462921443	510.00	1315.20
0.583250889	782.00	2634.88
0.695479447	582.00	1884.80
0.287244615	415.00	1088.00
0.236617809	520.00	1280.00
0.258297568	530.00	958.08
0.112077521	462.00	968.32
0.136083032	594.00	1628.16
0.341514892	534.00	1578.24
0.025809864	528.00	–
0.378800217	836.00	2842.24
0.358205378	648.00	–
0.33250332	598.00	–
0.411593515	558.00	1541.76
0.245320088	500.00	1875.20
0.342150603	318.00	2097.92
0.228665859	300.00	739.00
0.204625792	179.00	428.00
0.201714231	199.00	402.00
0.169508701	230.00	425.60
0.181540093	140.00	281.60
0.095375135	230.00	496.00
0.260247479	340.00	620.80
0.221754306	230.00	486.40
0.122480385	280.00	556.80

Results and Discussions

There is a direct relation between the variation of TDS and *S*. In Fig. 4a, in the eastern region, high TDS contours shown in white tone match perfectly with high *S* zone shown in white tone in the eastern zone. The low TDS contours shown in black tone in the south western portion and grey tone in north western portion match significantly with low *S* values with similar tones. The parameters of *S* and TDS have also shown significant direct relation when both the parameters are correlated quantitatively, the graph of correlation is shown in Fig. 4c. The correlation coefficient r^2 is 0.5274 which amounts to 73 %, hence one of the parameters are quantitatively estimated if either one is known.

There is significant qualitative correlation between *S* and total hardness (TH). In the contour map shown in Fig. 4b in the eastern region the contours of high longitudinal unit conductance match well with contours of higher values of total hardness. Similarly in the western region low values of contours of *S* match significantly with low values of contours of total hardness. Figure 4b shows the correlation of *S* vs TH. There is a remarkable direct relation between *S* and TH. The correlation coefficient r^2 is 0.4025 which amounts to 64 %. Hence one of the parameters can be quantitatively estimated if either is known.

In the contour maps shown in Fig. 5a, there is total correlation between contour pattern of *S* and Na. Contours showing higher values of Na match remarkably with contours showing higher values of *S* significantly in space. Similarly, contours showing lower values of Na in space match well with lower values of contours of *S*. In the contour maps shown in Fig. 5a, white tone represents higher values and darker tone represents lower values of parameters namely *S* and Ca. It is clearly observed that high level contours of *S* match with high level contours of calcium and vice-versa. Hence there is direct qualitative relationship between *S* and Ca.

Figure 5b shows a direct correlation of *S* vs Na. The correlation coefficient r^2 is 0.3236, which amounts to 56 %. Figure 5c shows correlation between *S* and Ca. The correlation coefficient r^2 which is 0.3709 and amounts to 61 % shows a significant quantitative relationship between *S* and calcium. Hence one of the parameters can be quantitatively estimated if either is known.

In Fig. 6a the contours of specific conductance and longitudinal unit conductance are shown. The contours in the white tone are higher values, and the contours in grey and black tones are lower values of the parameters. There is total match of white grey and dark areas in the map of *S* with white grey and dark areas observed in the map of specific conductance. Hence, there is a significant qualitative relationship between *S* and specific conductance. Specific conductance increases with increase in the values of *S* and vice-versa. Figure 6b shows the correlation of *S* and specific conductance, the correlation shows a direct relation between *S* and specific significant. Hence one of the parameters can be quantitatively estimated if either is known. In Fig. 6a in the contour map, white tone indicates higher values, and the contours in grey and black tones indicate lower values. There is significant qualitative relationship between *S* and sodium adsorption ratio, because the grey and white tone regions match significantly with each other. Figure 6c shows correlation of *S* and sodium adsorption ratio, a direct relationship is observed between these parameters. The correlation coefficient r^2 is 0.4662 which amounts to 68 % which is significant. Hence, one of the parameters can be quantitatively estimated if either is known.

In Fig. 7a the contour map shows that except a minor discrepancy, the correlation in the north central parts of the study areas, a complete match between the patterns of contours *S* and Cl can be observed. Figure 7b shows that the quantitative relation of *S* and Cl is almost direct. The correlation coefficient r^2 is 0.4688 which amounts to 68 %. Hence, one of the parameters can be quantitatively estimated if either is known. In Fig. 7a the nitrate contour map indicates the correlation in the north central parts of the study area, there is complete match between *S* and nitrate. In Fig. 7c

the quantitative relation shows almost direct relation of both the parameters. The correlation coefficient r^2 is 0.2853 which amounts to 53 %.

The above mentioned qualitative and quantitative relationship between longitudinal unit conductance (*S*) and hydrochemical parameters of Cl, SAR, EC, TDS, Ca, Na, NO_3 illustrate significant relationship between the geophysical parameter, longitudinal unit conductance and various hydrochemical parameters.

The correlation can be improved to further levels of better significance if the geophysical data is collected exactly at the same spot from where the water samples were collected from bore wells for chemical quality analysis. However, in the present studies the correlation coefficients for the various parameters are all above 60 %, hence it is possible to estimate the chemical quality parameter by just carrying out simple Vertical Electrical Soundings (VES) at many sites and by conducting water quality analysis at few sites.

Geophysical surveys can be conducted in short field seasons and are appreciably cost effective compared to the expenditure in detailed water quality analysis in any study area. The qualitative and quantitative results shown in the correlation patterns and correlation graphs clearly illustrate the geophysical expression of water quality.

Conclusions

In the contour map the parameters of *S* and TDS have shown significant direct relation, the correlation coefficient r^2 is 0.5274 which amounts to 73 %. In the eastern region the contours of high longitudinal unit conductance match well with contours of higher values of total hardness. Similarly in the western region low values of contours of *S* match significantly with lower values of contours of total hardness. The correlation coefficient r^2 is 0.4025 which amounts to 64 %. Contours showing higher values of Na match remarkably with contours showing higher values longitudinal unit conductance in space. The correlation coefficient of r^2 is 0.3236 which amounts to 57 %. High level contours of longitudinal unit conductance match well with high level contours of calcium and vice-versa. Hence, there is direct qualitative relationship between *S* and calcium, the correlation coefficient r^2 is 0.3709 and shows significant quantitative relationship between *S* and calcium which amounts to 61 %. Specific conductance increases with increase in the values of *S* and vice-versa. The correlation coefficient r^2 which is 0.4294 amounts to 66 % which is significant. There is a complete match between the patterns of contours *S* and Cl. The qualitative relation of the *S* and chloride is almost direct. The correlation coefficient r^2 is 0.4688 which amounts to 68 %. The qualitative and quantitative relationship between longitudinal unit conductance (*S*) and hydrochemical parameters of Cl, SAR, EC, TDS, Ca, Na and NO_3 illustrate significant relationship.

In present study the correlation coefficients for the various parameters are all above 60 %, hence it is possible to estimate the chemical quality parameter by just carrying out simple vertical electrical soundings (VES) at many sites and by con-

ducting water quality analysis at few sites. The correlation can be improved to further levels if the geophysical data is collected exactly at the same spot from where the water samples are collected from bore wells for chemical quality analysis. The qualitative and quantitative results shown in the correlation patterns and correlation graphs clearly illustrate the geophysical expression of water quality.

Acknowledgements The author expresses his sincere thanks to staff of A.P. Groundwater Board, and G.K. Hodlur, Emeritus Scientist N.G.R.I for their continued support for carrying this research. I also express profound gratitude to Prof. M. Muralidhar, Professor, Department of Geology, Osmania University for his supervision, constant discussion and invaluable help in completing this research work.

References

Hodlur GK, Ravi Prakash M, Deshmuck SD, Singh VS (2002) Role of some geophysical, geochemical, and hydrogeological parameters in the exploration of groundwater in brackish terrain. Environ Geol 41:861–866

Hodlur GK, Singh UK, Das RS, Rangarajan R, Chand R, Singh SB (2003) Geophysical expression of natural recharge in different geological terrains. Groundwater 41(6):1–10

Hodlur GK, Dhakata R et al (2006) Correlation of vertical electrical sounding and borehole-log data. Geophysics 71:G11

Maillet R (1947) The fundamental equation of electrical prospecting. Geophysics 12:529–556

Sree Devi PD (1999) Assessment and management of groundwater resources of Pageru river basin, Cuddapah district, Andhra Pradesh, India. Unpublished Ph.D. thesis, S.V. University, Tirupati

Zohdy AAR (1965) The auxiliary point method of electrical sounding interpretation and its relationship to the Dar-Zarrouk parameters. Geophysics 30:644–660

Zohdy AAR (1974) Applications of surface geophysics to groundwater investigations. U.S. Department of Interior Geological Survey Book No. 2

Geospatial Analysis of Fluoride Contamination in Groundwater of Southeastern Part of Anantapur District, Andhra Pradesh

B. Muralidhara Reddy, V. Sunitha, and M. Ramakrishna Reddy

Introduction

The occurrence of fluoride (F^-) concentration in groundwater is mainly due to natural or geogenic pollution and the source of contamination is often unknown (Handa 1975a; Saxena and Ahmed 2002). Geogenic contamination of groundwater depends mainly on the geological setting of an area. As rain water infiltrates through soil and reaches the water table, it can dissolve partly certain component of bedrock. The F^- content of groundwater can thus originate from the dissolution of fluorine-bearing minerals in the bed rock. In other words, bed rock mineralogy is a primary factor in general for the variations in F^- content of groundwater (Chae et al. 2007; Raju et al. 2012). F^- contamination of groundwater is a function of many factors such as availability and solubility of fluorine-bearing minerals, temperature, pH, concentration of calcium and bicarbonate ions in water, etc. (Chandra et al. 1981; Largent 1961). In contrast to anthropogenic pollution of surface water, geogenic contamination of groundwater is difficult to detect and even more difficult to control. The presence of excessive concentrations of F^- in groundwater may persist for years, decades or even centuries and can reach the food system (Todd 1980). In recent years, there has been an increased interest in F^- research because high concentration of F^- in groundwater causes adverse impact on human health. In order to mitigate the excessive F^- in groundwater, it is essential to determine and monitor the casual factors of enrichment of F^- concentration in groundwater in time and space (Ahmed et al. 2002; Raju et al. 2009).

B. Muralidhara Reddy (✉) • V. Sunitha
Department of Geology, Yogi Vemana University, Kadapa 516003, Andhra Pradesh, India
e-mail: bandi.murali@yahoo.co.in

M. Ramakrishna Reddy
Department of Earth Sciences, Yogi Vemana University,
Kadapa 516003, Andhra Pradesh, India

© Capital Publishing Company 2015

N.J. Raju et al. (eds.), *Management of Natural Resources in a Changing Environment*, DOI 10.1007/978-3-319-12559-6_4

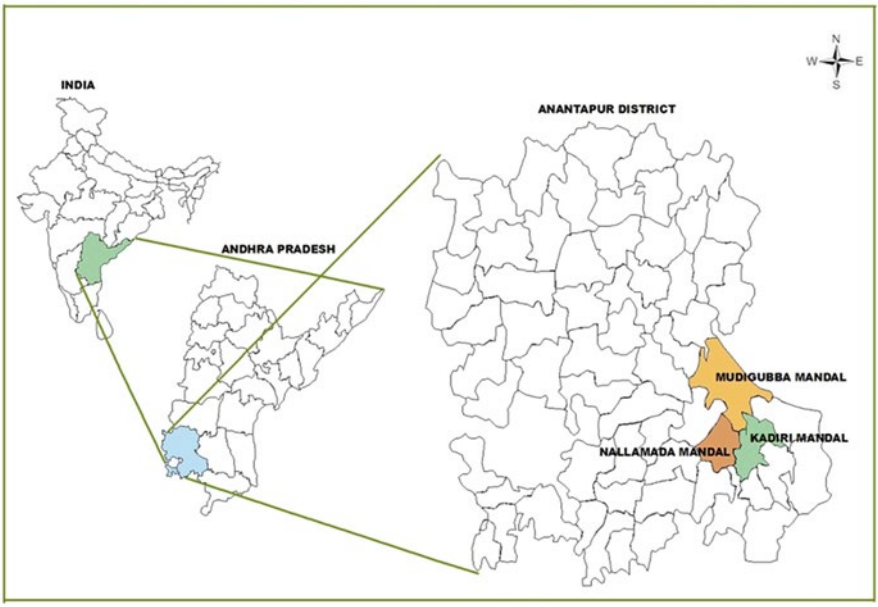

Fig. 1 Study area location map

Study Area

The study area covers an extent of about 1,136.3 km^2 extending in the revenue mandals such as Mudigubba, Kadiri and Nallamada (Fig. 1) in the southeastern part of Anantapur District, Andhra Pradesh and lies between east longitudes from 77°30′ to 78°15′ and north latitudes from 14°0′ to 14°30′ covering in the Survey of India Toposheet Nos. 57 F/14, F/15, J/3 and J/4. The geological map of the study area is shown in Fig. 2. The major geomorphic units are denudational hills, dissected pediments, pediplain and alluvium. Geologically, it is underlain mainly by Peninsular gneisses of Archean age comprising pink granites, schists and composite gneisses (equivalents of the Dharwars), intruded by a few pegmatite dykes, numerous dolerite dykes and volcanic flows. It experiences a semiarid climate, with a moisture index of 33.7 % and monthly mean temperatures of a low of 15 °C in January and high of 39 °C in May. The normal rainfall in the district is 553 mm that is the least, when compared to that in the other districts of Andhra Pradesh.

Hydrogeology

The district is underlain by granite gneisses and schists of Archaean age. The northeastern part of the district is covered by consolidated sedimentary formation of Cuddapah Super Group belonging to upper Precambrian to lower Paleozoic Age. River

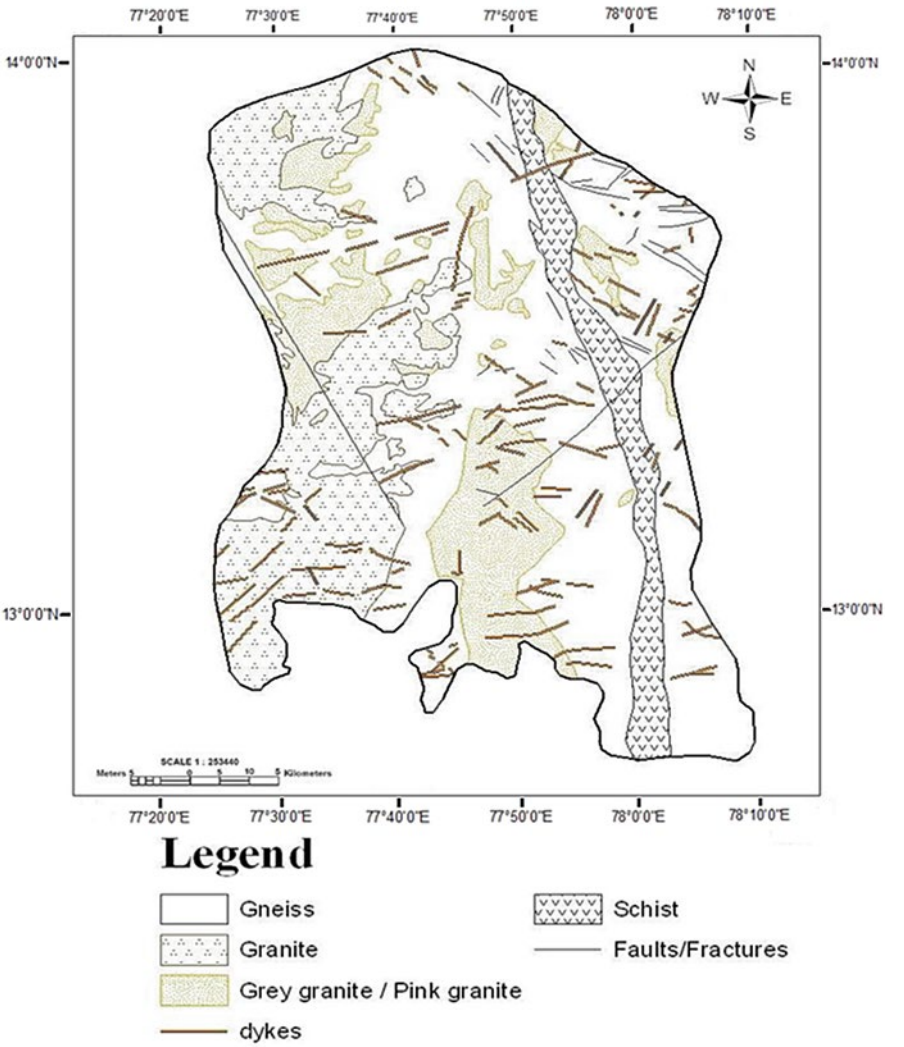

Fig. 2 Geological map of the study area (GSI District Resource Map, Anantapur District, 1994)

alluvium occurs along the major river courses and to some extent along minor stream courses. The Archaean crystalline rocks include granites, gneisses and Dharwarian schists. The ground water in these formations occurs in the weathered and fractured zones under water table and semi-confined conditions, respectively. These rock types do not possess primary porosity. Due to fractures and weathering, they have developed secondary porosity often giving rise to potential aquifers at depth. The degree of weathering in the Archaean formation is less than 20 m depth. This weathered zone has been tapped extensively by the dug wells and dug-cum-bore wells, which invariably tap the fractures occurring below the weathered zone. Ground water occurring in these formations is generally developed by dug wells, dug-cum-bore wells and bore wells. The

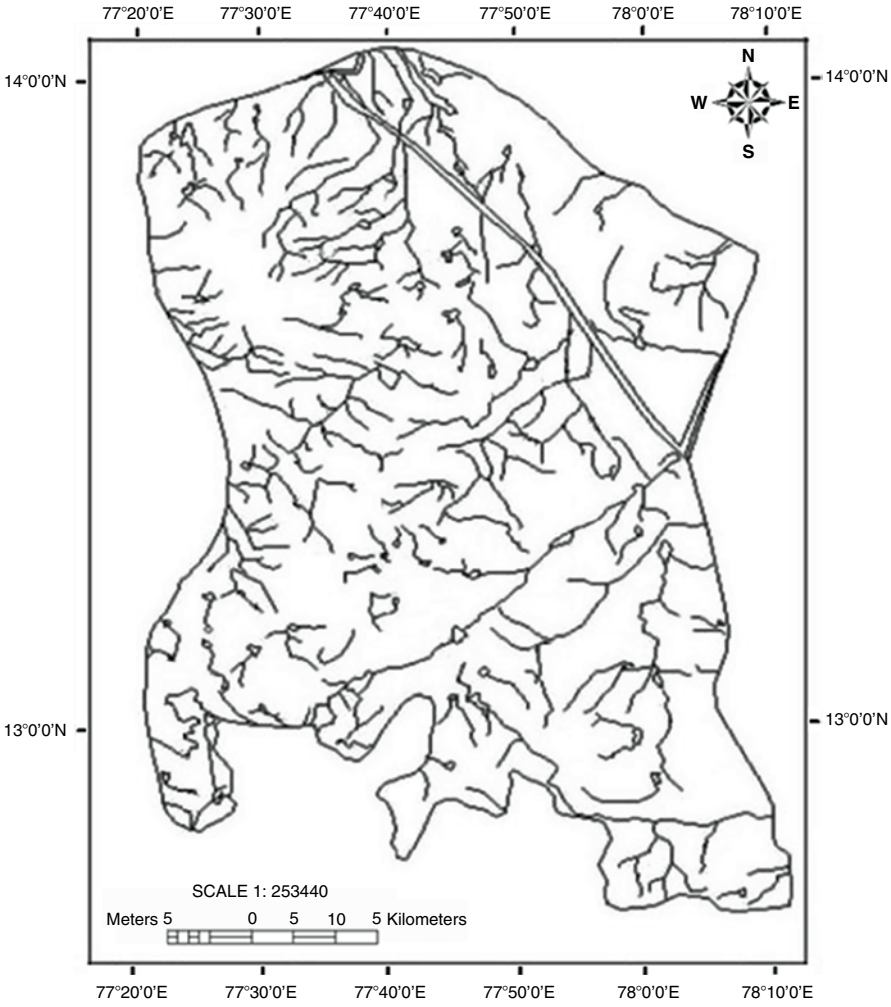

Fig. 3 Drainage map of the study area

depth of open wells range from 6.0 to 25.0 m below ground level and depth to water level vary from 1.5 to 23 m bgl. The yield of dug wells varies 10–200 cm/day for a pumping period of 3–6 h/day. The drainage map of the study area is shown in Fig. 3.

Materials and Methods

In the present study, water samples were collected from 50 tube wells in the study area. The study is carried out with the help of topographic maps, Garmin GPS MAP 76, Arc GIS 9.3 corroborating with fieldwork. The Survey of India toposheets are used to prepare the basemap, drainage map and to understand the general nature of the study area.

GPS is used to map the location of each sampling well and finally the results were taken to the GIS for further analysis. The field work included water level measurements, well inventory and collection of water samples from tube wells and the study of geological and geomorphological features of the area in general. The pre-monsoon water samples were collected during September 2009 and the post-monsoon water samples were collected during April 2010. The groundwater samples were analyzed, as per the procedure of American Public Health Association (APHA 1995) and suggested precautions were taken to avoid contamination. The various parameters determined were: pH, total hardness (TH), chloride (Cl^-), nitrate (NO_3^-) and fluoride (F^-). pH was determined by pH meter; TH, Cl^- by titrimetry; F^- and NO_3^- were determined by using ion selective electrode (Orion 4 star ion meter, Model: pH/ISE). The location of each well was taken into the GIS environment and the results of each parameter analysed was added to the concerned wells. Spatial analyst, an extended module of Arc GIS 9.3 was used to find out the spatiotemporal behaviour of the fluoride parameters.

Results and Discussion

Chemical Analysis

Fluoride concentration in natural waters depends on several factors such as temperature, pH, presence or absence of ion complexes or precipitation of ions and colloids, solubility of fluorine-bearing minerals, anion exchange capacity of aquifer materials, the size and type of geological formations through which the water flows and the time water is in contact with a particular formation (Apambire et al. 1997). The concentration of fluoride in groundwaters is principally governed by the climate, the composition of host rock, and the hydrogeology. Areas of semiarid climate, crystalline rocks and alkaline soils are mainly affected (Handa 1975b). High fluoride concentrations in groundwater suggest that favourable conditions exists for the dissolution of fluoride bearing minerals present in the granite and gneissic rocks in the study area. Fluoride bearing minerals occupy the joints, fractures, faults and vertical openings in the gneissic and granitic formations which are the oldest geological formations in Anantapur and have undergone maximum weathering (Subba Rao 2003). Granitic rocks are known to contain a relatively large proportion of fluorine minerals (Edmunds and Smedley 2005). Fluorite, the main mineral that controls the geochemistry of fluoride in most environments is found in significant amounts in granite, granite gneisses and pegmatite (Deshmukh et al. 1995; Rama Rao 1982; UNICEF 2008; Mamatha and Sudhakar Rao 2010).

The results of analyzed chemical and statistical parameters including minimum, maximum, mean and standard deviation are given in Table 1. Understanding the quality of ground water is an important aspect because it is the main factor determining its suitability for drinking, domestic, agricultural and industrial purposes. The pH values of ground water range from 7 to 8.6 with an average of 7.98 during September 2009, with a mean of 8 indicating an alkaline condition which favours the solubility of fluoride-bearing minerals. In acidic medium (acidic pH), fluoride is adsorbed in clay; however, in alkaline medium it is desorbed, and thus alkaline pH is more favourable for

Table 1 Result of chemical analysis and statistical parameters of groundwater samples collected from the study area

S. No	pH		TH (mg/l)		Cl^- (mg/l)		F^- (mg/l)		NO_3^- (mg/l)	
	Sept. 09	April 10	Sept. 09	April 10	Sept. 09	April 10	Sept. 09	April 10	Sept. 09	April 10
W_1	7.4	7.2	678	712	140	130	3.5	3.4	58	54
W_2	7.6	7.4	650	696	170	170	4.2	4.0	55	50
W_3	7.3	7.2	655	705	190	180	4.0	3.8	60	58
W_4	7.5	7.2	346	413	170	160	5.0	4.8	68	65
W_5	8.3	8.0	413	471	80	75	5.2	5.0	90	85
W_6	8.2	8.2	496	529	82	80	1.4	1.2	92	92
W_7	8.3	8.0	246	1,030	190	180	1.1	1.0	70	70
W_8	8.3	8.3	505	530	95	90	4.3	4.2	30	28
W_9	8.3	8.0	538	555	98	95	3.8	3.6	62	60
W_{10}	8.4	8.2	596	637	110	100	3.3	3.0	45	40
W_{11}	7.2	7.0	662	695	120	110	4.2	4.0	48	45
W_{12}	7.0	7.0	728	787	130	120	4.6	4.4	56	50
W_{13}	8.0	7.6	630	696	134	128	3.3	3.0	70	68
W_{14}	8.3	8.3	621	754	220	130	3.5	3.2	72	70
W_{15}	8.4	8.4	637	736	210	210	3.8	3.6	56	54
W_{16}	8.5	8.5	494	703	190	200	2.2	2.0	48	40
W_{17}	8.6	8.4	478	536	94	190	1.9	2.0	98	95
W_{18}	7.9	7.2	490	462	96	90	1.6	1.6	78	70
W_{19}	8.2	8.0	596	471	110	90	2.2	2.0	65	65
W_{20}	8.3	8.3	530	580	124	100	1.8	1.8	60	60
W_{21}	8.0	8.2	539	534	128	120	3.4	3.2	20	78
W_{22}	8.6	8.6	580	564	330	110	3.6	3.4	70	70
W_{23}	7.5	7.2	639	622	410	320	3.0	3.0	100	95
W_{24}	7.6	7.5	540	623	210	400	2.8	2.8	46	45
W_{25}	8.2	7.6	398	456	180	150	2.4	2.2	56	50
W_{26}	8.6	8.2	480	514	170	160	2.8	2.6	90	85
W_{27}	8.0	8.4	539	584	130	120	2.1	2.0	97	90
W_{28}	7.6	8.0	621	655	170	150	3.5	3.4	88	85
W_{29}	8.0	7.2	605	638	178	170	2.2	2.0	70	70
W_{30}	8.2	7.8	704	696	180	140	2.8	2.6	66	65
W_{31}	8.3	8.0	721	741	210	200	7.1	7.0	20	20
W_{32}	8.0	8.0	537	562	220	210	4.4	4.2	68	65
W_{33}	7.4	7.2	562	595	240	230	2.7	2.6	49	45
W_{34}	7.6	7.4	528	557	160	150	2.6	2.5	56	50
W_{35}	7.2	7.6	478	503	72	70	3.4	3.2	70	68
W_{36}	8.0	7.8	548	561	240	220	4.3	4.3	77	70
W_{37}	8.2	8.0	594	619	260	250	4.6	4.5	56	50
W_{38}	8.6	8.2	628	665	270	260	5.2	5.0	72	70
W_{39}	8.3	8.6	648	694	290	270	4.6	4.4	54	52
W_{40}	8.0	8.3	744	827	360	350	4.3	4.3	80	75
W_{41}	8.2	7.8	835	902	310	300	3.6	3.6	80	75

(continued)

Table 1 (continued)

S. No	pH		TH (mg/l)		Cl^- (mg/l)		F^- (mg/l)		NO_3^- (mg/l)	
	Sept. 09	April 10	Sept. 09	April 10	Sept. 09	April 10	Sept. 09	April 10	Sept. 09	April 10
W_{42}	7.6	8.0	910	1,000	280	270	3.8	3.8	63	60
W_{43}	7.8	7.6	926	1,017	210	200	3.7	3.5	33	30
W_{44}	7.6	7.8	969	964	220	200	4.5	4.4	35	35
W_{45}	8.0	7.6	1,067	1,133	320	300	3.7	3.7	32	30
W_{46}	8.2	8.0	1,124	1,219	410	400	3.8	3.8	90	85
W_{47}	8.3	8.2	1,240	1,306	378	370	4.0	3.8	100	90
W_{48}	8.5	8.3	1,322	1,413	480	460	4.2	4.0	110	95
W_{49}	8.0	8.0	1,333	1,898	450	290	4.5	4.2	90	100
W_{50}	8.2	7.8	1,474	1,479	380	300	4.0	4.5	78	90
Min	7.0	7.0	246	413	72	70	1.1	1	20	20
Max	8.6	8.6	1,474	1,898	480	460	7.1	7.0	110	100
Mean	8.0	7.86	676.4	744.7	211.9	195.3	3.53	3.4	65.94	64.14
S.D	0.40	0.44	256.8	295.6	102.8	94.8	1.12	1.12	21.02	19.75

fluoride dissolution activity (Saxena and Ahmed 2001). However, during April 2010 it ranges from 7 to 8.6 with an average value of 7.84. This shows that the ground water of the study area is mainly alkaline in nature. The total hardness values range from 246 to 1,474 mg/l during September 2009 and 413 to 1,898 mg/l during April 2010; around 80 % of the samples were found to be very hard in nature. The high value of total hardness in supply water may cause corrosion of pipes, resulting in the pressure of certain heavy metals such as cadmium, copper, lead and zinc in drinking water. Chlorides ranged between 72 and 480 mg/l for September 2009 and 70–460 mg/l during April 2010, respectively. The fluoride values range from 1.1 to 7.1 mg/l during September 2009 and 1 to 7.0 mg/l during April 2010. Nitrate (NO_3^-) in the ground water varies from 20 to 110 mg/l during September 2009 and 20 to 100 mg/l during April 2010.

The analytical results of physical and chemical parameters of ground water were compared with the standard guideline values as prescribed by the World Health Organization (WHO 1983) and Indian Standards Institute (ISI 1983) for drinking and public health purposes (Table 2). The table shows the most desirable limits of various parameters and found that all the parameters analyzed were above the desirable limits of both the standards.

Impact of Fluoride on Human Health

Dental Fluorosis

Generally, present ingestion of ground water having a fluoride concentration above 1.5–2.0 mg/l may lead to dental mottling, an early sign of dental fluorosis which is characterized by opaque white patches on teeth. In advanced stages of dental

Table 2 A comparison of drinking water quality parameters of the study area with WHO and Indian Standards

Parameters	WHO international standard (1983)	Indian standards for drinking water specification	Mean value of parameters under analysis	
			Sept. 09	April 10
pH	7.0–8.5	6.5–8.5	8.0	7.8
TH (mg/l)	100	300	676.4	744.7
Cl^- (mg/l)	200	250	211.9	195.3
F^- (mg/l)	1.5	1.5	3.53	3.40
NO_3^- (mg/l)	45	45	65.94	64.14

Fig. 4 Dental fluorosis from Bapanakunta village of Anantapur district

fluorosis, teeth display brown to black staining followed by pitting of teeth surfaces. Dental fluorosis produced considerable added dental costs (tooth deterioration) and significant physiological stress for affected population. Dental fluorosis is endemic in 14 states and 150,000 villages in India. The problems are most pronounced in the states of A.P., Bihar, Gujarat, M.P., Punjab, Rajasthan, Tamil Nadu and Uttar Pradesh (Pillai and Stanley 2002).

The main source of drinking water are dug wells and hand pumps in Mudigubba mandal of Anantapur district. Major health problem in this village is because of high profile of natural fluoride concentration in ground water. High fluoride level in drinking water causes dental decay and physiological deformations. Manifestation of dental fluorosis in Bapanakunta village of the Mudigubba mandal is shown in Fig. 4.

Skeletal Fluorosis

Skeletal fluorosis may occur when fluoride concentrations in drinking water exceeds 4–8 mg/l, which leads to increase in bone density, calcification of ligaments, rheumatic or arthritic pain in joints and muscles along with stiffness and rigidity of the joints, bending of the vertebral column and excessive bone formation or osteosclerosis, a basic symptom of skeletal fluorosis (Teotia and Teotia 1988); while excess F^- may include hypocalcaemia (Sherlin and Verma 2000; Pius et al. 1999; Ekambaram and

Fig. 5 Skeletal fluorosis from Ralla Anantapuram village of Anantapur district

Vanaja 2001). Crippling skeletal fluorosis can occur when a water supply contains more than 10 mg/l (WHO 1984; Boyle and Chagnon 1995). Figure 5 shows the skeletal fluorosis from Ralla Anantapuram village of Mudigubba mandal where the fluoride concentration is 4.6 mg/l. Ralla Anantapuram, Mallepalli, Pathabathalapalli, Dorigallu and Yerravankapalli villages are having fluoride concentration more than 4.0 mg/l limit while samples from five other locations have fluoride less than even 1 mg/l. This low fluoride may be used safely as the fluoride traces are useful for healthy growth of teeth and bones. A concentration less than 0.8 mg/l results in 'dental caries'. Other samples have fluoride well within the lower and upper limits recommended and therefore potable. Due to the higher fluoride level in drinking water several cases of dental and skeletal fluorosis have appeared at alarming rate in this region.

Spatial Analysis of Groundwater Quality

The GIS based analysis of spatiotemporal behaviour of the groundwater quality in the study area was done by using the spatial analyst module of Arc GIS 9.3. Powerful spatial analysis is feasible once the database is established. The interpolation technique used in the analysis is inverse distance weighted (IDW) method. The IDW is an algorithm for spatially interpolating or estimating values between measurements. Each value estimated in an IDW interpolation is a weighted average of the surrounding sample points. The weights are computed by taking inverse of the distance

from an observations location to the location of the point being estimated (Burrough and Mc Donnell 1998). The inverse distance can be raised to a power (e.g. linear, squared and cubed) to model different geometries (e.g. line, area, volume) (Guan et al. 1999). In a comparison of several different deterministic interpolation procedures, Burrough and Mc Donnell (1998) and Mathes and Rasmussen (2006) found that using IDW with a squared distance term yielded results most consistent with

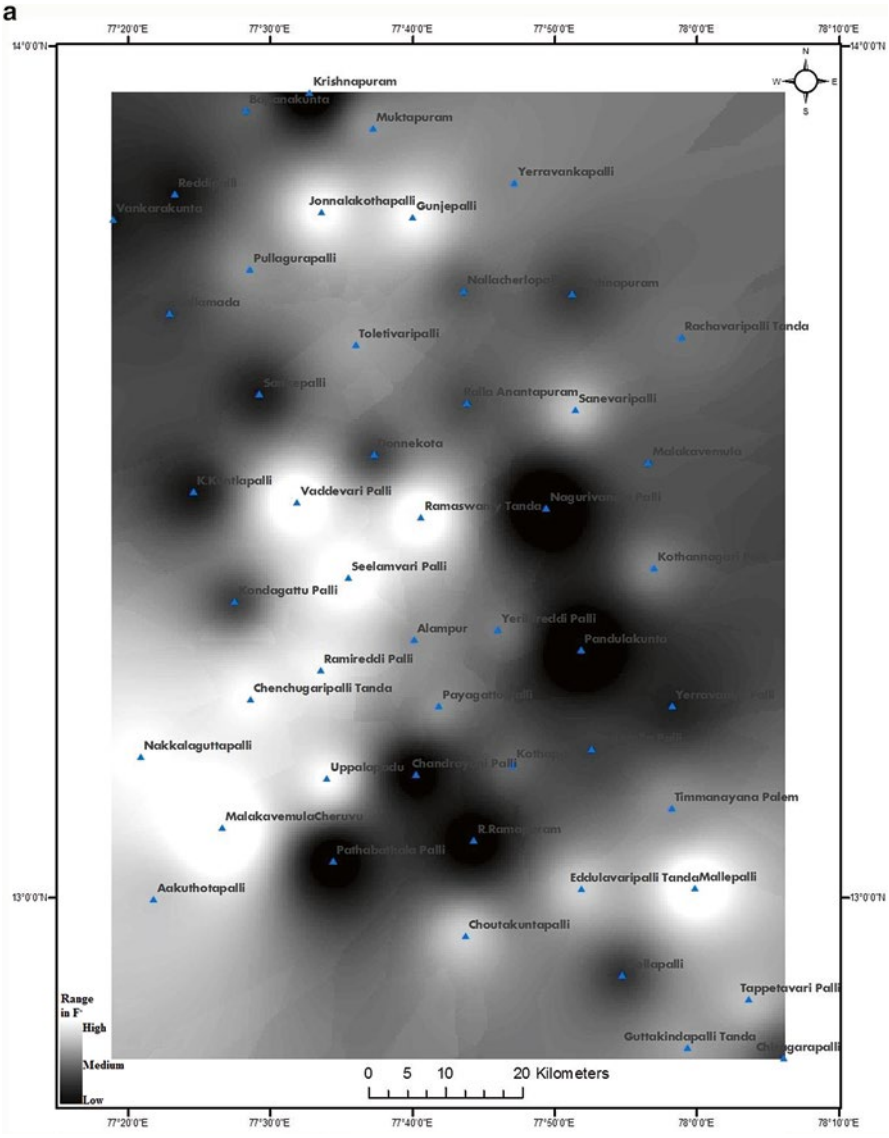

Fig. 6 Maps (**a**, **b**) showing the variations in spatiotemporal distribution of F^- in the study area

original input data. This method is suitable for datasets where the maximum and minimum values in the interpolated surface commonly occur at sample points (ESRI 2002). The spatial pattern of parameters was analyzed in two seasons, i.e. pre-monsoon (April 2010) and post-monsoon seasons (September 2009). Spatial distribution of the fluoride is shown in Fig. 6.

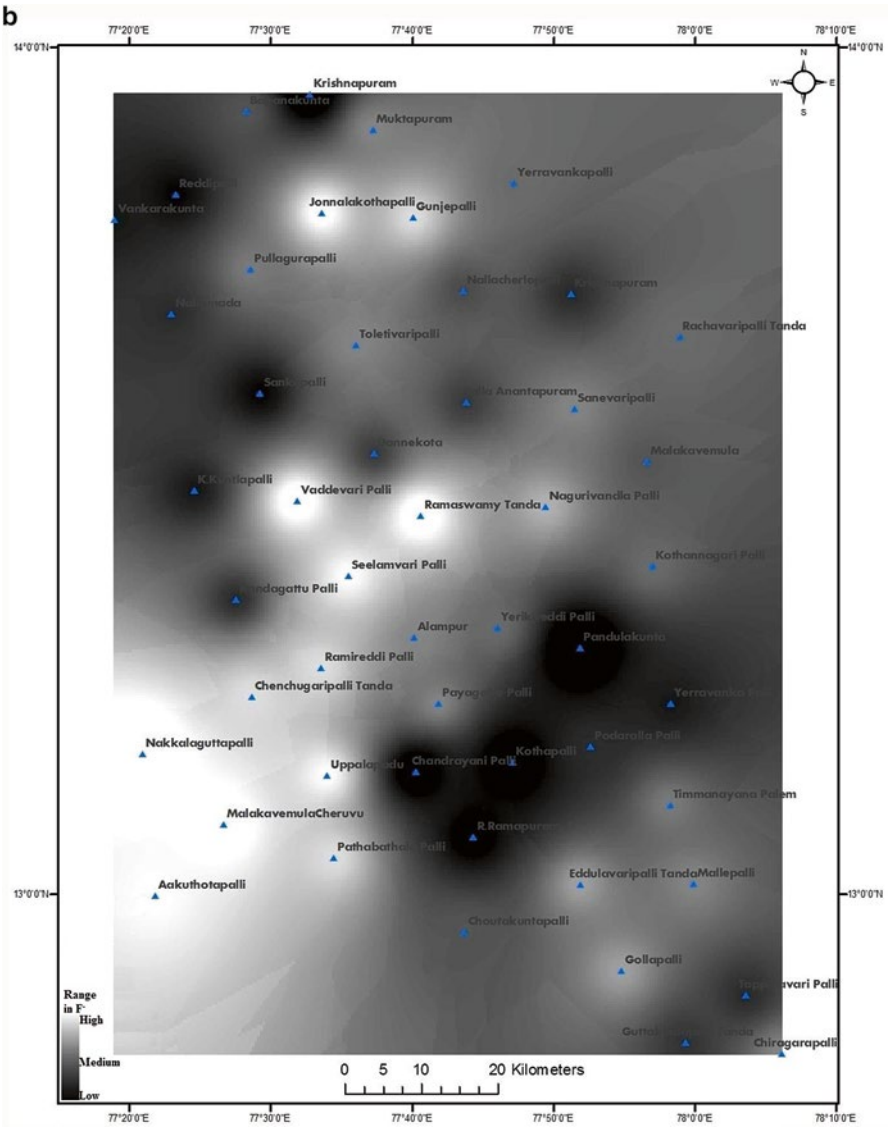

Fig. 6 (continued)

Conclusions

The Anantapur district of Andhra Pradesh state in India is a typical region showing endemic fluorosis caused by drinking water. Ground water (wells, hand pumps and tube wells) is the main source of drinking water for village residents. The geological formation is found to be the main source for the fluoride concentration in most of the sampling points. The present study suggests that alkaline environment is the dominant controlling factor for leaching of fluoride from the source material in the ground water. The chemical analysis of water samples from the study area do not comply with the water quality standards. The chemical compositions of the water samples reveal slight seasonal variations. The ground water in the study area is alkaline in nature. All the other parameters analysed such as pH, total hardness (TH), chloride (Cl^-), nitrate (NO_3^-) and fluoride (F^-) are above the desirable limits of WHO and Indian Standards for drinking water. Hence, the ground water in the study area is not suitable for drinking purpose. The post-monsoon groundwater samples show maximum deviation, as this is the time when precipitation is less so that the concentration of ions will increase considerably. The spatial highs of pH are showing a clear alignment in pre-monsoon season but in post-monsoon season it shows an eastward shift with a spatial maximum in the northwestern side. The spatial distributions of chloride (Cl^-) highs are very prominent in post-monsoon season when compared to pre-monsoon season. However, in the case of NO_3^- and F^-, the spatial highs show a spread in post-monsoon season and during pre-monsoon season the isolated patches of highs are distributed in the study area. Several reports on dental and skeletal manifestations of fluorosis were also reported in the study area, which shows that the population of the study area is at higher risk due to excessive fluoride intake. The worst fluoride affected villages in Mudigubba mandal are: Ralla Anantapuram, Bapanakunta, Gunjepalli, Muktapuram, Yerikareddipalli; Nallamada mandal: Nallamada, Toletivaripalli, Malakavemula, Yerravankapalli, Patha Bathalapalli, R. Ramapuram; Kadiri mandal: Alampur, Kutagulla and Nagurivandlapalli. Most of the people in these villages suffer from dental and skeletal fluorosis such as mottling of teeth, deformation of ligaments, bending of spinal column and ageing problem.

Acknowledgements The work was funded by the Department of Science and Technology (DST), New Delhi under the Fast track Young Scientist scheme (Project no: SR/FTP/ES-50/2007). One of the authors Dr. V. Sunitha is grateful to the DST for providing the financial assistance in the form of fast track Young Scientist Project.

References

Ahmed S, Bertrand F, Saxena V, Subramaniyam K, Touchard F (2002) A geostatistical method of determining priority of measurement wells in a fluoride monitoring network in an aquifer. J Appl Geochem 4(2B):576–585

American Public Health Association (APHA) (1995) Standard methods for the examination of water and wastewater. 19th Edition of American Public Health Association, Washington
Apambire WB, Boyle DR, Michel FA (1997) Geochemistry, genesis, and health implications of fluoriferous groundwater in the upper regions of Ghana. Environ Geol 33(1):13–24
Boyle DR, Chagnon M (1995) An incident of skeletal fluorosis associated with ground waters of the maritime carboniferous basin, Gaspe region, Quebec, Canada. Environ Geochem Health 17:5–12
Burrough PA, Mc Donnell RA (1998) Principles of Geographical Information Systems. Oxford University Press, Oxford
Chae GY, Seong TM, Bernhard K, Kyoung-Ho K, Seong-Young K (2007) Fluorine geochemistry in bedrock groundwater of South Korea. Sci Total Environ 385(1–3):272–283
Chandra S, Thergaonkar VP, Sharma R (1981) Water quality and dental fluorosis. Indian J Public Health 25:47–51
Deshmukh AN, Valadaskar PM, Malpe DB (1995) Fluoride in environment: a review. Gondwana Geol Mag 9:1–20
Edmunds M, Smedley P (2005) Fluoride in natural waters. In: Selnius O, Alloway B, Centeno JA, Finkleman RB, Fuge R, Lindh U (eds) Essentials of medical geology—impacts of the natural environment on public health. Academic, Amsterdam
Ekambaram P, Vanaja P (2001) Calcium preventing locomotor behavioral and dental toxicities of fluoride by decreasing serum fluoride levels in rats. Environ Toxicol Pharmacol 9:141–146
Environmental Systems Research Institute (ESRI) (2002) Using Arc GIS spatial analyst. ESRI Press, Redlands
Guan W, Chamberlain RH, Sabol BM, Doering PH (1999) Mapping submerged aquatic vegetation in the Caloosahatchee Estuary: evaluation of different interpolation methods. Mar Geol 22:69–91
Handa BK (1975a) Geochemistry and genesis of fluoride containing groundwater in India. Groundwater 13:275–281
Handa BK (1975b) Natural waters, their chemistry pollution and treatment with a chapter on the use of saline water, CGWB technical report 2 (unpublished)
Indian Standards Institution (ISI) (1983) Indian standard for drinking water IS: 10500
Largent EJ (1961) The health aspects of fluoride compound. Ohio State University Press, Columbus
Mamatha P, Sudhakar Rao M (2010) Geochemistry of fluoride rich groundwater in Kolar and Tumkur Districts of Karnataka. Environ Earth Sci 61:131–142
Mathes ES, Rasmussen TC (2006) Combining multivariate statistical analysis with Geographic Information Systems mapping: a tool for delineating groundwater contamination. Hydrogeol J. doi:10.1007/S10040-006-0041-4
Pillai KS, Stanley VA (2002) Implications of fluoride—an endless uncertainty. J Environ Biol 23:81–87
Pius A, Appa Rao BV, Karthikeyan G (1999) Role of calcium in the amelioration of fluorosis: a case study. Indian J Environ Health 41:121–125
Raju NJ, Dey S, Das K (2009) Fluoride contamination in groundwater of Sonbhadra District, Uttar Pradesh, India. Curr Sci 96(7):979–985
Raju NJ, Dey S, Gossel W, Wycisk P (2012) Fluoride hazardous and assessment of groundwater quality in the semi-arid upper Panda river basin, Sonbhadra District, Uttar Pradesh, India. Hydrol Sci J 57(7):1433–1452
Rama Rao NV (1982) Geochemical factors influencing the distribution of fluoride in rocks, soils and water sources of Nalgonda District, A.P. Unpublished Ph.D. thesis, Osmania University, Hyderabad
Saxena VK, Ahmed S (2001) Dissolution of fluoride in groundwater: a water-rock interaction study. Environ Geol 40:1084–1087
Saxena VK, Ahmed S (2002) Inferring the chemical parameter for the dissolution of fluoride in groundwater. Environ Geol 25:475–481
Sherlin DMG, Verma RJ (2000) Amelioration of fluoride induced hypocalcaemia by vitamins. Hum Exp Toxicol 19:632–634

Subba Rao N (2003) Groundwater quality: focus on fluoride concentration in rural parts of Guntur district, Andhra Pradesh. Hydrol Sci J 48:835–847

Teotia SPS, Teotia M (1988) Endemic skeletal fluorosis clinical and radiological variants. Fluoride 21:39–44

Todd DK (1980) Groundwater hydrology, 2nd edn. Wiley International Editions, Wiley, New York

United Nations Children's Emergency Fund (UNICEF), United Nations Children's Fund (2008) UNICEF handbook on water quality. United Nations Children's Fund, New York

World Health Organization (WHO) (1983) International standards for drinking water. World Health Organization, Geneva

World Health Organization (WHO) (1984) The guidelines for drinking water quality recommendations. World Health Organization, Geneva

Identification of Surface Water Harvesting Sites for Water Stressed Area Using GIS: A Case Study of Ausgram Block, Burdwan District, West Bengal, India

C. Prakasam

Introduction

Water is the most vital element for survival on earth. It has become one of the emerging environmental issues our ecosystems are facing today. Issues of water quantity, quality and availability are the three major concerns and are vital to the quality of life on earth. It is one of the most essential resources in our day-to-day life. It is depleting fast in rural as well as urban areas mainly because of increase in agricultural and domestic demands (Kumar et al. 2008). In water resources planning, ground water is attracting an ever-increasing interest due to scarcity of good quality subsurface water and growing need of water for domestic, agricultural and industrial uses. In a densely populated country like India, groundwater resource is in high demand. In undulating terrains, availability of water resource is of limited extent. Efficient management and planning of water resources in these areas are of utmost importance.

Surface water is naturally replenished by precipitation and naturally lost through discharge to the oceans, evaporation, evapo-transpiration and subsurface seepage. Although the only natural input to any surface water system is precipitation within its watershed, the total quantity of water in that system at any given time is also dependent on many other factors. Human activities can have a large and sometimes devastating impact on these factors. Humans often increase storage capacity by constructing reservoirs and decrease it by draining wetlands. Natural surface water can be augmented by importing surface water from another watershed through a canal or pipeline. Availability of water plays very important role in deciding the nature and extent of land use land cover (LULC) of any region. LULC—the assemblage of biotic and abiotic components and their modification for beneficial output—is one

C. Prakasam (✉)
School of Civil Engineering, Chitkara University, Solan, Himachal Pradesh 174103, India
e-mail: cprakasam@gmail.com

© Capital Publishing Company 2015

N.J. Raju et al. (eds.), *Management of Natural Resources in a Changing Environment*, DOI 10.1007/978-3-319-12559-6_5

of the most crucial properties of the earth's system. At present, the LULC are severely being affected due to depletion of much needed water.

Since time immemorial, farmers in dry areas harvested surface water for irrigation. Water harvesting is here defined as the collection of surface runoff mainly for agricultural and domestic purposes. Present days watershed approach has been adopted to collect water from precipitation. It is a resource region where the eco-system is closely interconnected with basic resource water. A watershed or river basin is considered as an ideal water management unit (Prinz 1995, 1996) but present surface water harvesting study is made through administrative approach.

Mainly for agriculture purpose, surface water resource (pond, lake, canal, river) is very essential. Present study area (Ausgram block) is basically a good agriculture region in Burdwan district but due to water stressed problem cultivation is not successful every year. In Ausgram block, surface water bodies are present but water is not available many months in a year. Due to this problem farmers are not able to cultivate the crops more than one in a year, because of water stress. This region landform or physical landscape is the main controlling factor of surface water resource, because of undulating surface topography. This regional surface water harvesting is needed mainly for agriculture purpose. Present surface water harvesting study is made through the geomorphic resources i.e., Ruggedness Index (RI), Relative Relief (RR), Drainage Density (DD), Slope and Frequency of Surface Water Bodies (FSWB). These analyses have been done from Survey of India topographical maps and satellite imagery 1 km^2 grid-wise using GIS techniques. For delineating the surface water potential zones, Geographical Information System (GIS) has been found to be an effective tool. In recent years, use of satellite remote sensing data along with GIS, topographical maps, collateral information and limited field checks have made it easier to establish the base line information on surface water prospective zones.

The world's usable freshwater supply is being depleted because of increasing water use associated with population growth, industrial and agricultural usage. Agriculture is the largest consumer of water, constituting an average 80 % of water consumption in developing countries (Gately 1995). Rice is one of the major grain crops that is grown primarily as a human food source. More efficient use of water in rice production is critical in view of projected increase in rice production needed to meet a growing world population (65 % increase during 1992–2020) (International Rice Research Institute [IRRI] 1993). Approximately 50 % of the freshwater used in Asian agriculture is used for rice production (IRRI 2002).

West Bengal is endowed with 7.5 % of the water resource of the country and that is becoming increasingly scarce with the uncontrolled growth of population, expansion of irrigation network and developmental needs (Rudra 2012). The Bengal Delta, which was described as areas of excess water in the colonial document, now suffers from acute dearth of water during lean months. The spatial and temporal variability of rain within the state causes the twin menaces of flood and drought. Both the flood and drought isopleths are expanding with time in spite of ever-increasing investment in water management. The navigation even in the southern tidal regime has become an extremely difficult task for the country boats that require minimum draft (Rudra 2012). Burdwan district generally have lots of surface water body. It is the main source of agriculture specifically for paddy cultivation but some parts of Burdwan

district are affected by the water stressed problem due to the undulating topography and seasonal rainfall. Ausgram blocks I & II are agricultural (paddy) potential zones in Burdwan district, West Bengal. Recent agriculture researches suggest that water demand in rice fields can be substantially reduced through implementation of new management techniques (Tuong et al. 2005).

Water harvesting involves the storage of runoff and rainwater, so that it can be channelled onto targeted land areas when needed, thereby improving agricultural cultivation. The potential of surface water harvesting is a function of geomorphology, rainfall frequency and cropping potential. Maps, based on Geographical Information Systems (GIS) and models, can give a clear idea of the areas where the surface water can be effectively harvested at the community level.

In all past studies, geomorphic analysis of the concerned drainage basin was the key aspect for the study. In almost all the cases the unit of study was river basin but seldom the drainage basin confined within the administrative region and hence it becomes difficult for the administrators for implementation of the developmental plans. Present geomorphic analyses have been done in an administrative region for identification of the surface water harvesting potential zones. Present surface water harvesting potential study considered Ruggedness Index (RI), Relative Relief (RR), Drainage Density (DD), Slope and Frequency of Surface Water Bodies (FSWB) of Ausgram Blocks I and II of Burdwan district, West Bengal as geomorphic resources. The geomorphic resources have been evaluated and the potentiality of surface water in this administrative region is identified and further suggestions are made for the suitable zones for water storing or harvesting. Existing geomorphic resources and surface water bodies are measured and analysed using Survey of India (SOI) topographical maps. The zones can be used to store excess rainfall for the use in the drier periods. The present study identified and mapped the existing geomorphic and surface water resources to propose surface water harvesting zones in Ausgrm blocks through overlay method using GIS techniques.

Study Area

The study area, Ausgram blocks I and II are located in the central part of Burdwan district. The blocks are surrounded by Birbhum district in the north, Mangalkote and Bhatar blocks, Galsi block and Kanksa blocks of Burdwan district in the west, south and east (Fig. 1). Its geographical area is distributed between 23°21′47″ N–23°37′04″ N latitude and 87°28′57″ E–87°47′07″ E longitude, covering 493 sq. km of area. Total population of the block is 2,43,113 as per Census of India (2001). Agriculture is main economic activity of the region. The altitude varies between 40 and 60 m above MSL. Slope gradually decreases from south west to north east. Its maximum area is covered with clay with caliche concretion, laterite and clay alternating with silts and sand as another extensive soil cover of the region. The blocks experience a climate which is transitional between CWg3 and AW1 types, where ‘C’ stands for ‘warm temperate rainy climates with mild winter’, ‘W’ for ‘dry winter not compensated for by total rain in the rest of the year’, ‘g3’ for ‘eastern

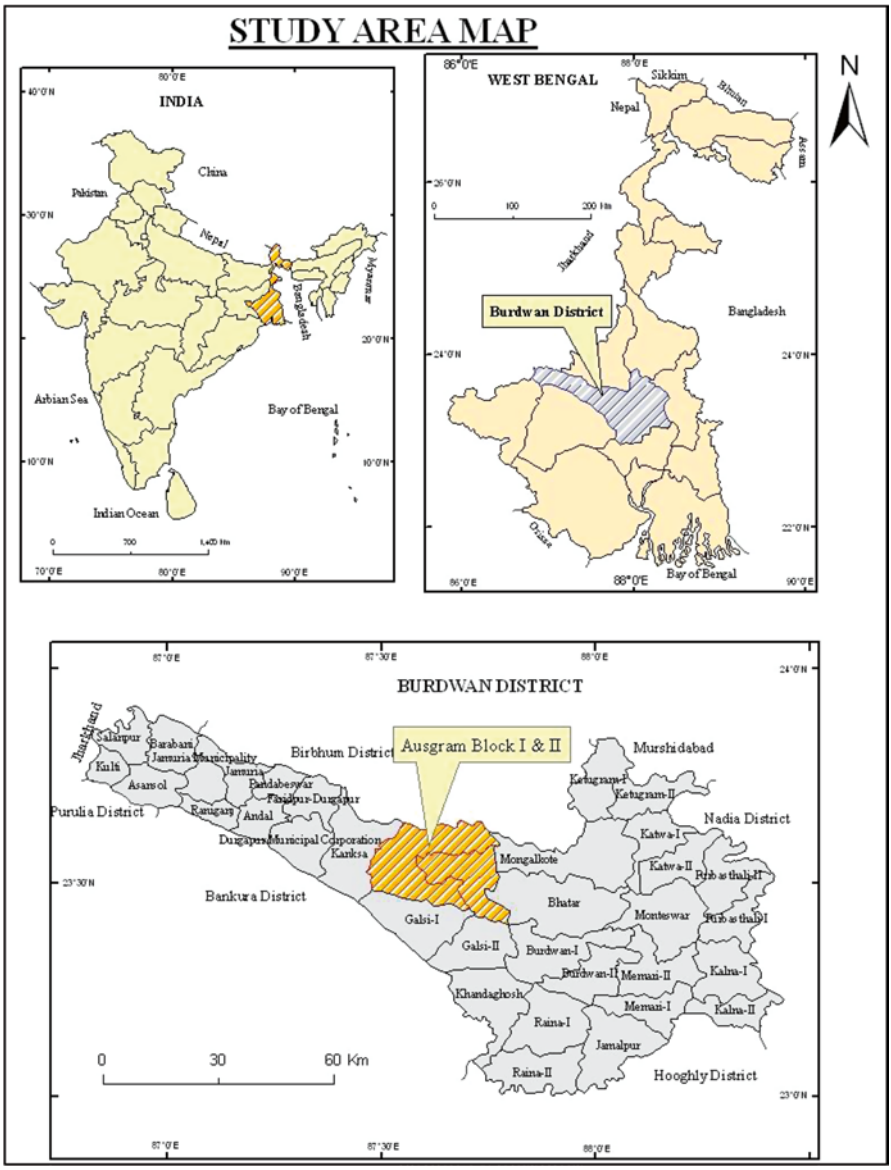

Fig. 1 Study area map

Ganges type of temperature trend' and 'AW1' for 'tropical savanna climates' (http://bardhaman.nic.in/home.htm). Average temperature in hot season is 30 °C while at the cold season is 20 °C and average rainfall is 1,500 mm. The important rivers are Ajoy, Kunur and Khari. The important canals are Durgapur Branch Canal, Damodar Branch Canal and Panagarh Branch Canal.

Methodology

Ausgram blocks I and II are affected by water stress condition due to serenity of surface water; cultivation is done only once in a year in majority of the areas. Present study tried to identify and map the surface water harvesting potential zones using the geomorphic resources. Geomorphic resource layers (Ruggedness Index (RI), Relative Relief (RR), Drainage Density (DD), Slope and Frequency of Surface Water Bodies (FSWB)) were superimposed over each other and the suitable zones identified for surface water harvesting based on methodology described as follows.

Existing geomorphic resource have been evaluated from Survey of India (SOI) topographical maps (73 M/06, 10, 11, 14 and 15; published in 1972) as a base data at 1:50,000 scale. Physical information is extracted from every 1 km^2 grid. Features like contours, spot heights, bench marks, drainage lines and surface water bodies (pond, tank, lake) are taken into consideration for characterisation of the physical resources of the region. These phenomena were measured and analysed to generate information on Ruggedness Index (RI), Relative Relief (RR), Drainage Density (DD), Slope and Frequency of Surface Water Bodies (FSWB). These resources are directly or indirectly controlling and influencing the availability of surface water resources which in turn dictate the land use land cover, water stressed situation and agriculture resources in Ausgram blocks I and II.

The basic methodologies to identify the surface water harvesting potential zones are as follow:

1. Minimum Ruggedness Index + Minimum Relative Relief + Maximum Drainage Density + Maximum Frequency of Surface Water bodies + Minimum Slope = *Maximum Surface Water Harvesting Potential Zone*.
2. Moderate Ruggedness Index + Moderate Relative Relief + Moderate Drainage Density + Moderate Frequency of Surface Water bodies + Moderate Slope = *Moderate Surface Water Harvesting Potential Zone*.
3. Maximum Ruggedness Index + Maximum Relative Relief + Minimum Drainage Density + Minimum Frequency of Surface Water bodies + Maximum Slope = *Minimum Surface Water Harvesting Potential Zone*.

With the help of the above mentioned methodology and Table 1, surface water harvesting potential zones have been identified and classified in three categories. GIS tool has been used to prepare the different thematic layers and surface water harvesting potential zone map through overlay analysis method.

Result and Discussion

Evaluation of the existing geomorphic resources is the fundamental key to understand the surface forms and process. Geomorphic resources are the natural phenomena on the earth's surface, which have originated due to the active geomorphic processes. The resources directly or indirectly control various

Table 1 Identification of the surface water harvesting potential zones

Sl. No	Geomorphic resources	Value	Zones
1	Minimum Ruggedness Index	<0.0078 RI/km^2	**Maximum** Surface water harvesting potential zone
	Minimum Relative Relief	<3.00 m/km^2	
	Maximum Drainage Density	3.00 km length of river/km^2	
	Minimum Slope	<20.00′	
	Maximum Frequency of Surface Water Bodies	>15/km^2	
2	Moderate Ruggedness Index	0.0078–0.0157 RI/km^2	**Moderate** Surface water harvesting potential zone
	Moderate Relative Relief	3.00–6.00 m/km^2	
	Moderate Drainage Density	2.00–3.00 km length of river/km^2	
	Moderate Slope	20.00–30.00′	
	Moderate Frequency of Surface Water Bodies	10–15/km^2	
3	Maximum Ruggedness Index	>0.0157 RI/km^2	**Minimum** Surface water harvesting potential zone
	Maximum Relative Relief	>6 m/km^2	
	Minimum Drainage Density	<1.00 km length of river/km^2	
	Maximum Slope	>30.00′	
	Minimum Frequency of Surface Water Bodies	<10/km^2	

Source: Author's calculation

anthropogenic activities to a great extent. Study and analysis of geomorphic resources are very much essential to understand the availability of natural resources which in turn influence the probability of economic and social development of the region as well. Ruggedness Index (RI), Relative Relief (RR), Drainage Density (DD), Slope and Frequency of Surface Water Bodies (FSWB) are considered very important indicators and they are used to evaluate geomorphic parameters, because these are all controlling the surface water resource in present study area. Evaluations of these resources are considered essential for implementation of any type of regional and economic planning, especially for water resource planning and management.

Geomorphic Resources

Geomorphic resources are measured and analysed using Survey of India (SOI) topographical maps. One square kilometre grids are generated and grid-wise information are measured and collected for analysis. The geomorphic resources are controlling the surface water bodies and present land use land cover of Ausgram blocks I and II; in the present paper surface water harvesting potential zones are identified and proposed based on the geomorphic resources through GIS tool. It is very essential for Ausgram blocks I and II, for controlling the water stressed conditions. As a result farmers can do good crop cultivation at least two times in a year.

Ruggedness Index (RI)

Ruggedness Index describes the complexity of the topography and the roughness of the terrain. The ruggedness indicates the degree of dissection of a region where drainage has also been taken as an important parameter. Chorley (1962) has devised the formula of ruggedness index as:

$$Ruggedness\,\text{Index} = \frac{Relative\,\text{Relief}\,(\text{M}) \times \text{Drainge density}\left(\text{km}/\text{km}^2\right)}{1{,}000}$$

This index is being widely used by the earth scientists in connection with the morphological studies of terrain and it leads to better understanding of the surface configuration evolved under complex geomorphic processes. Actually, it is more than development of slope or dissection index as it incorporates a number of determinant factors related to the development of landforms. This index reflects the combined effects of evolutionary rhythmic processes in the development of relief (Mukhopadhyay 1984).

Roughness index follows the same trend and indicates a close relationship with other morphometric attributes like relative relief, slope and dissection index (Mukhopadhyay 1973, 1979).

Ruggedness index value has been generated using 1 km^2 grid like other morphometric parameters and isolines are drawn for the whole region. Ruggedness index of the study area is divided into three categories with the help of isolines. The zones are <0.0078, 0.0078–0.0157 and >0.0157. Minimum ruggedness value is distributed over maximum study area and it covers 99 % of the total area. 0.0078–0.0157 ruggedness value is distributed over the central west and central part of study area and it covers 0.52 % of total area. More than 0.0157 ruggedness index value is distributed over central part of the study area and it covers 0.33 % area of land only (Fig. 2). With the low ruggedness index value, minimum effort is needed to manage surface water which can make the area a good agricultural region.

Relative Relief (RR)

Relative relief is one of the various methods evolved to measure the average slope. The term was invented and used by Smith (1935) to ascertain the amplitude of available relief to relate the altitude of the highest and the lowest points of any particular area. The study of relative relief depicts the relief of an area in relation to the surrounding areas. The relative relief map gives a clear conception of the nature and amount of the slope of the area under study.

$$Relative\,\text{Relief} = \text{Maximum Elevation} - \text{Minimum Elevation}$$

Relative relief is one of the methods to depict the local relief of any part of the earth's surface. The study area is having less drainage development and it

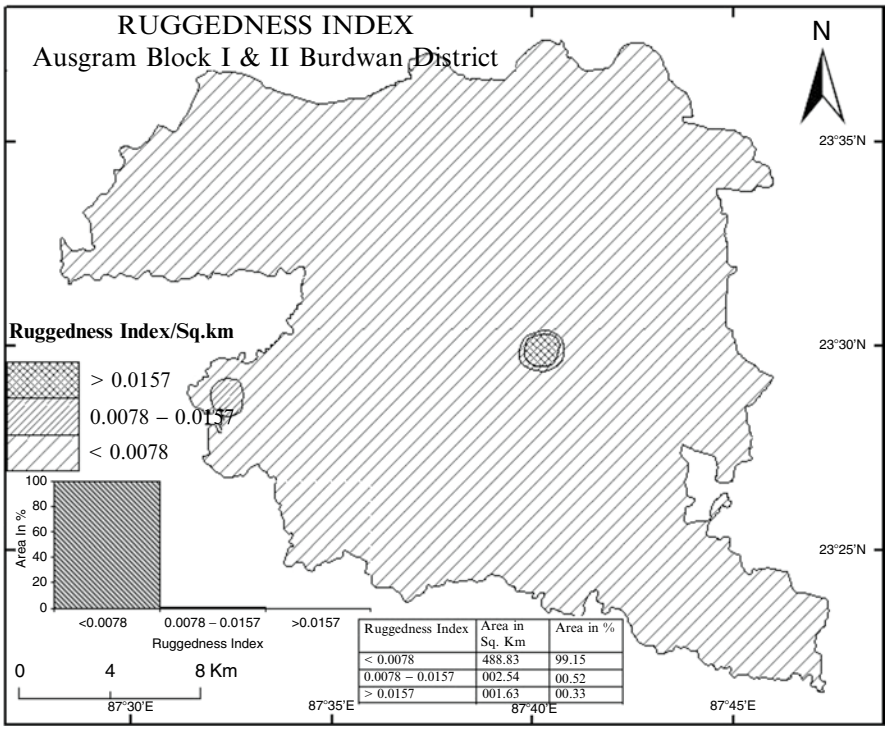

Fig. 2 Ruggedness index map (*Source*: 73 M/10, 11, 14 & 15)

will generate lower relative relief. Highest relative relief is only 11.20 m/km^2 and is found at the west central part of the study area. Relative relief of the study area is classified in four relative relief zones, like <3, 3–6, 6–9 and >9 m/km^2. Around 84 % of the total study area is under <3 m relative relief category. Next category of relative relief zone is 3–6 m/km^2 and it covers 13 % of total area. This zone is distributed over the south central, central, west central, north west and north east parts of study area. The third category of relative relief is 6–9 m/km^2 and it covers about 3 % of area. This zone is distributed in west central, north west central and central parts of study area. Last category is more than 9 m/km^2. It covers less than 1 % (0.42 %) of the area and is located in central part of study area (Fig. 3). The lower relative relief indicates that the region is almost flat land and appearing mature stage of geomorphic evolution. Lower relative relief suggests the availability of water, hence the region can be converted to a very good agricultural region. Although maximum area is covered under <3 m/km^2 relative relief zone but the presence of surface water resources are limited.

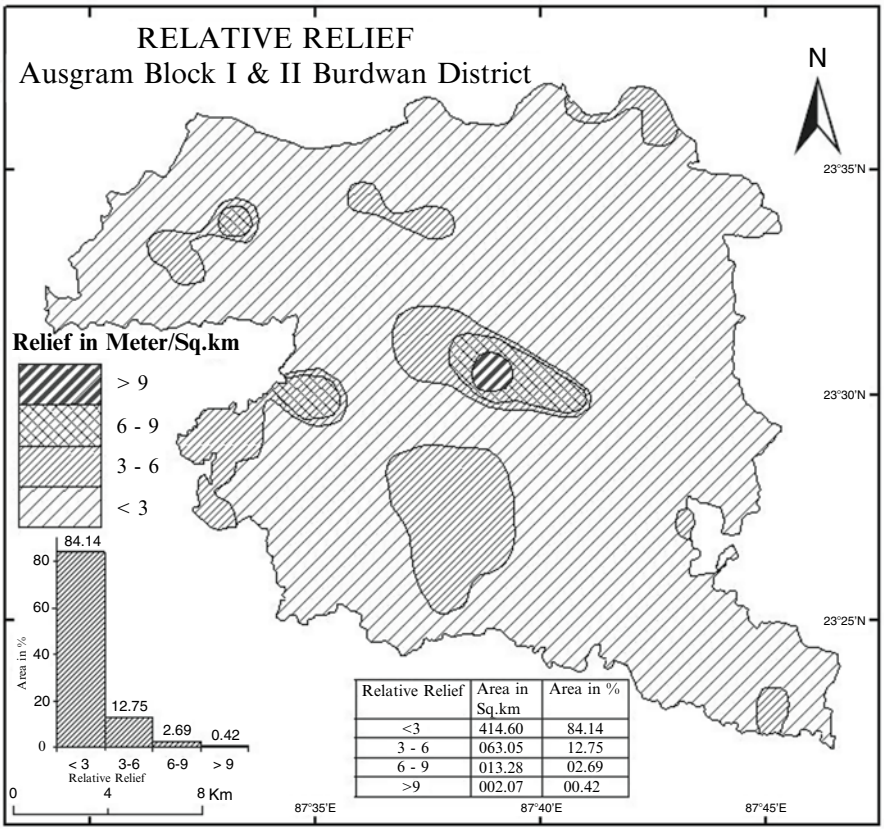

Fig. 3 Relative relief map (*Source*: 73 M/10, 11, 14 & 15)

Drainage Density (DD)

Drainage density is defined as the total length of streams/km^2. Density factor is related to climate, rock type, relief, infiltration capacity, vegetation cover, surface roughness and run-off intensity index. The drainage density explains the stage of fluvial eroded landscape. The importance of drainage density analysis is due to two reasons. Firstly, it reflects the potential rate of discharge of water to be transmitted through the respective region or basin and secondly, it reflects climatic conditions of particular area. The drainage density indicates the closeness of spacing of channels (Horton 1932).

$$Drainage\ \text{density}\left(D\right) = \left(\frac{Lu}{A}\right)$$

where *Lu* is total length of stream channels per unit area (km) and *A* is area of the unit (km^2) (Horton 1932).

Drainage density map of Ausgram blocks I and II have been prepared and analyzed through 1 km^2 grid. The study area is located in relatively drier part of the district Burdwan. The region falls in the water stressed part and it is expected that the region is having very low drainage development.

Again, the region is located in moderately higher relief zone and many first order streams are there. As a result, some parts of the block may have higher drainage density, but in reality it may have no significant contribution towards the availability of water resources. Using isolines ~~of~~ drainage density have divided the whole study area in four categories i.e. <1, 1–2, 2–3 and >3 km length of stream km/km^2. The data reveals that the region is poorly drained and 47 % of the total land has drainage density <1 km/km^2. The other, highest drainage density i.e. >3 km/km^2 covers negligible percentage of land of the study region. Highest drainage density, 3.63 km/km^2 is observed in the central part of the study area (Fig. 4). The central part of the study area is characterized by high land and resulted in the origin of some ephemeral drainage lines. This has resulted in maximum drainage density in this part of the region. But the ground reality shows that the highest drainage density does not add significantly to the availability of water in the region.

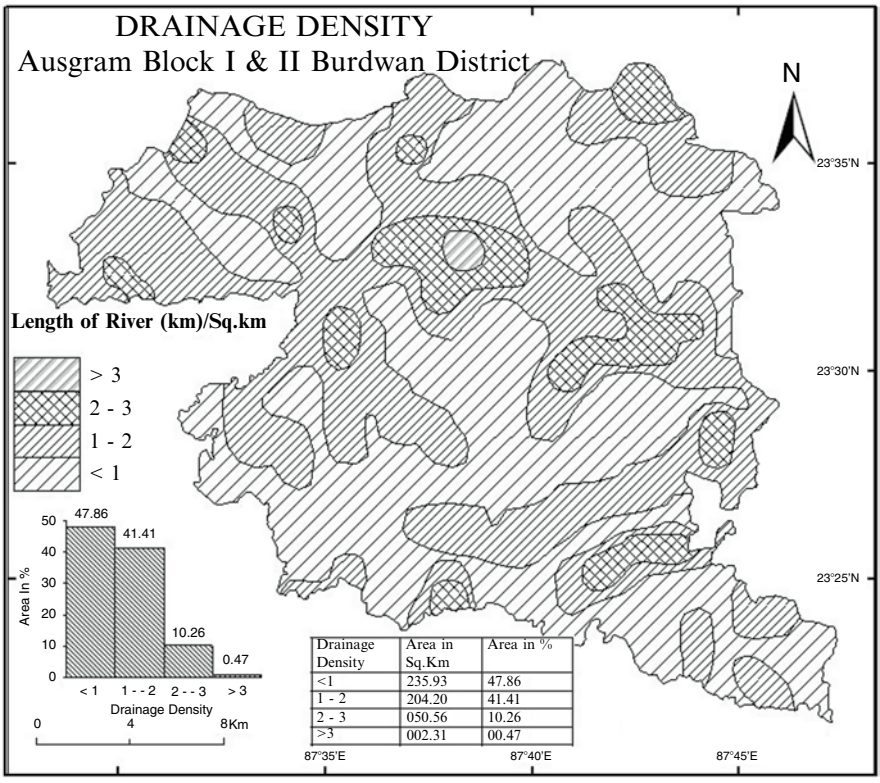

Fig. 4 Drainage density map (*Source*: 73 M/10, 11, 14 & 15)

About 10 % land of the block is having drainage density of 2–3 km/km^2. It has been observed that this portion of the block is having significantly good amount of available surface water resources.

Slope (Raisz and Henry Method)

The term slope in its broadest sense means an element of earth's solid surface, including both terrestrial and submarine surfaces (Strahler 1956). Terrain morphology is characterized by slope condition which is governed by a number of factors including climatic, geologic and tectonic conditions. There is also a close relationship between slope condition and morphometric attributes of terrain i.e. absolute relief, relative relief, dissection index, drainage density and drainage frequency. Slopes are ubiquitous elements of the landscape (King 1962). Slopes are the fundamental types of landscape feature. Slope may be defined as the tangent of the angle of inclination of a line or plane defined by a land surface. It is the result of a complex and continuous interaction between internal and external forces acting upon the earth's surface. It depends on rock and climatic conditions, which may in certain regions be constant over long periods of time and on the thickness, texture and mobility of surface layers of soil, organic matter etc. (Baulig 1959).

In a drainage system, valley side and channel slopes control directly the potential and kinetic energy of water flows and thus the intensity of runoff, erosion and transport processes. These factors tend to be in a state of equilibrium in relation to overall local geographical conditions. The slope angle indicates the magnitude of the component of the gravitational surface acting to produce movement of solid bodies, water or soil particles down a slope (Strahler 1956). Slope also plays an important role in river processes. Neither the formation of runoff, the movement of floods, the power potential of river courses, the modelling and evolution of river channels, nor the erosion and transport processes occurring in the latter can be approached without knowing the slopes of the land surface and river network (Zavoianu 1985).

$$Slope\left(\text{Raisz and Henry method}\right)=\tan\theta=\frac{Vertical}{Base}$$

An understanding of slope distribution is essential, as a slope map provides data for planning, settlement, mechanization of agriculture, reforestation, engineering structures, conservation practices etc. Though various methods are used to carry out the slope analysis, Raisz and Henry (Monkhouse and Wilkinson 1994) slope analysis method have been used in the study region. Raisz and Henry have divided the large scale topographical map into small region, within each of which the contour lines have the same standard spacing.

According to Raisz and Henry method present study area is divided into five slope category zones i.e. <10′, 10′-20′, 20′-30′, 30′-1° and >1°. In this study area maximum slope is found in the south west central part and minimum slope is found in the north east and south east parts. First category, <10′ slope is distributed in north east and south east parts of study area. It covers 28 % of the total area. Second category 10′-20′ slope zone is distributed in south and north parts of the study area and covers maximum area, about 52 % of the total area. Third category, 20′-30′ slope zone is distributed in central, central east and west parts of the study area. It covers 13 % of land of the total study area. Fourth category zone, 30′-1° is distributed in west central and north central parts of study area. It covers 5 % of the land area. Last category, more than 1° slope zone, is distributed in south west central and north west central parts of the study area. It covers 1 % of land. Generally slope is from west to east and from south west to north east direction (Fig. 5).

This slope is controlling the nature and distribution of surface water resources. Where the slope is <30′ in the Ausgram block, those parts have lots of surface water

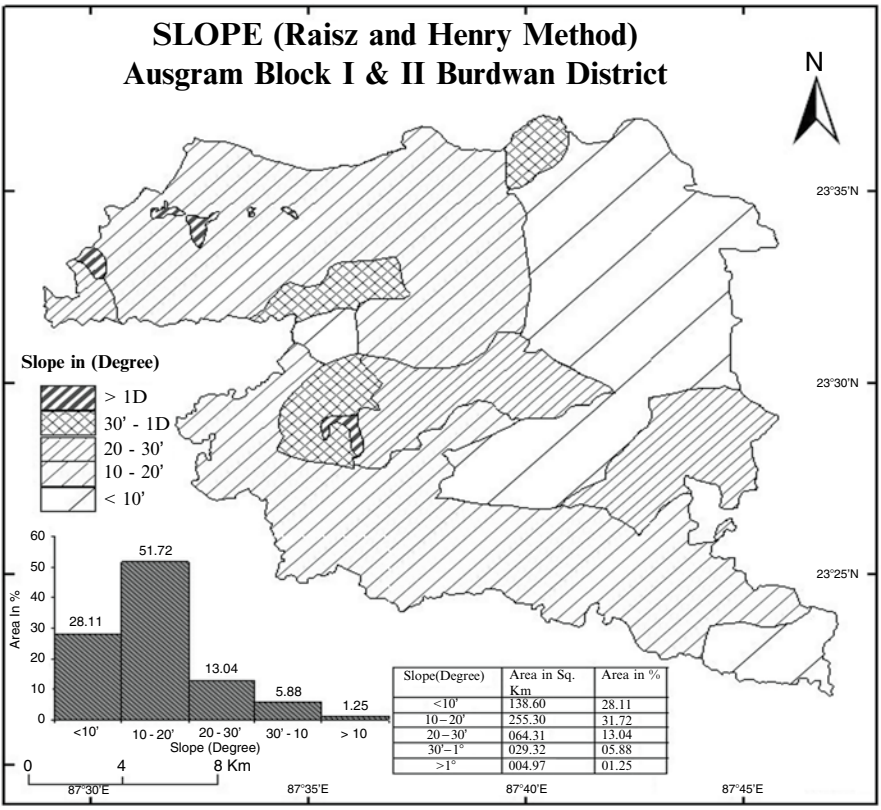

Fig. 5 Slope map (*Source*: 73 M/10, 11, 14 & 15)

bodies (ponds, tanks, river and canals). Where the slope is 1° or more, relatively the surface water bodies are few in these areas.

Frequency of Surface Water Bodies (FSWB)

Frequency of surface water bodies can be defined as the number of water bodies per km^2 area (Prakasam and Biswas 2010). Water is an important locating factor for settlement and it remains present on the earth's surface in the form of rivers, ponds and lakes. The quantity of water directly used by man is comparatively small, but for agriculture in the form of irrigation is very large.

In Ausgram block availability of surface water bodies are calculated using frequency of surface water bodies per km^2. Distributions of surface water bodies are very much irregular in Ausgram block. As already stated, the data has been generated using 1 km^2 grid; here also the same methodology has been followed. Isolines have been drawn to analyse the data in better way. It has been observed that some region is having more than 30 number of surface water bodies per km^2 area and in some cases it is less than two surface water bodies per km^2 area. Using isolines, present study area is divided into four zones i.e. <2, 2–10, 10–15 and >15 water bodies per square kilometre. Maximum concentration of water bodies within 1 km^2 area is located in north east central part (36 water bodies/km^2) of the study area.

The first zone of surface water frequency, <2 number of water bodies/km^2, covers about 42 % of the total study area; 2–10 number of water bodies/km^2 covers about 39 % of the total study area. More than 15 water bodies/km^2 zone is distributed in north east, north east central, south east and north west parts of the present study area (Fig. 6). It covers 10 % of the total study area. Generally in Ausgram block many water bodies are present but water is not available from those water bodies in most of the months of a year. The ground reality shows that these water bodies add little water to the region in drier periods.

Surface Water Harvesting Potential Zone (SWHPZ) Identification

Most of the areas in Ausgram blocks I and II are affected by water stressed conditions. As a result cultivation of the study region suffers almost every year. Most of the agricultural lands are being cultivated only once in a year. An attempt has been made to identify the surface water harvesting potential zones of the study region. The geomorphic resources (Ruggedness Index (RI), Relative Relief (RR), Drainage Density (DD), Slope and Frequency of Surface Water Bodies (FSWB)) are used to prepare the zones through overlay method. In this overlay method, GIS tool has been adapted for identification and classification of the surface water harvesting zones.

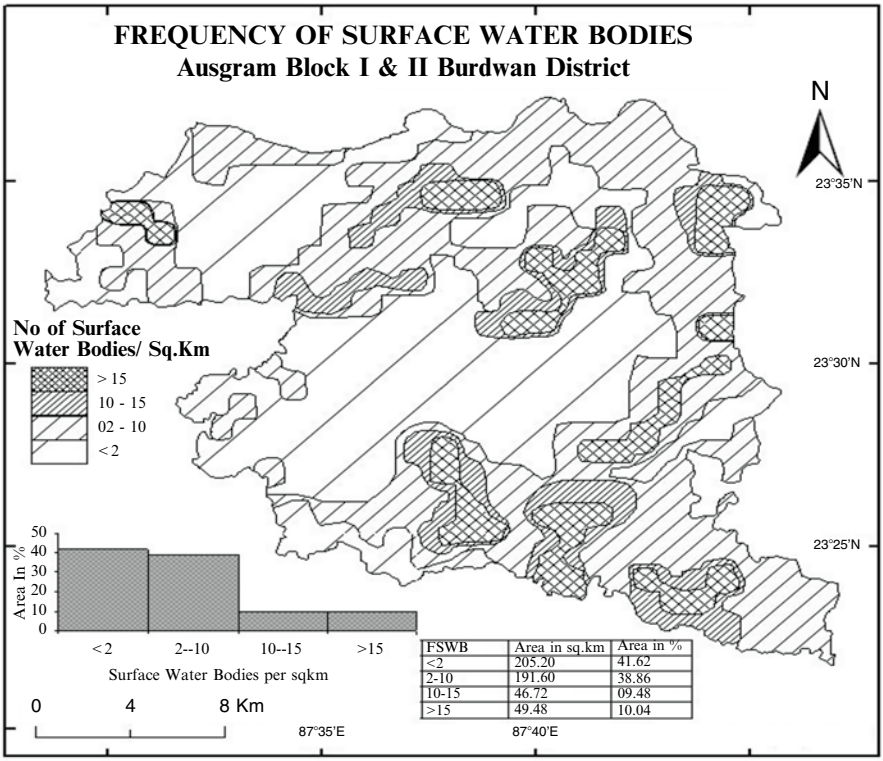

Fig. 6 Frequency of surface water bodies map (*Source*: 73 M/10, 11, 14 & 15)

With the help of the above criteria and methodology (Table 1), the surface water harvesting potential zones are identified and classified in three categories i.e. Maximum Surface Water Harvesting Potential Zone, Moderate Surface Water Harvesting Potential Zone and Minimum Surface Water Harvesting Potential Zone of Ausgram blocks I and II (Fig. 7).

Maximum Surface Water Harvesting Potential Zone covered 13 % of land surface and is distributed in central, south east, north west and north east parts of the study area. Moderate Surface Water Harvesting Potential Zone covered 6 % of the land surface and is distributed in north west, south central, south east parts of the study area. Minimum Surface Water Harvesting Potential Zone or not suitable for surface water storage covered 81 % of the land surface and is distributed in maximum study area land; because these 81 % land have rough topography, covered by minimum surface water bodies and drainage density, it is poorly suitable for water storage. The surface water potential zone map (Fig. 7) shows maximum area affected by water stressed problem (around 81 %). Generally this study concludes that surface water resource is poor in the study area.

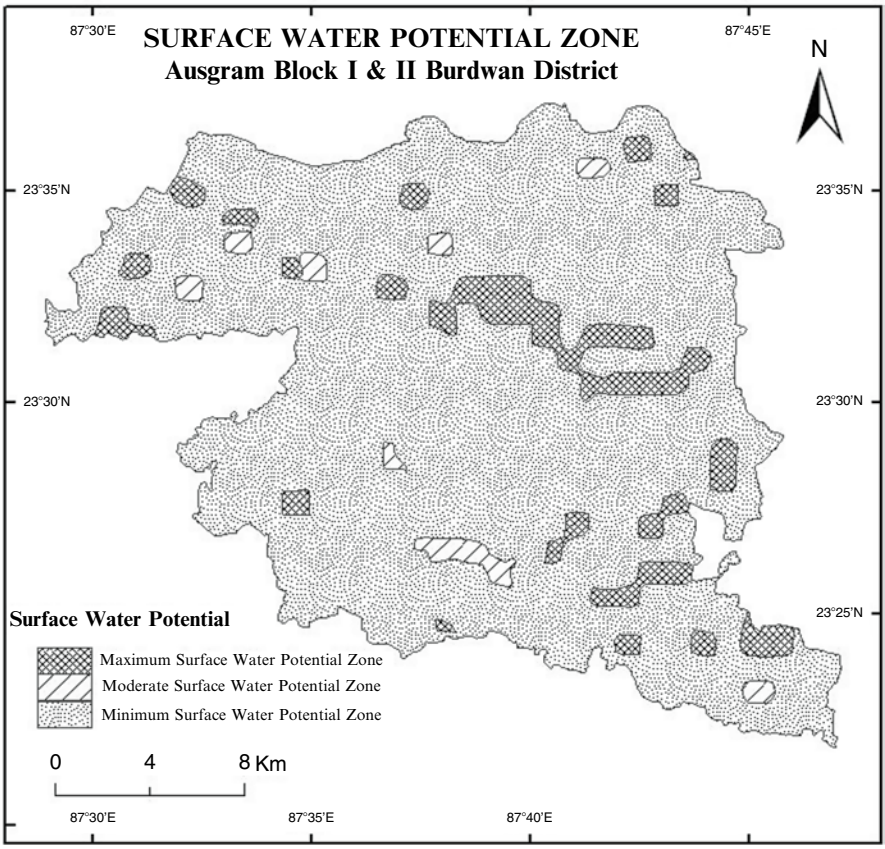

Fig. 7 Surface water potential zone map (*Source*: Author's Calculation)

Conclusions

India is facing the problem of water scarcity for agriculture, domestic and other purposes almost every year. The problem varies both in its spatial and temporal scale. In the present study, only agriculture has been taken into consideration because agriculture is the main source of income for the local people in Ausgram I and II blocks. Present paper has selected some geomorphic attributes and analysed them i.e., Ruggedness Index (RI), Relative Relief (RR), Drainage Density (DD), Slope and Frequency of Surface Water Bodies (FSWB) of the region.

Present study has identified three surface water harvesting potential zones in Ausgram block, i.e., Maximum Surface Water Harvesting Potential Zone (13 %), Moderate Surface Water Harvesting Potential Zone (6 %) and Minimum Surface Water Harvesting Potential Zone (81 %). The presence of water resource dictates the nature and extension of primary economic activities. Some part of the study area is

falling directly in the water stressed condition and agriculture is affected severely due to non-availability of water. If water resource is secured, the region can easily be converted to a good agricultural region.

Based on the geomorphic resources, present paper has suggested some surface water harvesting potential zones. In these zones, study considers that excess water of rainy season can be stored for future use. These zones can be of immense help to increase the intensity of agriculture and be able to increase the earnings of the people dependent on the agricultural activities. Maximum water harvesting potential zones are highly suitable for the water harvesting during the rainy season. The region is having the river Kunur, an ephemeral river carrying lots of water resources during the rainy season. The region is having undulating topography and has efficient drainage system. If the running water is made to be delayed or stored in the existing depressions, ponds for future usage, the running water can be converted into much more usable resources.

During the rainy season if surface water is stored in existing water bodies and check dams, it may be useful for the irrigation to the agriculture land. So the economy of the region can positively be changed. The dry ponds can be converted into permanent water storage zones, which may have much more other economic possibility along with the much-needed ecological importance.

References

Baulig H (1959) Morphombtrie. Ann Glogr 68(369):386–408

Chorley RJ (1962) Geomorphology and general system theory, Professional Paper 500-B. U.S. Geological Survey, Washington, DC

Gately D (1995) Potential for international and national water conflicts is high in coming years according to research organization. www.ifpri.org

Horton RE (1932) Drainage basin characteristics. Trans Am Geophys Union 13:350–361

International Rice Research Institute (IRRI) (1993) Rice research in a time of change. IRRI's medium term plan for 1994–1998. IRRI, Los Banos

International Rice Research Institute (IRRI) (2002) International Rice Research Institute. Los Banos. www.RiceWeb.org/

King LC (1962) The morphology of the earth. Oliver & Boyd, Edinburgh/London

Kumar MG, Agarwal AK, Bali R (2008) Delineation of potential sites for water harvesting structures using remote sensing and GIS. J Indian Soc Remote Sens 36:323–334

Monkhouse FJ, Wilkinson HR (1994) Maps and diagram. B.I. Publications, New Delhi

Mukhopadhyay SC (1973) Geomorphology of the Subarnarekha basin with a special reference to its cycle of erosion. Ph.D. thesis, Calcutta University, Calcutta

Mukhopadhyay SC (1979) Some aspects of Geomorphology of part of the Subarnrekha basin around Mahali Murup, Bihar. Geogr Rev India XXXI(2):33–40

Mukhopadhyay SC (1984) The Thisa basin – a study in fluvial geomorphology. K.P. Banchi & Co., Calcutta

Prakasam C, Biswas B (2010) Identifying the surface water resource in Ausgram blocks I & II, Burdwan District, West Bengal, India, based on morphometric analysis, using GIS. J Water Land-Use Manage 10(1):12–28

Prinz D (1995) Water harvesting in the Mediterranean environment – its past role and future prospects. In: Tsiourtis NX (ed) Water resources management under drought or water shortage conditions. Proceedings, EWRA 1995 symposium 14–18 March 1995, Nicosia, Cyprus

Prinz D (1996) Water harvesting – history, techniques and trends. Zf Bewässerungs wirtschaft 31(1):64–105

Rudra K (2012) The status of water resources in West Bengal: a brief report. www.indiawaterportal.org/sites/indiawaterportal.org/files/Rudra_Water_WB.doc

Smith GH (1935) The relative relief of Ohio. Geogr Rev 25:10–12

Strahler AN (1956) Quantitative geomorphology of drainage basins and channel networks. In: Chow VT (ed) Handbook of applied hydrology. McGraw Hill Book Company, New York

Tuong TP, Bouman BAM, Mortimer M (2005) More rice, less water: Integrated approaches for increasing water productivity in irrigated rice-based systems in Asia. Plant Prod Sci 8:231–241. http://bardhaman.nic.in/home.htm

Zavoianu I (1985) Morphometry of drainage basins, developments in water science, 20. Elsevier Publications, Amsterdam

Forecasting Groundwater Level Using Hybrid Modelling Technique

Sumant Kumar and Surjeet Singh

Introduction

In India, groundwater serves about 70 % of rural population, 50 % of urban population and about 60 % of agricultural area. There are more than 20 million groundwater extraction structures in place which are being used to meet requirement for domestic, industrial and agricultural activities. There is intensive development of groundwater in certain pockets of India, which has resulted in over-exploitation of groundwater resources and led to steep declining trend in levels of groundwater. As per the assessment of groundwater resources (CGWB 2007), out of 5,723 assessment units (blocks/mandals/taluks) in the country, 839 units in various states have been categorized as "over-exploited" meaning that annual groundwater extraction exceeds the annual replenishable resource. In addition, 226 units are critical with stage of groundwater development hovering between 90 % and 100 % of annual replenishable resource.

In recent years, the artificial neural network (ANN) technique has been found successfully applied to solve various water resource problems including time-series forecasting (ASCE 2000; Sudheer et al. 2002; Yoon et al. 2007; Maier and Dandy 2000). Nayak et al. (2006) and Krishna et al. (2008) successfully predicted the GWL fluctuation in coastal aquifers using ANN models with meteorological information with GWL data as the input variables. Daliakopoulos et al. (2005) simulated groundwater level using optimum ANN structure and provided acceptable prediction upto 18 months ahead. Coulibaly et al. (2001) and Coppola et al. (2005) have also applied ANN model in groundwater sector to predict water table fluctuation. Jalalkamali and Jalalkamali (2011) used hybrid model of ANN and genetic algorithm

S. Kumar (✉) • S. Singh
Groundwater Hydrology Division, National Institute of Hydrology, Roorkee 247667, India
e-mail: sumantk@nih.ernet.in

© Capital Publishing Company 2015

N.J. Raju et al. (eds.), *Management of Natural Resources in a Changing Environment*, DOI 10.1007/978-3-319-12559-6_6

(GA) in forecasting groundwater level in an individual well. Das et al. (2010) attempted to develop a hybrid neural model (ANN-GA) employing an ANN model in conjunction with famous optimization strategy called genetic algorithms (GA) for accurate prediction of groundwater levels in the lower Mahanadi river basin of Orissa State, India. Jain and Kumar (2009) used a hybrid ANN regression model structure for knowledge extraction from trained neural network hydrologic models. In this paper, hybrid model, which comprises ANN and non-linear regression model, was developed to predict the GWL fluctuations.

Study Area

The study area is located in the Sagar city, Sagar district of Madhya Pradesh, India. The well is located in the catchment of Sagar lake of Sagar city (Fig. 1). The Sagar city is located at the latitude of 23° 50′ N and longitude of 78° 45′ E. The catchment area of Sagar lake is 18 km^2 and the land use pattern of the area is 40.9 % barren land, 20.9 % agriculture, 18.7 % settlement, 11.5 % open forest and 8.1 % water body. The soils of this area are of two types: the red or reddish brown lateritic soil on hill tops and the black soil at the foothills.

The geological formation of the area mainly comprises quartzite sandstone of Vindhyan age and Deccan traps. The Deccan traps are basaltic in nature having vertical, polygonal and columnar joints. The Vindhyan quartzite sandstone is hard and compact with nearly vertical joints.

The data acquired from the area consisted of rainfall and GWL. The GWL time series data were measured at a particular location (bus stand) in the Sagar city and the precipitation data were collected from the meteorological station located in the Sagar city. The rainfall and GWL data were available for the period from June 1999 to July 2000. The data were divided into two sets: a training data set consisting of daily rainfall and GWL data for 9 months (June to February), and a testing data set of 5 months (March to July).

Development of Hybrid Model

A hybrid model is comprised of both ANN and regression modelling techniques. In the hybrid model, the output layer was replaced by a non-linear regression model (NLRM). The structure of the hybrid model is depicted in Fig. 2. The input was fed through input layers and the intermediate output i.e. hidden neurons output was calculated at the hidden layer using ANN. The outputs from hidden neurons were the inputs to the NLRM of the hybrid model. Jain et al. (2004) used the output of hidden layer for identification of physical processes inherent in artificial neural network rainfall runoff models.

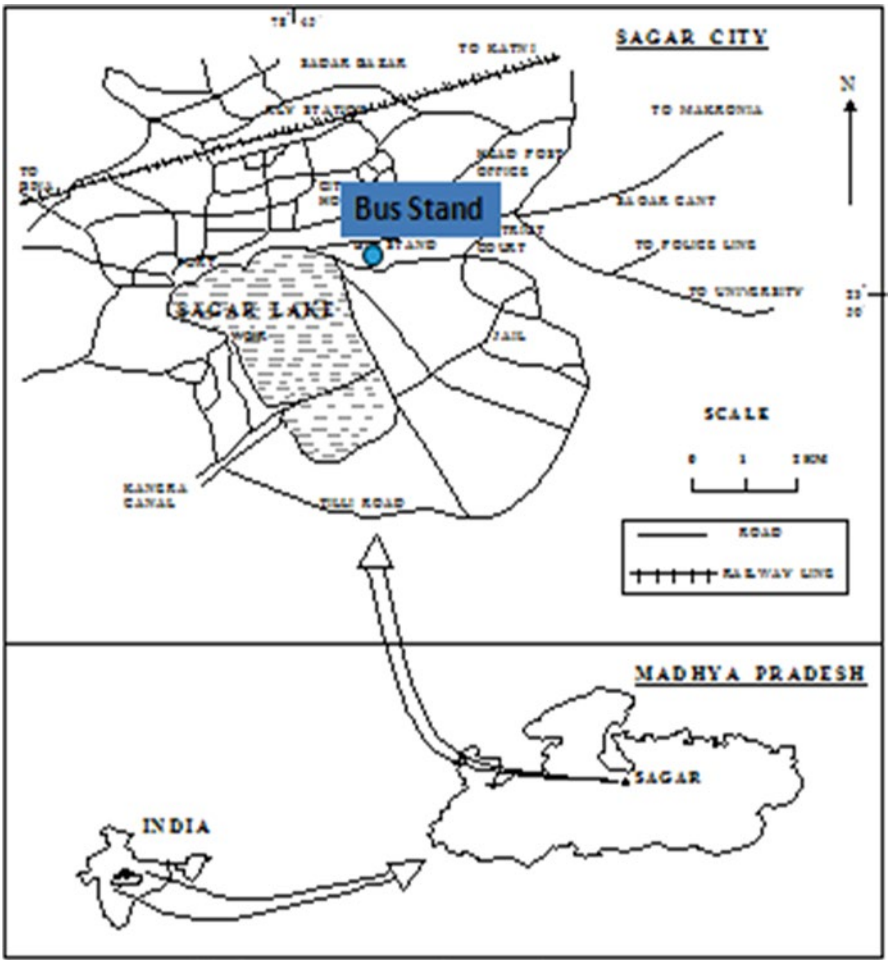

Fig. 1 Location map of the study area. *Blue dot* represents the location of the observation well

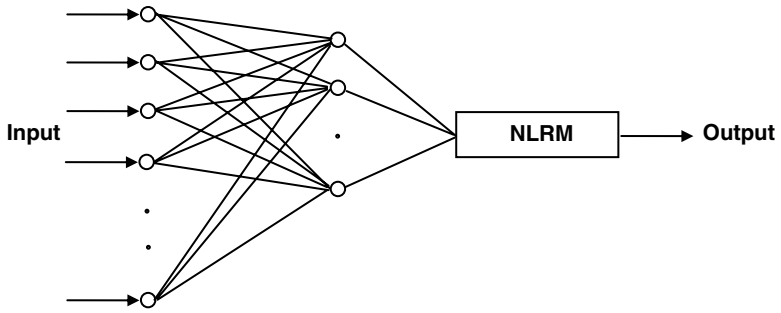

Fig. 2 The structure of the hybrid model

The structure of the NLRM is given below:

$$O = \alpha_1 H1 + \alpha_2 H2 + \beta_1 H1^2 + \beta_2 H2^2 \ldots + \alpha_n HN + \beta_n HN^2 \quad (1)$$

where O is the observed output, α_1, α_2, β_1, β_2 … α_n, β_n are the regression coefficients and H's are the hidden neuron outputs.

The structure of ANN model was found to be 7-2-1. Therefore, there are only two hidden neurons and their output (H1, H2) are taken as input for NLRM. The calibration data were used to determine the values of the regression coefficients.

Evaluation of Model Performance

Five different standard statistical performance evaluation criteria are used to evaluate the performance of various models. These include Average Absolute Relative Error (AARE), Coefficient of Correlation (*R*), Nash-Sutcliff Efficiency (*E*), Normalized Root Mean Square Error (NRMSE), and Threshold Statistics (*TS*). The lower AARE values, the higher TS_x and *R* values close to 1.0 would indicate a sufficient condition for a good model. The AARE, NRMSE and *TS* statistical measures give the effectiveness of a model in terms of its ability to accurately predict data from a calibrated model. The other statistic, such as *R*, quantifies the efficiency of the model in capturing the complex, dynamic and non-linear nature of the physical process being modelled.

Results and Discussion

The statistical results from the hybrid model are presented in Table 1. The values of *E* and *R* in excess of 0.97 were obtained during both training and testing sets for the model, which is excellent. The performance in terms of *TS* and AARE statistics is also very good. A major fraction of the computed groundwater level (90 %, for the models, during testing) had ARE of less than 5 %.

The scatter plots during testing data set (unseen by the model during training) are presented in Fig. 3. The graphical performance indicator gives better results when the data pairs are closing to 45° line and the good superposition between the observed and calculated values in the testing phase. The results demonstrate that the

Table 1 Results of the various statistical measures

Hybrid model	NRMSE	E	R	AARE	TS 5	TS 10
During training/calibration	0.0343	0.9973	0.9984	3.21	78.84	92.97
During testing/validation	0.0310	0.9725	0.9862	2.19	90.00	96.47

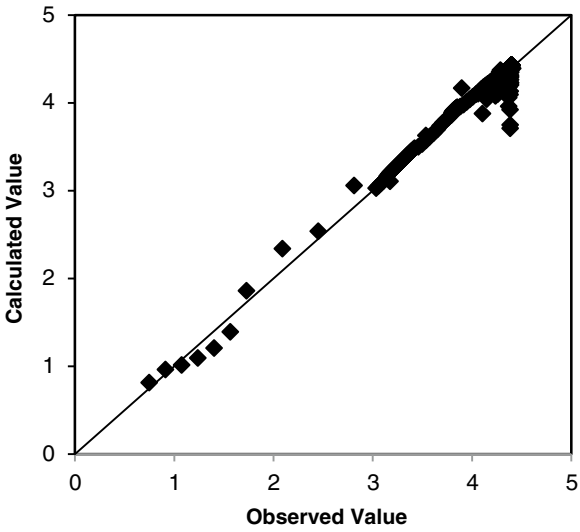

Fig. 3 Scatter plot of hybrid model during testing

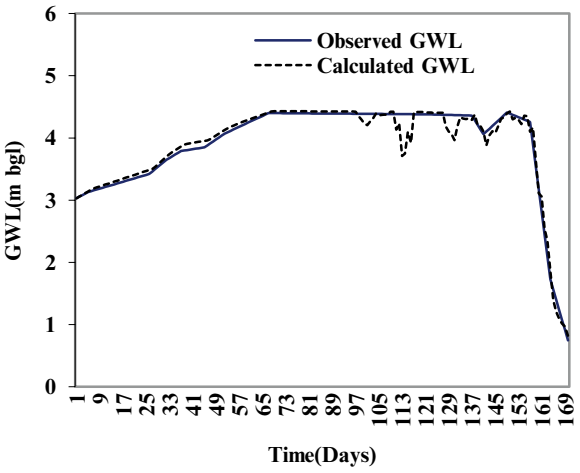

Fig. 4 Time series plot of hybrid model during testing

model is able to extract the input-output mappings inherent in the respective data employed for the model. From Fig. 3, it can be seen that the data pairs (observed and calculated GWL values) for the models are closer to 45° line and hence the model would give better result.

The time series plot of the observed GWL and calculated GWL of the hybrid model for the testing case is shown in Fig. 4. From Fig. 4 it is clearly evident that both the observed and computed profiles match closely and hence the proposed model gives quite accurate results.

Conclusions

The dependence on ground water as a reliable source to meet the requirements for irrigation, drinking and industrial uses in India has been rising rapidly during the last few decades. This has resulted in depletion of groundwater table in some areas causing concerns for the long-term sustainability. For the effective management of ground water, it is important to predict groundwater level (GWL) fluctuations. In this study, hybrid model has been developed to forecast the groundwater level fluctuations. The proposed model is developed by comprising both ANN and regression modelling techniques. The model is developed by replacing the output layer of ANN structure by non-linear regression model. The model is calibrated and tested based on the training and testing of the time-series data of rainfall and GWL in the Sagar city. The model uses the rainfall and the preceding GWL as the input data to predict the proceeding GWL. The performance of the models has been evaluated using standard statistical measures, namely: Average Absolute Relative Error (AARE), Coefficient of Correlation (R), Nash-Sutcliff Efficiency (E), Normalized Root Mean Square Error (NRMSE), and Threshold Statistics (TS). The results of the model are found to predict the GWL accurately and hence hybrid model can successfully be used for prediction of GWL of the Sagar city, Madhya Pradesh, India.

References

ASCE Task Committee on Application of Artificial Neural Networks in Hydrology (2000) Artificial neural networks in hydrology. I: preliminary concepts. J Hydrol Eng 5:115–123

CGWB (2007) Manual on artificial recharge to groundwater. Central Ground Water Board, Ministry of Water Resources, Government of India

Coppola E, Rana AJ, Poulton MM, Szidarovszky F, Uhl VV (2005) A neural network model for predicting aquifer water level elevations. Ground Water 43:231–241

Coulibaly P, Anctil F, Aravena R, Bobee B (2001) Artificial neural network modeling of water table depth fluctuations. Water Resour Res 37:885–896

Daliakopoulos IN, Coulibaly P, Tsanis IK (2005) Groundwater level forecasting using artificial neural networks. J Hydrol 309:229–240

Das NB, Panda SN, Remesan R, Sahoo N (2010) Hybrid neural modeling for groundwater level prediction. J Neural Comput Appl 19:1251–1263

Jain A, Kumar S (2009) Dissection of trained neural network hydrologic model architectures for knowledge extraction. Water Resour Res 45(7). doi:10.1029/2008WR007194

Jain A, Sudheer KP, Srinivasulu S (2004) Identification of physical processes inherent in artificial neural network rainfall runoff models. Hydrol Process 18(3):571–581. doi:10.1002/hyp.5502

Jalalkamali A, Jalalkamali N (2011) Groundwater modeling using hybrid of artificial neural network with genetic Algorithm. Afr J Agric Res 6(26):5775–5784

Krishna B, Satyaji R, Vijaya T (2008) Modelling groundwater levels in an urban coastal aquifer using artificial neural networks. Hydrol Process 22:1180–1188

Maier HR, Dandy GC (2000) Neural networks for the prediction and forecasting of water resources variables: a review of modeling issues and applications. Environ Model Softw 15:101–124

Nayak PC, Satyaji R, Sudheer KP (2006) Groundwater level forecasting in a shallow aquifer using artificial neural network approach. Water Resour Manag 20:77–90

Yoon H, Hyun Y, Lee KK (2007) Forecasting solute breakthrough curves through the unsaturated zone using artificial neural networks. J Hydrol 335:68–77

Alterations in Physico-chemical Parameters of Water and Aquatic Diversity at Maneri-Bhali Phase I Dam Site on River Ganges in District Uttarkashi, Uttarakhand

Madhu Thapliyal, Poonam Tiwari, and Ashish Thapliyal

Introduction

Rivers and lakes comprise approximately 0.009 % of earth's water but they harbour about 43 % of fish biodiversity (Nelson 2006; Helfman 2007). These fresh water systems also support various zoo-planktons and phyto-planktons which are important bio-indicators of an ecosystem. Greatest threats to freshwater ecosystems globally are: anthropogenic activities that cause habitat degradation, fragmentation, and loss; flow modifications; translocation of species outside their native ranges; over exploitation and pollution. Humans appropriate fresh water globally for direct consumption, crop irrigation, hydro-electric energy production and other purposes. The direct and indirect competition with humans for limited freshwater resources is largely why fishes and other aquatic organisms are among the most imperiled faunas on earth (Baxter 1977; Leidy and Moyle 1998; Duncan and Lockwood 2001).

Blocking the rivers/streams by construction of dams converts it into slow flowing lentil aquatic ecosystem. Benefits of impounding rivers are: flood control, hydro power generation, navigation, water supply, fishery etc. However, major drawbacks of construction of dams which exists in relation to aquatic flora and fauna are: blockage to fish migration, efficiency of fish passes, reduction in flood plain fish production etc. Impacts of dams can be grouped into direct and indirect effects. Direct effects include: (i) Physical barriers and preventing passage of migrating fish to their usual breeding, rearing, and feeding grounds. This results in massive failure of recruitment and eventual extinction of stock. The blank niche so created may be filled by the undesirable species. (ii) Change in physico-chemical

M. Thapliyal • P. Tiwari
Department of Zoology, Pt. L.M.S. Government PG College, Rishikesh, Uttarakhand, India

A. Thapliyal (✉)
Department of Biotechnology, Graphic Era University, Dehradun 248001, Uttarakhand, India
e-mail: ashish.thapliyal@gmail.com

© Capital Publishing Company 2015

N.J. Raju et al. (eds.), *Management of Natural Resources in a Changing Environment*, DOI 10.1007/978-3-319-12559-6_7

and biological parameters upstream and downstream as well as in surrounding environment and also causes fluctuations in planktonic, crustacean and molluscan fauna (the natural fish food) and (iii) Mortality or damage to fishes in a number of ways including abrasion against rough surfaces, turbine blade mangling, rapid pressure changes, water shearing effects and nitrogen super saturation in the stilling basin.

The indirect effects include: (i) Thermal stratification of reservoirs in warm season which can result in de-oxygenation of the hypo-limnion. Cool and/or anoxic water discharged from the hypo-limnion can severely reduce water quality downstream and negatively impact fish stock and fisheries. Fish may be eliminated from the river as far downstream from the dam as de-oxygenation persists. (ii) Sediment released from the reservoir can hasten turbidity which can create severe problems for the downstream flora and fauna. (iii) Sediments trapped in the reservoir may be contaminated with pesticides and industrial chemicals from catchment sources and residues can enter the reservoir food chain and make fish poisonous. (iv) Change in fish biodiversity and stock abundance over time. (v) Extensive de-oxygenation and acidification may occur due to rotting of submerged vegetation in reservoirs which may result in the extensive kill of the original riverine population in the lower layers of water (Heppner and Loague 2009; Ziegeweid et al. 2008; Burlakova and Karatayev 2007; Mérona et al. 2005; Todd et al. 2005; Turner and Erskine 2005; Santucci et al. 2005; Johnson et al. 2004; Park et al. 2004; Taylor et al. 2001).

The Garhwal Himalayan region, located in middle Himalaya in India, harbours many endemic species and is known as a global hotspot for biodiversity (Fig. 1a). This region also has an extensive network of fresh water rivers and streams (Fig. 1b). According to estimates, there are approximately 10 major rivers in Garhwal region of Uttarakhand that supports some 60–70 species of fishes within a short radius of 200 miles (Badola 2009). These fresh water systems are also known to harbour a wealth of benthic fauna and flora. These river systems of Garhwal Himalaya are being used extensively to generate hydro-electric projects by construction of dams. In Uttarkashi district, there are about 18 proposed hydro-electric projects within a span of 100 km on river Bhagirathi (Fig. 1a) out of which five major dams under construction (Dabrani, Lohari-Nag, Pala, Maneri and Asiganga) are in district Uttarkashi. It is surprising to see that these many dams/barrages exist within such a short distance and there have been no initiatives to conserve/manage/monitor the aquatic fresh water biodiversity. Water from the reservoirs of these dams is channelized through tunnels to power houses located at distant part somewhere downstream causing drastically reduced water levels in river between dam wall and power house (Fig. 2a, b). There has been no base line data effect of these drastically reduced water levels on aquatic biodiversity (flora and fauna) of the region including that in Uttarkashi district. During this study, efforts were made to investigate various parameters including variation in aquatic flora and fauna, changes in physico-chemical parameters of water in river before and after the dams on river Bhagirathi at Maneri Bhali Phase I hydro-electric power project, Uttarkashi district.

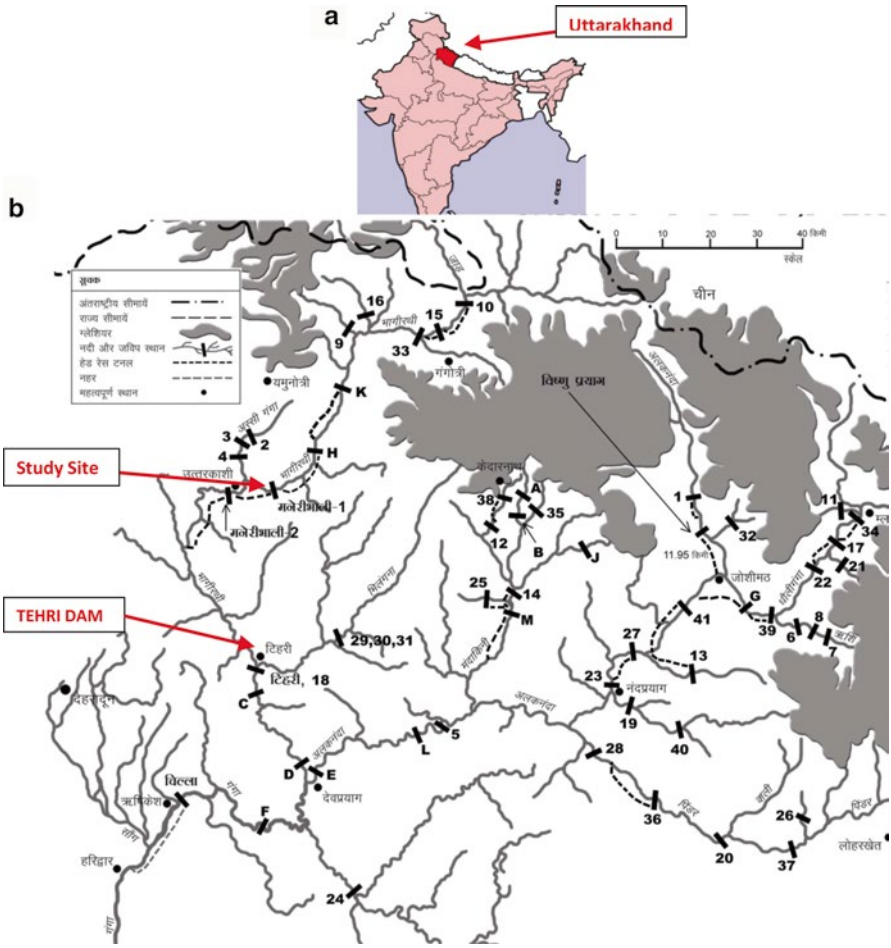

Fig. 1 (**a**) Location of Uttarakhand in India. (**b**) Network of rivers in Garhwal Himalaya, Uttarakhand. All the major tributaries supporting the Ganges are marked in the figure along with sites (total 41) for major hydro-electric power projects. Already functional Tehri Dam is also marked in the figure

Methods

Study Site

Study site was Maneri Bhali Phase I power project located in District Uttarkashi, Uttarakhand, India (latitude 30.75°N, longitude 78.60°E). The study sites were upto 5 km upstream and from 500 m to 2 km downstream from dam wall. Specific sampling sites, upstream and downstream were marked and all the sampling was done at these sites.

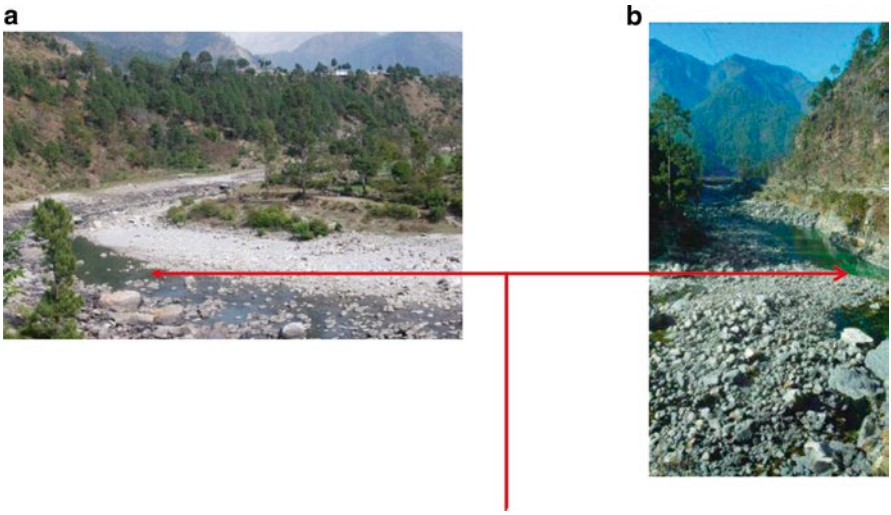

Fig. 2 Severely reduced water levels during winters. (**a**) Reduced water levels after Maneri Bhali – Phase II, Location village Barethi. This site is approximately 5 km downstream from Uttarkashi where Phase II project dam wall is located. (**b**) Reduced water levels after Maneri Bhali – Phase I, Location near village Gangori. This site is approximately 3 km down-streams from the dam wall of Maneri Bhali – Phase I, project site

Field Methodology

Field methodology included sampling for fishes, collection of zoo-planktons, phyto-planktons and measurement of physico-chemical parameters of water.

Zoo-planktons

Samples were collected using plankton net and preserved. A quadrate of 1 m × 1 m was marked and the collection was made from these quadrates. These samples were photographed and identified using existing zoo-plankton key of Needham and Needham (1962).

Phyto-planktons

Plankton-net method was used for this sampling. Amount of water to be filtered for collection of phyto-planktons was standardized. Five volumes of a 5 L capacity bucket were filtered for each collection from specific study sites. The collected samples were preserved in 4 % formalin. The samples were identified using the key of Needham and Needham (1962) and their numbers were counted using Sedgwick-Rafter slide.

Physico-chemical Properties of Water

After collection the water samples were stored in refrigerator to avoid any microbiological decomposition. Parameters like temperature, pH, electrical conductance (EC) and dissolved oxygen (DO) and carbon-dioxide (CO_2) were measured immediately. AR grade reagents and double distilled water were used for reagent preparation.

Physico-chemical parameters were measured following methods of Welch (1952), APHA (1992), Trivedi and Goel (1986) and Munshi and Munshi (1995).

1. Physical Parameters

Water temperature: Water temperature was recorded with the help of mercury thermometer by dipping it into water.

2. Chemical Parameters

(*a*) *pH:* pH was measured on the sampling sites by the portable pH meter (Hanna pocket pH meter-H196-107 Systronic-361 pH meter).

(*b*) *Free carbon dioxide:* Method of Trivedi and Goyal (1986) was used for CO_2 estimation. Free CO_2 was determined by titrating the sample using a strong alkali (pH 8.3). The analysis was done on the sampling site. Drops of neutralized phenolphthalein indicator were added to 100 ml of water sample taken in an Erlenmeyer's flask and titrated with 0.05 N sodium hydroxide (NaOH) until a pink colour appears. The volume of titrant was noted down and free CO_2 was calculated using following equation:

$$\text{Free}\,CO_2\left(\text{mg}/\text{L}\right)=\left(\text{ml}\times\text{N}\right)\text{of NaOH}\times 1{,}000\times 44/\text{ml sample}$$

(*c*) *Total alkalinity:* Alkalinity is the expression of the total quantity of base (usually in equilibrium with carbonate or bicarbonate) and was determined by titration with a strong acid (as per Hutchinson 1957).

(*d*) *Dissolved oxygen (DO):* The DO was estimated on the site by the Winkler's Iodometric method. The estimation of oxygen in water depends on the fact that sodium hydroxide together with manganese sulphate gives a white precipitate of manganese hydroxide.

$$MnSO_4+2NaOH\rightarrow Mn\left(OH\right)_2+Na_2SO_4$$

Water sample was taken in a 300 ml BOD bottle. 1.0 ml of both manganese sulphate ($MnSO_4$) and alkaline iodide (KOH + KI) were added to the sample and mixed gently. Addition of 2.0 ml of conc. sulphuric acid (H_2SO_4) liberates iodine equivalent to DO. 200 ml of the aliquot was titrated with the standardized sodium thiosulphate $Na_2S_2O_3$ (0.025 N), aqueous starch was used as indicator. The volume of titrant used was recorded and the result was expressed as milligram per litre (mg/L). The formula used to calculate DO was:

$$\text{DO}\left(\text{mg}/\text{L}\right)=\left(\text{ml}\times\text{N}\right)\text{of titrant}\times 8\times 1{,}000/V_2\left(V_1-V\right)=V_1$$

where V_1 is volume of sample bottle after placing the stopper, V_2 is volume of the part of the contents titrated and V is volume of $MnSO_4$ and KI added.

(*e*) *Total calcium (EDTA method):* 50 ml of sample water was taken in a conical flask and 0.1 ml of 8 % NaOH along with few drops of indicator (Murexide indicator) was added to it and the colour changed to pink (Munshi and Munshi 1995). This was titrated with EDTA (0.01 M) till the colour turned purple.

(*f*) *Total Hardness (EDTA method):* 50 ml of sample water was taken in a conical flask. Added 1 ml of ammonia buffer (Sigma Aldrich – product code 318604) along with five drops of indicator (Eriochrome black T) (Munshi and Munshi 1995). Above solution turns wine red. Titrated the above solution by EDTA (0.01 M) until clear blue colour appears.

(*g*) *Total magnesium hardness* = Total hardness – calcium level (Munshi and Munshi 1995)

(*h*) *Total chlorides:* Chlorides were estimated by the method of Munshi and Munshi (1995). In short about 50 ml of water sample was taken in a conical flask and 2 ml of potassium chromate indicator was added. The solution was titrated against standardized silver nitrate (0.01 N) until a brick red colour precipitate of silver chromate started appearing. The volume of silver nitrate consumed was noted down and amount of chloride was calculated with following equation:

$$\text{Free Cl}\left(\text{mg} = \text{L}\right) = \left(\text{ml} \times \text{N}\right)\text{of AgNO}_3 \times 1{,}000 \times 35.5 / \text{ml sample}$$

Electrical conductivity (EC) and total dissolved solids (TDS) (Systronic – soil and water analysis kit – model director new BC) and turbidity – Nephelometeic method (Systronic – digital nephlo-turbidity meter 132) were determined using available electronic instruments.

Fish Population Estimates

Data on fish populations was obtained from sampling sites established during the original survey. These sites were chosen to capture the existing range of fish communities (e.g., dominated by native fishes vs. exotic fishes) as well as the range of habitat types and quality. Fish were sampled using a combination of hired fisherman and other efforts (e.g., three pass depletion technique), and population estimates were completed based on modified depletion technique (Zippin 1958). For fish population estimates, a specifically marked area of 800 m to 1 km was quardened off with nets and then the sampling was conducted. All the sample collections and measurements were done from these specifically marked sites.

Statistics

Statistical comparisons were done using Origin 8.6 software from origin labs.

Results

The result from this site shows trends of drastic changes in various parameters.

Phyto-planktons

The diversity of phyto-planktons was assessed and the summary is presented in Table 1. Three prominent class of phyto-planktons: Bacilariophyceae (19 genus), Chlorophyceae (8 genus) and Myxophyceae (5 genus) were observed. Clear variation in species can be seen. Before dam, the abundance/presence of almost all the species was recorded. After dam wall these species are beginning to dwindle but most of the species are intact/present. A total of 32 genus were observed before dam wall (Table 1) and out of total 32 genus, 10 genus were not observed in site after dam wall.

Zoo-planktons

Eleven species of other fauna were observed (Table 2) in total before dam wall site. Out of total 11, only six species were observed after dam wall. Significant reduction in overall diversity was observed. Copepod, Diptomus, Kertella, Rotaoria and Nolthoca were not observed in samples after the dam wall.

Physico-chemical Properties

The results on water temperature show a clear increase in average water temperature in the regions after the dam wall (Table 3). The temperature range before the dam wall was 14.46 ± 0.99 to 10.46 ± 0.73 °C while after the dam wall the temperature ranged from 17.00 ± 1.16 °C to 11.00 ± 0.80 °C in the same area. Similar pattern was observed in case of dissolved CO_2 and DO. Before dam average CO_2 range was 2.71 ± 0.27 mg/L while after dam it was 3.09 ± 0.32 mg/L. DO before dam wall was 10.02 ± 0.30 mg/L while after dam it became 8.42 ± 0.30 mg/L. All these values were significantly different ($p > .001$).

Fish Population Estimates

Drastic changes in fish number is observed (Table 4). Before dam wall the number of fishes was 44.14 ± 6.15 and after dam wall 21.7 ± 2.95 ($p > .001$).

Table 1 Phyto-planktons of river Ganges before and after dam wall at Maneri Bhali Phase I hydro-electric power project

	After dam	Before dam
	Presence/absence	Presence/absence
Bacilriophyceae		
Navicula	+++	+++
Cymbella	++	+++
Ditoma	+	+
Meridon	++	+
Syndra	++	+++
Denticula	+	++
Euonotia	++	++
Nistichia	+	++
Crentonies	–	+
Pinnularia	–	+
Gyrosigma	–	+
Hechentia	+	+
Stauriens	–	+
Coconies	–	+
Amphora	+	+
Epitima	–	+
Gomphonema	–	+
Fragilaria	–	++
Centorlla	–	+
Chlorophyceae		
Clostrium	+	+
Cosmerium	+	+
Desmidium	+	+
Ulotirix	+	+
Microspora	+	+
Ankistrudemus	–	+
Penium	–	+
Cladophora	–	+
Myxophyceae		
Anabena	+	+
Phormodium	+	+
Ocitierilaria	++	++
Rivularia	+	+
Urenema	–	+
Species richness	19	32

Discussion

Very little to almost no literature on impact of dam on aquatic environment is available on upper Garhwal Himalayan especially on river Ganges (Bhagirathi). Most of the work done so far has been on documentation of some fish species in the region. We could find only couple of studies carried out in this region by the group of

Table 2 Macro invertebrate fauna of river Ganges before and after dam wall at Maneri Bhali Phase I hydro-electric power project

	After dam	Before dam
	Presence/absence	Presence/absence
Crustaceans	+	+
Cladocera	++	+
Bosmania	+	+
Daphnia	+	+
Copepod	–	+
Cyclops	+	+
Diptomus	–	+
Rotifera	+	+
Kertella	–	+
Rotaoria	–	+
Nolthoca	–	+
Species richness	6	11

Table 3 Physico-chemical parameters of river Ganges before and after dam wall at Maneri Bhali Phase I hydro-electric power project

	Maneri phase I – before dam site I		Maneri phase I – after dam site I		*t*-test–paired *P* value
	Mean	SEM	Mean	SEM	Sig. level 0.05, 95 % CI
Temp. Max (°C)	**14.46**	0.99	**17**	1.16	S*
Temp. Min (°C)	**10.46**	0.73	**12**	0.80	S*
pH	**7.2**	0.14	**7.30**	0.12	NS
CO_2 (mg/L)	**2.71**	0.27	**3.09**	0.32	NS
Alk (mg/L)	**21.26**	1.35	**20.15**	1.45	NS
DO (mg/L)	**10.02**	0.30	**8.42**	0.30	S*
Conductance (siman/cm^2)	**116.53**	3.66	**111.46**	9.22	NS
Ca^{++} (mg/L)	**52.65**	3.21	**51.46**	3.27	NS
TH (mg/L)	**77.76**	6.42	**72.69**	7.03	NS
Cl^- (mg/L)	**19.90**	2.77	**22.11**	2.12	NS
Mg^{++} (mg/L)	**5.54**	1.45	**6.08**	1.46	NS
TDS	**73.76**	2.41	**76.56**	2.94	NS
TUR nNTU)	**27.80**	11.75	**41.19**	15.57	NS

Dr. RC Sharma (2003) but that too studied the effect of excessive road construction on river eco-system.

Aquatic habitat includes all of the physical, chemical and biological features of the environment needed to sustain life. Examples include suitable water quality and habitat-migration routes, spawning grounds for fishes, feeding and resting sites and shelter from predators and adverse environment conditions (Orth and White 1993), phytoplankton's, zoo-plankton's and other biotic components. Therefore habitat quality influences the numbers, sizes and species of aquatic eco-system that can be sustained in a particular area (Milner et al. 1985), and changes to that habitat can

Table 4 Variation in number of fishes sampled before and after dam wall from river Ganges at Maneri Bhali Phase I hydro-electric power project

	Before dam wall	After dam wall
Months	No. of fishes	No. of fishes
Aug.	20	8
Sept.	25	15
Oct.	44	25
Nov.	62	39
Dec.	44	17
Jan.	53	25
Feb.	86	35
March	93	38
April	60	32
May	45	24
June	25	18
July	16	8
Aug.	20	9
Sept.	25	12
Mean ± SEM	**44.14 ± 6.15**	**21.7 ± 2.95**

result in altered species characteristics. Also, legal mandates (e.g. the US National Environmental Protection Act, 42 USC – 4321 to 4361 and the US Endangered Act, 16 USC – 1531 to 1544) require assessment of habitat and predication of changes to it under different management scenarios. Such legislation spawn the development of habitat models designed to quantify the effect of flow alterations and other habitat changes on species populations (Terrell 1984; Orth 1987; Gore and Nestler 1988).

In specific case related to fishes, the blockage of fish movements upstream can have a very significant and negative impact on fish biodiversity. Many findings reveal that large number of aquatic fauna have been lost as a consequence. In the Columbia River, USA, more than 200 stocks of anadromous, Pacific salmonids became extinct. Sturgeon populations in the Caspian Sea rely on hatcheries, mainly in Iran, since Russian dams block natural spawning migrations. Hydroelectric dams in the Amazon basin have halted the long distance upstream migration of several species of catfishes and interrupted the downstream migration of their larvae. On the Araguaia-Tocantins River basin, Brazil, several species of migrating catfish have been drastically reduced in abundance as a result of dams; catches in the downstream fisheries have been reduced by 70 %. Artificial barriers also lead to the dramatic decline of the endangered cyprinid fish, *Anaecypris hispanica* in Iberia.

In general, a river is a one-way system for molluscs, as many molluscs can only move downstream by drifting or being dislodged by flood events and moved downstream. But some species with a larval form can move significant distances upstream with the aid of a third party, e.g. host fish during the larval stage. A single dam and more significantly multiple dams along a given river interfere with the genetic bridging function of the main stem.

Water quality, flow and seasonality of flow are not normally disrupted in the upstream area above the reservoir so impacts are generally less than for the reservoir and downstream areas. Nevertheless, the dam and the reservoir affect migratory movements of species into and out of this upstream area. The genetic exchange with downstream segments is reduced or prevented. A study was made of molluscs upstream in a braided river that enters a reservoir on the River Inn in Austria (Foeckler et al. 1991). Data shows that there was a decline of species upstream of the reservoir.

In the construction of reservoirs, the clearing of vegetation, movement of earth and rock, the presence of humans and machinery, bringing in construction materials, use of explosives, noise, and reducing or cutting off river flow and increasing turbidity, will affect biodiversity. Removal of forests or other vegetation over a wide area, excavation, earth and rock movement and reduction in river flow are the most significant. Some of the on-site activities are mirrored in off-site disturbances such as the mass displacement of earth and rocks and road building. During reservoir filling the river and any associated wetland areas become inundated. Riffles, runs and pools of the river are lost beneath the rising waters, leading to the extirpation (or extinction) of habitat sensitive riverine species with tightly defined niche requirements. Fishes in rivers are generally well adapted to flowing water. Similarly molluscs are often restricted to specific habitats within the river system, e.g. some species are bottom-dwelling filter feeders, and others live in weeds at the edge of the channel. The construction of reservoirs converts lotic (running) into lentic (still water) habitats. Species dependent on running water will diminish or disappear. In almost all cases, the diversity of fish species will drop (McCully 1996).

The changed or fluctuating conditions in the reservoir may lead to opportunities for weed or exotic species e.g. the water hyacinth, *Eichhornia crassipe*. Increases in the number of mollusc-borne diseases following dam construction in various countries. For example at least four genera of mollusc-borne human diseases have increased as a result of impoundments in Thailand (Woodruff and Upatham 1992).

Our results show that the minimum and maximum temperatures of water have shown a significant variation. This change might be attributed mostly due to reduced water level. As water levels are low, the heating and cooling of river bed might be having an effect on water temperature. Due to this change in water temperature, the habitat and tolerance of aquatic species might be showing variations. During the study, it was noted that the characteristics of water after the dam wall is more "stream like" rather than "river". Change in DO level might also be another reason for difference of species richness in case of phytoplankton and micro invertebrate fauna. As per the review of literature done by our lab, very few to almost none of the long studies have ever been conducted in Garhwal Himalaya on impact of hydro-electric power project/plant's dam wall on aquatic fauna. Our study has thrown light on this aspect and came up with data that should be a cause of concern and clearly highlight the need of long-term data sets on various aspects of river ecology especially in areas of hydro-electric power projects.

Our study clearly shows that the fauna and flora is clearly being affected due to construction of power projects. The main cause is drastic changes in water level. The situation is alarming and immediate steps will have to be taken to counter the situation. Either the hydro-electric power companies need to follow the recommended guidelines or policy makers will have to think about new policies on this issue.

Conclusions

River Ganges originates from Gomukh in Uttarakhand, India. Uttarakhand, a state located in northern part of India is also referred to as an "Energy State" because of the potential that it possesses for generation of hydro-electric power. This potential is due to the immense number of streams/rivers in this state and their perianal nature due to their origin in snow clad mountains of Himalaya. Approximately 18 hydroelectric projects have been planned in Tehri and Uttarkashi districts on this river, a region within 100 km of its origin. Like most of the sites for hydro-electric power projects, at Maneri Bhali (Phase I), reservoir water is diverted into tunnels and stretch(s) of river after dam wall has drastically reduced water levels. Temperature before dam wall ranged from 14.46 ± 0.99 °C to 10.46 ± 0.73 °C while after the dam wall it ranged from 17.00 ± 1.16 °C to 12 ± 0.80 °C. Before dam average CO_2 range was 2.71 ± 0.27 mg/L while after dam it was 3.09 ± 0.32 mg/L. DO before dam wall was 10.02 ± 0.30 mg/L while after dam it became 8.42 ± 0.30 mg/L. Population of fishes (mostly *Schizothorax*) was estimated at 44 ± 6 fishes before dam while it was 21 ± 3 fishes after wall. All the variations were significant. Absence of phytoplankton and zooplankton species was also recorded after dam wall. The overall situation in areas after dam wall needs immediate attention for habitat restoration. Besides the Ganges and the Yamuna, there are many other rivers that are tributaries of these two rivers. Policy makers in Central Government and the State Government have marked several hydro-electric projects in many of these rivers. Environmentalists have objected to the clearance of these projects because the project report on paper differs widely from the ground realities in terms of minimal water flow policies. The river water flow after every dam wall is so drastically changed that it is impacting the river ecology. The present study reports one such startling finding where there are significant alterations in physico-chemical properties of water before and after the dam wall have altered along with the aquatic fauna. It is a wakening call for the policy makers; we still have time to save a region if we act now. Further long-term studies will also have to be undertaken to keep a baseline date for year to year variations that might occur.

Acknowledgement Funding for Major Project from University Grants Commission (UGC), India (grant number – F.No. 40-372/2011 (SR) dated 5th July, 2011) to Dr. Madhu Thapliyal is duly acknowledged.

References

Almeida EF, Oliveira RB, Mugnai R, Nessimian JL, Baptista DF (2009) Effects of small dams on the benthic community of streams in an Atlantic forest area of Southeastern Brazil. Hydrobiology 94(2):179–193

American Public Health Association (1992) Standard methods for the examination of water and waste-water, 18th edn. APHA, Washington, DC

Badola SP (2009) Ichthyology of central Himalaya. Transmedia Publication

Baxter RM (1977) Environmental effects of dams and impoundments. Annu Rev Ecol Syst 8:255–283
Burlakova LE, Karatayev AY (2007) The effect of invasive macrophytes and water level fluctuations on unionids in Texas impoundments. Hydrobiologia 586(1):291–302
Christopher A, Taylor JH, Knouft TMH (2001) Consequences of stream impoundment on fish communities in a small North American drainage. Regul Rivers Res Manag 17(6):687–698
Duncan JR, Lockwood JL (2001) Spatial homogenization of the aquatic fauna of Tennessee: extinction and invasion following land use change and habitat alteration. Lockwood & McKinney
Foeckler F, Diepolder U, Deichner O (1991) Water mollusc communities and bioindication of lower salzach floodplain waters. Regul Rivers Res Manag 6:301–312
Furey PC, Nordin RN, Mazumder A (2006) Littoral benthic macroinvertebrates under contrasting drawdown in a reservoir and a natural lake. J N Am Benthol Soc 25(1):19
Gillette DP, Tiemann JS, Edds DR, Wildhaber ML (2005) Spatiotemporal patterns of fish assemblage structure in a river impounded by low-head dams. Copeia 2005(3):539
Gore JA, Nestler JM (1988) In-stream flow studies in perspective. Regul Rivers Res Manag 2:93–101
Greathouse EA, Pringle CM, Mcdowell WH, Holmquist JG (2006) Indirect upstream effects of dams: consequences of migratory consumer extirpation in Puerto Rico. Ecol Appl 16(1):339
Gunkel G, Lange U, Walde D, Rosa JWC (2003) The environmental and operational impacts of Curua-Una, a reservoir in the Amazon region of para, Brazil. Lakes Reserv Res Manag 8(3–4):201–216
Helfman S (2007) Fish conservation: a guide to understanding and restoring global aquatic biodiversity and fishery resources. Island Press, Washington, DC
Heppner CS, Loague K (2009) A dam problem: simulated upstream impacts for a Searsville-like watershed. Ecohydrology 1(4):408–424
Hutchinson GE (1957) A treatise on limnology, vol I. Geography, physics and chemistry. Wiley, New York
Johnson BM, Saito L, Anderson MA, Weiss P, Andre M, Fontane DG (2004) Effects of climate and dam operations on reservoir thermal structure. J Water Resour Plan Manag 130(2):112
Kang B, He D, Perrett L, Wang H, Hu W, Deng W, Wu Y (2009) Fish and fisheries in the upper Mekong: current assessment of the fish community, threats and conservation. Rev Fish Biol Fish 19:465–480
Leidy RA, Moyle PB (1998) Conservation status of the world's freshwater fish fauna: an overview. In: Fieldler PL, Kareiva PM (eds) Conservation for the coming decade, 2nd edn. Chapman and Hall, New York
Lucas MC, Bubb DH, Jang M, Ha KK, Masters JEG (2009) Availability of and access to critical habitats in regulated rivers: effects of low-head barriers on threatened lampreys. Freshw Biol 54(3):621–634
McCully P (1996) Silenced rivers: the ecology and politics of large dams. Zed Books, London
Mérona B, Vigouroux R, Leonardo Tejerina-Garro F (2005) Alteration of fish diversity downstream from Petit-Saut dam in French Guiana implication of ecological strategies of fish species. Hydrobiologia 551(1):33–47
Milner NJ, Hemsworth RJ, Jones BE (1985) Habitat evaluation as a fisheries management tool. J Fish Biol 27(A):85–108
Munshi JD, Munshi JD (1995) Fundamentals of freshwater biology. U.P. Sharma, Bhagalpur
Needham JG, Needham PR (1962) A guide to the study of freshwater biology. Holden-Day Inc., San Francisco
Neil JM (2008) Anthropogenic effects of reservoir construction on the parasite fauna of aquatic wildlife. EcoHealth 4(4):374–383
Nelson JS (2006) Fishes of the world, 4th edn. Wiley, New York
New T, Xie Z (2009) Impacts of large dams on riparian vegetation: applying global experience to the case of China's three gorges dam. Biodivers Conserv 17(13):3149–3163
Orth DJ (1987) Ecological consideration in the development and application of instream flow-habitat models. Regul Rivers Res Manag 1:171–181

Orth DJ, White RJ (1993) Stream habitat management. In: Kohler CC, Hubert WA (eds) Inland fisheries management in North America. American Fisheries Society, Bethesda

Park YS, Chang J, Sovan L, Cao W, Brosse S (2004) Conservation strategies for endemic fish species threatened by the three gorges dam. Conserv Biol 17(6):1748–1758

Santucci VJ Jr, Gephard SR, Pescitelli SM (2005) Effects of multiple low-head dams on fish, macroinvertebrates, habitat, and water quality in the Fox River, Illinois, North America. J Fish Manag 25(3):975

Seong-Yong P, Seo-Jun K, Seung-Hwi L, Byung-Man Y (2008) An experimental study on the swimming performance of pale chub (Zacco platypus). J Korea Water Resour Assoc 41(4):423–432

Sharma RC (2003) Protection of an endangered fish Tor Tor and Tor Putitora population impacted by transportation network in the area of Tehri dam project, Garhwal Himalaya, India. UC Davis, Road Ecology Center. Retrieved from: http://escholarship.org/uc/item/53g2s0vp

Terrell JW (ed) (1984) Proceedings of a workshop on fish habitat suitability index model, US fish and wildlife service biological report, 85(6)

Tiemann JS, Gillette DP, Wildhaber ML, Edds DR (2004) Effects of low-head dams on riffle-dwelling fishes and macroinvertebrates in a midwestern river. Trans Am Fish Soc 133(3):705

Todd CR, Ryan T, Nicol SJ, Bearlin AR (2005) The impact of cold water releases on the critical period of post-spawning survival and its implications for Murray cod (Maccullochella Peelii Peelii): a case study of the Mitta Mitta River, southeastern Australia. River Res Appl 21(9):1035–1052

Trivedi RK, Goyal PK (1986) Chemical and biological methods for water pollution studies. Environmental Publications

Turner L, Erskine WD (2005) Variability in the development, persistence and breakdown of thermal, oxygen and salt stratification on regulated rivers of southeastern Australia. River Res Appl 21(2–3):151–168

Welch PS (1952) Limnology. McGraw-Hill, New York

Woodruff DS, Upatham ES (1992) Snail-transmitted diseases of medical and veterinary importance in Thailand and the Mekong valley. J Med Appl Malacol 4:1–12

Ziegeweid JR, Jennings CA, Peterson DL (2008) Thermal maxima for juvenile shortnose sturgeon acclimated to different temperatures. Environ Biol Fish 82(3):299–307

Zippin C (1958) The removal method of population estimation. J Wildlife Manag 22:82–90

Part II
Bio-remediation for Resource Enrichment

Effective Removal of Heavy Metals and Dyes from Drinking Water Utilizing Bio-compatible Magnetic Nanoparticle

Dwiptirtha Chattopadhyay and Keka Sarkar

Introduction

Heavy metal contamination in environment is being resulted mainly from natural weathering processes and anthropogenic activities. Freshwater chromium (Cr) concentrations are dependent on soil chromium levels in the surrounding watershed areas. Extensive industrial usage of chromium leads to generation of large volumes of chromium-containing wastes that are discharged into the environment. Chromium has been known to be extremely toxic at low concentration (Waalkes et al. 1992; Bruins et al. 2000), although they have no significant biological function so far reported. Malachite Green (MG) has effective application as an anti-fungal, anti-microbial and anti-parasitic agent in food industry (Afkhami et al. 2010) but the chemical causes toxic effects to human cells with mutagenic and carcinogenic properties as well.

Due to the low concentration of pollutants in water samples, separation and pre-concentration before instrumental analysis are very important. Nanoscale iron particles represent a new generation of environmental remediation technologies that could provide cost effective solutions to some of the most challenging environmental cleanup problems (Zhang 2003). They pose high surface area along with high surface reactivity and provide enormous flexibility for in-situ application. Iron nanoparticles are very effective for the transformation and detoxification of a wide variety of common hazardous contaminants. Application of magnetic property along with further surface modification of iron nanoparticle enhances the speed and efficiency of remediation.

D. Chattopadhyay • K. Sarkar (✉)
Department of Microbiology, University of Kalyani, Kalyani 741235, West Bengal, India
e-mail: keka@klyuniv.ac.in

© Capital Publishing Company 2015

N.J. Raju et al. (eds.), *Management of Natural Resources in a Changing Environment*, DOI 10.1007/978-3-319-12559-6_8

Typically iron nanoparticles are synthesized either by aqueous routes using co-precipitation of iron (II and III) salts (Bandyopadhyay et al. 2011) or by high temperature route using toxic iron pentacarbonyl compounds. Further purification of these particles is needed and surface modifications of these are also a laborious task. Here we demonstrate a low cost novel synthetic method for the preparation of a stable suspension of iron nanoparticles. One-pot synthesized mono-dispersed iron nanoparticles were characterized using UV-vis Spectrophotometer, DLS, TEM, SEM and its bio-compatibility has been checked on bacterial viability. The as-synthesized iron nanoparticles were then utilized for Cr(VI) and MG remediation from contaminated water.

Methodology

Reagents and Materials

All the chemicals and reagents used in this work were of analytical grade and purchased from Merck India. Double distilled water (DDW) made at our laboratory was used throughout the study. The stock solutions of Chromium (VI) (2.0 μg/mL) and of MG (50 mg/mL) was prepared in DDW and experimental solutions of their desired concentrations were obtained by successive dilutions of the stock solution with DDW. For measurement of Cr(VI) and Malachite Green (MG) DDW was artificially contaminated and was used for all the experiments.

Instrumentation

A dual beam Techcomp UV2300 UV-vis spectrophotometer was used for determining concentrations of Cr(VI) and MG in the water samples. Size distribution and Zeta potential (ζ) of the MNPs were characterized using transmission electron microscopy (TEM; Tecnai S-Twin, FEI, USA), scanning electron microscopy (SEM; S-2300, Hitachi, Japan) and dynamic light scattering (Zetasizer, Malvern Instruments Ltd, UK).

Bacterial Culture

Gram-negative *E. coli DH5α* and gram-positive *B. subtilis* were obtained from Department of Molecular Biology and Biotechnology, University of Kalyani. The bacteria were maintained and incubated in shaking incubators, using Luria-Bertani (LB) medium at a temperature of 37 °C.

Methods

Preparation of Magnetic Nanoparticles (MNPs)

The basic principle of our method for development of an MNP was reduction of ferrous sulfate with ammonia solution in presence of potassium nitrate. For this 0.1 g of ferrous sulfate was dissolved in 100 μL MiliQ water. In a separate container 0.1 g of potassium nitrate was dissolved in 1,000 μL of ammonia solution. Both solutions were mixed and instantly vortexed (mixed vigorously using a cyclomixer) for 10 min. During addition of ammonia to the ferrous solution the solution first turns green and after vigorous mixing black slurry is generated. Now the generated MNPs were maintained in a highly reducing (basic) medium for long storage and before application the MNPs were washed several times with MiliQ water. The MNPs are separated from impurities and excess ammonia by means of magnetic separation. After removal of impurities the MNPs are resuspended in 2,000 μL MiliQ water. These MNPs could be stored for at least a month in an airtight container without considerable oxidation.

Synthesis of Glutathione (GSH) Coated Iron Nanoparticle

100 mL 30 mM glutathione was prepared in water ($pH \approx 9.0 \pm 0.5$) and under constant steering condition (2,000 rpm) 1 g of as-synthesized iron nanoparticles were added. It was kept under constant steering condition for 120 min at room temperature. The glutathione coated iron nanoparticles were separated from excess unbound glutathione using magnetic decantation and washing with double distilled water for three times.

Synthesis of Sodium Dodecyl Sulfate (SDS) Coated Iron Nanoparticle

For SDS coating 5 % (w/v) SDS solution was prepared in 100 mL water and to it 1 g of iron nanoparticles were added slowly. During addition of the iron nanoparticles the SDS solution was kept under steering condition (at 515 rpm). After 120 min of steering the SDS coated iron nanoparticles were separated from the excess unbound SDS by magnetic decantation and it was washed with DDW for three to four times for complete removal of any unbound SDS.

Growth Experiment

The comparative study on growth of bacteria under normal condition and under the influence of magnetic nanoparticles has been carried out (Chatterjee et al. 2011). Various concentrations of nanoparticles (i.e. 100 μg/mL, 200 μg/mL) were added

into 50 mL LB medium containing *E. coli DH5α and B. subtilis inoculums separately, leaving one as a control to track the normal microbial growth and shaken at 180 rpm at 37 ± 2 °C. Optical density measurement* at 600 nm indicates the bacterial growth interacting with nanoparticle and the viability was determined from a plot of the log of the optical density versus time.

Uptake Studies of Chromium (VI) in Batch Process

Cr(VI) uptake studies have been performed in a batch process in which glutathionated iron nanoparticles were evaluated for chromium(VI) removal efficiency. Adsorption studies were performed by adding 25 mL of the solution in 100 mL Erlenmeyer flask containing different concentration (0.1–1.0) μg/mL of potassium di-chromate to 100 μg/mL and 200 μg/mL of GSH-loaded iron nanoparticles separately. The pH of the solutions and iron nanoparticles were separately adjusted at 7.0. Flasks were placed on a rotary shaker and shaken at 120 rpm at 37 ± 2 °C. After desired incubation (24 h), Cr(VI) loaded nanoparticles were separated with magnetic decantation and the supernatant has been analyzed for Cr(VI) concentration.

Chromium(VI) Analysis

Cr(VI) removal was measured as the decrease of chromate using Cr(VI) specific colorimetric reagent S-diphenylcarbazide (DPCZ). About 1 mL of 0.05 % DPCZ (w/v in acetone) was added to 1 mL of water sample and additionally 3 mL of 0.16 M sulfuric acid was poured for minimizing the deterioration (Urone 1955). A purple complex was formed due to the reaction of DPCZ with chromate. The absorbance was taken immediately at 540 nm in a spectrophotometer. Quantity of Cr(VI) was measured obtaining the calibration curve using potassium di-chromate ($K_2Cr_2O_7$) solution as standard.

Effect of pH on Cr(VI) Adsorption

Aqueous chromium solution (2 μg/mL) was adjusted to the required pH (3, 11) using 0.1 N HCl or 0.1 N NaOH. Flasks were shaken with 120 rpm at 37 ± 2 °C for required incubation time (24 h).

Absorption Studies of Malachite Green (MG)

MG uptake studies were performed in a batch process according to Afkhami et al. (2010) with some modification. Effect of pH has been studied with SDS iron nanoparticles as absorbent. Adsorption studies were performed by adding 25 mL of

the solution containing 0.1–2 μg/mL of MG to 1 g of SDS-loaded iron nanoparticles in an Erlenmeyer flask. The pH of the solutions and iron nanoparticles were separately adjusted at 3.0 using 0.1 m/L HCl and/or 0.1 m/L NaOH and the solutions were stirred for 24 h. The MG loaded nanoparticles were separated with magnetic decantation. The concentration of MG in the supernatant was monitored spectrophotometrically by measuring the absorbance of the solution at 627 nm.

Results and Discussion

The nanoparticle synthesized in the laboratory was characterized using a dual beam Techcomp UV2300 UV-vis spectrophotometer. The size of magnetic nanoparticle was found to be 8 nm by TEM image whereas the scanning electron microscopy (SEM; S-2300, Hitachi, Japan) revealed amorphous nature of the as-synthesized iron nanoparticle (Fig. 1). The DLS data indicated the Zeta potential (ζ) of nanoparticle and was found to be −26.9 mV.

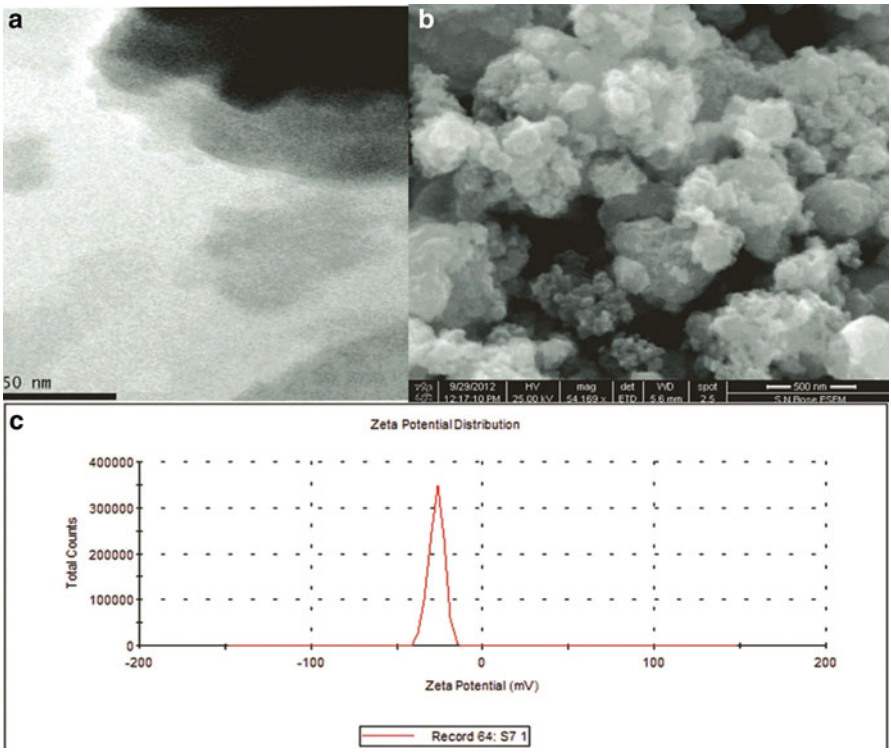

Fig. 1 TEM (**a**), SEM (**b**) images and zeta potential data (**c**) of the synthesized bare magnetic nanoparticles

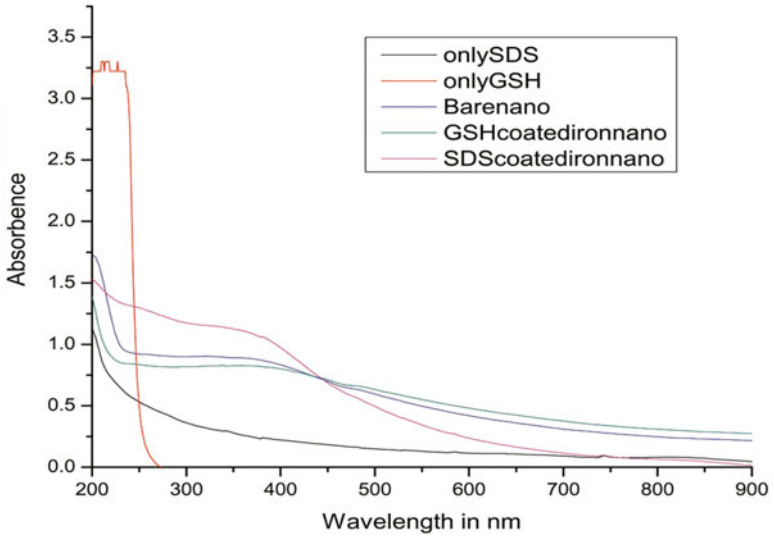

Fig. 2 UV-vis spectrophotometric data to demonstrate the surface fictionalization of iron nanoparticle by SDS and GSH with control

To investigate the effect of surface modification on absorption spectra, the surface modified nanoparticles were subjected into UV-vis spectrum and observed spectrophotometrically. Figure 2 shows the UV-vis absorption spectrum of bare nanoparticle, free SDS and SDS coated nanoparticle, Glutathione and Glutathione coated nanoparticle. The free glutathione exhibited a characteristic absorption peak at 280 nm (curve red). No absorption peak was observed for free SDS (curve black). However, the SDS (curve purple) and Glutathione (curve green) modified nanoparticle showed different absorption spectra compared with the bare nanoparticle (curve blue) and considered as successfully modified.

The growth curve data of *E. coli DH5α* and *B. subtilis* under normal condition clearly depicted the separate growth phases as shown in Fig. 3a, b) but under the influence of various concentration of iron nanoparticle (100 and 200 μg/mL), the log phase was shown to be affected for both species with increasing concentration of nanoparticle in negligible quantity, indicating the least toxic nature of the nanoparticle at the studied concentration.

Glutathione fictionalized nanoparticle was taken into Erlenmeyer flask under continuous shaking condition containing various concentration of potassium dichromate and the amount of Cr(VI) remained in the liquid phase after magnetic separation was determined spectrophotometrically against standard. The concentration of the nanoparticle has significant effect on the removal of Cr(VI) (Fig. 4i) and its role has been studied at various pH (3 and 11) (Fig. 4iia, b). Among the various concentrations of nanoparticle as adsorbent (100, 200 and 400 μg/mL), 200 μg/mL nanoparticle concentration was found to be maximum with respect to the Cr(VI) adsorption efficiency and this concentration was selected for further studies.

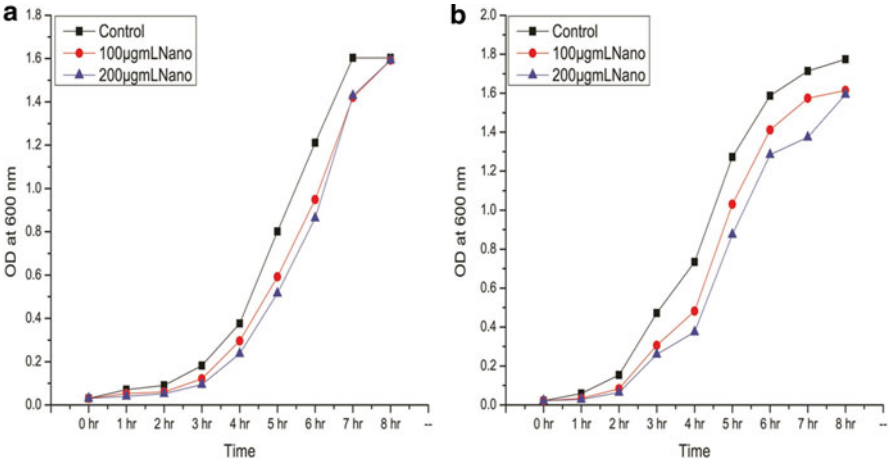

Fig. 3 Effect of bare iron nanoparticle on growth curve of *E. coli DH5α* (**a**) and *B. subtilis* (**b**) compared to the normal condition

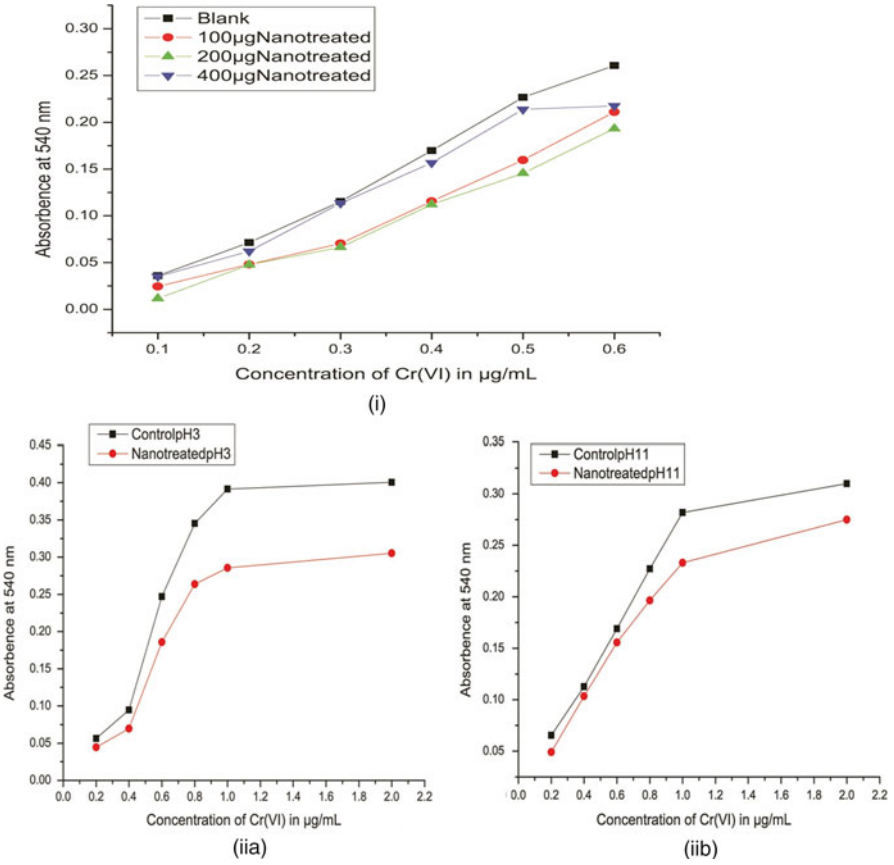

Fig. 4 GSH functionalized magnetic nanoparticle mediated chromium(VI) adsorption

Since the carboxyl (COO^-) of glycine residue electrostatically interacts with the positively charged iron nanoparticle to form glutathione modified iron nanoparticle, the free end (γ-glutamyl residue) of glutathione posses an amine group and a carboxyl group among which the amine group nonspecifically interacts with the negatively charged heavy metals forming a reversible electrostatic complex of Cr-Glutathione-iron nanoparticle hybrid.

In order to study the effect of pH (basic and acidic) on adsorption behaviour, glutathione fictionalized iron nanoparticle along with different concentration of potassium dichromate have been taken together into different flasks at pH 3 and pH 11 separately (Fig. 4iia, b). However, both pH 3 and 11 have shown to be the better adsorption condition but at pH 3 the adsorption capacity increases sharply. These results may be due to the fact that in the acidic pH, there is a competition between the chromate and amine group.

In another experiment in this study, SDS modified iron nanoparticle was employed for adsorption of MG as described by Afkhami et al. (2010). The as-synthesized amorphous nanoparticle which was developed in our laboratory by a novel method was found to be very useful when coated with SDS for removal of this dye. SDS being anionic surfactant will adsorb onto the surface of iron nanoparticle through the negative moiety of sulfate (Li et al. 2008) and makes the surface of the nanoparticle hydrophobic. The dye could be trapped into the aggregates of SDS on iron nanoparticle (Hiraide et al. 1994). The effect of different amount of SDS modified nanoparticle on the adsorption of MG was studied to determine the optimum amount for removal of MG in flask containing 1–2 μg/mL MG solution mixed with 200 $\mu g/mL$ SDS coated nanoparticle at pH 3. As Fig. 5 shows, the absorption of MG increased by increasing concentration of MG at constant adsorbent concentration. This result is consistent with

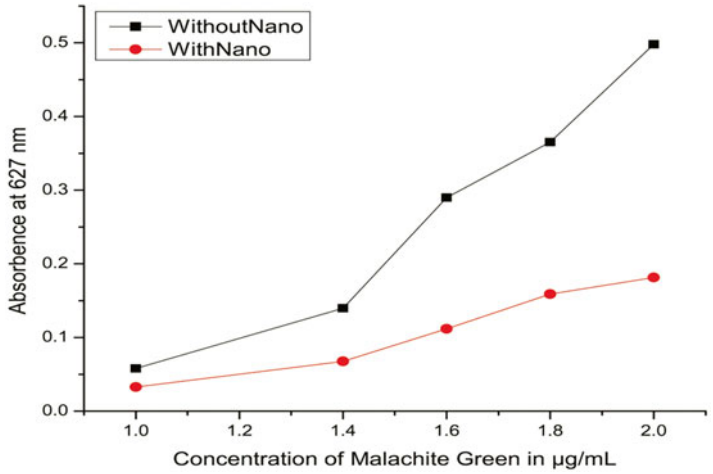

Fig. 5 SDS functionalized magnetic nanoparticle mediated Malachite Green (dye) adsorption

the report of Afkhami et al. (2010). The pK_a value for MG is 6.9 and in aqueous solution it has two cationic and colourless carbinol forms (Culp and Beland 1996). The balance between these two forms depends on the pH of the solution; the decrease in the positive charge of adsorbent surface sites can cause a decrease in the adsorption of SDS.

Conclusion

An efficient and effective system for heavy metals and dye removal from drinking water should meet several requirements like high adsorptive capacity, high rate of adsorption, selectivity etc. The functionalized nanomagnets described here remove heavy metals (Cr(VI)) and dye (MG) from contaminated water efficiently by adsorption and magnetic separation with excellent efficiency. It was found that the adsorption capability was increased by increasing the concentration of nanoparticles and it was pH dependent. This as-synthesized, surface functionalized novel iron oxide nanoparticle is very promising material as adsorbent and this convenient procedure is safe, rapid and inexpensive for removal of toxic compounds from water compared to the other troublesome methods. Further study to optimize the adsorption efficiency should be performed that would develop cost effective, reusable platform to mitigate the pollution.

Acknowledgement The research work has been carried out with the financial support of University Grant Commission, Govt. of India (Major Research Project-41-1178/2012(SR)) and University of Kalyani, Nadia, West Bengal. TEM facility was provided by Dr Pulak Ray, SINP, Kolkata.

References

Afkhami A, Moosavi R, Madrakian T (2010) Preconcentration and spectrophotometric determination of low concentrations of malachite green and leuco-malachite green in water samples by high performance solid phase extraction using maghemite nanoparticles. Talanta 82:785–789

Bandyopadhyay A, Chatterjee S, Sarkar K (2011) Rapid isolation of genomic DNA from E. coli XL1 Blue strain approaching bare magnetic nanoparticles. Curr Sci 101:210–214

Bruins MR, Kapil S, Oehma FW (2000) Microbial resistance to metals in the environment. Ecotoxicol Environ Saf 45:198–207

Chatterjee S, Bandyopadhyay A, Sarkar K (2011) Effect of iron oxide and gold nanoparticles on bacterial growth leading towards biological application. J Nanobiotechnol 9:34

Hiraide M, Sorouradin MH, Kawaguchi H (1994) Immobilization of dithizone on surfactant-coated alumina for preconcentration of metal ions. Anal Sci 10:125–128

Li J, Shi Y, Cai Y, Mou S, Jiang G (2008) Adsorption of di-ethyl-phthalate from aqueous solutions with surfactant-coated nano/microsized alumina. Chem Eng J 140:214–220

Urone PF (1955) Stability of colorimetric reagent for chromium, S-diphenylcarbazides in various solvents. Anal Chem 27:1354–1355
Waalkes MP, Coogan TP, Barter RA (1992) Toxicological principles of metal carcinogenesis with special emphasis on cadmium. Crit Rev Toxicol 22:175–201
Zhang W (2003) Nanoscale iron particles for environmental remediation: an overview. J Nanoparticle Res 5:323–332

UASBR: An Effective Wastewater Treatment Option to Curb Greenhouse Gas Emissions

Rajesh Singh and C.K. Jain

Introduction

Anaerobic digestion is used for treating high strength organic wastewater. Since late seventies, anaerobic digestion has experienced an outstanding growth in research and full scale application, particularly for the treatment of food and beverage industry effluent and to a lesser extent for municipal wastewater (Hulshoff-Pol et al. 1998; Yu et al. 2004; Fountoulakis et al. 2004; Filik-Iscen et al. 2007). Anaerobic digestion is a complex, natural, and multi-stage process in which organic compounds are degraded through a variety of intermediates into methane and carbon dioxide, by the activity of a consortium of micro organisms. Interdependence of the bacteria is a key factor in the anaerobic digestion process (Parawira et al. 2005) and the deciding factor for quality of treated effluent as well as gas generation.

The upflow anaerobic sludge blanket reactor (UASBR) is a reactor of upflow where the organic material on its way through the covering of sludge composed of a large population of anaerobic bacteria begins its biodegradation. The reactor is composed of three essential parts: a zone of digestion, a zone of sedimentation, and a separator of gas-solids-liquids. These are integrated into one column where the primary sedimentation process, the bio-digestion of the sludge and the secondary sedimentation is done simultaneously as a primary and secondary treatment of residual waters, achieving efficiency in the removal of organic material up to 85 % (Sponza 2001). Anaerobic digestion treatment is one of the technologies being considered to provide a solution to the treatment of high strength organic wastewater and maximum amount of biodegradable fraction can be converted into useful energy end product in the form of biogas and fertilizer in the form of digestate (Fernandez et al. 2001; Saravanan et al. 2004; Song et al. 2004).

R. Singh (✉) • C.K. Jain
Environmental Hydrology Division, National Institute of Hydrology, Roorkee 247 667, India
e-mail: rsingh@nih.ernet.in

© Capital Publishing Company 2015

N.J. Raju et al. (eds.), *Management of Natural Resources in a Changing Environment*, DOI 10.1007/978-3-319-12559-6_9

The upflow anaerobic sludge blanket process is one of the most commonly used wastewater treatment system, with several installations treating industrial wastewater (Techobanoglous et al. 2004).

Ion exchange resins consist of a polymeric matrix and a functional group with a mobile ion. The most common synthetic structures are: cross linked polystyrene, cross linked polymethacrylate, phenol-formaldehyde etc. The manufacture of ion exchange resins involve the preparation of a cross linked copolymer followed by sulfonation in the case of strong acid cation resins, or chloromethylation and amination of the copolymer for anion resins (Dow 2000). The production process involves use of variety of chemicals like styrene, divenyl benzene, ethylene glycol dimethacrylate, isobutyl alcohol, formaldehyde, methanol, ethylene dichloride, trimethyl amine, dimethyl amine, methacrylates, polyvinyl alcohol, oleum, etc. The unused solvents and chemicals make the effluent from the manufacturing process high in organics, total dissolved solids, and low in pH. The presence of different chemicals in the wastewater makes the treatment challenging and requires a cost effective as well as robust process with minimum GHG emissions to meet the international commitments.

The objective of the work was to study the anaerobic treatability and possibility of utilizing UASBR in order to optimize the operational cost, reduce green house gas emissions and convert waste into useful end products.

Methodology

Pilot Scale Digester

The UASB reactor was constructed from MS-FRP sheet with 2 m length, 1 m width and 4 m height. The working volume of the reactor was 7 m^3 (Fig. 1). Sampling ports were provided for the collection of samples. A centrifugal pump (Grundfos, Chiu) of capacity 5 m^3/h was used for feeding wastewater into the reactor. A HDPE tank of 500 L capacity was utilized as buffer tank.

Seed and Inoculation

The reactor was initially seeded with inoculum from an anaerobically digested sludge of a sewage treatment plant. On subsequent days, jaggery solution along with urea and DAP was added to obtain the desired mixed liquor suspended solids (MLSS) and mixed liquor volatile suspended solids (MLVSS) in the reactor. After achieving 4 % MLSS and 0.75 MLVSS/MLSS ratio, effluent injection at the rate of 0.5 m^3/day started for acclimatization of the micro organisms. The acclimation period in this study was 60 days.

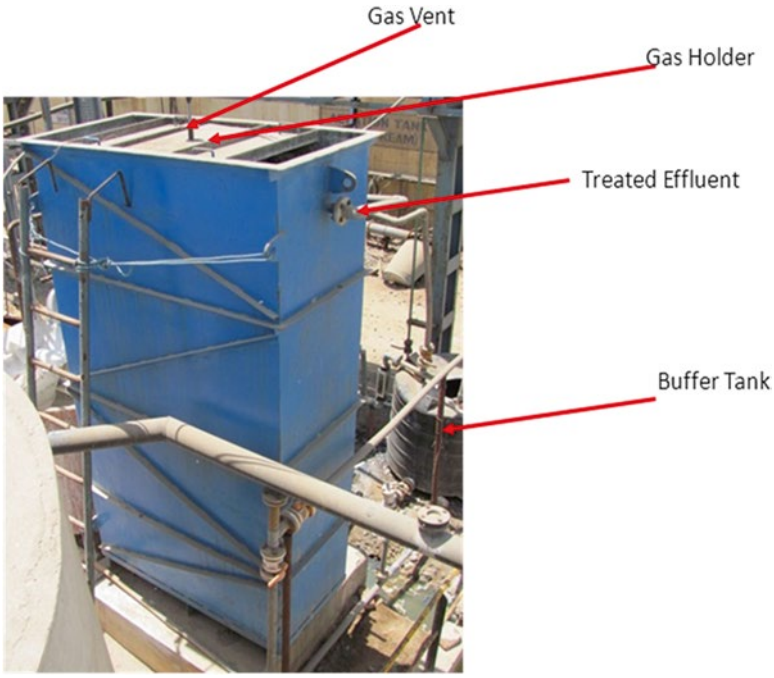

Fig. 1 Pilot upflow anaerobic sludge blanket reactor

Sampling and Analysis

The functioning of the reactor was monitored over a period of 4 months. The samples at feed, in the reactor and treated effluent were taken on regular basis to monitor the performance of the reactor. Chemical oxygen demand (COD), total suspended solids (TSS), total dissolved solids (TDS), MLSS and MLVSS were regularly analyzed for the untreated and treated effluent as well as sludge according to the standard methods (APHA 1995).

Operating Conditions

The reactor was operated in fill, react and withdrawal mode during initial period of operation. After stabilization of the process, the reactor was operated in continuous mode for a period of 3 months.

Results and Discussion

Characterization of Wastewater

The pilot plant was installed in the ion exchange resin manufacturing facility located in Ankleshwar, Gujarat to understand the actual operational conditions and the associated difficulties. The manufacturing facility was already having a state of the art effluent treatment facility consisting of collection tank, solids contact clarifier, aerobic reactor based on membrane technology and hence, it was decided to install the pilot plant after clarifier (Fig. 2) in order to get rid of suspended solids which are polymeric in nature and non-biodegradable and replicate the future condition. Hence, the samples were collected from the outlet of solids contact clarifier and the characterization is given in Table 1. The effluents were rich in organics with high COD (7,000–8,000 mg/L), BOD (2,500–3,500 mg/L) and TDS (15,000–25,000 mg/L) values. Presence of high organics in the wastewater was due to unused chemicals and washing of reactors. Apart from these harsh parameters, the BOD/COD ratio (0.3–0.35) is not very much favourable for biological treatment.

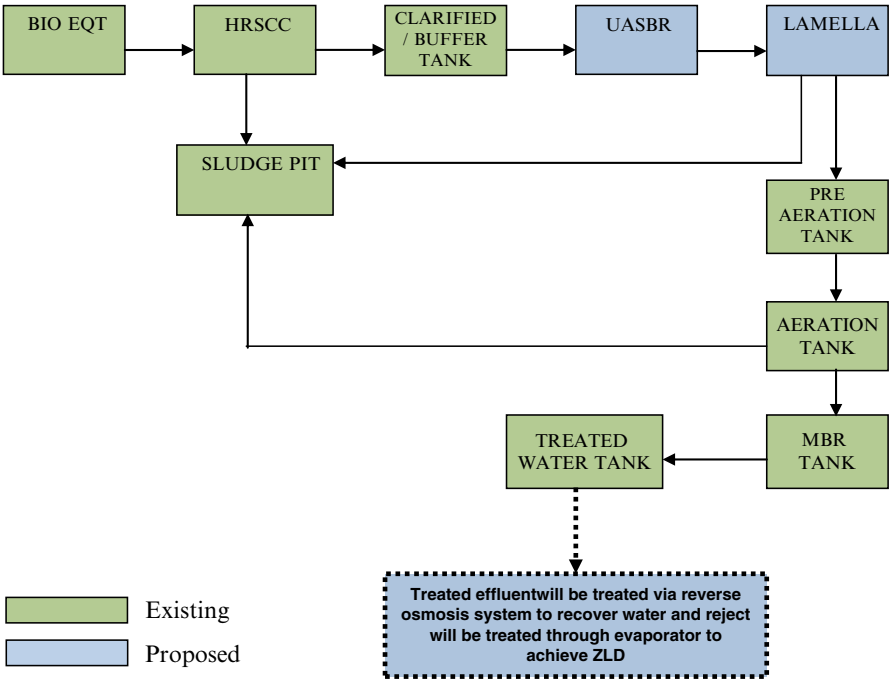

Fig. 2 Schematic diagram of effluent treatment plant for resin manufacturing facility

Table 1 Wastewater characteristics

Sr. No.	Parameters	Unit	Inlet
1	pH	–	7.0–9.0
2	Total dissolved solids	mg/L	15,000–25,000
3	Total suspended solids	mg/L	100–200
4	Volatile suspended solids	mg/L	50–150
5	COD	mg/L	7,000–8,000
6	BOD	mg/L	2,500–3,500
7	Oil and grease	mg/L	<30

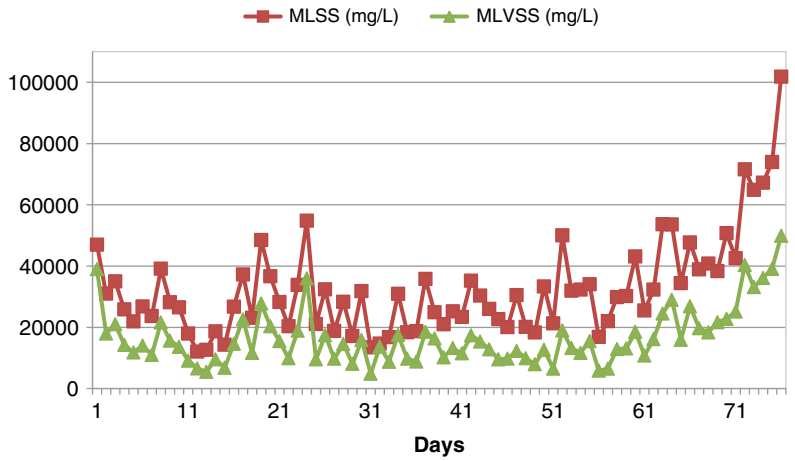

Fig. 3 MLSS and MLVSS trend

UASBR Performance

Acclimatization of micro organisms for the wastewater was judged from the analysis of MLSS and MLVSS in the reactor. MLVSS represents the micro organisms in the reactor, responsible for biodegradation of organics. The organic loading rate (OLR) was increased or decreased based on the MLVSS in the reactor. During start up phase, ups and downs were observed in the MLVSS value. If sharp reduction of 25 % in MLVSS value was observed during acclimatization period, part of wastewater feed was replaced with jaggery solution in order to maintain 0.5 food/microorganism (f/m) ratio. The process stabilized in 60 days and after that continuous increase in MLVSS was observed (Fig. 2).

OLR was always maintained above 1 kg COD/m^3/day by combination of organics supplied from process effluent and jaggery. Initial OLR from effluent was kept as low as 0.5 kg/m^3/day and increased in a stepped manner to 4.5 kg/m^3/day over a period of 75 days (Fig. 3). The process was found stabilized at this point and the system was operated for almost 1 month with this OLR. Consistency in the treated effluent was observed during this period.

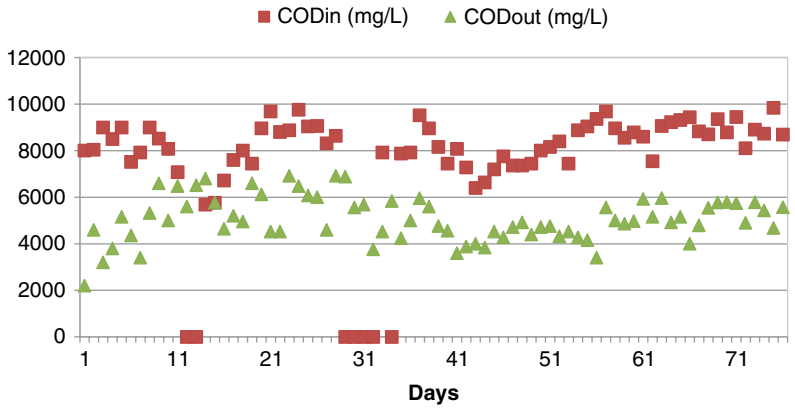

Fig. 4 COD profile over the trial period

Upflow velocity is regarded as one of the key parameter significantly affecting microbial ecology and characteristics of UASBR. It also helps in flushing the hazardous gases thereby keeping the system in healthy condition. The optimum upflow velocity for the wastewater and the system under study was found to be 0.5 m/h. In order to maintain the desired OLR and upflow velocity, the feed to UASBR is 4–5 times of the influent and hence the same was recycled back to buffer tank/UASBR feed tank. This also helps in minimizing the toxicity and shock load to UASBR.

The COD reduction in the initial phase of the start up was on the higher side due to higher percentage of COD from the jaggery which is easily biodegradable. COD reduction stabilized to 47–50 % (Fig. 4) which was desired by the manufacturing facility. COD reduction of 90–95 % was achieved with the combination of anaerobic followed by aerobic reactor, whereas only 85–90 % of COD reduction was observed with two-stage aerobic reactor. This may be due to presence of facultative micro organisms present in the reactor which releases certain enzymes which are able to convert high molecular aliphatic/aromatic compounds into smaller linear chain molecules which are easily biodegradable (Singh and Choubey 2012). Based on pilot plant observations, full scale plant was designed.

Cost Economics

The manufacturing unit was planning to increase the production of IX resins, which will lead to increase in flow as well as organic load to the ETP. The expansion of the manufacturing facility will lead to increase in the flow to ETP from 180 m^3/day to 240 m^3/day with marginal or no change in the COD and BOD. A cost comparison of UASBR against installation of an aerobic reactor was carried out which is presented in Table 2.

Table 2 Cost comparison for aerobic reactor versus UASBR

Sr. No.	2-stage aerobic reactor		Anaerobic followed by aerobic reactor	
1	Mechanical equipments			
	AT blower ($2 \times 1{,}200$ m^3/h)	5,60,000	UASBR feed pump (60 m^3/h)	68,000
	Sludge pump (2×10 m^3/h)	50,000	Sludge recirculation pump (1 m^3/h)	50,000
	Sec. clarifier mechanism	1,80,000	Lamella clarifier	5,00,000
	Diffuser (100)	4,50,000	UASBR internals + Gas flare system	40,00,000
	Total	**12,40,000**		**46,18,000**
2	Civil equipments @ 6,000 INR/m^3			
	Aeration tank (1,145 m^3)	68,70,000	UASBR tank (700 m^3)	42,00,000
	Sec. clarifier (60 m^3)	3,60,000		
	Total	**72,30,000**		**42,00,000**
	Grand total (1 + 2)	**84,70,000**		**88,18,000**
3	Operating cost @ 4.5 INR/kWh (INR/Annum)			
	AT blower	10,08,000	UASBR feed pump	1,41,000
	Sec clarifier mechanism	52,000	Sludge pump	29,000
	Sludge recirculation pump	42,000		
	Total	**11,02,000**		**1,70,000**

$$\begin{aligned}\text{Extra investment in case of UASBR} &= (88.18 - 84.70)\,\text{Lacs INR}\\ &= 3.48\,\text{Lacs INR}\\ \text{Savings in operating cost} &= (11.02 - 1.70)\,\text{Lacs INR}\\ &= 9.32\,\text{Lacs INR}\\ \text{Pay back period} &= 3.48 / 9.32\\ &= 0.37\,\text{year} = 4.5\,\text{months}\end{aligned}$$

The capital cost associated with the installation of anaerobic reactor is more than that of aerobic reactor for achieving almost similar reduction in organics but the operating cost is almost six times less which makes the UASBR a better choice for developing countries.

Reduction in GHG Emissions

The degradation of organics by anaerobic bacteria results in methane and carbon dioxide. Methane is a source of energy which can be utilized for heating requirements or power generation. Generation of methane and reduction in operating cost results in huge reduction of GHG emissions.

(a) Methane generation and power production

$$\begin{aligned}\text{COD reduction in the reactor} &= 3{,}500\,\text{mg/L} \times 240\,\text{m}^3/\text{day}/1{,}000\\ &= 840\,\text{kg/day}\\ \text{Approx. methane generation @ } 0.30\,\text{m}^3\text{CH}_4/\text{kg COD reduced}&\\ &= 0.30 \times 840 = 252\,\text{m}^3/\text{day}\\ &= 10.5\,\text{m}^3/\text{h}\\ \text{Power production} &= (\text{Vol. of methane} \times \text{cal. value} \times \text{engine eff.})/860\\ &= 10.5\,\text{m}^3/\text{h} \times 9{,}500\,\text{kcal/m}^3 \times 0.35/860\\ &= 40.6\,\text{kWh} = 974\,\text{kWh/day}\end{aligned}$$

(b) Power consumption of 1,494 kWh/day can be achieved due to installation of UASBR in place of aerobic reactor as provided in Table 3. This reduction is due to elimination of aeration tank blowers which are major power consumer in effluent treatment plant. Considering 330 days of manufacturing facility operation, the annual saving in power consumption results to 4,93,020 kWh.

(c) Total savings in power consumption $(a+b) = (3{,}21{,}420 + 4{,}93{,}020)$
$= 8{,}14{,}440\,\text{kWh/annum}$

(d) Considering, 1 tonne CO_2 is released with generation of 800 kWh electricity (www.carbonfootprint.com), reduction in GHG emissions for 8,14,440 kWh consumption is 1,020 tonnes per annum CO_2 emissions.

(e) To offset 1,020 tonnes of CO_2 emissions, 6,50,000–10,00,000 INR should be invested in clean energy and reforestation (Fig. 5).

Table 3 Power consumption comparison for aerobic reactor versus UASBR

Sr. No.	Equipments for aerobic reactor	Power consumption (kWh/day)	Equipments for UASBR	Power consumption (kWh/day)
1	AT blower	1,536	UASBR feed pump	85
2	Sec clarifier mechanism	35	Sludge pump	20
3	Sludge recirculation pump	28		
	Total	**1,599**		**105**

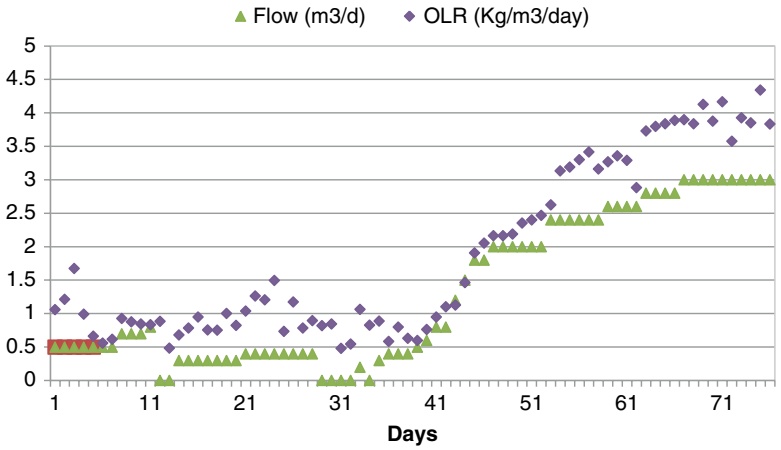

Fig. 5 Flow and OLR profile over the trial period

Conclusions

The results of the study reflect that UASBR is a cost effective option for the treatment of IX resin manufacturing facility wastewater. The process is able to degrade high molecular weight compounds through action of consortium of microorganisms. The optimum COD removal efficiency of reactor was 50 % corresponding to HRT and organic loading rate of 3 days and 4.5 kg/m^3/day respectively which is expected to improve over the extended period of operation. The stabilization/acclimatization period for the system is 60 days with sludge recycling option for reducing hazardous gases and to minimize shock loading. UASBR along with EASP results in COD reduction up to 95 %. Cost benefit analysis indicates that UASBR is a better choice if compared to extended aerobic reactors. Moreover, UASBR is helpful in reducing green house gas emissions and a natural option to minimize global warming.

Acknowledgements The authors gratefully acknowledge Ion Exchange (I) Ltd., Mumbai and Ankleshwar for providing the support and infrastructure required during study.

References

APHA (1995) Standard methods for the examination of water and wastewater. American Public Health Association, Washington, DC

DOW (2000) Fundamentals of ion exchange. DOW Chemical Company, Midland

Fernandez B, Porrier R, Chammy R (2001) Effect of inoculums-substrate ratio on the start up of solid waste anaerobic digesters. Water Sci Technol 44:103–108

Filik-Iscen C, Ilhan S, Yildirim ME (2007) Treatment of cake production wastewater in upflow anaerobic packed bed reactors. Int J Nat Eng Sci 1:75–80

Fountoulakis M, Drillia P, Stamatelatou K, Lyberatos G (2004) Toxic effect of pharmaceuticals on methanogenesis. Water Sci Technol 50:335–340

Hulshoff-Pol LW, Lens P, Stams AJM, Lettinga G (1998) Anaerobic treatment of sulfate rich wastewaters: microbial and process technological aspects. Biodegradation 9:213–224

Parawira W, Mutto M, Zvauya R, Mattasson B (2005) Comparative performance of a UASB reactor and an anaerobic packed bed reactor when treating potato waste leachate. Renew Energy 31:893–903

Saravanan R, Sivasankaran MA, Sundararaman S, Sivacoumar R (2004) Anaerobic sustainability for integration of sugar mill waste and municipal sewage. J Environ Sci Eng 46:116–122

Singh R, Choubey VK (2012) Removal of organics and colour from the wastewater of Denim industry. WARMICE 2012 proceedings, pp 605–611

Song YC, Kwon SJ, Woo JH (2004) Mesophilic and thermophilic temperature co-phase anaerobic digestion compared with single stage mesophilic and thermophilic digestion of sewage sludge. Water Res 38:1653–1662

Sponza DT (2001) Anaerobic granule formation and tetrachloroethylene (TCE) removal in an upflow anaerobic sludge blanket reactor. Enzym Microb Technol 29:417–427

Techobanoglous G, Burton F, Stensel HD (2004) Wastewater engineering: treatment and reuse. McGraw-Hill, New York

Yu Y, Park B, Hwang S (2004) Co-digestion of lignocellulosics with glucose using thermophilic acidogens. Biochem Eng J 18:225–229

Biogas Upgrading and Bottling Technology for Vehicular and Cooking Applications

Virendra Kumar Vijay, Rimika Kapoor, Abhinav Trivedi, and Pradip Narale

Introduction

Enhanced energy security and climate change mitigation are the main drivers for the transformation of the energy system from fossil to renewable sources. Biomass has to play a key role in this transformation to a low carbon economy. Worldwide, biomass accounts for more than two thirds of all renewable energy supplies. Among biomass sources, biogas is an interesting option with a large potential, offering many exciting possibilities to supplement and therefore reduce our dependence on fossil fuels.

Biogas is an energy source which is produced from biodegradable/organic wastes, and hence contributes simultaneously to waste management and to build a sustainable environment. Wastes of variable qualities and quantities, such as animal dung, agricultural wastes and municipal solid waste, are available in rural and urban areas. Biogas production is the most feasible option in developing nations as biogas can be produced at the same site as locally available wastes. The raw biogas can be upgraded using simple technologies and can be bottled, thus facilitating its use in applications such as domestic and commercial cooking, power generation via engines and as vehicular fuel. A specific advantage of biogas technology is in the utilisation of organic wastes and other organic by-products for energy production, as opposed to disposal via landfills, which inevitably leads to further emissions of greenhouse gases by the process of slow decomposition.

Biogas produced from anaerobic digestion is a green and cost effective replacement of wastes. Anaerobic digestion has the potential to meet the energy requirements in rural areas, and also counter the effects of reckless burning of biomass resources. An additional benefit is that the quantity of digested slurry is the same as

V.K. Vijay (✉) • R. Kapoor • A. Trivedi • P. Narale
Centre for Rural Development and Technology, Indian Institute of Technology Delhi, New Delhi 110016, India
e-mail: vkvijay@rdat.iitd.ac.in

© Capital Publishing Company 2015

N.J. Raju et al. (eds.), *Management of Natural Resources in a Changing Environment*, DOI 10.1007/978-3-319-12559-6_10

that of the feedstock fed in a biogas plant. This slurry can be dried and sold as high quality compost. This means increased income for the farmers.

Biogas Production in India

Small scale digestion plants using primarily animal wastes have seen widespread use throughout the world, with many plants in developing countries. These plants are generally used for providing raw biogas for cooking and lighting for households.

In India, widespread options of biomethanation organic wastes are available. Presently, out of 960 million tonnes of solid waste being generated annually, around 350 million tonnes are organic wastes generated from agricultural sources. A wide range of organic wastes are available which are widespread throughout the nation. Rapid industrialization and increase in population has resulted in the generation of huge quantity of wastes, both solid and liquid, in industrial sectors such as pulp and paper, fruit and food processing, sugar/starch, distilleries, dairies, tanneries, slaughterhouses, poultries, etc.

Despite requirements for pollution control measures, these wastes are generally dumped on land or discharged into water bodies, without adequate treatment, and thus become a large source of environmental pollution and health hazard. These include animal/agro waste, human waste, wastes from agro-based industries (paper and pulp production, sugarcane processing, distilleries, and other food and food-processing industries).

Biogas, therefore, is an obvious choice and has a very promising future in India due to the tropical location and very high population of livestock of over 300 million. Use of cattle dung is widespread in rural areas either as cooking fuel in the form of dung cakes or as compost. This resource, when used through biomethanation route, can provide biogas as clean fuel and digested slurry as good quality compost (Fig. 1).

An estimate indicates that India has the potential of generating 6.38×10^{10} Nm^3 of biogas from 980 million tonnes of cattle dung produced annually (Vijay et al. 2006). If organic wastes such as sewage, MSW, industrial effluent, and distillery wastes are also taken as feedstock for biogas production, the total biogas potential would increase further. There are around 300 distilleries throughout India which collectively have a potential of producing 1,200 million Nm^3 biogas, and 2,000 tannery units capable of producing 787,500 Nm^3 of biogas (MNRE 2001). The increasing number of poultry farms can also add to biogas productivity as with a current population of 649 million birds, another 2,173 million Nm^3 of biogas can be generated (Mittal 1996). Different categories of urban municipal and industrial organic wastes and their estimated quantity available in India are shown in Table 1.

Since there is widespread availability of organic wastes in India, biogas can be produced at different scales. India has a vast potential of biogas production

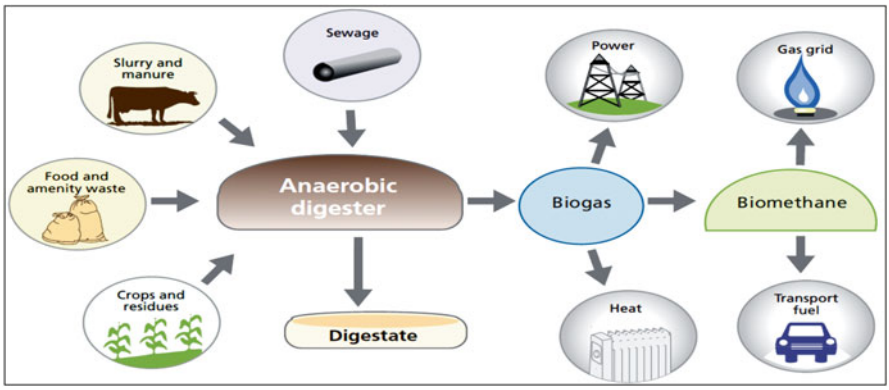

Fig. 1 Biogas production and utilization (*Source*: OGFEM 2011)

Table 1 Organic wastes and their estimated availability in India

Waste	Estimated quantity
Municipal solid waste	30 million tonnes/year
Municipal liquid waste	12,000 million litres/day
Distillery (243 units)	8,057 kilolitres/day
Press mud	9 million tonnes/year
Food and fruit processing wastes	4.5 million tonnes/year
Willow dust	30,000 tonnes/year
Dairy industry waste	50–60 million litres/day
Paper and pulp industry waste (300 mills)	1,600 m^3/day
Tannery (2,000 units)	52,500 m^3 waste water/day

Source: MNES Report, Renewable energy in India and business opportunities, MNES, Govt. of India, New Delhi, 2001

per annum from wide variety of organic waste produced. There are number of cattle farms, dairies, village communities having large number of cattle which have potential of producing biogas from medium to large scale. Large scale biogas can be produced in industries like distilleries, food processing, pulp and paper etc., sewage treatment plants and landfills in urban areas. Family size biogas plants are not considered as the amount of biogas produced is quite less in few cubic metres and is not viable for bottling. Resources like industrial wastes from distilleries, food processing, pulp and paper, waste water treatment plants and landfills etc. are also not taken into consideration as these produce large scale biogas which become viable for large scale biogas upgrading and bottling. Hence, for small scale biogas upgrading and bottling resources which have potential to produce medium and community level are considered like cattle manure, dairy farms, canteens, hostels, community toilets, institutional and community biogas plants etc.

Biogas Composition, Properties and Utilization

Raw biogas produced from anaerobic digestion is often around CH_4 55–65 % and CO_2 35–45 % (Persson 2003), with trace components of H_2S and moisture. Methane is extremely flammable. It combusts very cleanly with hardly any soot particles or other pollutants, making it a clean fuel. But CO_2, the non-combustible part of the biogas, lowers the calorific value of the biogas (de Hullu et al. 2008). On an average, the calorific value of biogas is 21.5 MJ/m^3 whereas that of biomethane is 35.8 MJ/m^3 (Aebiom 2009). Depending on the end use, different biogas treatment steps are necessary. For some applications like cooking and lighting, it is important only to purify biogas i.e. remove H_2S and moisture, whereas in some, e.g. as vehicle fuel or for grid injection, it is important to have a high energy content in the gas, the raw biogas needs to be purified as well as upgraded. The energy content of biogas is in direct proportion to the methane concentration; hence by removing carbon dioxide in the upgrading process the energy content of the gas is increased.

Need and Methods of Biogas Upgrading

Raw biogas produced from anaerobic digestion is often around 55–65 % methane and 35–45 % CO_2, with trace components of H_2S and moisture. Raw biogas is therefore not ideal for use as a vehicular fuel. The traces of H_2S produces H_2SO_4 which corrode the internals of pipes, fittings etc. The solution is to use biogas upgrading process, whereby other constituents such as carbon dioxide and hydrogen sulphide in the raw biogas stream are adsorbed in water, leaving above 90–95 % methane per unit volume of gas (Vijay 1989).

In different countries, there are different fuel quality standards for vehicle fuel use. This upgraded gas is generally referred to as biomethane and this is the term best representing upgraded biogas used in vehicles as opposed to the raw gas produced by the anaerobic digestion process. Gas upgradation and bottling is normally performed in two steps where the main step is the process that removes the CO_2 and H_2S from the gas followed by its moisture removal and compression at 200 bar. The processes used in biogas upgrading are reasonably well developed.

Despite several advantages, the biogas technology continues to suffer from certain limitations. Prime amongst these are the non-storability of biogas for longer period and use nearby plant only. It can be overcome if biogas is compressed and stored in cylinders like other gases, since liquefaction of biogas under normal conditions is not possible. But, biogas contains a sizable amount of CO_2, H_2S and water vapour, which have practically no use as fuel.

Presence of CO_2 in biogas poses following problems:

- It lowers the power output of the engine;
- It takes up space when biogas is compressed and stored in cylinder; and
- It can cause freezing problems at valves and metering points where the compressed gas undergoes expansion during engine running.

Removal of CO_2 enriches the biogas in terms of methane content. Methane burns faster and hence yields a higher specific output and thermal efficiency compared to raw biogas when used as engine fuel. Moreover absence of carbon dioxide in the gas will enable an additional volume of air to be inducted into the engine cylinder thereby improving the volumetric efficiency of the engine. H_2S usually amounts to less than 1 % on volume basis in cattle dung based biogas, which is very harmful. Its concentration more than this may cause corrosion in pipe lines and in engine. Also, biogas usually contains water vapour which enhances corrosion and decreases heating value of the fuel. Therefore, it is essential to enrich the biogas before compression by removing CO_2, H_2S and water vapour to make it a suitable engine fuel.

Compressing biogas reduces storage space requirements, concentrates energy content and increases pressure to the level needed to overcome resistance to gas flow. Sometimes the production pressure of a biogas source does not match the pressure requirements of the gas utilization equipment. Compression can eliminate the mismatch of pressures and guarantee the efficient operation of the equipment. Instead of raw biogas if enriched biogas is compressed, it will reduce the cost of compression. Also it will produce a gas with a high heating value, making it more suitable for uses in internal combustion engines and in particular automobile engines.

Biogas Upgrading Processes

A variety of processes are available for upgrading of methane content in biogas by removing insignificant contents for practical purposes i.e. carbon dioxide (CO_2), and hydrogen sulphide (H_2S). Most of these processes have been developed for use in the natural gas, petroleum and petrochemical industries. As a consequence, some of them may not be suited for biogas applications unless high flow rates are involved. Commonly CO_2 removal processes also remove H_2S.

Removal of CO_2 from Biogas

For an effective use of biogas as a vehicle fuel, it has to be enriched in methane. This is primarily achieved by carbon dioxide removal, which also provides a consistent gas quality with respect to energy value. A variety of processes are being used for removing CO_2 from natural gas in petrochemical industries. Several basic mechanisms are involved to achieve selective separation of gas constituents. The feasible processes of CO_2 removal from biogas can be split into following four groups. At present four different methods are used commercially for carbon dioxide removal, but the most common technologies for biogas upgrading are the water scrubber technology and the pressure-swing absorption technology.

- Absorption into liquid (Physical/Chemical)
- Adsorption on solid surface

- Membrane separation
- Cryogenic separation

Selection of the appropriate process for a particular application depends on the scale of intended operation, composition of the gas to be treated, degree of purity required and the need for CO_2 recovery.

Existing biogas upgrading systems are suitable and optimised for large-scale operations and hence demand high capital investment costs. Improvements in new and traditional techniques can lower investment and operational costs. For biogas upgrading, technologies such as water scrubbing, pressure swing absorption (PSA), chemical and physical absorption and cryogenic processing are commercially available and many others are at the pilot phase study level. The most widely used technologies for biogas upgrading are water scrubbing, PSA, organic physical and chemical scrubbing. Out of these technologies, water scrubbing and PSA are considered to be most appropriate at a small scale due to low cost and easy maintenance.

Hydrogen Sulphide Removal

Hydrogen sulphide is always present in biogas, although concentrations vary with the feedstock. It has to be removed in order to avoid corrosion in compressors, gas storage tanks and engines. Several methods have been developed. Based on the Swedish experience, air-oxygen dosing in the biogas and iron chloride dosing to the digester slurry are the most suitable for small-scale operations. For larger scale operations when upgrading to natural gas quality is the objective, chemical absorption of H_2S might become more feasible.

Moisture Removal

Several methods are available based on separation of condensed water or using gas drying. For upgrading to natural gas quality, gas drying techniques like refrigeration, PSA silica gel adsorption etc. is preferred.

Versatility of Biogas Use

Biogas can be divided into two grades: raw biogas (CH_4 55–65 % and CO_2 35–45 %) and upgraded ($CH_4 > 90$ % and <10 % other gases). Both forms of biogas have different approaches for utilisation as shown in Fig. 2. Raw biogas is a low-grade fuel as it has a lower percentage of methane and hence it is the cheapest fuel for rural people. It can be utilised on the site of production itself or nearby for cooking with biogas cook stoves and for electricity production by using it in dual fuel 100 % biogas engines. If raw biogas needs to be utilised at a distance from the production

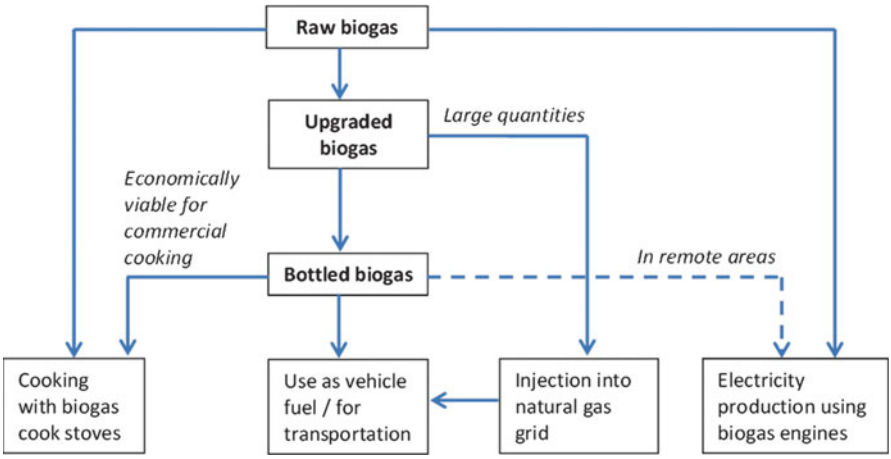

Fig. 2 Different uses of biogas

site then it must be stored in biogas balloons and taken to the site of utilisation or it can be transported by pipelines. Hence raw biogas being economical and easily available can fulfil the basic cooking and electricity needs of rural people.

Upgrading biogas widens the scope of its utilisation. When produced in centralised plants in large quantities, upgraded biogas can be injected directly into the natural gas grid and then dispensed into vehicles as a transport fuel. In developing countries, biogas is produced mainly in small to medium-size decentralised biogas plants, hence upgrading and then injection into the grid is not possible due to limitations in quantity and quality and cost constraints. For the purposes of feeding-in, however, the gas must meet the quality specifications of the relevant legal provisions and may only deviate within the range of these quality standards.

Adaptability of Bottled Biogas in Natural Gas Infrastructure and Network in India

With a large number of Indian cities implementing the natural gas vehicle programme, consumption has increased rapidly within the past decade. As per the Ministry of Petroleum, Government of India, India has an estimated current demand for natural gas of around 57.32 billion m^3 $year^{-1}$, which is made up of around 45.58 billion m^3 $year^{-1}$ from domestic supplies and the rest from imported LNG (Jain and Sen 2011). India's future demand for gas could reach 113.61 billion m^3 $year^{-1}$ by 2015 and 135 billion m^3 $year^{-1}$ by 2025, depending on how the gas market develops (Roychowdhury 2010). India currently has around 12,000 km of natural gas pipeline. Most of these gas pipelines are in the northern and western regions and much development is needed in southern, eastern and central regions. The network density is low when compared with some of the more developed natural gas markets.

Presently, the transportation sector in India, with around 1.1 million natural gas vehicles, consumes less than 2 % of the total natural gas consumption (MPNG 2012). It is expected that within the next decade the number of natural gas vehicles will increase to over 5.8 million. It is also expected that the pipeline network will increase to 15,000 km and implementation of city gas distribution networks will cover around 150–200 cities by 2014. This would further increase the share of natural gas imports to India (Roychowdhury 2010).

There are over 860 CNG service stations providing a blend of CNG and upgraded biogas (bio-CNG) to over 90,000 natural gas vehicles in some developed countries like Sweden and Germany; two of these stations only sell upgraded biogas (Power 2011). Such development is yet to begin in India, as no commercial upgraded biogas facilities are currently in operation.

CNG Conversion Kits

Upgraded biogas can be directly used in natural gas vehicles without any modifications in the engine architecture. If an existing petrol or diesel vehicle has to run on biogas, easily-available CNG conversion kits can be installed as shown in Fig. 3.

A CNG conversion kit is a set of components and tools that are installed in a vehicle so that it can operate using both petrol and CNG. These usually include parts such as regulator, high pressure tubing and fittings, pressure gauge, filling nozzle, hoses, hose clamps, closed loop fitting system, emulator, timing advance processor, fuel change over switch as well as the necessary wiring, straps and screws

Fig. 3 Car with CNG conversion kit (*Source*: http://naturalgasconversion.net/)

as shown in Fig. 3. The fuel change over switch allows the driver to switch from petrol to CNG with the flick of a button. CNG conversion kits usually do not include the CNG tank or cylinder or the cylinder valve, which are purchased separately. The price of a CNG conversion kit is usually in the range of Rs 40,000–65,000.

Creating a market for upgraded biogas takes time and there are many obstacles. As natural gas and upgraded biogas are interchangeable in vehicles, the two fuels may be used in parallel. In this way a market can be built up for biogas powered vehicles fuelled mainly by natural gas, and upgraded biogas can then be phased in as it becomes available in sufficient volumes. Natural gas as vehicle fuel reduces the CO_2 emissions by about 25 % compared to petrol because of the lower carbon content per energy value. Running vehicles on upgraded biogas may reduce overall CO_2 emissions even further, if the biogas comes from waste products.

Biogas Upgradation and Bottling Unit

IIT Delhi has successfully developed an automated biogas upgrading and bottling system as shown in Fig. 4. The aim of experimental work was to increase the efficiency and performance of the existing biogas upgrading and bottling facility at Indian Institute of Technology Delhi, according to the standard requirements for biogas bottling in India.

The system was modified for an automatic control so as to get biomethane of high purity (90–92 % methane) with relatively less losses of gases. This research work has focused on the study of biogas purification by water scrubbing, at ambient temperature (25 °C) using automated controls. Our principal goal was to identify an optimum column diameter and to optimize the pressure throughout the column. The purified

Fig. 4 Biogas upgrading and bottling plant at IIT Delhi

biogas with methane content of <90 % was bottled using high pressure compressor at 200 bar and filled in biogas operated car and three-wheeler using CNG dispensing system. The car was tested for its performance with biomethane as fuel.

Biogas Upgrading and Bottling Experimental Setup at IIT Delhi

To meet the gaps in existing biogas purification plant installed at Indian Institute of Technology Delhi, the research was done to minimize losses to yield high purity methane by automated controlling system. The whole setup was divided into two main components: (i) Packed tower for removal of CO_2 and H_2S and (ii) High-pressure compressor and cylinder cascade for storage of purified gas.

Packed Tower for Removal of CO_2 and H_2S

Water scrubbing based biogas upgradation system developed at IIT Delhi is shown in Fig. 5. Raw biogas is first compressed using intermediate compressor and fed to the bottom of the packed bed at 10 bar pressure. Rotor pump was used to pressurize water so as to get constant flow rate and then fed to the top of the packed bed. In the packed bed, gas and water come into contact and water physically absorbs the CO_2 of the biogas. Water sealing is maintained in the bottom section of tower in order to prevent the gas to escape from water outlet. Due to high turbulence inside the tower, purified gas contains water droplets with it; a mist eliminator is used to prevent it. Water coming from the packed tower goes in to a flash tower, which is hollow vessel at near atmospheric pressure. At the normal pressure, water releases the absorbed CO_2 and H_2S into another tower, where after further upgradation CO_2 can be used for other purposes. After releasing the absorbed gases, same water is recycled for further upgradation. The H_2S level of up to 1,000 ppm can be purified satisfactorily along with CO_2 in water scrubbing method.

Compression and Bottling Unit

Bottling consists of a high pressure compressor having suction at 0.1 bar, discharge pressure at 200 bar and having capacity 5 Nm^3/h. Compressed natural gas cylinders are used having water volume of 60 l capacity. Dispensing nozzle NZ type is used for filling the compressed purified gas in the vehicles. Dried and purified gas goes into the suction of high-pressure compressor, where it compresses the gas to desired (~20 Mpa) pressure and fill into the storage cylinders. In the system, a multi-stage compressor is used for the compression of methane-enriched biogas at 200 bar pressure in CNG cylinder. Pressure swing adsorption (PSA) is used for the moisture

Fig. 5 Modified purification plant

removal. The storage cylinders used are of high pressure, seamless, steel cylinders that are already being used for compressed natural gas (CNG) application (Fig. 6).

Policies and Regulations Pertaining to Biogas Bottling in Developing Economies

In India during 2008–2009, the Ministry of New and Renewable Energy (MNRE) undertook an initiative to demonstrate an integrated technology-package in entrepreneurial mode on medium size (200–1,000 Nm^3 day^{-1}) biogas fertiliser plants (BGFP) for generation, purification/upgrading, bottling and piped distribution of biogas. A 50 % subsidy of the total project cost for compressed biogas plant (Biogas Bottling) was extended for another six months by the MNRE, Government of India.

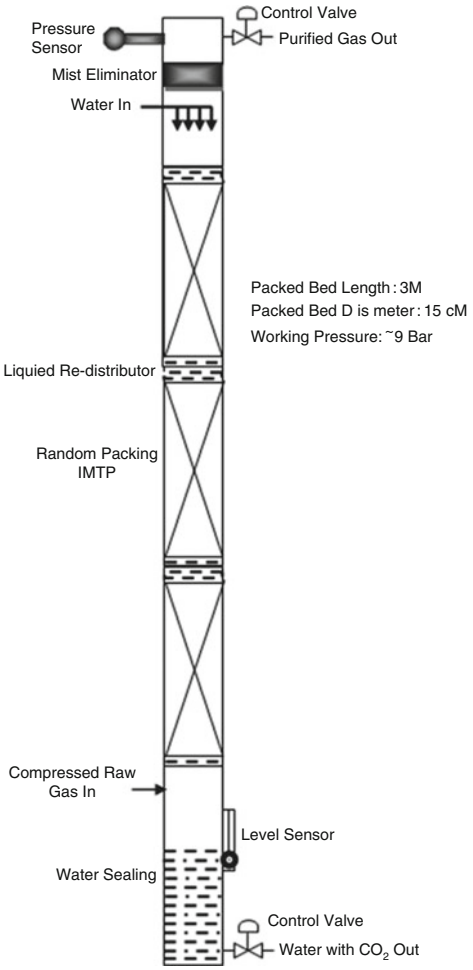

Fig. 6 Schematic diagram of modified packed bed tower

The available term loan was up to 30 % from financing institutions with a 20 % entrepreneur's share (MNRE 2011a, http://www.mnre.gov.in/mnre-2010/schemes/decentralized-systems/schems-2/). Installation of such plants aimed at production of Compressed Biogas (CBG) of the quality of Compressed Natural Gas (CNG) to be used as vehicle fuel in addition to meet stationary and motive power, cooling, refrigeration and electricity generation needs in a decentralised manner through establishment of a sustainable business model in this sector. The purified biogas, compressed at 200 bar pressure and filled into CNG cylinders for various applications, should be in accordance with the approval given by Petroleum Explosive and Safety Organisation (PESO) India (Annual Report, PESO 2011). A compressed biogas project is eligible to obtain Carbon Emissions Reduction certificates for methane avoidance and replacing fossil fuels (compression and utilisation of methane gas vehicle fuel). Standards for biogas composition have also been developed, and are being processed through Bureau of Indian Standards (BIS) (Figs. 7, 8, and 9).

Fig. 7 Upgraded compressed biogas dispensing nozzle and a two-cylinder CNG cascade

Fig. 8 Simple low cost upgraded biogas dispensing system

Fig. 9 Upgraded biogas dispensing system being used to fill biogas vehicle demonstrated at IIT Delhi

Table 2 Suggested standards for biogas composition in India

No.	Biogas component	Percentage
1	Methane (CH_4)	≥90 %
2	Carbon dioxide (CO_2)	≤4 %
3	Hydrogen sulphide (H_2S)	≤20 ppm
4	Moisture	≤0.02 g m^{-3}

In India, Bureau of Indian Standards has formulised standards for upgraded biogas use in stationary engines and in vehicles. But these standards can only be implemented if the other legal authorisations are fulfilled for the utilisation of biogas in vehicles or as a transport fuel. Standards for biogas composition have been developed and are being processed through Bureau of Indian Standards (BIS).

The purpose of these standards and policies is to provide general guidelines for the upgraded biogas composition, and its filling into CNG cylinders. In the proposed standards, the composition of purified biogas suitable for filling in CNG cylinders (at 200 bar) is as shown in Table 2.

Status of Biogas Upgrading and Bottling Plants Sanctioned by the Ministry of New and Renewable Energy

In India four pilot-scale biogas upgrading and bottling projects have been installed since 2006 where the bottled biogas is used as a vehicle fuel for captive use (MNRE 2011b, http://www.mrne.gov.in/mnre-2010/related-links/r-d/rd-projects/). Details of these are given in Table 3. Under the demonstration stage, the Ministry is providing central financial assistance (CFA) for implementation of projects on entrepreneurial mode. So far 21 biogas bottling projects with an aggregate capacity of 37,016 cum/day have been sanctioned in ten states in India which are Chhattisgarh, Gujarat, Haryana, Karnataka, Maharashtra, Punjab, Madhya Pradesh, Andhra Pradesh, Uttar Pradesh and Rajasthan (Bamboriya 2012).

Under technology demonstration of new RDD&D Policy of the Ministry of New and Renewable Energy (MNRE), the Ministry took up a new initiative for bottling of biogas to demonstrate an Integrated Technology-package in entrepreneurial mode on medium size (200–1,000 cum/day) mixed feed biogas-fertilizer plants (BGFP) for generation, purification/upgrading, bottling and piped distribution of biogas. Installation of such plants aims at meeting stationary and motive power, cooling, refrigeration and electricity needs in addition to cooking and heating requirements. There could be a huge potential of installation of medium size biogas-fertilizer plants in the country. Under the demonstration phase, the Ministry is providing a central financial assistance of 50 % of the cost (excluding cost of land) for a limited number of such projects for implementation following an entrepreneurial mode on Built Own and Operate (BOO) and re-imbursement basis.

Table 3 Biogas bottling in India at demonstration level

No.	Place	Substrate	Utilisation	Raw biogas composition	Purified biogas composition	Technology	Plant capacity ($Nm^3\ h^{-1}$ raw gas)	In operation since
1	Rajasthan Go Seva Sangh Plant, Jaipur	Cow dung	Vehicle fuel and electricity production for medicine making and lighting	55–60 % CH_4, 35–40 % CO_2	95 % CH_4, 3–4 % CO_2, H_2S below detectable level, 1–2 % other gases	Water scrubbing	20	2006
2	MGVAS Bhilwara Plant	Cow dung	Transport fuel in CNG vehicle electricity generation, battery charging for inverter operation	55 % CH_4, 32 % CO_2	95 % CH_4, 3–4 % CO_2, H_2S below detectable level, 1–2 % other gases	Water scrubbing	20	2008
3	Nasik, Maharashtra	Cow dung, agricultural waste etc.	Power generation, cooking and industrial application	55 % CH_4, 32 % CO_2	98 % CH_4, 1–2 % CO_2, H_2S below detectable level, 1–2 % other gases	Water scrubbing and pressure swing adsorption	Water scrubbing capacity: 20 Pressure swing adsorption (PSA) capacity: 50	2011
4	Abohar, Mukatsar, Punjab	Cow dung, agricultural waste etc.	Heating/cooking demand of the hotel industry nearby	55 % CH_4, 32 % CO_2	95 % CH_4 3–4 % CO_2, H_2S below detectable level, 1–2 % other gases	Water scrubbing	20	2010

Fig. 10 Water scrubbing and PSA system (*Left*) and Gas analyser system at Nasik (*Right*)

500 Nm^3 Nasik, Maharashtra—Bottled Biogas Used as a Fuel for Captive Vehicle

A 500 Nm^3 biogas generation per day capacity BGFP project for generation, upgradation and bottling of biogas was sanctioned by the MNRE with central financial assistance during the year 2009–2010 to Ashoka Biogreen Pvt Ltd at village Talwade, District Nasik, Maharashtra. The biogas bottling plant was commissioned on 16th March, 2011 after obtaining license for filling and storage of compressed biogas in CNG cylinders. The purified gas is filled in two cylinder cascades of 20 cylinders each (80 L capacity) using a high pressure compressor of 5 Nm^3/h. Upgraded biogas is used primarily to generate electricity and to provide energy to the entire plant. 5 KW CNG Kirloskar generators are installed for this purpose. The cylinders are filled upto 150 bar only, as per the license conditions. For experimental purpose, Ashoka Biogreen runs a CNG vehicle (TATA Magic) within its premises from the gas generated at the site since at present there are no regulations and authorizations for running vehicles on upgraded biogas in India (Fig. 10).

600 Nm^3 Abohar, Mukatsar (Punjab)—Bottled Biogas Used as a Commercial Cooking Fuel

Another project was sanctioned by the MNRE during the year 2009–2010 to Anand Energy for 600 Nm^3 per day biogas generation capacity for generation, upgradation and bottling of biogas. The plant is located at Abohar, Mukatsar (Punjab) and has started its operation after having received the consent to operate from Punjab Pollution Control Board and licence for filling and storage of compressed biogas in CNG cylinders. The biogas is produced by using UASB digesters and the biogas

Fig. 11 Biogas plant (*Left*) and Upgradation plant at Abohar (*Right*)

upgrading technology used is water scrubbing. Cylinder cascade is used for compressed biogas filling and stored at 15 MPa. The plant is producing purified biogas with methane composition of around 95 %. The purified gas is filled in cylinder cascades using a high pressure compressor and is being sold to meet the cooking demand of the hotel industry nearby (Fig. 11).

600 m^3 Tohana, Haryana—Bottled Biogas Used as a Commercial Cooking Fuel

The biogas fertilizer plant at Tohana, Haryana is owned by Shashi Energies. They procure 14 t/day cattle dung from the nearby villages and cattle farms. This dung is mixed with digester slurry and fed into a 600 m^3/day CSTR type biogas digester. The raw biogas from the digester is stored in a balloon of 200 m^3. The raw biogas is then fed into the low pressure water scrubbing tower operated at 0.8 bar. The capacity of the water scrubbing tower is 50 m^3/h. Upgraded biogas is compressed using a three-stage high pressure compressor and filled and stored in cascade of CNG cylinders. These cylinders are sold and used to replace commercial LPG cylinders in nearby hotels and restaurants. The biogas fertilizer plant is shown in Figs. 12 and 13.

At present in India there are no norms for using upgraded biogas in vehicles. There are strict regulations and legal authorisations required for dispensing biogas in vehicles. Also special permissions are required for filling biogas in CNG cylinders from legal authorities like CPCB, PESO etc.

Fig. 12 50 m^3/h low pressure water scrubbing tower

Fig. 13 Bottling of upgraded biogas in CNG cylinder cascade (*Left*) and bottled biogas being used for cooking (*Right*)

References

Aebiom (2009) A biogas road map for Europe. European Biogas Association, Aebiom

Annual Report (2010–2011) Petroleum and Safety Organisation (PESO). http://peso.gov.in/PDF/AR2010_11.pdf

Bamboriya ML (2001) Biogas bottling in India – a case study. Available from: http://mnre.gov.in/filemanager/UserFiles/casestudy_biogas_bottling_in_India_mlbamboria.pdfMNRE

Bamboriya ML (2012) Biogas bottling in India. Akshay Urja 5(5)

de Hullu J, Maassen JI, van Meel PA, Shazad S, Vaessen JM (2008) Comparing different biogas upgrading techniques. Dirkse Milieutechniek and Eindhoven University of Technology, Eindhoven

Jain A, Sen A (2011) Natural gas in India: an analysis of policy, Working paper. Oxford Institute for Energy Studies, Oxford

Mittal KM (1996) Biogas systems: principles and applications. New Age International (P) Limited, New Delhi

MNRE (Ministry of New and Renewable Energy) (2011a) http://www.mnre.gov.in/mnre-2010/schemes/decentralised-systems/schems-2/. Accessed Dec 2011

MNRE (Ministry of New and Renewable Energy) (2011b) http://mnre.gov.in/mnre-2010/related-links/r-d/rd-projects/. Accessed Nov 2011

MNRE Annual Report (2001) Renewable energy in India and business opportunities. MNRE (Ministry of New and Renewable Energy), Government of India, New Delhi

MPNG (2012) Basic statistics on Indian Petroleum and Natural Gas, 2011–12. Ministry of Petroleum and Natural Gas, India. http://petroleum.nic.in/petstat.pdf

OFGEM (2011) Bio-methane – a renewable gas source. Factsheet. http://www.ofgem.gov.uk/Media/FactSheets/Documents1/biomethanearenewablegassourceFS.pdf. Accessed Nov 2012

Persson M (2003) Evaluation of upgrading techniques for biogas. Lund School of Environmental Engineering, Lund. http://www.sgc.se/dokument/Evaluation. Accessed Sept 2012

Persson M, Jönsson O, Wellinger A (2006) Biogas upgrading to vehicle fuel standards and grid injection. IEA Bioenergy. Task 24. http://www.iea-biogas.net/_content/publications/publications.php. Accessed Sept 2012

Petersson A, Wellinger A (2009) Task 37—biogas upgrading technologies—developments and innovations. http://www.iea-biogas.net/_download/publi-task37/upgrading_rz_low_final.pdf. Accessed Sept 2012

Power G (2011) Potential of small to medium scale transport biomethane development in Ireland. In: Proceedings of the Irish Transport Research Network Conference, 31st August–1st September, University College Cork

Roychowdhury A (2010) CNG programme in India: the future challenges, fact sheet series. Centre for Science and Environment. http://www.cseindia.org/userfiles/cngfuture_pdf.pdf

Vijay VK (1989) Studies on utilisation of biogas for improved performance of duel fuel engine. ME (Ag.) thesis, CTAE, Udaipur

Vijay VK, Chandra R, Subbarao PMV, Kapdi SS (2006) Biogas purification and bottling into CNG cylinders: producing Bio-CNG from biomass for rural automotive applications. In: The 2nd joint international conference on Sustainable Energy and Environment, 21–23 November, Bangkok. http://balajibiopower.com/

Use of Indigenous Bacteria from Arsenic Contaminated Soil for Arsenic Bioremediation

Ivy Mallick, Sk Tofajjen Hossain, Sangram Sinha, and Samir Kumar Mukherjee

Introduction

Arsenic (As) is a ubiquitous element found in the earth's crust. It is now ranked first in a list of 19 hazardous substances by the Agency for Toxic Substances and Disease Registry and United States Environmental Protection Agency (Goering et al. 1999; Prerna et al. 2007). Among different chemical forms of As in the environment, the most often encountered toxic forms are arsenite [As(III)] and arsenate [As(V)] (Buchet and Lauwerys 1981; Leonard 1991; Mukhopadhyay et al. 2002). The abundance of different arsenic forms and its mobility in soil depends on several factors like pH, redox potential, presence of other elements, organic matter content, texture and biotic functions therein (Woolson 1977). When environmental conditions change, the speciation and mobility of arsenic may also change. As(III) is more toxic due to its affinity to bind with functional groups, like SH^- and imidazolium nitrogens of different biomolecules including catalytic proteins (Krumova et al. 2008). On the other hand, arsenate (AsO_4^{3-}) mimics phosphate (PO_4^{3-}); thus it affects cell metabolism by interfering with phosphorylation processes (Tseng 2004).

Due to irrigation of agricultural fields with As-contaminated groundwater, the concentration of As is also being increased in the crop fields, thereby creating a potential risk in lower Gangetic plain of Indian sub-continent (Rahman et al. 2007, 2008; Bhattacharya et al. 2009) including the sampling site, a paddy field of Nadia district, West Bengal, India, where the level of arsenic is above 0.05 mg/l (Bhattacharya et al. 2009), a level that is much above the WHO's recommended limit. To have an effective measure of increasing As pollution in the environment,

I. Mallick • S.T. Hossain • S.K. Mukherjee (✉)
Department of Microbiology, University of Kalyani, Kalyani 741235, WB, India
e-mail: dr.samirmukherjee@gmail.com

S. Sinha
Department of Botany, Vivekananda Mahavidyalaya, Haripal, Hooghly 712405, WB, India

© Capital Publishing Company 2015

N.J. Raju et al. (eds.), *Management of Natural Resources in a Changing Environment*, DOI 10.1007/978-3-319-12559-6_11

many procedures have been documented earlier (US EPA 2002). The need for low-cost and eco-friendly technologies for removing As from the environment is recently being emphasized. For survival under metal-stressed conditions, microorganisms have evolved several resistance mechanisms like exclusion, intra- and extra-cellular complexation, precipitation, volatilization, enzymatic oxidation/reduction, and adsorption (Nies 1999). Microbial isolates having either of the mechanisms would be useful to select a possible As bioremediating candidate.

The aim of the present study was to find an arsenic resistant indigenous bacterial isolate from paddy field rhizosphere soil irrigated with As-containing groundwater, which could effectively remove arsenic under aerobic culture condition and that can be used for bioremediation without the need for pre-processing. We found a *Brevibacillus* sp. strain KUMAs1, capable of removing arsenic, suggesting the possibility that it could be used for bioremediation of arsenic.

Methodology

Rhizosphere soil of paddy field, Nadia District, West Bengal, India (Fig. 1), was collected in sterile container to avoid any contamination. The pH value and organic carbon content of the soil sample were determined following standard method (Walkley and Black 1947; ASA 1982). Total As content in the soil sample was measured after acid digestion and was quantified by atomic absorption spectroscopy (AAnalyst 400, Perkin Elmer, Singapore).

Fig. 1 Geographic location of arsenic resistant bacterial strain KUMAs1 isolation site

Arsenic resistant bacterial strains were isolated from soil sample by serial dilution and plating on nutrient agar medium (HiMedia, India) supplemented with various concentration of arsenite (0.5–2 mM) as $NaAsO_2$ (HiMedia, India). The isolate which showed maximum level of As resistance (20 mM) was finally selected for further experiment. The isolate was then purified to have a pure culture by cycles of single colony isolation and liquid culture transfer on minimal broth (MB) supplemented with 2 mM As(III) and maintained for further experiment. The obtained bacterial isolate was designated as KUMAs1.

The isolate was identified based on the morphological and standard biochemical tests according to Bergey's Manual of Systematic Bacteriology (Sneath 1986). The ~1.309 Kb 16S rDNA fragment was amplified from the genomic DNA of KUMAs1 using 16S rRNA bacterial specific forward and reverse primer sets 5′-AGAGTYTGATC(AC)TGNCTYAG-3′ and 5′-TACGG(CT) TAYCTTGTNACRACYT-3′ respectively (Amnion Bioscience, India). The sequence data were aligned and analyzed using NCBI Blast function (Altschul et al. 1990) and Ribosomal Database Project (Maidack et al. 1997). The phylogenetic lineage of KUMAs1 was built from 16S rDNA sequence using MEGA 4.0 (Tamura et al. 2007).

Minimum inhibitory concentration (MIC) values of As(V) as $Na_2HAsO_4.7H_2O$ (HiMedia, India) and As(III) as $NaAsO_2$ (HiMedia, India) were determined in both Nutrient broth (NB) and MB having pH 7.2. Cells of KUMAs1 were grown in NB and MB initially for 14 h at 37 °C; 1 % culture (v/v) was inoculated in 5 ml of both media separately having different concentrations of As(III) (0–25 mM) and As(V) (0–500 mM) and incubated at 37 °C for 48 h. MIC was determined by counting colony forming units (CFU/ml) by serial dilution plating on respective medium. MIC values of other heavy metals like cadmium ($CdCl_2.H_2O$), zinc ($ZnSO_4.7H_2O$), chromium (K_2CrO_4), cobalt ($CoCl_2.6H_2O$) and nickel ($NiCl_2.6H_2O$) against KUMAs1 were also determined in NB and MB following the same procedure as mentioned above.

Twelve different antibiotics discs (HiMedia, India) namely, Tetracycline (30 µg/disc), Imipenem (10 µg/disc), Tobramycin (10 µg/disc), Polymyxin B (300 units), Ticarcillin/Clavulanic acid (75/10 µg/disc), Gentamycin (10 µg/disc), Amikacin (30 µg/disc), Netillin (30 µg/disc), Colistin (10 µg/disc), Ciprofloxacin (5 µg/disc), Kanamycin (50 µg/disc) and Ampicillin (50 µg/disc) were tested against KUMAs1 to determine the sensitivity on Mueller-Hinton agar medium (HiMedia, India).

Growth response of KUMAs1 under aerobic condition was determined in presence of As (2 mM) both in NB and MB supplemented with either in the form of As(V) or As(III) and compared with their respective control sets. The growth response was determined by counting the CFU/ml at different time intervals. The effect of pH and temperature on growth was also determined in MB supplemented with 2 mM of either As(V) or As(III).

For determining the effect of arsenic on cell morphology, cells of KUMAs1 were grown in NB medium for 14 h and 1 % culture (v/v) was later inoculated in fresh medium having 2 mM As(V) and 2 mM As(III), respectively and incubated for 4 h. Microscopic observation of the cells was carried out under a phase contrast

microscope (Leica DM 750, Germany). The cell morphology was compared with the cells grown without arsenic.

Reduction of As(V) to As(III) was studied following Hu et al. (2012). It was carried out in presence of 0.07 mM, 0.14 mM, and 0.21 mM of As(V) in MB inoculated with 1 % (v/v) of 14 h grown culture. The medium was incubated at 37 °C with shaking. The cell-free supernatant was used to determine the amount of As(III) produced through reduction. Due to limitation of the spectrophotometric method of arsenic species analysis, in this experiment such low concentration was used. The cell-free supernatants were obtained at intervals of 24 h by centrifugation (6,000× g, at 4 °C for 10 min). Cell-free extract (30 ml) was then acidified with 1 % HCl and 10 µM/l phosphate. Three parallel sub-samples, 10 ml each, were treated with 1 ml of an oxidizing reagent ($KMnO_4$), a reducing reagent (NH_4N_2S) and deionized (DI) water (untreated sub-sample), respectively. Sample treated with reducing agent was incubated at 80 °C for 30 min and cooled to room temperature. After 30 min, 1 ml colour reagent [a mixture of 10.8 % $C_6H_8O_6$; 3 % $(NH_4)_6Mo_7O_{24}.4H_2O$; 0.56 % $C_8H_4K_2O_{12}Sb_2.3H_2O$ and 13.98 % H_2SO_4 in a volume ratio of 2:2:1:5] was added to each sub-samples and the absorbance was measured after 5 min at 880 nm using a spectrophotometer. The As(III) and As(V) concentrations were calculated using the equations: Total As = Oxidized – Reduced; As (III) = Oxidized – Untreated; As (V) = Untreated – Reduced. The percentage of As(V) reduction by the biomass was calculated using the equation: $R(\%) = (Co - Ce) \times 100/Co$; Co and Ce are the initial and equilibrium concentration of arsenate (mg/l) in the solution, respectively.

To determine arsenic removal efficiency of KUMAs1, 1 % (v/v) of 14 h grown culture was inoculated in MB supplemented with 2 mM of either As(V) or As(III) and incubated for 96 h on a rotary shaker at 37 °C. Control sets were prepared with same concentration of either form of As but without inoculation to determine the artifacts might arise due to the metalloid sorption on the glass surface of the container. Cell pellet from each treatment regime were harvested by centrifugation at 6000× g for 10 min after 48 h, 72 h and 96 h of incubation. The cell pellets were then acid-digested and the total arsenic content in the digest was determined by atomic absorption spectroscopy. The As removal percentage by the biomass was calculated using the equation: $R(\%) = Ce \times 100/Co$; Co and Ce are the initial and equilibrium concentration of As (mg/l) in the solution and pellet respectively.

Results and Discussion

Soil Analysis

The pH, organic carbon and arsenic concentrations of the experimental soil were found to be 7.39, 0.83 % and 3.86 ppm (mg/kg soil), respectively. Average total As content in such kind of agricultural soil irrigated with ground water has earlier been reported to be between ~1.38 and 12.27 mg/kg (Bhattacharya et al. 2009).

Table 1 Phenotypic and biochemical characteristics of the isolate KUMAs1

Colony features on NA[a]	Cell morphology	Biochemical features and carbon source utilization	
		Negative	Positive
Off-white	Gram positive	Catalase /Amylase activities	Mannitol utilization
Punctiform	Rod shaped	Starch hydrolysis	IAA production
Smooth	Motile	Methyl red test	
Convex with entire edge	Endospore-forming H_2S production	Carbohydrate fermentation (glucose/ fructose/lactose/ sucrose)	
		Voges-Proskauer test	
		P-solubilization	
		Citrate utilization	
		Siderophore production	

[a]NA = Nutrient agar medium

Isolation and Characterization of As Resistant Bacteria

The isolated bacterial strain KUMAs1 was found to be gram-positive rod shaped, endospore forming and motile in nature. Morphological and biochemical features of KUMAs1 have been summarized in Table 1. Based on the biochemical tests and analysis of the 16S rDNA sequence (~1,309 bp) using BLAST function at NCBI database and Ribosomal Database Project, the isolate KUMAs1 was identified as a strain of *Brevibacillus* sp. (NCBI GenBank Accession No. KC460322). The phylogenetic lineage of KUMAs1 was constructed from 16S rDNA sequence using MEGA 4.0 (Fig. 2).

Toxic Metal and Antibiotic Sensitivity of KUMAs1

KUMAs1 showed varied degree of resistance to different heavy metals including arsenic and the order of toxicity in both the NB and MB was found to be Co > Zn > Cd > Ni > Cr > As(III) > As(V). Respective MIC values of different heavy metals tested are given in Table 2. The differences in MIC values in NB and MB might be attributed by the fact that metal bioavailability was reduced due to complexation with undefined components in the NB medium (Chatterjee et al. 2009); for the same reason magnitude of As resistance was found to be more in solidified medium. The bacterial strain was found to be sensitive to most of the antibiotics tested (Table 3) that offers the scope for using it as suitable bioremediating candidate, as there are many reports suggesting that metal contamination in natural environments could have an important role in the maintenance and proliferation of antibiotic resistance (Summers 2002).

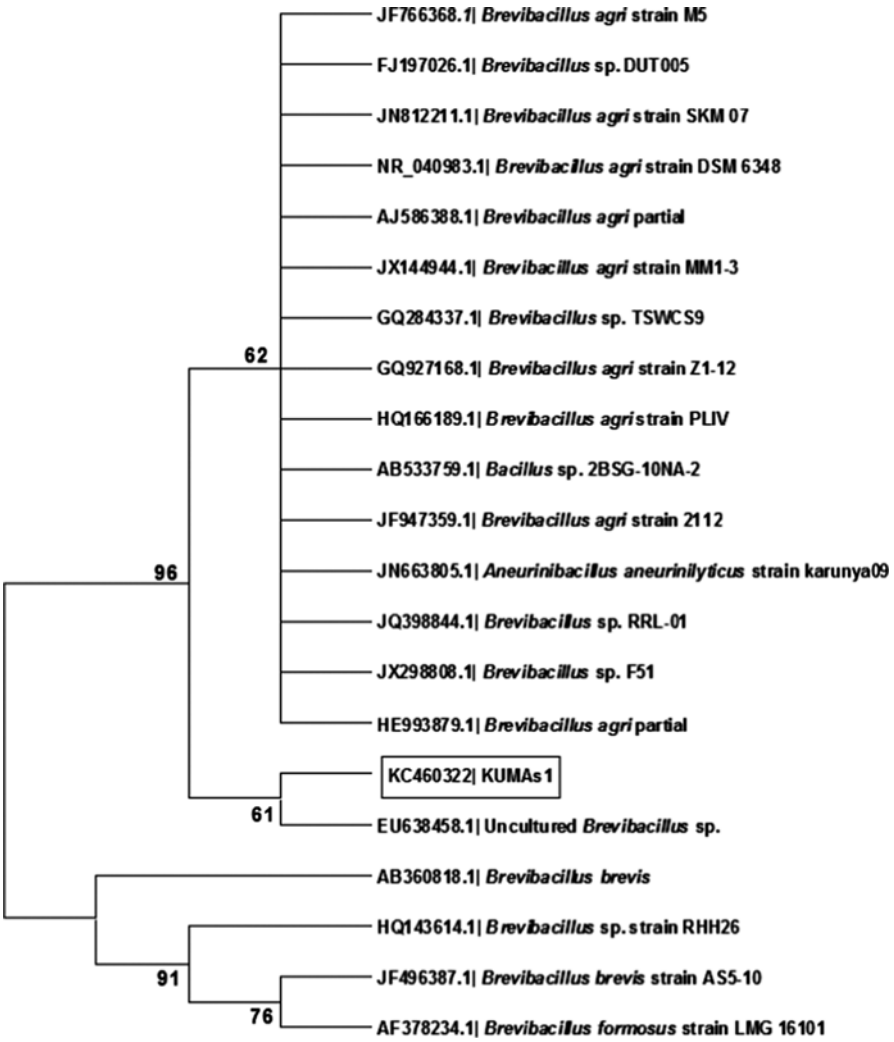

Fig. 2 Phylogenetic lineage of *Brevibacillus* sp. KUMAs1 showing relatedness with 20 closely related members based on 16S rDNA sequence comparison

Growth Response

The growth responses of KUMAs1 under As(III) or As(V) stress conditions both in NB and MB are presented in Fig. 3a, b. Due to reduced growth rate of KUMAs1 at higher level of As, in this experiment 2 mM concentration was used, which is much higher than that found in the rhizosphere soil. In NB medium after 2 h the strain showed steady state of growth but in MB log phase was achieved after 4 h of incubation both in presence and absence of As. KUMAs1 comparably grew well in

Table 2 Minimum inhibitory concentration (MIC) of the test metals to KUMAs1 in two different media

Metal tested	MIC values (mM) in	
	Nutrient broth	Minimal broth
As(III)	17	15
As(V)	395	355
Cd(II)	4	2
Zn(II)	2	1
Cr(VI)	15	9
Co(II)	1	0.2
Ni(II)	8	3

Table 3 Sensitivity of KUMAs1 to different antibiotics

Antibiotics discs	Diameter of inhibition zone (cm)
Tetracycline (30 µg/disc)	3
Imipenem (10 µg/disc)	3
Tobramycin (10 µg/disc)	–
Polymyxin B (300 units)	1
Gentamycin (10 µg/disc)	2.5
Amikacin (30 µg/disc)	2.2
Netillin (30 µg/disc)	2.7
Colistin (10 µg/disc)	–
Ciprofloxacin (5 µg/disc)	3
Kanamycin (50 µg/disc)	–
Ampicillin (50 µg/disc)	3.5
Ticarcillin/Clavulanicacid (75/10 µg/disc)	2.9

presence of 2 mM As(V) than in presence of equimolar As(III), which might be due to less toxicity of As(V) than As(III) to the strain. However, the requirement of As(V) for its growth warrants further investigation, as it grew better in presence of As(V) in comparison to the control set. Earlier it has been advocated that the microorganisms can use As(V) for their growth as electron acceptor suggesting possible mechanism of arsenic resistance (Ahmann et al. 1994; Anderson and Cook 2004). KUMAs1 grew optimally at 37 °C (Fig. 3c, d) and at pH 7.0 (Fig. 3e, f) in presence of either As(V) or As(III). In phase contrast microscopic study, the treated cells showed no difference in shape and size (Fig. 4) when compared with the cells of control set suggesting non-toxic effect of both forms of arsenic at that concentration.

Arsenate Reduction

Study of As(V) reduction was carried out in presence of 0.07 mM, 0.14 mM, and 0.21 mM of As(V) in MB as mentioned earlier. The strain grew well in presence of As(V) comparably with the control set and reduced As(V) optimally during steady

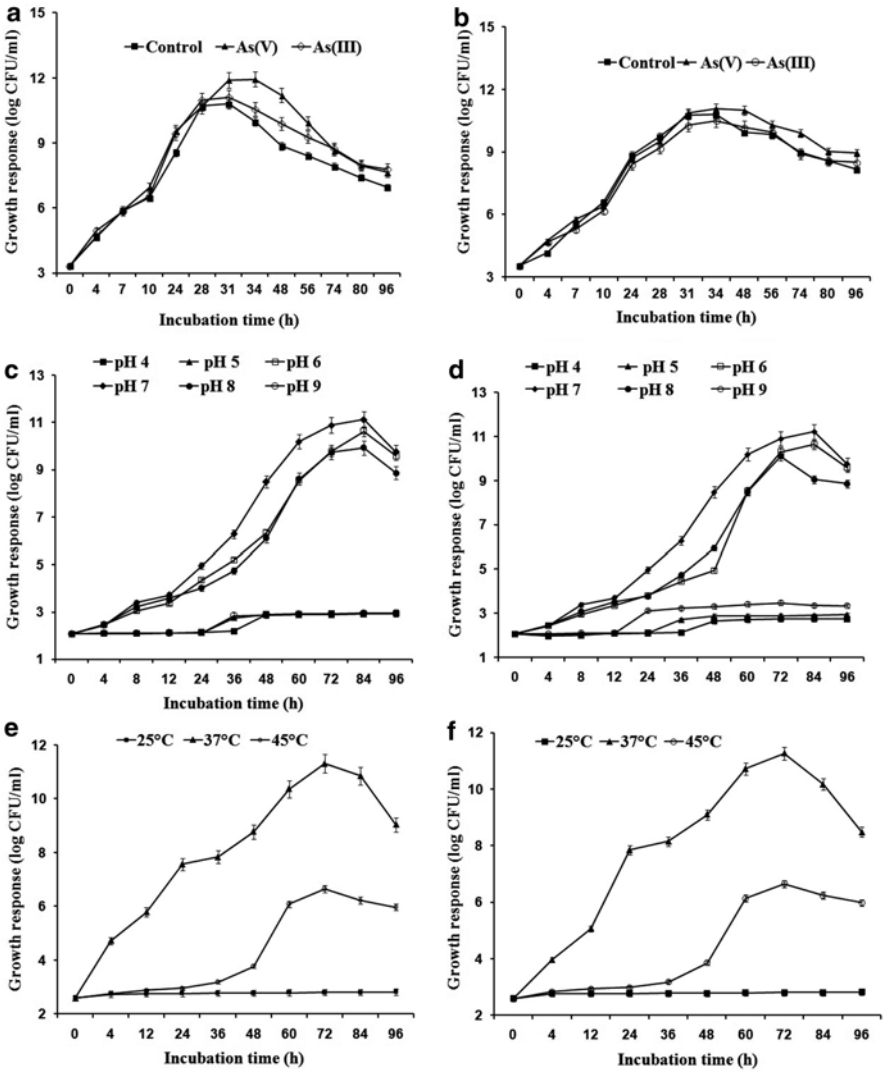

Fig. 3 Growth response of KUMAs1 in nutrient (**a**) and minimal liquid medium (**b**) supplemented with 2 mM As(III) and As(V); growth response of KUMAs1 under different pH in minimal medium supplemented with 2 mM arsenate (**c**) and 2 mM arsenite (**d**); and growth response of KUMAs1 under different temperature in minimal medium supplemented with 2 mM arsenate (**e**) and 2 mM arsenite (**f**). Data are the mean of three replications for each treatment regime with ±SD ($p = 0.05$)

growth phase. The As(V) reduction was found to be cell mass dependent in this strain, i.e. with increasing biomass As(V) reduction increased (Table 4). In the first 24 h the reduction rate was slowed irrespective of initial concentration of As(V). Growth response was found to be better at 0.21 mM and reduced ~33 % of As(V). But at lower concentration (0.07 mM) reduction rate was very slow and it was up to

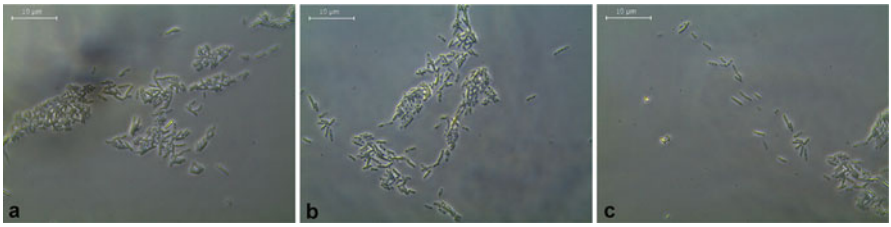

Fig. 4 Phase contrast micrographs of KUMAs1 cells grown in nutrient broth supplemented with 2 mM of arsenate (**b**) and 2 mM of arsenite (**c**) exposed for 4 h, and compared with untreated cells (**a**)

Table 4 As(V) reduction by KUMAs1 under aerobic culture condition with different initial As(V) concentration

Incubation time (h)	Growth and As(V) reduction versus initial concentration of As(V) in medium					
	0.07 mM		0.14 mM		0.21 mM	
	Growth[a]	% reduction	Growth	% reduction	Growth	% reduction
24	4.43	8.23	4.93	10.12	5.21	11.42
48	6.27	19.57	8.48	32.34	8.93	32.98
72	5.04	17.73	7.87	29.79	8.76	31.56
96	3.93	13.54	7.24	28.96	8.09	29.65

[a]Growth responses are presented as log number of CFU/ml. All the treatment regimes were inoculated with same inoculum load as stated

~20 % after 48 h of incubation, which might be due to reduced growth. It seems at lower concentration, growth phase was lengthened and thus slowed down As(V) reduction. The result also indicates that minimum amount of As was needed for the substantial growth of the bacteria as stated earlier. It was also earlier suggested that the bacteria capable of As(V) reduction might be used as possible arsenic bioremediation candidates in arsenic-contaminated environment (Bachate et al. 2009; Banerjee et al. 2011; Jareonmit et al. 2012).

Arsenic Removal

In this study, total As removal was found to be significantly higher in comparison to the As(V) reduction by the active cell mass of KUMAs1 under culture condition. The amount of As removal by KUMAs1 increased with increasing cell mass (Table 5). After 48 h of incubation, cell mass removed ~55 % and ~56 % of total As when the medium was supplemented with As(III) and As(V) respectively. It seems KUMAs1 could remove As following the same mechanism as hypothesized by Miyatake and Hayashi (2009) in case of *Bacillus megaterium* strain UM-123, which could reduce As(V) under aerobic conditions and could also remove As by adsorption.

Table 5 Growth response versus as removal by KUMAs1 under aerobic culture condition

	Growth and As removal			
	As(III)		As(V)	
Incubation	Growth[a]	% removal	Growth	% removal
48	9.19	54.67	10.24	56.13
72	8.93	51.22	9.09	50.95
96	7.51	35.34	7.95	37.89

[a]Growth responses are presented as log number of CFU/ml

All the treatment regimes were inoculated with same inoculum load as stated

Conclusions

It appears that strain KUMAs1 is effective in removing As under aerobic conditions, though it showed As(V) reducing ability. Furthermore, this activity is maintained even at low concentrations of As. Based on the present study, it seems that KUMAs1 could be used as potential As bioremediating candidate. Being an indigenous isolate, KUMAs1 might be assumed to have better rhizosphere colonizing ability in the paddy field; additional feature of this isolate makes it important that it could produce IAA, thus it might be used as biofertilizer candidate as well. Though, its efficiency under environmental condition conducive for decontamination of arsenic requires further investigation.

Acknowledgements This work was supported by the financial grants received from DST, Govt. of India under INSPIRE Programme and DBT, Govt. of India.

References

Ahmann D, Roberts AL, Krumholz LR, Morel FMM (1994) Microbe grows by reducing arsenic. Nature 371(6500):750

Altschul SF, Gish W, Miller W, Myers EW, Lipman DJ (1990) Basic local alignment search tool. J Mol Biol 215(3):403–410

Anderson CR, Cook GM (2004) Isolation and characterization of arsenate-reducing bacteria from arsenic-contaminated sites in New Zealand. Curr Microbiol 48:341–347

ASA (1982) Methods of soil analysis. Part 2. Chemical and microbiological properties, 2nd edn. Page AL (ed). Agronomy Society of America, Madison

Bachate SP, Cavalca L, Andreoni V (2009) Arsenic-resistant bacteria isolated from agricultural soils of Bangladesh and characterization of arsenate-reducing strains. J Appl Microbiol 107:145–156

Banerjee S, Datta S, Chattyopadhyay D, Sarkar P (2011) Arsenic accumulating and transforming bacteria isolated from contaminated soil for potential use in bioremediation. J Environ Sci Health A Tox Hazard Subst Environ Eng 46:1736–1747

Bhattacharya P, Samal AC, Majumdar J, Santra SC (2009) Transfer of arsenic from groundwater and paddy soil to rice plant (*Oryza sativa* L.): a micro level study in West Bengal, India. World J Agric Sci 5(4):425–431

Buchet JP, Lauwerys R (1981) Evaluation of exposure to inorganic arsenic in man. Analytical techniques for heavy metals in biological fluids. Elsevier, Amsterdam

Chatterjee S, Sau GB, Mukherjee SK (2009) Plant growth promotion by hexavalent chromium reducing bacterial strain, *Cellulosimicrobium cellulans* KUCr3. World J Microbiol Biotechnol 25:1829–1836

Goering PL, Aposhian HV, Mass MJ, Cebrian M, Beck BD, Waalkes MP (1999) The enigma of arsenic carcinogenesis: role of metabolis. Toxicol Sci 49(1):5–14

Hu S, Lu J, Jing C (2012) A novel colorimetric method for field arsenic speciation analysis. J Environ Sci 24(7):1341–1346

Jareonmit P, Mehta M, Sadowsky MJ, Sajjaphan K (2012) Phylogenetic and phenotypic analyses of arsenic-reducing bacteria isolated from an old tin mine area in Thailand. World J Microbiol Biotechnol 28(5):2287–2292

Krumova K, Nikolovska M, Groudeva V (2008) Characterization of arsenic-transforming bacteria from arsenic contaminated sites in Bulgaria. Biotechnol Biotechnol Equip 22(2):729–735

Leonard A (1991) Arsenic. Metals and their compounds in the environment. VCH, Weinheim

Maidack BL, Olsen GJ, Larson N, Overbeek R, McCaughey MJ, Woese CR (1997) The RDP (Ribosomal Database Project). Nucleic Acids Res 25(1):109–111

Miyatake M, Hayashi S (2009) Characteristics of arsenic removal from aqueous solution by *Bacillus megaterium* strain UM-123. J Environ Biotechnol 9(2):123–129

Mukhopadhyay R, Rosen BP, Phung T, Silver S (2002) Microbial arsenic: from geocycles to genes and enzymes. FEMS Microbiol Rev 26:311–325

Nies DH (1999) Microbial heavy metal resistance. Appl Microbiol Biotechnol 51:730–750

Prerna CP, Goulhen F, Boothman C, Gault AG, Charnock JM, Kalia K, Lloyd JK (2007) Arsenate detoxification in a *Pseudomonad* hypertolerant to arsenic. Arch Microbiol 187(3):171–183

Rahman MA, Hasegawa H, Rahman MM, Rahman MA, Miah MAM (2007) Accumulation of arsenic in tissues of rice plant (*Oryza sativa* L.) and its distribution in fractions of rice grain. Chemosphere 69:942–948

Rahman MA, Hasegawa H, Rahman MM, Miah MAM, Tasmin A (2008) Arsenic accumulation in rice (*Oryza sativa* L.): human exposure through food chain. Ecotoxicol Environ Saf 69:317–324

Sneath P (1986) Endospore-forming Gram-positive rods and cocci. In: Sneath PHA, Mair NS, Sharpe ME, Holt JG (eds) Bergeys manual of systematic bacteriology. Williams and Wilkins, Baltimore

Summers AO (2002) Generally overlooked fundamentals of bacterial genetics and ecology. Clin Infect Dis 34:S85–S92

Tamura K, Dudley J, Nei M, Kumar S (2007) *MEGA4*: Molecular Evolutionary Genetics Analysis (MEGA) software version 4.0. Mol Biol Evol 24(8):1596–1599

Tseng CH (2004) The potential biological mechanisms of arsenic induced diabetes mellitus. Toxicol Appl Pharmacol 197:67–83

US EPA (2002) Arsenic treatment technologies. United States Environmental Protection Agency. EPA 542, pp 2–4

Walkley A, Black IA (1947) A critical examination of a rapid method for determining organic carbon in soil: effect of variation in digestion and inorganic soil constituents. Soil Sci 63:251–264

Woolson EA (1977) Fate of arsenicals in different environmental substrates. Environ Health Perspect 19:73–81

Adsorption of Arsenite and Fluoride on Untreated and Treated Bamboo Dust

Sanjoy Kumar Nath and Krishna G. Bhattacharyya

Introduction

Pollution of water with anionic contaminants represents an important environmental concern due to the toxicity of these ions and their accumulation throughout the food chain. The fresh water wealth of India is under threat due to variety of natural and human influences. The high concentration of some toxic elements in anionic state such as fluorine as fluoride, and arsenic as arsenite and arsenate, etc. is of concern as they cause serious health hazards.

Of all chemical elements in the Periodic Table, fluorine is the most electronegative and the most reactive element. Because of its great reactivity, fluorine cannot be found in nature in its elemental state, it exists as fluorides. It occurs in nature and it is an essential constituent for both humans and animals in low concentration (Liang et al. 2006). Fluorine, a fairly common element of the earth's crust, is present in the form of fluorides in a number of minerals and in many rocks and hence it can be leached out by rainwater thereby allowing it to contaminate ground and surface water. On the other hand, several fluoride compounds have industrial applications (e.g. it is extensively used in semiconductors, fertilizers, aluminium industries, and nuclear applications) and are used widely and these also contribute to fluoride pollution (Oguz 2005).

Fluoride in drinking water has dual significance. If its content is less than the permissible limit, it may result in problems like dental caries. On the other hand, excess fluoride in drinking-water causes harmful effects such as dental and skeletal fluorosis. World Health Organization (WHO) recommends a permissible range of 0.1–1.5 mg/L. The standard for India is between 1 and 1.5 mg/L. Thus, the requirement of fluoride content varies among countries and depends on the geography and the age

S.K. Nath • K.G. Bhattacharyya (✉)
Department of Chemistry, Gauhati University, Guwahati 781014, Assam
e-mail: kgbhattacharyya@gmail.com

© Capital Publishing Company 2015

N.J. Raju et al. (eds.), *Management of Natural Resources in a Changing Environment*, DOI 10.1007/978-3-319-12559-6_12

of people involved. The high fluoride levels in drinking water and its impact on human health in many parts of India have increased the importance of defluoridation studies.

Arsenic and its compounds are well known poisonous substances and are widely distributed in the earth crust, which is the main cause of epidemiological problems to human health. The most common arsenic species found in aqueous media are the oxoanions of arsenate and arsenite. Arsenic contamination is a serious environmental problem, and its increasing concentration in natural water has been reported in many areas all over the world including in large areas in Bangladesh (Yokota et al. 2001) and West Bengal of India (Maiti et al. 2007). Recent reports reveal that groundwater of North Eastern India especially that of the Assam valley are affected by arsenic contamination especially in the districts of the Brahmaputra flood plain viz. Barpeta, Dhemaji, Dhubari, Darrang and Golaghat.

Arsenic in water is removed by different methods, viz. precipitation with lime, co-precipitation with ferric sulfate, precipitation with alum or with sodium sulfide and hydrogen sulfide. Iron coprecipitation method has been reported as one of the most successful methods in lowering the arsenic content to drinking water standard level, but it suffers from the post-treatment problem of disposal of the alkaline sludge produced during the treatment (Ghimire et al. 2003). A number of other adsorptive materials, such as impregnated activated carbon (Chang et al. 2010), activated alumina (Su et al. 2008), exchange resin (Issa et al. 2011), low cost (Chakravarty et al. 2002) and natural materials (Jordan et al. 2009; Gimenez et al. 2010), have been more or less successfully tested for the removal of toxic anions (Szlachta et al. 2012).

During the last few years, many low cost materials, such as waste orange peel, banana pith, bottom ash, de-oiled soya, rice husk, kaolin, bentonite clay, neem leaf powder, powdered activated sludge perlite, powdered peanut hull, natural and modified clays like sepiolite, zeolite, saw dust, coconut shell, groundnut shell, rice straw, duck weed, sewage sludge, saw dust carbon, agricultural waste and timber industry waste carbons and gram husk, etc., have been tested as adsorbents for treating contaminated water (Mane and Vijay Babu 2011; Demirbas 2009). The wastes from forestry and agricultural industries are abundant in nature, inexpensive, require little processing and are shown to be effective water treatment materials (Demirbas 2009).

Bamboo dust is an abundant by-product of the paper industry and is easily available at negligible price. The aim of the present work is to study the adsorption capacity of bamboo dust under various conditions and its acid treated modified forms as adsorbents.

Methodology

Reagent grade NaF (Merck, Mumbai, India), $NaAsO_2$ (Devam Chemicals Calcutta), HCl, HNO_3 and H_2SO_4 (all from E. Merck, Mumbai, India) were used without further purification.

For the adsorption experiments, stock solutions of fluoride and arsenite having 1,000 mg of F^- and As(III) per litre were prepared by dissolving appropriate amounts

of the salts respectively in 1 L of distilled water. For As(III) stock solution, $NaAsO_2$ was first dehydrated by drying at 105 °C for 4 h. The pH of the aqueous solutions of F^- - and As(III) as prepared was 6.50 ± 0.05 and 5.70 ± 0.05 respectively. The working solutions for adsorption experiments were freshly prepared by diluting the stock solution (1,000 mg/L).

Preparation of Adsorbent

Waste bamboo dust was collected from Nagaon Paper Mill. The material was thoroughly washed to get rid of the dyes and pigments, and other soluble impurities, oven dried, ground, and sieved to get the fraction between mesh size 50 and 100. The materials were modified by treating with 0.5 N HCl, HNO_3 and H_2SO_4 for 5 h. After modification, they were again washed with distilled water to remove the excess acid. In total, four adsorbents, namely, raw bamboo dust (B1), 0.5 N HCl treated bamboo dust (B2), 0.5 N HNO_3 treated bamboo dust (B3) and 0.5 N H_2SO_4 treated bamboo dust (B4) were prepared.

Surface Area Determination

The surface area measurement was based on adsorption of the dye, Methylene Blue, on the adsorbent (Hang and Brindley 1970; Percival and Lindsay 1997). In this method, the material was exposed to progressively increasing concentrations of Methylene Blue solution (25, 30, 40, 50, 60 and 70 mg/L) under continuous agitation and kept for 6 h in contact with the dye solution. The amount of dye adsorbed on unit mass of the adsorbent at equilibrium (q_e mg/g) was obtained from the amount of dye remaining unadsorbed (C_e mg/L) measured spectrophotometrically for each dye concentration. The amount of dye required to form a complete monolayer (q_m) was computed from Langmuir isotherm,

$$C_e/q_e = \left(1/bq_m\right) + \left(1/q_m\right) C_e \tag{1}$$

where the slope of the plot of C_e/q_e vs. C_e gives the Langmuir Monolayer Capacity, q_m. The specific surface area (s_g) of the adsorbent was obtained from the relation,

$$s_g = M_f \times A_m \times N_A \tag{2}$$

where M_f is number of milliequivalents of Methylene Blue adsorbed per 100 g of material, A_m = surface area of the Methylene Blue molecule (1.30×10^{-18} m^2/molecule), and N_A is Avogadro Number ($=6.023 \times 10^{20}$ molecules per milliequivalent).

Determination of Anion Exchange Capacity

The anion exchange capacity (AEC) was determined conductometrically. 0.2 g of the adsorbent in 20 mL conductivity water was titrated against standard $AgNO_3$ solution. The titration was repeated for standard NaCl with the same $AgNO_3$ solution and the equivalence point in each case was obtained. From the difference in volumes of $AgNO_3$ solutions required, AEC was calculated using the formula, $AEC = NV/W$ where N is the normality of $AgNO_3$ solution and V is its volume required by W g of the adsorbent.

Adsorption Experiments

The adsorption experiments were carried out by batch adsorption process, in which 50 mL of aqueous adsorbate solution was mixed with 1 g of the adsorbent in an Erlenmeyer flask (polypropylene Erlenmeyer flasks were used for F^- adsorption). The mixture was agitated in a thermostatic water bath shaker (Navyug India Q 5247) for a pre-determined time interval and the mixture was centrifuged. Unadsorbed As(III) in the supernatant was determined using atomic absorption spectrometer (Varian SpectrAA 220 using hydride generator, wavelength 192.5 nm, lamp current 5 mA, slit width 0.5 nm, working range 0–100 µg/mL). Unadsorbed fluoride was estimated using SPDNS reagent spectrophotometrically (Shimadzu UV 1800).

When the effect of pH was studied, the pH of the adsorbate solution was adjusted by adding aqueous solution of 0.01 N NaOH or 0.01 N HNO_3 in drops. The conditions for different sets of experiments are given in Table 1.

Results and Discussion

Effects of pH

The pH of the aqueous solution is a significant controlling factor in adsorption mechanism. The experiments were conducted by varying pH of the solution from 6.0 to 8.5 and taking 1.5 mg/L fluoride and 100 µg/L arsenite solutions at room temperature for 4 h and 5 h respectively. The amount adsorbed per unit mass of the adsorbents (q_e) increased up to pH = 7 in both the cases (Fig. 1), but the increase was not as sharp for arsenite as it was for fluoride.

In basic medium, adsorption decreased. As pH increased toward 7.0, the anions had to compete with increasing number of hydroxyl ions in the solution resulting in less adsorption. Similar results were obtained by using pumice (Malakootian et al. 2011). As pH increased toward 7.0, the anionic species, $H_2AsO_3^-$, increased and thus more As(III) uptake was expected due to specific binding. Relative adsorption inhibition was observed at basic pH range and could be attributed to the accumulation

Table 1 Experimental conditions

Type of study	Conditions
Effects of pH	Adsorbent 1 g/L
	F^- and As(III) volume 50 mL
	Concentration F^- 1.50 mg/L, As(III) 100 µg/L
	Temperature 300 K
	Adsorption time F^- 240 min/As(III) 300 min
	pH 6.0–8.5 (intervals of 0.5) for both F^- and As(III)
Kinetics	Adsorbent 1 g/L
	F^- and As(III) volume 50 mg/L
	Concentration F^- 1.50 mg/L, As(III) 100 µg/L
	Temperature 303 K
	Adsorption time 0, 5, 10, 15, 30, 45, 60, 90, 120, 180, 40 min
	pH F^- 5.7 ± 0.05, As(III) 6.5 ± 0.05
Effects of adsorbent amount	Adsorbent 1.0, 1.5, 2.0, 2.5, 3.0, 3.5 g/L
	F^- and As(III) volume 50 mL
	Concentration F^- 1.50 mg/L, As(III) 100 µg/L
	Temperature 300 K
	Adsorption time F^- 240 min, As(III) 300 min,
	pH as prepared for both F^- and As(III)
Effects of anion concentration	Amount of Adsorbent 1 g/L;
	F^- and As(III) volume 50 mg/L;
	Temperature 300 K
	Adsorption time F^- 240 min, As(III) 300 min
	Concentration F^- 2.5, 5.0, 7.5, 10.0, 12.5, 15.0, 17.5, 20.0 mg/L
	As(III) 10, 20, 30, 40, 50, 60, 70, 80, 90, 100 µg/L
Isotherm	Adsorbent 1 g/L
	F^- and As(III) volume 50 mg/L
	Temperature 300 K
	Adsorption time F^- 240 min, As(III) 300 min
	Concentration F^- 2.5, 5.0, 7.5, 10.0, 12.5, 15.0, 17.5, 20.0 mg/L
	As(III) 10, 20, 30, 40, 50, 60, 70, 80, 90, 100 µg/L

of hydroxyl ions on the surface leading to formation of aqua-complexes and reducing sorption (Venkata Mohan et al. 2003).

Effects of Adsorption Time and Kinetics

Adsorbent-adsorbate interaction was studied as a function of time at pH 5.70 ± 0.05 for fluoride and 6.50 ± 0.05 for arsenite at 300 K for 4 and 5 h respectively. Amount adsorbed per unit mass increased gradually with time and attained equilibrium

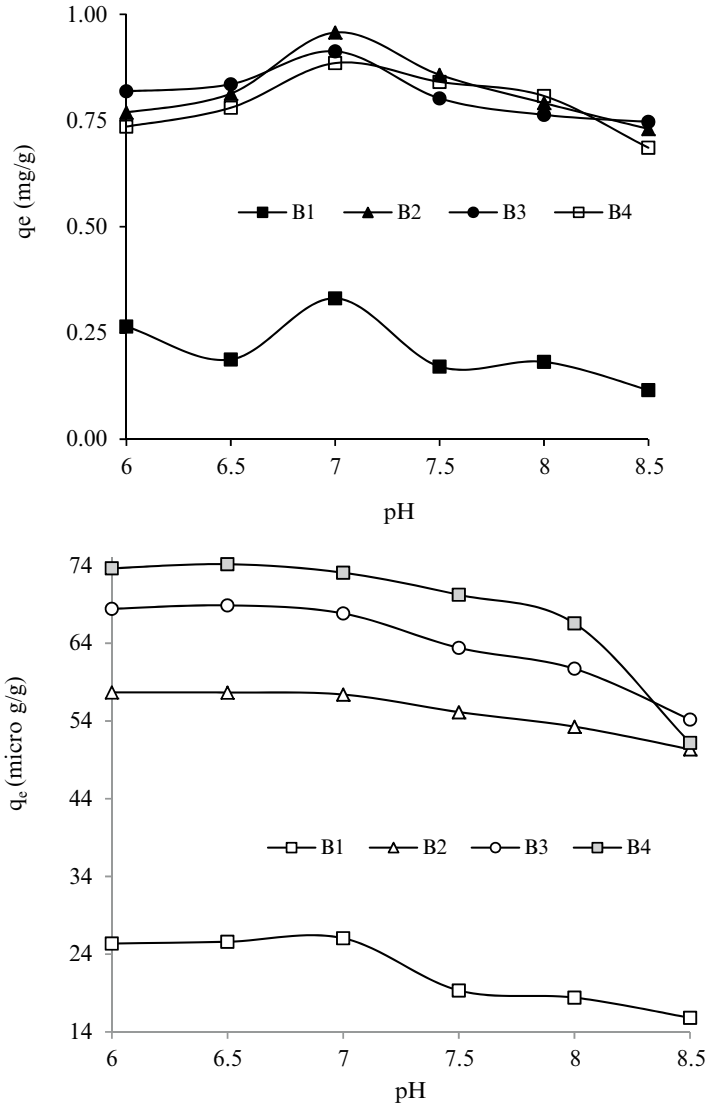

Fig. 1 Influence of pH on adsorption of fluoride (*top*) and arsenite (*bottom*)

(Fig. 2) after 180 min for fluoride and 240 min for arsenite. In both the cases, H_2SO_4 activated bamboo dust (B4) showed the highest adsorption.

At low coverage, arsenite adsorption was very rapid, but as the coverage increased, the number of available surface sites came down, and the adsorption rate decreased until equilibrium was approached. At equilibrium, the uptake was controlled by the rate at which the metal ions were transported from the external surface to the interior sites of the adsorbents (Yu et al. 2000).

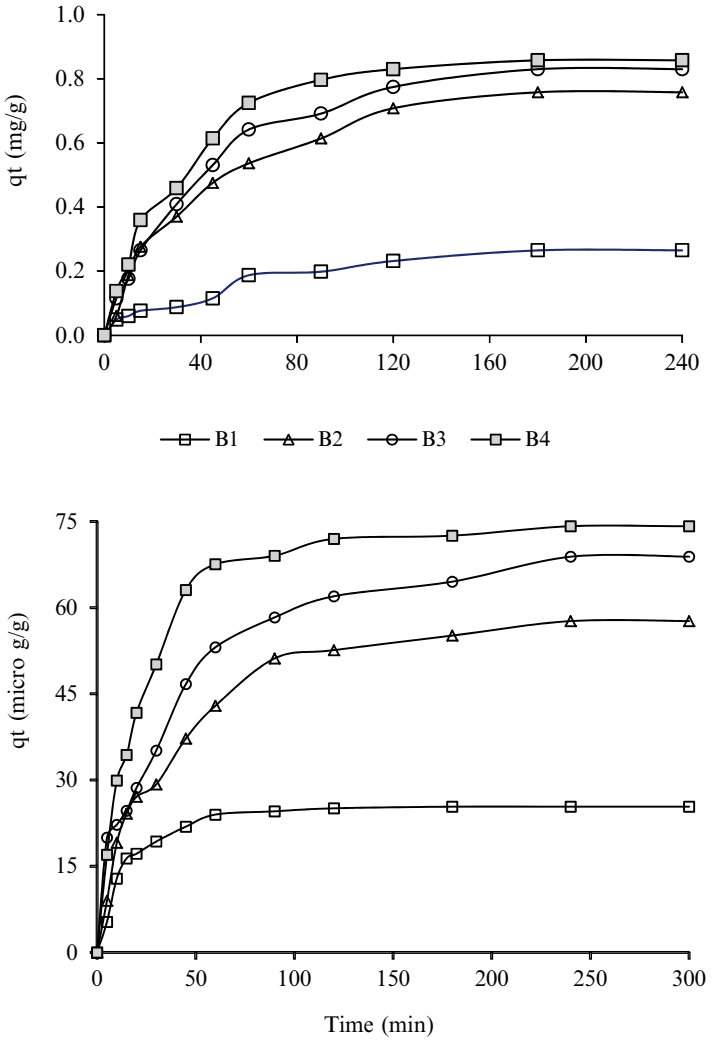

Fig. 2 Effects of adsorption time on fluoride (*top*) and arsenite (*bottom*) uptake

Different models were used to test the kinetics of adsorbent-adsorbate interactions. The Lagergren plots of log $(q_e - q_t)$ vs. time are based on the pseudo first order kinetics (Lagergren 1898; Ho 2004) given by

$$\ln q_e - q_t = \ln q_e - k_1 t \tag{3}$$

where q_e and q_t are the amounts adsorbed per unit mass at equilibrium and at any time t, and k_1 is the first order adsorption rate coefficient. The plots are linear (r lies between 0.98 and 1.00 for fluoride and 0.95 and 0.99 for arsenite) and the first-order rate coefficient (k_1) is 1.63×10^{-2} min^{-1} (B1), 2.09×10^{-2} min^{-1} (B2), 2.17×10^{-2} min^{-1}

(B3), and 2.88×10^{-2} min^{-1} (B4) for fluoride adsorption and 3.99×10^{-2} min^{-1} (B1), 1.73×10^{-2} min^{-1} (B2), 1.50×10^{-2} min^{-1} (B3) and 2.16×10^{-2} min^{-1} (B4) for arsenite adsorption. However, the validity of the first-order kinetics for arsenite is not good because the equilibrium adsorption capacity, q_e, obtained from the plots deviated by 20.03–40.79 % from the experimental value (Table 2).

The second order kinetics (Ho and McKay 1999) given by the equation

$$t / q_t = 1 / \left(k_2 q_e^{\,2} \right) + \left(1 / q_e \right) t \tag{4}$$

also yielded good linear plots of t/q_t vs t (r lies between +0.92 and +0.99 for fluoride and is ~ +1.00 for arsenite). The second order rate coefficient, k_2, has values of 6.73×10^{-2} g mg^{-1} min^{-1} (B1), 1.75×10^{-2} g mg^{-1} min^{-1} (B2), 2.06×10^{-2} g mg^{-1} min^{-1} (B3) and 2.56×10^{-2} g mg^{-1} min^{-1} (B4) for fluoride and 2.87×10^{-3} g µg^{-1} min^{-1} (B1), 0.54×10^{-3} g µg^{-1} min^{-1}(B2), 0.53×10^{-3} g µg^{-1} min^{-1} (B3), 0.73×10^{-3} g µg^{-1} min^{-1} (B4) for arsenite. The deviations in the q_e values (experimental and those obtained from the slopes of the second-order plots) for arsenite adsorption are now quite tolerable being in the range of −7.4 to −1.8 % (Table 2). On the other hand the deviation is more for fluoride adsorption.

These results indicate that fluoride adsorption follows Lagergren pseudo first order kinetics, while arsenite adsorption follows second order kinetics.

Influence of Concentration

When the initial concentration of the anion adsorbate was increased at a constant adsorbent amount, the amount adsorbed per unit mass of the adsorbent at equilibrium (q_e) also increased (Fig. 3) as expected.

For example, by increasing fluoride concentration from 2.5 mg L^{-1} to 20 mg L^{-1} (adsorbent 1 g L^{-1}), the amount of fluoride adsorbed per unit mass of adsorbent increased from 0.56 mg g^{-1} to 2.65 mg g^{-1} for B1, 1.50 mg g^{-1} to 8.43 mg g^{-1} for B2, 1.67 mg g^{-1} to 8.87 mg g^{-1} for B3 and from 1.67 mg g^{-1} to 9.03 mg g^{-1} for B4. Similarly by increasing arsenite concentration from 10 µg L^{-1} to 100 µg L^{-1} (adsorbent 1 g L^{-1}), the amount adsorbed per unit mass increased from 3.31 µg g^{-1} to 25.37 µg g^{-1} for B1, from 7.16 µg g^{-1} to 57.66 µg g^{-1} for B2, from 7.79 µg g^{-1} to 68.87 µg g^{-1} for B3, and from 8.93 µg g^{-1} to 74.17 µg g^{-1} for B4.

At low initial adsorbate concentration, the ratio of the number of anions to the number of available adsorption sites on the adsorbent surface is small and consequently the adsorption is independent of the initial concentration. With an increase in the number of ions, the situation changes and the number of ions available per unit volume of the solution rises. This results in an increased competition for the binding sites (Ucun et al. 2003), resulting in a higher uptake by unit mass and consequently an increase in q_e. A good number of works related to fluoride and arsenite uptake have reported similar results e.g. removal of fluoride from water by using granular red mud (Tor et al. 2009), adsorption of arsenite using natural laterite as adsorbent (Maiti et al. 2007), etc.

Table 2 Deviations in q_e (experimental and those obtained from first order and second order plots)

	qe for fluoride					qe for arsenite				
	qe Expt.	First order		Second order		qe Expt.	First order		Second order	
Sorbent		Plot	% Dev	Plot	% Dev		Plot	% Dev	Plot	% Dev
B1	0.26	0.26	3.75	0.31	−15.72	25.37	20.29	20.03	27.55	−8.59
B2	0.76	0.74	2.76	1.03	−35.88	57.66	44.11	23.51	64.47	−11.82
B3	0.83	0.80	3.58	1.07	−28.46	68.87	49.37	28.32	73.96	−7.40
B4	0.86	0.84	2.03	1.10	−27.75	74.17	43.91	40.79	80.97	−9.17

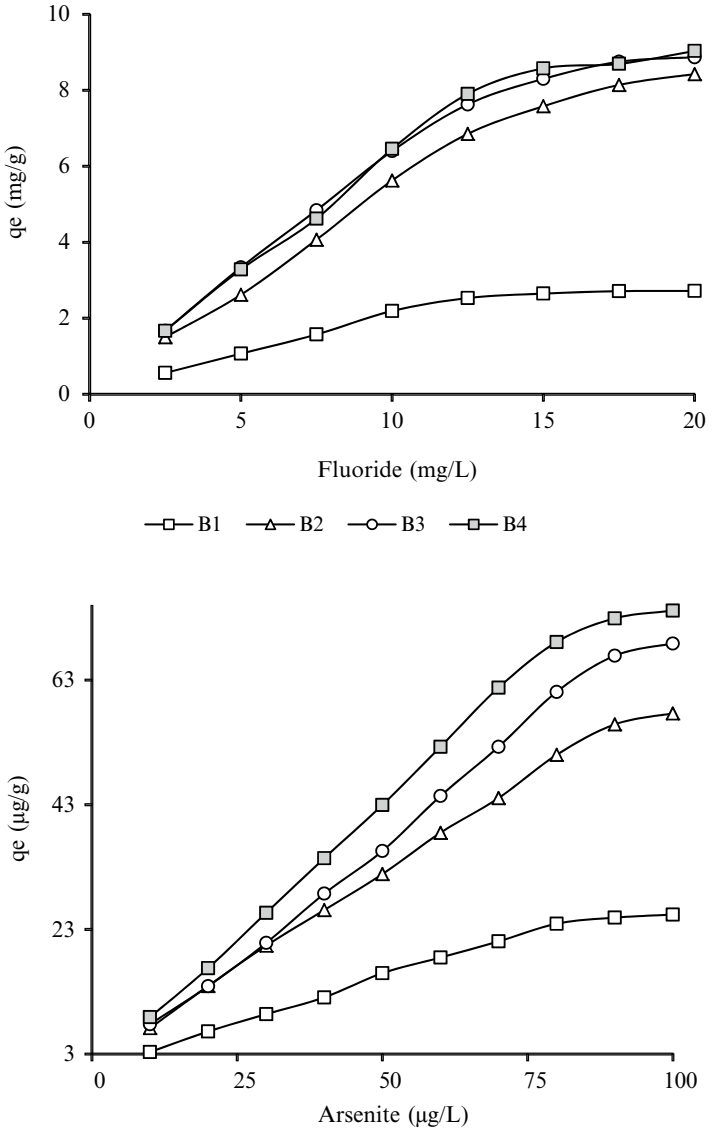

Fig. 3 Influence of concentration on adsorption of fluoride (*top*) and arsenite (*bottom*)

Influence of Adsorbent Amount

When the amount of the adsorbent was increased from 1 to 3 g/L (fluoride 1.5 mg/L and arsenite is 100 µg/L), the amount adsorbed per unit mass of the adsorbent decreased (Fig. 4) in both the cases. This may be due to two reasons: (i) a large adsorbent amount reduces the unsaturation of the adsorption sites and,

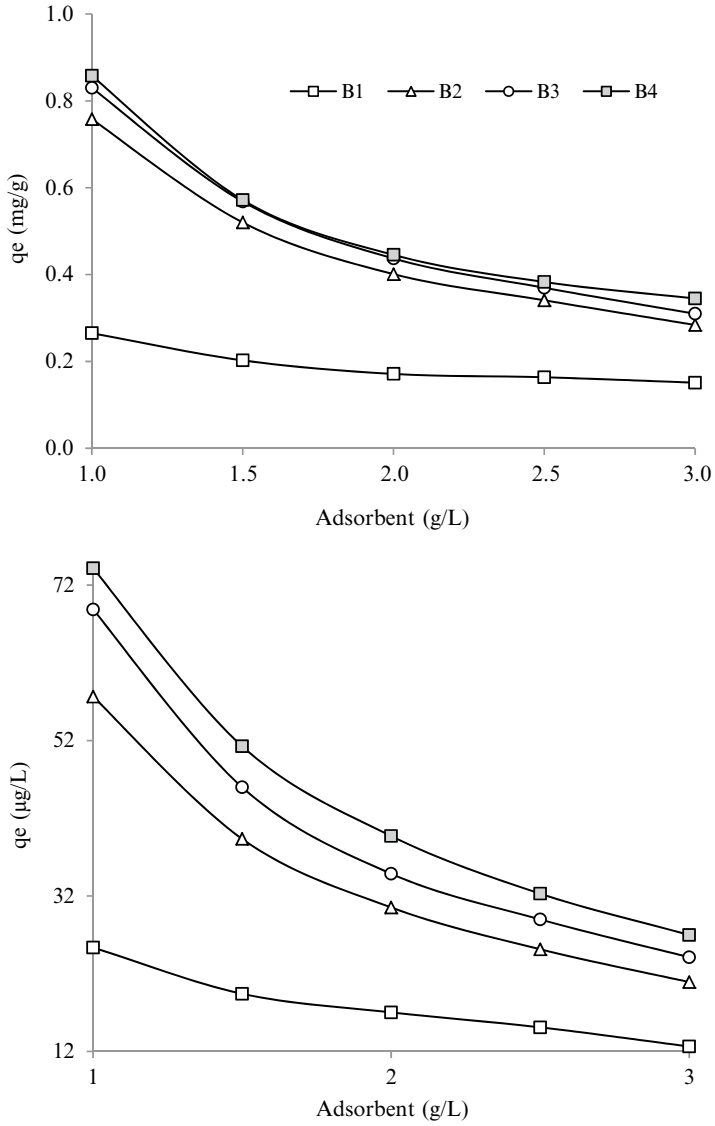

Fig. 4 Influence of adsorbent amount on adsorption of fluoride (*top*) and arsenite (*bottom*)

correspondingly, the number of such sites per unit mass comes down, resulting in comparatively less adsorption at higher adsorbent amount, and (ii) higher adsorbent amount creates particle aggregation, resulting in a decrease in the total surface area and an increase in diffusional path length, both of which contribute to a decrease in amount adsorbed per unit mass (Yu et al. 2000).

Adsorption Isotherm and Adsorption Capacities

Application of the empirical Freundlich isotherm (Freundlich 1906) (Eq. 5) and its linearized form (Eq. 6), given by

$$q_e = k_f C_e^{\,n} \tag{5}$$

$$\log q_e = n \log C_e + \log K_f \tag{6}$$

showed that the plots of log q_e vs. log C_e were linear (r from +0.96 to +0.98 for fluoride and +0.95 to +1.00 for arsenite). The values of the adsorption coefficient 'n' obtained from the plots are 0.76, 0.76, 0.65 and 0.67 for fluoride adsorption and 0.88, 0.80, 0.94 and 0.76 for arsenite respectively for B1, B2, B3 and B4. The adsorption intensity is $n<1$ for both the cases and indicates favourable adsorption on the adsorbents.

The values of the Freundlich adsorption capacity, K_f, on untreated and acid treated bamboo dust are in the order of B1 (0.39 $mg^{1-1/n}\,L^{1/n}\,g^{-1}$) < B2 (1.56 $mg^{1-1/n}\,L^{1/n}\,g^{-1}$) < B4 (2.26 $mg^{1-1/n}\,L^{1/n}\,g^{-1}$) < B3 (2.32 $mg^{1-1/n}\,L^{1/n}\,g^{-1}$) for fluoride adsorption, and B1 (0.66 $\mu g^{1-1/n}\,L^{1/n}\,g^{-1}$) < B3 (3.13 $\mu g^{1-1/n}\,L^{1/n}\,g^{-1}$) < B2 (3.23 $\mu g^{1-1/n}\,L^{1/n}\,g^{-1}$) < B4 (9.09 $\mu g^{1-1/n}\,L^{1/n}\,g^{-1}$) for arsenite adsorption.

Langmuir adsorption isotherm models the monolayer coverage of the sorption surfaces and assumes that sorption take places on a structurally homogeneous surface of the adsorbent. This isotherm (Langmuir 1916) is given by the equation:

$$C_e / q_e = 1/(bq_m) + (1/q_m)C_e \tag{7}$$

The Langmuir plots of C_e/q_e vs. C_e are also linear (r from +0.99 to +1.00 in fluoride adsorption and +0.98 to +1.00 in arsenite adsorption). Langmuir equilibrium coefficient, b, has values of 0.04–0.11 L g^{-1} for fluoride and 0.005–0.070 L g^{-1} for arsenite adsorption. Langmuir monolayer adsorption capacity, q_m, has the values 8.70 mg g^{-1} (B1), 17.24 mg g^{-1} (B2), 20.41 mg g^{-1} (B3) and 20.41 mg g^{-1} (B4) for fluoride adsorption and 111.23 µg g^{-1} (B1), 112.74 µg g^{-1} (B2), 123.00 µg g^{-1} (B3) and 123.92 µg g^{-1} (B4) for arsenite adsorption.

Acid activation has a positive influence on the monolayer adsorption capacity of the adsorbent materials as it has been found that q_m values increase on acid activation.

Conclusions

All the adsorbents were effective in the adsorption of fluoride as well as arsenite. The amount adsorbed per unit mass of the adsorbent also increases on acid activation. Acid activation increases the adsorption capacity compared to the untreated bamboo dust, which is due to the increase in surface area and anion exchange capacity.

The pH has significant influence on adsorption and it was observed that all the adsorbents were effective at neutral pH range for both fluoride and arsenite. The adsorption of fluoride reached equilibrium around 180 min, while the same for arsenite took 240 min.

The adsorption of fluoride followed Lagergren pseudo first order kinetics while arsenite adsorption followed second order kinetics. Application of Freundlich and Langmuir isotherms indicated good adsorption capacities for both fluoride and arsenite.

The results show that waste bamboo dust could be explored as a suitable material for removal of fluoride and arsenite from water.

Acknowledgements This work was sponsored partly by the Department of Science and Technology, Government of India under its Water Technology Initiative Programme and partly by the University Grants Commission under the Basic Science Research scheme.

References

Chakravarty S, Dureja V, Bhattacharyya G, Maity S, Bhattacharjee S (2002) Removal of arsenic from groundwater using low cost ferruginous manganese ore. Water Res 36:625–632

Chang Q, Lin W, Ying W-c (2010) Preparation of iron-impregnated granular activated carbon for arsenic removal from drinking water. J Hazard Mater 184:515–522

Demirbas A (2009) Agricultural based activated carbons for the removal of dyes from aqueous solutions: a review. J Hazard Mater 167:1–9

Freundlich HMF (1906) Uber die adsorption in Lusungen. Z Phys Chem 57:385–470

Ghimire KN, Inoue K, Yamaguchi H, Makino K, Miyajima T (2003) Adsorptive separation of arsenate and arsenite anions from aqueous medium by using orange waste. Water Res 37:4945–4953

Giménez J, de Pablo J, Martínez M, Rovira M, Valderrama C (2010) Reactive transport of arsenic(III) and arsenic(V) on natural hematite: experimental and modeling. J Colloid Interface Sci 348:293–297

Hang Pham T, Brindley GW (1970) Methylene blue absorption by clay minerals. Determination of surface areas and cation exchange capacities (Clay-Organic Studies XVIII). Clays Clay Miner 18:203–212

Ho YS (2004) Citation review of Lagergren kinetic rate equation on adsorption reactions. Scientometrics 59:171–177

Ho YS, McKay G (1999) Batch lead(ii) removal from aqueous solution by peat: equilibrium and Kinetics. Trans IChemE 77(B):165–173

Issa NB, Rajaković-Ognjanović Vladana N, Marinković Aleksandar D, Rajaković Ljubinka V (2011) Separation and determination of arsenic species in water by selective exchange and hybrid resins. Anal Chim Acta 673:191–198

Jordan N, Lomenech C, Marmier N, Giffaut E, Ehrhardt J-J (2009) Sorption of selenium(IV) onto magnetite in the presence of silicic acid. J Colloid Interface Sci 329:17–23

Lagergren S (1898) Zur theorie der sogenannten adsorption gelöster stoffe. Kungliga Svenska Vetenskapsakademiens. Handlingar Band 24(4):1–39

Langmuir I (1916) The constitution and fundamental properties of solids and liquids. Part I Solids J Am Chem Soc 38:2221–2295

Liang L, He J, Wei M, Duan X (2006) Kinetic studies on fluoride removal by calcined layered double hydroxides. Ind Eng Chem Res 45:8623–8628

Maiti A, Das Gupta S, Basu JK, De S (2007) Adsorption of arsenite using natural laterite as adsorbent. Sep Purif Technol 55(3):350–359

Malakootian M, Moosazadeh M, Yousefi N, Fatehizadeh A (2011) Fluoride removal from aqueous solution by pumice: case study on Kuhbonan water. Afr J Environ Sci Technol 5:299–306

Mane VS, Vijay Babu PV (2011) Studies on the adsorption of Brilliant Green dye from aqueous solution onto low-cost NaOH treated saw dust. Desalination 273:321–329

Oguz E (2005) Adsorption of fluoride on gas concrete materials. J Hazard Mater 117(2–3):227–233

Percival JB, Lindsay PJ (1997) Measurement of physical properties of sediments. In: Mudroch A, Azcue JM, Mudroch P (eds) Manual of physico-chemical analysis of aquatic sediments. Lewis Publishers, Boca Raton

Su T, Guan X, Gu G, Wang J (2008) Adsorption characteristics of As(V), Se(IV), and V(V) onto activated alumina: effects of pH, surface loading, and ionic strength. J Colloid Interface Sci 326:347–353

Szlachta M, Gerda V, Chubar N (2012) Adsorption of arsenite and selenite using an inorganic ion exchanger based on Fe–Mn hydrous oxide. J Colloid Interface Sci 365:213–221

Tor A, Nadide D, Gulsin A, Yunus C (2009) Removal of fluoride from water by using granular red mud: batch and column studies. J Hazard Mater 164:271–278

Ucun H, Bayhana YK, Kaya Y, Avni C, Algur OF (2003) Biosorption of lead (II) from aqueous solution by cone biomass of Pinus sylvestris. Desalination 154:233–238

Venkata Mohan S, Vijaya Bhaskar Y, Karthikeyan J (2003) Biological decolourisation of simulated azo dye in aqueous phase by algae Spirogyra species. Int J Environ Pollut 21(3):211–222

Yokota H, Tanabe K, Sezaki M, Akiyoshi Y, Miyata T, Kawahara K, Tsushima S, Hironaka H, Takafuji H, Rahman M, Ahmad SKA, Sayed MHSU, Faruquee MH (2001) Arsenic contamination of ground and pond water and water purification system using pond water in Bangladesh. Eng Geol 60:323–331

Yu B, Zhang Y, Shukla A, Shukla SS, Dorris KL (2000) The removal of heavy metal from aqueous solutions by sawdust adsorption—removal of copper. J Hazard Mater 80:33–42

Reducing the Toxicity of Carbon Nanotubes and Fullerenes Using Surface Modification Strategy

Jyoti Chawla and Arun Kumar

Introduction

Carbon-based nanoparticles have attracted much attention because of their unique properties like specific strength, lightness, electrical properties and also show several promising potential applications in biology and pharmacology. However, their growing use and mass production have raised several questions about their probable unfavourable effects on human health. For example, use of carbon nanotubes (CNTs) and fullerenes are there in maximum number of consumer products containing carbon-based nanomaterials and have been reportedly found in environmental samples (Farré et al. 2010).

A literature review showed that carbon nanotubes can produce effects very similar to those of asbestos fibres. The results of rodent studies showed that CNTs produce inflammation, epithelioid granulomas, fibrosis and biochemical/toxicological changes in the lung (Lam et al. 2006). Single-walled carbon nanotubes (SWCNTs) were found to be more toxic than quartz and carbon black. Pharmacokinetic studies with radio-labeled watersoluble C60 showed that after intravenous injection into mice the compound quickly migrates through the body, accumulates in the liver after a few hours, and is excreted, either slowly or rapidly depending on the functionalization of the C60 surface. CNTs were also identified in four of the seven WTC dust samples. Wu et al. (2010) investigated seven previously healthy individuals who were exposed to World Trade Centre dust and later developed severe respiratory impairment. SWCNTs of various lengths were identified in lung tissues of three

J. Chawla (✉)
Department of Chemistry, ManavRachna International University, Faridabad, India
e-mail: jyoti.chawla@gmail.com

A. Kumar
Department of Civil Engineering, Indian Institute of Technology Delhi, Delhi, India

© Capital Publishing Company 2015

N.J. Raju et al. (eds.), *Management of Natural Resources in a Changing Environment*, DOI 10.1007/978-3-319-12559-6_13

patients with interstitial disease. One other patient with CNT had mild chronic bronchiolitis and occasional peribronchiolar and submucosal fibrosis. However, lung tissue analysis showed variable amounts of aluminum and magnesium silicates, chrysotile asbestos, calcium phosphate and calcium sulfate, and shards of glass along with CNTs of various sizes. Though it remains uncertain whether the CNTs caused the lung pathology but it is the high time to assess and reduce the risk posed by these materials for safer use as their production rate is increasing rapidly. Studies also indicate the liver and spleen to be the main sites of CNT accumulation (Schipper et al. 2008). Interactions of nanoparticles with environment and biological systems are very important factors for risk assessment and reduction.

Functionalisation/surface modification of nanoparticle plays an important role in deciding the interaction of nanoparticles with environment and biological systems (Li et al. 2012). In order to support the use of modified materials, risk assessment needs to be done in order to compare their toxicities with unmodified ones.

The objective of this study was to explore possibility of using functionalised materials with possible lesser risk, including consideration of whether the modified materials maintain required properties to minimise the risk to consumers using reported toxicity studies based on secondary data. Fullerenes and carbon nanotubes were selected and attempt was made to evaluate their toxicity results to compare hazardous properties with their substitutes and also to identify related issues for further consideration.

Methodology

The study used following steps: (1) Overview of products containing CNTs and fullerenes with their application area and their presence in environment, (2) Review of the synthesis methods and possible substitution and modification options for CNTs and fullerenes, and (3) Review of toxicological studies to predict their comparative hazards for different options to identify better options for reducing toxicity and future needs. Towards this, scientific journal papers and reports were reviewed and their findings were synthesized.

Results and Discussion

Overview of Products Containing CNTs and Fullerenes

The range of carbon-based nanomaterials in variety of consumer products were identified from literature review. Carbon-based nanomaterials, such as CNTs, fullerenes, carbon nanofibres, graphene, carbon nano crystals, carbon black, and carbon onions

Table 1 Reported LD 50/LC 50 values

Derivative	LC 50/LD 50	References
Fullerene	LC 50–0.25 µg/ml	Isakovic et al. (2006)
C60(OH)n	LC 50–800–1,000 µg/ml	Isakovic et al. (2006)
SWCNT	LD 50 from acute oral toxicity studies >1,000 mg/kg bw in mice	Kolosnjaj-Tabi et al. (2010)
(1) Ultrashort (diam. ~1 nm, length ~20–80 nm, Fe <1.5 %);		
(2) Raw (diam. ~1 nm, length ~1–2 µm, Fe 25 %);		
(3) Purified (diam. ~1 nm, length ~1–2 µm, Fe <4 %)		
MWCNT (mean diameter 10–15 nm; mean length ~200–1,000 nm; Co 0.53 %)	LD 50 from acute oral toxicity studies >5,000 mg/kg bw in rats	Pauluhn (2010)

LC Lethal Concentration, *LD* Lethal Dose

are being widely applied in electronics, automotive, filtration and storage devices, OLEDs, computer RAM, cosmetics, computer hardware and sporting good products. As of March 2011, a total of 91 products are available worldwide that contains carbon-based nanomaterials *(Inventory done under Project on Emerging Nanotechnologies,* www.nanotechproject.org*)*. The number is more than double when compared to the figure given in the 2006 inventory.

Following sections compare toxic effects of fullerenes and carbon nanotubes with their derivatives, functionalized with groups, such as hydroxyl, carboxyl, etc. The available information about LC50 of some nanoparticles (i.e., nanoparticles concentration causing 50 % lethality to exposed species) supports the use of functionalized nanomaterials with more value of LC50/LD50 (where LD50 = nanoparticles dose causing 50 % lethality to exposed species) (Table 1).

Carbon Nanotubes

Synthesis, Substitution and Modification

Carbon nanotubes are cylindrical macromolecules, which have a radius of only a few nanometres and can be grown in different lengths. The cylinders are usually capped at the ends by a fullerene-type molecule. The common synthesis procedures for CNTs with average diameter 1–1.4 nm are Electric arc discharge, Laser ablation, Catalytic decomposition of gaseous hydrocarbons (maximum production rate), etc. (Balasubramanian and Burghard 2005). There are two major types of CNTs

discussed in current study: single-walled carbon nanotubes (SWCNTs) and multi-walled carbon nanotubes (MWCNTs). SWCNTs are composed of a single rolled up graphene sheet and MWCNTs are composed of a concentric arrangement of many cylinders.

Carbon nanotubes possess high chemical and mechanical stability, which makes it useful for different applications but due to this substitutions/modifications are difficult and have low conversion/functionalisation rate. Derivatization of CNTs gives products with side-wall substituents, wrapped with polymers, or with inclusion of guest molecules. Several approaches have been developed including defect functionalization, covalent functionalization of the side-walls, non-covalent exohedral functionalization and endohedral functionalization. Most commonly used approaches are functional group addition and surface modification by compositing with other materials (Table 2).

The known addition reactions of carbon nanotubes are carboxylation, anhydride conversion, amidization, and fluorination. These additions can potentially lead to decreased toxicity by increasing the hydrophilic character and therefore biocompatibility of the manufactured CNTs (Balasubramanian and Burghard 2005). However, such modifications may impact on other properties, e.g., mechanical and electrical properties (Chattopadhyay et al. 2008). Chemical modification is examined in detail in the following sections.

Table 2 Functional group addition and surface modification for CNTs

Type of CNT	Modification/reagents	Product	References
SWCNT	Carboxylation/Nitric and sulfuric acid	Carboxyl SWCNT	Zhang et al. (2003)
Carboxyl-SWCNT	Anhydride formation/Acid treatment	SWCNT anhydride	Sano et al. (2001)
Nitrogen doped MWCNT	Amidization/Amine groups of ferritin or Bovine Serum Albumin (BSA)	MWCNT ferritin or BSA amide	Katz and Willner (2004)
Carboxyl-functionalised MWCNTs	Covalent modification/polymeric material grafted polyetherimide	Grafted MWCNT	Ge et al. (2005)
MWCNT	Covalent modification/low molecular weight chitosan	Grafted MWCNT	Ke et al. (2007)
Polymer nanotubes composites	Covalent attachment/polymer precursors on the surface and the subsequent in situ polymerization.	Grafted nanotubes	Jia et al. (1999) and Shaffer and Koziol (2002)
Water soluble MWCNTs with temperature responsive shells	Covalent attachment of polymers/Grafting thermosensitive poly(Nisopropolyacrylamide) to the side walls	Grafted nanotubes	Guoyong et al. (2006)

Toxicology Comparison of CNTs With and Without Substitution/Modification

It was explained that inflammatory and granuloma responses were associated with long straight CNT fibres, having a structural aspect ratio similar to long fibre asbestos (Poland et al. 2008; Drew 2009). In case of CNTs, size is an important factor to control toxicity, which can be reduced by reducing their length below 5 μm. Curled-tangled CNT fibres are considered to be less pathogenic than long straight CNTs (Poland et al. 2008). Long fibre CNTs have a high potential to be retained in the pleural membrane and to cause diseases such as mesothelioma (Donaldson et al. 2009). Short CNT fibres (<5 μm) will transit through the parietal pleural stomata. However, long CNT fibres (>15 μm) can reach the pleura and cause genotoxicity and inflammation.

Unmodified CNTs may be classified as durable and biopersistent than modified one. Drew (2009) suggested that all biopersistent CNTs, or aggregates of CNTs, of pathogenic fibre dimensions could be considered as potential fibrogenic and mesothelioma hazards. As per recent studies, unfunctionalized carbon nanotubes show potent cytotoxicity toward alveolar macrophages, HacaT cells, and HEK293 cells. SWCNTs present in the lungs of mice produce respiratory impairment, damage DNA in the aorta, increase aortic plaques, induce atherosclerotic lesions in arteries of the heart and retard bacterial clearance. Carcinogenic and fibrogenic behaviour of MWCNTs in the intraperitoneal cavity of mice has been discussed in vivo studies (Poland et al. 2008). Dutta et al. (2007) suggested that the uptake of proteins can be significantly reduced by a coating on the surface of CNTs. It was found that SWCNT sample became less cytotoxic with sidewall functionalisation of SWCNTs. This functionalisation was also considerably less cytotoxic than surfactant-stabilised SWCNTs (Sayes et al. 2006).

It is noticeable in Table 3 that functionalisation of CNTs reduces the toxicity in most of the cases except acid functionalization. Cytotoxic response of human dermal fibroblast cells was also found to be dependent on the degree of functionalisation of single-walled carbon nanotubes. Carbon nanotubes modified with suitable biomimetic polymers are found to be biocompatible while the uncoated carbon nanotubes lead to cell death. Studies support that functionalization of MWNTs reduces toxicity and improves biocompatibility of cells in vitro. The excretion rate of SWCNTs after injection in mice was investigated in a study. Ammonium functionalised SWCNTs (diam. 1 nm, length 300–1,000 nm) were rapidly excreted through the renal route (Singh et al. 2006), whilst polyethylene glycol functionalised SWCNTs (dimensions not reported) persisted for 4 months within the liver and spleen in mice (Schipper et al. 2008). It is difficult to conclude that the rate of excretion was affected by functionalisation because of variation in experimental conditions. The other two studies used functionalised CNTs to investigate different toxicity properties: acid functionalised SWCNTs showed increased cardiopulmonary toxicity in mice (Tong et al. 2009) and carboxylic functionalised MWCNTs did not affect the immune responses in human dendritic cells in vitro (Wang et al. 2009). The selected toxicity results have been compared and summarized in Table 3.

Table 3 Selected toxicity comparison studies of modified/unmodified carbon nanotubes

Modified product	Test	Results	References
SWCNT without modification	Albumin absorption and anti-inflammatory response	Inhibited albumin absorption and anti-inflammatory response	Dutta et al. (2007)
SWCNT after polymer coating with Pluronic F127			
SWCNTs	Cytotoxic response of human dermal fibroblast cells	Cytotoxic response of human dermal fibroblast cells was dependent on the degree of functionalisation of SWCNTs. This sidewall functionalisation was also substantially less cytotoxic than surfactant-stabilised SWCNTs	Sayes et al. (2006)
Functionalisation of SWCNTs with addition of phenyl-(COOH)2 or phenyl-SO3H moieties			
MWCNT	Emission levels of various types of carbon nanoparticles in laboratory activities	Emissions were higher for raw MWCNT	Johnson et al. (2010)
MWCNT-OH			
Functionalisation of SWCNTs following the 1,3-dipolar cyclo-addition reaction and the oxidation/amidation treatment	The impact of functionalised carbon on cells of the immune system	Both types of f-CNTs are uptaken by B and T lymphocytes as well as macrophages in vitro, without affecting cell viability	Dumortier et al. (2006)
CNTs modified with suitable biomimetic polymers	Demonstrated a strategy for interfacing biocompatible CNTs with cell surfaces	Carbon nanotubes modified with suitable biomimetic polymers are found to be biocompatible while the uncoated carbon nanotubes lead to cell death.	Chen et al. (2006)
CNTs	Cytotoxicity	Unfunctionalised CNTs show potent cytotoxicity toward alveolar macrophages, HacaT cells, and HEK293 cells	Jia et al. (2005) and Shvedova et al. (2003)
Functionalised SWCNTs	Histology and Raman microscopic mapping	Functionalised SWCNTs persisted within liver and spleen macrophages for 4 months without apparent toxicity.	Schipper et al. (2008)

Fullerenes

Synthesis, Substitution and Modification

The carbon allotrope C_{60}, usually referred to as a 'buckyball', is geometrically shaped as a truncated dodecahedron with a carbon atom sitting at each corner of the polyhedron (Sayes et al. 2004). Synthesis of fullerenes (Grushko et al. 2007) involves the vapourisation of carbon fragments into an inert atmosphere in which they combine and deposit to form fullerenes and other carbon-based compounds, including CNTs. Another method involves the production of fullerene-containing soot deposits through chemical vapour deposition. Fullerenes are known to be essentially insoluble in water. However, their solubility can be increased (up to 2 mM) through appropriate coatings or by being suspended in colloidal solution. Functional groups may be added to the fullerene in order to increase its water solubility (Table 4). Hence, it is useful to consider the exposure of biological molecules, such as DNA, to fullerenes in aqueous solutions.

The cytotoxic and photocytotoxic effects of two water-soluble fullerene derivatives, a dendritic C (60) mono-adduct and the malonic acid C (60) tris-adduct were tested (Rancan et al. 2002) on Jurkat cells. It was proposed that the two fullerene derivatives may interact with the cell membrane in different ways. Tris-malonic acid fullerene was found to be more phototoxic than the dendritic derivative.

Toxicology Comparison of Fullerenes With and Without Substitution/Modification

Pristine C_{60} can cause membrane leakage. Qiao et al. (2007) also found that the functionalization of C_{60} dramatically lowered toxicity with no resultant membrane leakage. It has been reported that attaching water solubilising groups such as carboxyl or alcohol groups increase the solubility and reduce the toxicity of fullerene.

Table 4 Functional group addition and surface modification for fullerenes (C60)

Modification/Reagents	Product	References
Hydroxylation/Reaction with nitroniumborofluoride and a carboxylic acid followed by basic hydrolysis	Hydroxylated fullerene	Schneider et al. (1994)
Carboxylation	Carboxylated fullerene	Sayes et al. (2004)
Adding polymers, macromolecules	C60-containing polymers, fullerodendrimers	Kong et al. 2004 and Nierengarten (2003)
Hydroxyl, amino or carboxylic acid functional groups to fullerene followed by coupling to a protected amino acid or peptide	Fulleryl amino acid and peptide derivatives	Burley et al. (1999)
Proline derivatives/1,3-Dipolar cycloaddition of azomethineylides	Fulleroproline derivatives	Bianco et al. (1996)

Mechanistic explanation has also been given in a study supporting the reduced acute toxicity of functionalized fullerenes. The differential cytotoxicity of a series of water-soluble fullerene species showed that changes in the fullerene cage structure had substantial impact on in vitro cytotoxicity. As the number of hydroxyl or carboxyl groups on the surface of the fullerene cage was increased, cytotoxicity decreased over seven orders of magnitude. In a study (Chen et al. 1998), polyalkyl-sulfonated fullerenes (in water) were not found to be lethal, subsequent to the oral exposure of rats in acute (50 mg/kg, single administration) or subacute (50 mg/kg daily for 12 days) exposure setups, and as a consequence was considered to be nontoxic. It should be noted that fullerol have proved to be less cytotoxic than fullerene in the in vitro fibroblast test system. Fullerol at 50 mg/L (Zhu et al. 2007) did not exert toxicity to zebrafish embryos. In contrast, nC60 at 1.5 mg/L delayed zebrafish embryo and larval development, decreased survival and hatching rates, and caused pericardial edema. However, tetrahydrofuran treated C60, C60(OH)18 generated cytotoxicity which was related to the residual THF. It was reported that tetrahydrofuran used for the purification and dispersion of C60 remained in C60 aggregates after the treatment and enhanced the cytotoxicity. THF-pre-treated C60 induced mortality in fathead minnows, whereas stirring of engineering nanoparticles in water did not affect survival. However, lipid peroxidation was observed in the gill. One of the publications linked the toxic effects directly to a THF degradation product (γ-butyrolactone) rather than to C60 and may explain toxicity attributed to C60 in other investigations (Kovochich et al. 2009). The selected toxicity results have been compared and summarized in Table 5.

Table 5 Selected toxicity comparison studies of modified/unmodified fullerenes

Type of fullerene	Study/test	Result	References
Fullerene, Substituted fullerene	In vitro Cytotoxicity	The unsubstituted fullerene exhibited the highest toxicity whereas more functionalised (and polar) derivatives showed decreased toxicity.	Sayes et al. (2004)
Fullerenols	Human epidermal keratinocytes	Hydroxylation of fullerenes caused no cytotoxicity or inflammation up to 8.55 μg/ml.	Saathoff et al. (2011)
Functionalised fullerenes, CD-C60, hexa-C60, and tris-C60	Cytokine secretion profile of dermal epithelial cells.	tris-C60 significantly reduces inflammatory cytokine release in a dose- and time-dependent manner; CD-C60 demonstrated a relatively pro-inflammatory cytokine response, while hexa-C60 did not significantly perturb cytokine responses	Gao et al. (2010)

(continued)

Table 5 (continued)

Type of fullerene	Study/test	Result	References
Pure fullerene suspension and water-soluble polyhydroxylated fullerene [C60(OH)n]	The mechanisms underlying the cytotoxic action. Crystal violet assay for cell viability	Pure fullerene was at least three orders of magnitude more toxic than C60(OH)n to mouse L929 fibrosarcoma, rat C6 glioma, and U251 human glioma cell lines.	Isakovic et al. (2006)
		LC50 of C60: 0.25 μg/ml; LC50 of C60(OH)n: 800–1,000 μg/ml	
C60, C70 and C60(OH)24	Embryonic zebrafish morphological and cellular responses	Exposure to 200 lg/L C60 and C70 induced a significant increase in malformations, pericardial edema, and mortality; while the response to C60(OH)24 exposure was less pronounced at concentrations an order of magnitude higher. Exposure to C60 induced both necrotic and apoptotic cellular death throughout the embryo.	Crystal et al. (2007)
C82(OH)22, C60(OH)22, C60(C(COOH)2)2	H2O2-induced oxidative injury within A549 lung epithelial and rat brain capillary endothelial cells	Protective effects of fullerenes are dependent on ability to scavenge ROS, which is increased by greater derivatization	Yin et al. (2009)
Non-treated C60, SWCNTs and MWCNTs	Macrophages	Cytotoxicity of C60 was lower than that of SWCNTs and MWCNTs	Jia et al. (2005)

Conclusions

This study identified the CNT/fullerene and its derivatives with lesser risks for given sets of required properties by exploring and analyzing the toxicity studies reported till date in published reports and literature. From number of toxicity studies of non-derivatized and derivatized fullerene it can be concluded that as the number of hydroxyl or carboxyl groups on the surface of the fullerene cage increases, cytotoxicity decreases. For non-derivatized fullerenes, generally organic solvents are used during the specimen treatment process to make it soluble in water and the residual organic solvents are capable of contributing toxicity. In case of CNTs it is reported that toxicity can be reduced by keeping their length less than 5 μm. CNT became

less cytotoxic after functionalisation and its extent depends on the degree of functionalisation. CNTs modified with suitable biomimetic polymers are also found to be biocompatible while the uncoated CNTs lead to cell death.

It is not possible to draw conclusions on the effect of specific functionalisation/modification on specific toxicity (Chawla and Kumar 2013) because of the limited studies available and due to many variables involved in different toxicity studies (i.e., dose, exposure time, exposure form, number, diameter, length, test species, end points observed, etc.). However, it can be summarised that the toxicity of fullerenes and carbon nanotubes can be controlled while formulating a product. The specimen treatment process plays a significant role in affecting the toxicity because of residual solvents in the sample. The sonication method should be preferred over the use of organic solvents. Attaching water solubilising groups, such as carboxyl or alcohol groups increase the solubility and reduce the toxicity of fullerene. After surface modification, one can minimize/avoid the use of organic solvents during specimen treatment process as it usually increases its solubility in water. Overall, it can be summarised that functionalization plays a significant role in reducing the toxicity of fullerenes and CNTs and may alter the properties to some extent. However, further studies are required in this area to make them compatible for required application.

Acknowledgements The authors would like to thank Department of Science and Technology (India) for supporting this study through the grant no: DST/TM/WTI/2K11/301(G) and Indian Institute of Technology Delhi (India) for offering the Summer Faculty Research Fellowship to the first author.

References

Balasubramanian K, Burghard M (2005) Chemically functionalized carbon nanotubes. Small 1:180–192

Bianco A, Maggini M, Scorrano G, Toniolo C, Marconi G, Villani C, Prato M (1996) Synthesis, chiroptical properties and configurational assignment of fulleroproline derivatives and peptides. J Am Chem Soc 118:4072–4080

Burley GA, Keller PA, Pyne SG (1999) Fullerene amino acids and related derivatives. Fuller Sci Technol 7:973–1001

Chattopadhyay CN, Billups WE, Bandaru PR (2008) Modification of the electrical characteristics of single wall carbon nanotubes through selective functionalization. Appl Phys Lett 93:243113–243116

Chawla J, Kumar A (2013) Ranking carbon-based nanomaterials using cytotoxicity to minimize public health risks. Int J Environ Eng Manag 4(3):301–308

Chen HH, Yu C, Ueng TH, Chen S, Chen BJ, Huang KJ, Chiang LY (1998) Acute and subacute toxicity study of water-soluble polyalkylsulfonated C60 in rats. Toxicol Pathol 26:143–151

Chen J, Swanang P, Seal S, McGinnis JF (2006) Rare earth nanoparticles prevent retinal degeneration induced by intracellular peroxides. Nat Nanotechnol 1:142–150

Crystal YU, Stacey LH, Robert LT (2007) In vivo evaluation of carbon fullerene toxicity using embryonic zebrafish. Carbon 45:1891–1898

Donaldson K, Murphy F, Poland C, Duffin R, Osmond M, Mccall M, Hawkins S (2009) High aspect ratio nanoparticles: the hazard from long biopersistent fibres. Presented at 4th interna-

tional conference on nanotechnology—occupational and environmental health, Helsinki, August 2009
Drew R (2009) Engineered nanomaterials: a review of the toxicology and health hazards. Prepared for safe work Australia. http://www.safeworkaustralia.gov.au. Accessed 15 Dec 2012
Dumortier H, Lacotte S, Pastorin G, Marega R, Wu W, Bonifazi D, Briand JP, Prato M, Muller S, Bianco A (2006) Functionalized carbon nanotubes are non-cytotoxic and preserve the functionality of primary immune cells. Nano Lett 6:1522–1528
Dutta D, Sundaram SK, Teeguarden JG, Riley BJ, Fifield LS, Weber TJ (2007) Adsorbed proteins influence the biological activity and molecular: targeting of nanomaterials. Toxicol Sci 100:303–315
Farre M, Pereza S, Gajda-Schrantz K, Osorio V, Kantiani L, Ginebreda A, Barcelo D (2010) First determination of C60 and C70 fullerenes and N-methylfulleropyrrolidine C-60 on the suspended material of wastewater effluents by liquid chromatography hybrid quadrupole linear ion trap tandem mass spectrometry. J Hydrol 383:44–51
Gao J, Wang HL, Iyer R (2010) Suppression of proinflammatory cytokines in functionalized fullerene-exposed dermal keratinocytes. J Nanomater 2010:1–9
Ge JJ, Zhang D, Li Q, Hou H, Graham MJ, Dai L, Harris FW, Cheng SZD (2005) Multiwalled carbon nanotubes with chemically grafted polyetherimides. J Am Chem Soc 127:9984–9985
Grushko YS, Sedov VP, Shilin VA (2007) Technology for manufacture of pure fullerenes C60, C70 and a concentrate of higher fullerenes. Russ J Appl Chem 80:448–455
Guoyong X, Wei-Tai W, Yusong W, Wenmin P, Pinghua W, Qingren Z, Fei L (2006) Synthesis and characterization of water-soluble multiwalled carbon nanotubes grafted by a thermoresponsive polymer. Nanotechnology 17:2458–2465
Isakovic A, Markovic Z, Todorovic-Markovic B, Nikolic N, Vranjes- Djuric S, Mirkovic M et al (2006) Distinct cytotoxic mechanisms of pristine versus hydroxylated fullerene. Toxicol Sci 91:173–183
Jia ZJ, Wang ZY, Xu C, Liang J, Wei BQ, Wu DH, Zhu SW (1999) Study on poly(methylmethacrylate)/carbon nanotubes composites. Mater Sci Eng A 271:395–400
Jia G, Wang HF, Yan L, Wang X, Pei RJ, Yan T, Zhao YL, Guo XB (2005) Cytotoxicity of carbon nanomaterials: single-wall nanotube, multi-wall nanotube, and fullerene. Environ Sci Technol 39:1378–1383
Johnson DR, Methner MM, Kennedy AJ, Steevens JA (2010) Potential for occupational exposure to engineered carbon-based nanomaterials in environmental laboratory studies. Environ Health Perspect 118:49–54
Katz E, Willner I (2004) Biomolecule-functionalized carbon nanotubes: applications in nanobioelectronics. ChemPhysChem 5:1085–1104
Ke G, Guan WC, Tang CY, Hu Z, Guan WJ, Zemg DL, Deng F (2007) Covalent modification of multiwalled carbon nanotubes with a low molecular weight chitosan. Chin Chem Lett 18:361–364
Kolosnjaj-Tabi J, Hartman KB, Boudjemaa S, Ananta JS, Morgant G, Szwarc H, Wilson LJ, Moussa F (2010) In vivo behavior of large doses of ultrashort and full-length single walled carbon nanotubes after oral and intraperitoneal administration to Swiss mice. ACS Nano 4:1481–1492
Kong H, Gao C, Yan D (2004) Controlled functionalization of multiwalled carbon nanotubes by in situ atom transfer radical polymerization. J Am Chem Soc 126:412–413
Kovochich M, Espinasse B, Auffan M, Hotze EM, Wessel LXT, Nel AE, Wiesner MR (2009) Comparative toxicity of C60 aggregates toward mammalian cells: role of tetrahydrofuran (THF) decomposition. Environ Sci Technol 43:6378–6384
Lam CW, James JT, McCluskey R, Arepalli S, Hunter RL (2006) A review of carbon nanotube toxicity and assessment of potential occupational and environmental health risks. Crit Rev Toxicol 36:189–217
Li X, Lee SC, Zhang S, Akasaka T (2012) Biocompatibility and toxicity of nanobiomaterials. J Nanomater, Article Id 591278, 2 Pages: 10.1155/2012/591278

Nierengarten JF (2003) Fullerodendrimers: fullerene-containing macromolecules with intriguing properties. Top Curr Chem 228:87–110

Pauluhn J (2010) Subchronic 13-week inhalation exposure of rats to multiwalled carbon nanotubes: toxic effects are determined by density of agglomerate structures, not fibrillar structures. Toxicol Sci 113:226–242

Poland CA, Duffin R, Kinloch I, Maynard A, Wallace WAH, Seaton A, Stone V, Brown S, MacNee W, Donaldson K (2008) Carbon nanotubes introduced into the abdominal cavity of mice show asbestos-like pathogenicity in a pilot study. Nat Nanotechnol 3:423–428

Qiao R, Roberts AP, Mount AS, Klaine SJ, Ke PC (2007) Translocation of C60 and its derivatives across a lipid bilayer. Nano Lett 7:614–619

Rancan F, Rosan S, Boehm F, Cantrell A, Brellreich M, Schoenberger H, Hirsch A, Moussa F (2002) Cytotoxicity and photocytotoxicity of a dendritic C(60) mono-adduct and a malonic acid C(60) tris-adduct on Jurkat cells. J Photochem Photobiol B 67:157–162

Saathoff JG, Inman AO, Xia XR, Riviere JE, Monteiro-Riviere NA (2011) In vitro toxicity assessment of three hydroxylated fullerenes in human skin cells. Toxicol in Vitro 25:2105–2112

Sano M, Okamura J, Shinkai S (2001) Colloidal nature of single-walled carbon nanotubes in electrolyte solution: the Schulze- Hardy Rule. Langmuir 17:7172–7173

Sayes CM, Fortner JD, Guo W, Lyon D, Boyd AM, Ausman KD, Tao YJ, Sitharaman B et al (2004) The differential cytotoxicity of watersoluble fullerenes. Nano Lett 4:1881–1887

Sayes CM, Liang F, Hudson JL, Mendez J, Guo W, Beach JM et al (2006) Functionalization density dependence of single-walled carbon nanotubes cytotoxicity in vitro. Toxicol Lett 161:135–142

Schipper ML, Nakayama-Ratchford N, Davis CR, Kam NWS, Chu P, Liu Z, Sun X, Dai H, Gambhi SS (2008) A pilot toxicology study of single-walled carbon nanotubes in a small sample of mice. Nat Nanotechnol 3:216–221

Schneider NS, Darwish AD, Kroto HW, Taylor R, Walton DRM (1994) Formation of fullerols via hydroboration of fullerene-CGO. J Chem Soc Chem Commun 4:463–464

Shaffer MSP, Koziol K (2002) Polystyrene grafted multi-walled carbon nanotubes. Chem Commun 18:2074–2075

Shvedova AA, Castranova V, Kisin ER, Schwegler-Berry D, Murray AR, Gandelsman VZ, Maynard A, Baron P (2003) Exposure to carbon nanotube material: assessment of nanotube cytotoxicity using human keratinocyte cells. J Toxicol Environ Health Part A 66:1909–1926

Singh R, Pantarotto D, Lacerda L, Pastorin G, Klumpp C, Prato M, Bianco A, Kostarelos K (2006) Tissue biodistribution and blood clearance rates of intravenously administered carbon nanotube radiotracers. Proc Natl Acad Sci U S A 103:3357–3362

Tong H, McGee JK, Saxena RK, Kodavanti UP, Devlin RB, Gilmour MI (2009) Influence of acid functionalization on the cardiopulmonary toxicity of carbon nanotubes and carbon black particles in mice. Toxicol Appl Pharmacol 239:224–232

Wang J, Sun RH, Zhang N, Nie H, Liu JH, Wang JN, Wang H, Liu Y (2009) Multi-walled carbon nanotubes do not impair immune functions of dendritic cells. Carbon 47:1752–1760

Wu M, Gordon RE, Herbert R, Padilla M, Moline J et al (2010) Case report: lung disease in world trade center responders exposed to dust and smoke: carbon nanotubes found in the lungs of world trade center patients and dust samples. Environ Health Perspect 118:499–504

Yin JJ, Lao F, Fu PP, Wame WG, Zhao Y, Wang PC, Qiu Y, Sun B, Xing G, Dong J et al (2009) The scavenging of reactive oxygen species and the potential for cell protection by functionalised fullerene materials. Biomaterials 30:611–612

Zhang J, Zou HL, Qing Q, Yang YL, Li QW, Liu ZF, Guo XY, Du ZL (2003) Effect of chemical oxidation on the structure of single-walled carbon nanotubes. J Phys Chem B 107:3712–3718

Zhu X, Zhu L, Li Y, Duan Z, Chen W, Alvarez PJ (2007) Developmental toxicity in zebrafish (Daniorerio) embryos after exposure to manufactured nanomaterials: buckminsterfullerene aggregates (nC60) and fullerol. Environ Toxicol Chem 26:976–979

Phytoremediation Study and Effect of pH on Biomass Productivity of *Eichhornia crassipes*

Ajay Kumar, Neetu Singh, Shilpa Gupta, Pallavi Joshi, Sukirti Tiwari, and Kavita Swaroop

Introduction

Hindon river is an important tributary of Yamuna river and originates from upper Shiwalik in Lower Himalayan Range (Jain et al. 2007). The river flows through Saharanpur, Muzaffarnagar, Meerut and Ghaziabad in western Uttar Pradesh and covers a distance of about 200 km before joining the Yamuna river downstream of Delhi (Jain et al. 2003).

The effluents of Nagdev nala and Star Paper Mill at Saharanpur generate the flow of water in the Hindon river. The industrial effluents from the cooperative distillery and municipal wastewater from Budhana town plunge into the river water in this stretch. In the Ghaziabad district, downstream of Karhera village, the majority of river flow is diverted to the Hindon cut canal at Mohan Nagar, which outfalls into the Yamuna upstream of the Okhla barrage. Thereafter, the river receives wastewater through the Dhasana drain at Bisrakh village in Ghaziabad district (Jain et al. 2003). The main objective of the study is to explore the phytoremediation potential of *Eicchornia crassipes* and evaluate its biomass productivity at different pH ranges.

Shoeb and Singh (2000) reported that under favourable conditions *Eichhornia crassipes* can achieve a growth rate of 17.5 metric tons per hectare per day. A typical biomass from land plants can have 30–50 % cellulose, 20–40 % hemicellulose and 15–30 % lignins (Bhattacharya and Kumar 2010; Bhetalu et al. 2012; Sagar and Kumari 2013). Masami et al. (2008) suggested a new method of ethanol production from the *Eichhornia crassipes* by using yeast isolated from different hydrospheres.

A. Kumar (✉) • N. Singh • S. Gupta • P. Joshi • S. Tiwari • K. Swaroop
Department of Biotechnology, Mewar Institute of Management, Ghaziabad, UP, India
e-mail: ajaykmr1986@gmail.com

© Capital Publishing Company 2015

N.J. Raju et al. (eds.), *Management of Natural Resources in a Changing Environment*, DOI 10.1007/978-3-319-12559-6_14

Research Methodology

As per the objective of our present investigation, wastewater was collected from a nearby wastewater body, Hindon river. Water sampling was carried out according to standard methods for examination of water and wastewater (APHA 2005).

The representative samples were filtered through a plastic sieve of pore opening size 0.5 mm. Thereafter the required quantity of wastewater samples were transferred into pre-washed "synthetic polyvinyl" culture containers of capacity 90 l each. Adequate individual *Eichhornia crassipes* plants were collected from sampling station in black coloured polyethylene bags. In order to explore the effect of different pH ranges on *Eichhornia* biomass production, it was decided to carry out an experiment under variable pH ranges. Acidic and basic pH was adjusted with 30 % liquid hydrochloric acid and sodium hydroxide respectively. Periodic maintenance of pH was carried out after every 24 h. Total of 12 polyvinyl culture containers were used on the basis of different pH ranges in order to carry out study in duplicates.

Accordingly, the wastewater sample was differentiated into a six pH range viz. Treatment Culture No. 1 (T-1): pH = 5, Treatment Culture No. 2 (T-2): pH = 6, Treatment Culture No. 3 (T-3): pH = 7, Treatment Culture No. 4 (T-4): pH = 8, Treatment Culture No. 5 (T-5): pH = 9 and culture container C-1 contained wastewater with actual pH (7.6) of Hindon river on initial day. As per the literature, it was confirmed that under optimal conditions, *Eichhornia crassipes* can potentially double its biomass in 2–3 weeks (Carignan et al. 1994). Hence, all the culture containers with the duplicates were placed strategically under careful observation for 20 days. In order to provide identical environmental conditions, an open field providing 10 h of uninterrupted light period was selected. All the culture containers were placed inside a 10 ft large polyhouse jacket in order to protect the cultures from any external injuries or disturbances.

For the purpose of nutrient analysis and measuring biomass, all the cultures were placed in periodical sequence. Representative samples from each culture were estimated for DO, BOD, COD, sulphate, phosphate and total-nitrogen on initial day and final day using standard methods of estimation as outlined in APHA (2005). Water samples were filtered through Whatman GF/C filters before analysis. Water loss by evapotranspiration during the wastewater culture study was adjusted by single distilled water from time to time.

Results and Discussion

In order to assess the suitability of *Eichhornia crassipes* for biomass production, wastewater sample was collected from Hindon river and analyzed for some important physicochemical properties. The physicochemical properties of Hindon river wastewater reflect a clear picture about the suitability of its use for *Eichhornia* biomass production except the higher concentration of some nutrients. In the present

investigation, the physicochemical analysis of wastewater was conducted on initial day and after 20 days of wastewater culture study. The details of physicochemical analysis of wastewater has been recorded in Tables 1 and 2.

The main objective of our study is to find out the best possible pH range for maximum *Eichhornia* biomass production. According to Haller and Sutton (1973), maximum growth of *Eichhornia crassipes* occurred in acid (pH 4.0) to slightly alkaline (pH 8.0) pH range. Therefore, it was decided to carry out the biomass production under variable pH range.

Temperature is one of the most important factors in an aquatic environment. In fact, no other single factor has so many profound influences and direct and indirect effects (Welch 1952). A close correlation between air and surface water temperature has also been reported by Mc Combie (1959) in one of his studies as has been noted in the present study also.

The mean air temperature fluctuated from 18.5 °C to 32.1 °C throughout the course of study. The mean air temperature at study site was recorded at 22.75 °C, 25.2 °C and 26.85 °C on initial, 10th and 20th days of wastewater culture study respectively. The surface water temperature followed a trend similar to that of air temperature. Mean water temperature fluctuated from 15.4 °C to 28.3 °C throughout the course of study. The mean water temperature at study site was recorded at 19.3 °C, 21.55 °C and 22.6 °C on initial, 10th and 20th days of culture study respectively.

The DO value 5.0 mg/l is the standard for drinking water (Bhanja and Patra 2000). The value of DO of Hindon river wastewater on initial day of culture study was recorded as 2.5 mg/l. The condition of DO is complex with respect to other parameters. The maximum mean value of DO was recorded as 5.8 mg/l while the minimum value was registered as 1.9 mg/l in T-4 (pH = 8) and T-1 (pH = 5) cultures respectively on 20th (final) day of study (Fig. 1).

Biochemical Oxygen Demand (BOD) is used to determine the relative oxygen requirements of wastewaters, effluents and polluted waters (APHA 1999). Maximum reduction in BOD was shown by treatment culture T-3 (pH = 7) [83.1 %] followed by treatment culture T-4 [81.3 %] during 20 days of wastewater culture study (Fig. 2).

The COD determines the chemical oxidisable organic matter present in water (Kolhatkar et al. 2012). The extent of sample oxidation in COD test can be affected by digestion time, reagent strength and sample COD concentration (APHA 1999). The COD value of Hindon river wastewater was found to be 184 mg/l on the initial day of culture study. The present investigation shows that the maximum reduction in COD value was found in T-3 (pH = 7) [69.7 %] while minimum reduction was found in T-5 (pH = 9) [67.1 %] during the 20 days course of wastewater culture study (Fig. 3).

Ansar and Khad (2005) reported that intolerable levels of phosphates and nitrates to local organisms have been known to deplete dissolved oxygen levels by causing algal blooms. The concentration of phosphate in wastewater was found desirable on initial day of culture study. The concentration of phosphate was consistently decreased in all the treatments. However the highest reduction rate was found in T-4

Table 1 Initial day physico-chemical properties of Hindon river wastewater

	C-1 (pH = 7.6)	T-1 (pH = 5)	T-2 (pH = 6)	T-3 (pH = 7)	T-4 (pH = 8)	T-5 (pH = 9)
Parameters	Mean ± SD	Mean ± SD	Mean ± SD	Mean ± SD	Mean ± SD	Mean ± SD
DO (mg/l)	2.50 ± 0.02	2.50 ± 0.02	2.50 ± 0.02	2.50 ± 0.02	2.50 ± 0.02	2.50 ± 0.02
BOD (mg/l)	48.20 ± 0.22	48.20 ± 0.22	48.20 ± 0.22	48.20 ± 0.22	48.20 ± 0.22	48.20 ± 0.22
COD (mg/l)	184.00 ± 0.20	184.00 ± 0.20	184.00 ± 0.20	184.00 ± 0.20	184.00 ± 0.20	184.00 ± 0.20
Sulphate (mg/l)	27.50 ± 0.02	27.50 ± 0.02	27.50 ± 0.02	27.50 ± 0.02	27.50 ± 0.02	27.50 ± 0.02
Phosphate (mg/l)	0.198 ± 0.03	0.198 ± 0.03	0.198 ± 0.03	0.198 ± 0.03	0.198 ± 0.03	0.198 ± 0.03
Total-nitrogen (mg/l)	292.06 ± 0.72	292.06 ± 0.72	292.06 ± 0.72	292.06 ± 0.72	292.06 ± 0.72	292.06 ± 0.72

Table 2 Final day physico-chemical properties of Hindon wastewater at different pH

	C-1 (pH = 7.6)	T-1 (pH = 5)	T-2 (pH = 6)	T-3 (pH = 7)	T-4 (pH = 8)	T-5 (pH = 9)
Parameters	Mean ± SD	Mean ± SD	Mean ± SD	Mean ± SD	Mean ± SD	Mean ± SD
DO (mg/l)	5.20 ± 0.25	1.90 ± 0.50	3.70 ± 0.67	5.20 ± 1.08	5.80 ± 0.44	2.20 ± 0.18
BOD (mg/l)	9.50 ± 0.93	15.40 ± 2.40	11.30 ± 1.12	8.10 ± 1.06	9.00 ± 1.80	17.20 ± 0.48
COD (mg/l)	66.40 ± 1.05	83.77 ± 0.33	80.60 ± 1.24	55.60 ± 0.02	60.40 ± 0.15	100.28 ± 0.42
Sulphate (mg/l)	8.00 ± 0.25	9.80 ± 0.07	9.24 ± 0.20	7.40 ± 0.18	8.13 ± 0.35	11.20 ± 0.24
Phosphate (mg/l)	0.032 ± 0.04	0.125 ± 0.05	0.087 ± 0.10	0.027 ± 0.04	0.020 ± 0.01	0.132 ± 0.14
Total-nitrogen (mg/l)	85.40 ± 0.39	63.05 ± 1.63	70.18 ± 0.10	110.54 ± 0.43	100.32 ± 0.14	65.50 ± 0.26

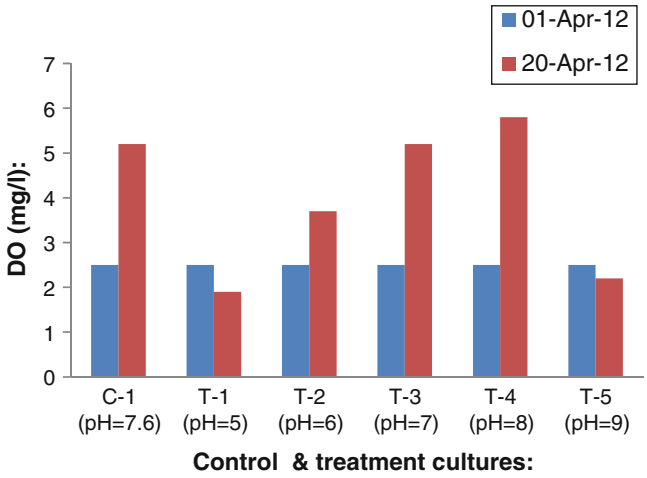

Fig. 1 Initial and final day DO values of Hindon river wastewater at different pH

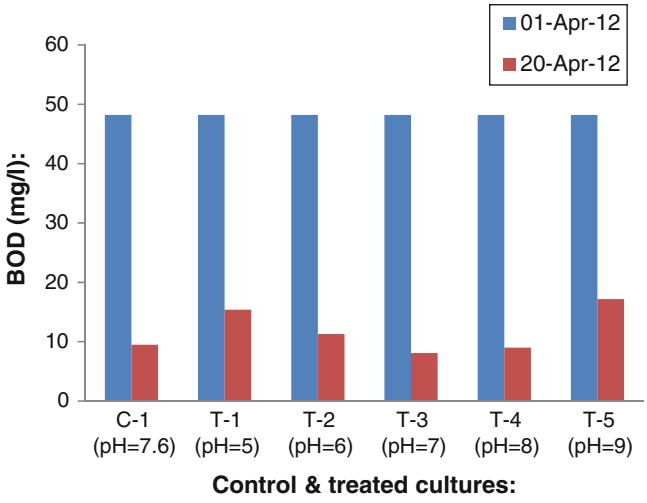

Fig. 2 Initial and final day BOD values of Hindon river wastewater at different pH

(89.8 %) (Fig. 4). The considerable availability of phosphate in Hindon river wastewater is expectedly high due to its accumulation over many decades.

High sulphate containing wastewaters are generated from various industrial activities (Lens et al. 1998). The concentration of sulphate in Hindon river wastewater was 27.5 mg/l on initial day of culture study. The present investigation shows that the maximum reduction in sulphate value was found in T-3 (pH = 7) [73.09 %] while minimum reduction was found in T-5 (pH = 9) [59.2 %] during the 20 days course of wastewater culture study (Fig. 5).

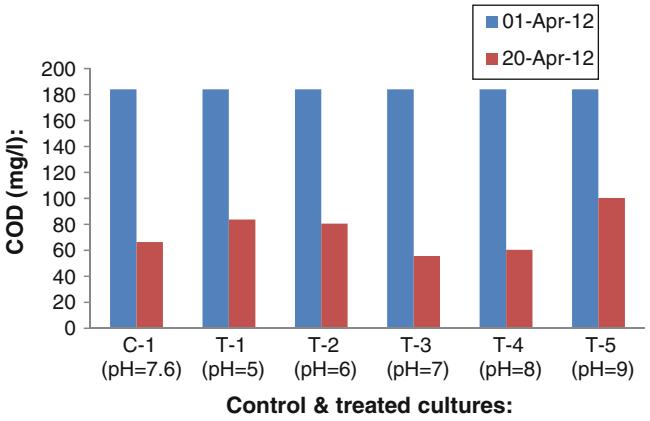

Fig. 3 Initial and final day COD values of Hindon river wastewater at different pH

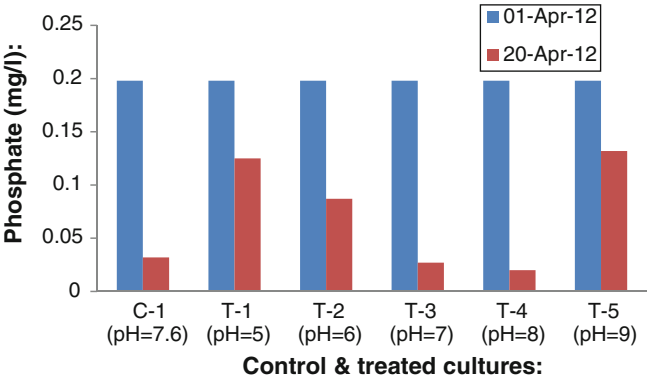

Fig. 4 Initial and final day phosphate values of Hindon river wastewater at different pH

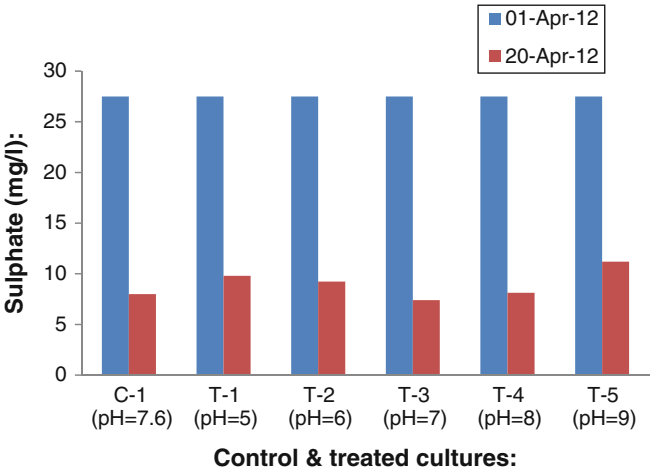

Fig. 5 Initial and final day sulphate values of Hindon river wastewater at different pH

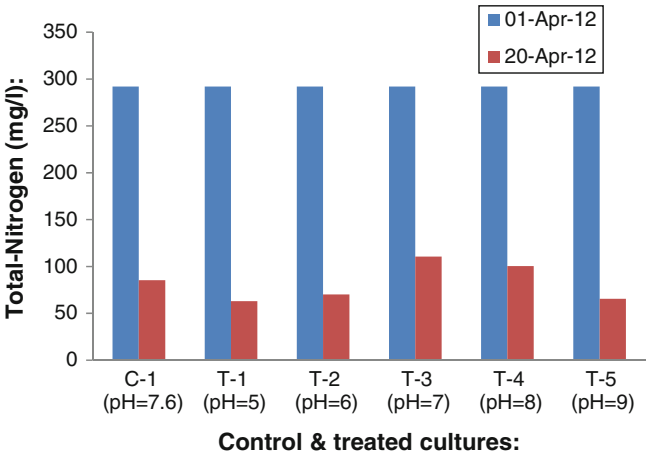

Fig. 6 Initial and final day total-nitrogen values of Hindon rive wastewater at different pH

Ammonia is toxic to aquatic life and toxicity is affected by pond pH. Ammoniacal-Nitrogen (NH_3-N) has an extensively high toxic form at high pH and a less toxic form at low pH. In addition, ammonia toxicity increases as temperature rises (Wurts 2003). The value of total-nitrogen in Hindon river wastewater was found to be 292.06 mg/l on initial day of culture study. The present investigation shows that the maximum reduction in total- nitrogen value was found in T-1 (pH = 5) [78.41 %] while minimum reduction was found in T-3 (pH = 7) [62.15 %] during 20 days course of culture study (Fig. 6).

As per our main objective of the present investigation, the effect of pH, in six different combinations was investigated (Table 3). All the data on biomass production at different pH were varying considerably. Maximum production of net biomass was recorded in T-3 as 197.60 ± 0.14 g, while minimum biomass production was recorded in T-1 as 87.49 ± 0.95 g on final day of wastewater culture study (Fig. 7). The maximum increase in biomass production at pH = 7 and pH = 8 may be due to increase in the nutrient uptake and immobilization capacity of *Eichhornia crassipes* at neutral and slightly alkaline pH.

Conclusion

According to Delgado et al. (1994), with an increase in pH, the ionic forms of the micronutrient cations change to hydroxides or oxides. This indicates that the *Eichhornia crassipes* has a tendency to neutralize an aquatic environment. Therefore, it is necessary to add a base or an acid in order to maintain the required pH range as outlined by Delgado et al. (1994). Minor fluctuations were observed in the pH values of treatment cultures; therefore periodic maintenance of pH was carried out after every 24 h.

Table 3 Periodical trend in *Eichhornia* biomass production under different pH on initial and final day of wastewater culture study

	C-1 (pH = 7.6)	T-1 (pH = 5)	T-2 (pH = 6)	T-3 (pH = 7)	T-4 (pH = 8)	T-5 (pH = 9)
Parameters	Mean ± SD	Mean ± SD	Mean ± SD	Mean ± SD	Mean ± SD	Mean ± SD
Fresh weight biomass (gms)						
Initial day (01 Apr, 2012)	40.27 ± 2.40	42.00 ± 1.03	40.35 ± 2.83	43.50 ± 4.95	44.28 ± 1.02	42.16 ± 0.75
Final (20th) day (20 Apr, 2012)	180.32 ± 4.82	90.13 ± 2.37	150.62 ± 4.31	203.75 ± 2.50	174.08 ± 1.8	100.21 ± 0.40
Dry weight biomass (gms)						
Final (20th) day (20 Apr, 2012)	5.40 ± 0.55	2.64 ± 1.42	4.33 ± 0.42	6.15 ± 2.36	5.18 ± 0.40	3.012 ± 0.15
Net biomass (gms)						
Final (20th) day (20 Apr, 2012)	174.92 ± 4.27	87.49 ± 0.95	146.29 ± 3.89	197.60 ± 0.14	168.90 ± 1.4	97.198 ± 0.25

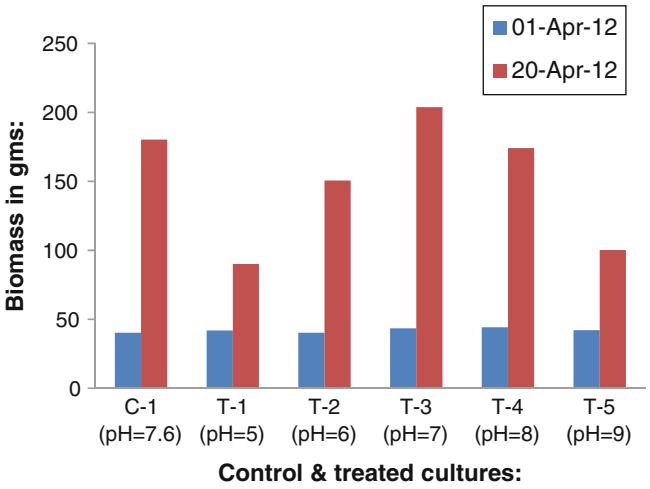

Fig. 7 Fresh weight biomass of *Eichhornia crassipes* on initial and final day of wastewater culture study at different pH

The pH culture study was conducted at different pH range i.e. 5, 6, 7, 8, 9 along with actual pH of Hindon river for a period of 20 days. The alkaline pH (7.6) of the wastewater was observed in our study which is due to the presence of ammoniacal nitrogen. Wastewater culture at pH = 7, pH = 8 and pH = 7.6 represents suitable medium for maximum nutrient removal as it seems to have commanding influence on the growth of *Eichhornia crassipes*. The *Eichhornia crassipes* biomass production on final day followed the trend in treatment cultures as follows: pH 7.0 > pH 8. 0 > pH 6.0 > pH 9.0 > pH 5.0.

Our study finally explored the potential of using wastewater under variable pH for the production of *Eichhornia crassipes* biomass and thereby conducted an array of methods to develop the wide possibilities of developing wastewater culture medium using different pH in order to attain maximum biomass production. This would consequently enhance the production of biofuel from *Eichhornia* biomass. The biofuel thus produced may possibly replace the traditional fuel, and ward off our present day fuel crisis. The possible use of aquatic plants to remove nutrients from wastewater effluents and eutrophic water has received considerable attention in recent years.

References

Ansar A, Khad F (2005) Eutrophication: an ecological vision. Bot Rev 71(4):449–482

APHA (1999) Standards methods for the examination of water and wastewater, 20th edn. APHA, Washington, DC

APHA (2005) Standards methods for the examination of water and wastewater, 21st edn. APHA, Washington, DC

Bhanja KM, Patra A (2000) Studies on the water quality index of river Sanamachhakandana at Keonjhar garh, Orissa, India. Poll Res 19(3):377–385
Bhattacharya A, Kumar P (2010) Water hyacinth as a potential biofuel crop. Electron J Environ Agric Food Chem 9(1):112–122
Bhetalu AD, Patil SS, Ingole NW (2012) Studies on generation of power alcohol as a non-conventional energy source from aquatic macrophytes—a critical review. J Eng Res Stud 3(1):9–17
Carignan R, Neiff JJ, Planas D (1994) Limitation of water hyacinth by nitrogen in subtropical lakes of the Paran floodplain (Argentina). Limnol Oceanogr 39(2):439–443
Delgado MDM, Bigeriego M, Walter I, Guardiola E (1994) Optimization of conditions for the growth of water hyacinth in biological treatment. Rev Int Contam Ambient 10(2):63–68
Haller WT, Sutton DL (1973) Effect of pH and high phosphorous concentrations on growth of water hyacinth. J Florida Agr Exp Sta, 4804 / Hyacinth Control J/J Aquat Plant Manag 11:59–61
Jain CK, Singhal DC, Sharma MK (2003) Hydrochemical studies of the Hindon River, India: seasonal variation and quality-quantity relationships. J Environ Hydrol 2:1–3
Jain SK, Agarwal PK, Singh VP (2007) Hydrology and water resources of India: volume 57 of water science and technology library—tributaries of Yamuna River. Springer
Kolhatkar DG, Shinde LP, Bhagure JC, Sahu NK (2012) Study of physicochemical characteristic of opium effluent in Govt. opium and alkaloid factory, Ghazipur (U.P.). Int J Pharm Bio Sci 3(1):363–367
Lens PNL, Visser A, Jansen AJH, Hulshoff Pol LW, Lettinga G (1998) Biotechnological treatment of organic sulphate-rich wastewaters. Crit Rev Environ Sci Technol 28:41–88
Masami GO et al (2008) Ethanol production from the water hyacinth Eichhornia crassipes by yeast isolated from various hydrosphere. Afr J Microbiol Res 2:110–113
Mc Combie AM (1959) Some relations between air temperature and the surface water temperature of lake. Assoc Sci Limnol Oceanogr 4(3):252–258
Sagar V, Kumari NA (2013) Sustainable biofuel production from water Hyacinth (*Eicchornia crassipes*). Int J Eng Trends Technol 4(10):4454–4458
Shoeb F, Singh HJ (2000) Kinetic studies of biogas evolved from water hyacinth. In: Proceedings of Agroenviron 2000, 2nd international symposium on new technologies for environmental monitoring and agroapplications, held at Tekirdag, Turkey, doi: 18–20th October 2000
Welch PS (1952) Limnology. McGraw Hill Book Company, New York
Wurts WA (2003) Daily pH cycle and ammonia toxicity. World Aquacult 34(2):20–21

Regeneration of White Oak (*Quercus leucotrichophora*) in Two Pine Invaded Forests in Indian Central Himalaya

Satish Chandra Garkoti

Introduction

A few species of oak found in the Himalaya are some of the largest forests forming species in the world (Singh et al. 2000). Among the various oak species that occur in central Himalaya viz., *Qurecus leucotrichophora*, *Q. floribunda*, *Q. glauca*, *Q. semecarpifolia* and *Q. lanuginosa* (Singh and Singh 1992), *Q. leucotrichophora* contributes to a greater proportion of ecosystem services than most of other species in the region (Singh 2002; Joshi et al. 2011).

In central Himalaya, white oak (*Q. leucotrichophora*), a climax species, is widely distributed between 1,200 and 2,200 m amsl (Troup 1921) and occupies approximately 12.3 % of the total area (24,413.20 km^2) of forest under the control of state forest department. White oak shares its dominance in this part of Himalaya with Chir pine (*Pinus roxburghii*), a successional species (Vishnu-Mittre 1974) that covers approximately 16.4 % of the above mentioned total forest area between 900 and 1,700 m amsl in the region. In most of the villages in the central Himalaya, despite huge socio-economic and infrastructural changes that have taken place in the recent past, local farming communities still heavily depend on forest resources for their subsistence. From the forests people collect fuel wood, fodder, forest litter for livestock beddings and various species for food and medicine (Singh et al. 2010; Joshi and Negi 2011). Among various species present in the region, oak is preferred most because it produces quality fuel wood and its leaves are perennial source of fodder. Leaf litter of white oak is also used as cattle bedding which ultimately after decomposition reach to crop fields for replenishing soil fertility year after year.

Studies show that chronic disturbances resulted in the degradation of white oak forests in the region and made them susceptible to fire damages that spread

S.C. Garkoti (✉)
School of Environmental Sciences, Jawaharlal Nehru University, New Delhi 110067, India
e-mail: sgarkoti@yahoo.com

© Capital Publishing Company 2015

N.J. Raju et al. (eds.), *Management of Natural Resources in a Changing Environment*, DOI 10.1007/978-3-319-12559-6_15

periodically from adjacent chir pine forests. Ecological literature during last few decades from the central Himalaya is full of the concerns that fire adapted chir pine (*Pinus roxburghii*) is replacing ecologically and socially valuable Indian white oak (*Qurecus leucotrichophora*), because the latter is subjected to various degree of anthropogenic disturbances like lopping, browsing, and recurrent forest fires (Singh et al. 1984, 1997; Singh 1998; Semwal and Mehta 1996; Semwal et al. 2003). Fire causes extensive damages to nearby degraded white oak especially on dry south facing slopes and has resulted into encroachment of *P. roxurghii* in oak forests (Singh et al. 1984; Singh and Singh 1992). Fire in chir pine forests occur at 3–5 years intervals and usually eliminate seedlings and saplings of other co-occurring species (Tewari 1982; Semwal and Mehta 1996). Chir pine being fire adapted successional species colonizes the burnt sites (Singh and Singh 1992). However, it has been observed that in oak-pine transition zones, fire damages during certain years have resulted in vigorous regeneration of white oak in several moist chir pine occupied sites (Garkoti personal observations). Owing to high social value local people prefer oak compared to chir pine and thus protect regenerating oak from fire and animal grazing in order to ensure sustainable supplies of goods and services from white oak forests. Although replacement of white oak by pine after disturbance is common in central Himalaya as well as natural because the pine is a successional species and the same has been widely reported by various ecologists (Singh and Singh 1992), there is no published record in ecological literature that describes the reverse.

Material and Methods

Study Area

The forest sites studied were located at 29° 20′11.6° N 80° 01′05.2° E (oak I) and at 29° 19′06.9° N 80° 01′26° E (oak II) at 1,849 m and 1,653 m amsl, respectively. Vegetation and soil characteristics of the study sites are presented in Table 1. Previously both the sites were under pine forest with a few scattered oak trees. The climate is temperate with an annual average rainfall 1,430 mm. In all the aspects in ridge sites pine occurs even above the present study site elevations. Monsoon rains in this part of Himalaya occur from late June/early July to the middle of September. The year is divisible into three main seasons: cool and usually dry winters (October–March), warm and dry summer (April–June), and warm humid rainy season (July–September).

Methods

Present study was conducted in two representative oak regeneration sites in the central Himalaya. Both the oak regeneration sites were located in oak-pine transition zone and were surrounded by old growth pine forests. Following Misra (1968) each regenerating stand was sampled by using ten, 10 m × 10 m randomly placed

Table 1 Site characteristics of two regenerating *Quercus leucotrichophora* forests of central Himalaya

Categories	16 years old stand	34 years old stand
Elevation (masl)	1,849	1,653
Tree density (trees ha^{-1})	1,280 (950)	1,100 (660)
Tree basal area (m^{-2} ha^{-1})	12.0 (10.4)	33.3 (28.3)
Soil N (%)	0.41 ± 0.03	0.48 ± 0.03
Available P (%)	0.024 ± 0.002	0.030 ± 0.002
Soil bulk density (g cm^{-3})	0.741 ± 0.05	0.631 ± 0.12
Soil pH	5.77 ± 0.11	5.36 ± 0.17
Soil moisture (%)	28.31 ± 2.13	31.46 ± 2.69

Values in parentheses are for *Q. leucotrichophora*

quadrats. Species richness, number of individuals of different species and circumference at breast height (cbh) of the individuals were recorded. Seedlings number was counted species wise.

Results and Discussions

Preliminary observations made on two regenerating oak forests indicate that on ridges pine occurs even at a higher elevation than the present oak regeneration site. In valleys, if the sites were kept free from disturbances for some time after the establishment of oak seedlings, the white oak was able to reoccupy the site. Some of these sites were in fact encroached by pine in the past and oak is now apparently again a dominant species.

In both the sites total five different tree species were recorded. In oak site I, pine was represented by only few seedlings while in oak site II, adult individuals of pine were also present (Figs. 1 and 2). In both the forests tree basal area was higher for *Q. leucotrichophora*, 10.4 m^2 ha^{-1} (86.9 %) and 28.4 m^2 ha^{-1} (85.3 %) in oak I and oak II, respectively (Table 1). *Quercus leucotrichophora* was the dominant species in both the forests followed by *Myrica nagi*. In general, two population structure categories have been derived from the size class distribution of tree species (Figs. 1 and 2): (a) expending or stable with many seedlings and gradual decline with increase in size class (e.g., *Q. leucotrichophora, R. arboreum*). This structure reflects continuous establishment of population of species. (b) Youthful with seedlings and saplings or young trees (e.g., *Q. floribunda, Pyrus pesia*, *Ficus nimalia*, *L. ovalifolia*). This type of species could be recent invaders and may increase their dominance in the community later. It seems that *Q. leucotrichophora* ameliorates the habitat conditions (e.g., N and moisture) and that in turn helps its associates to occupy the available niches in the community. In both the forests of present study, *Q. leucotrichophora* has expanding population structure. With the exclusion of disturbance in terms of forest fire and lopping for some period in the past the oak was able to regain and expand.

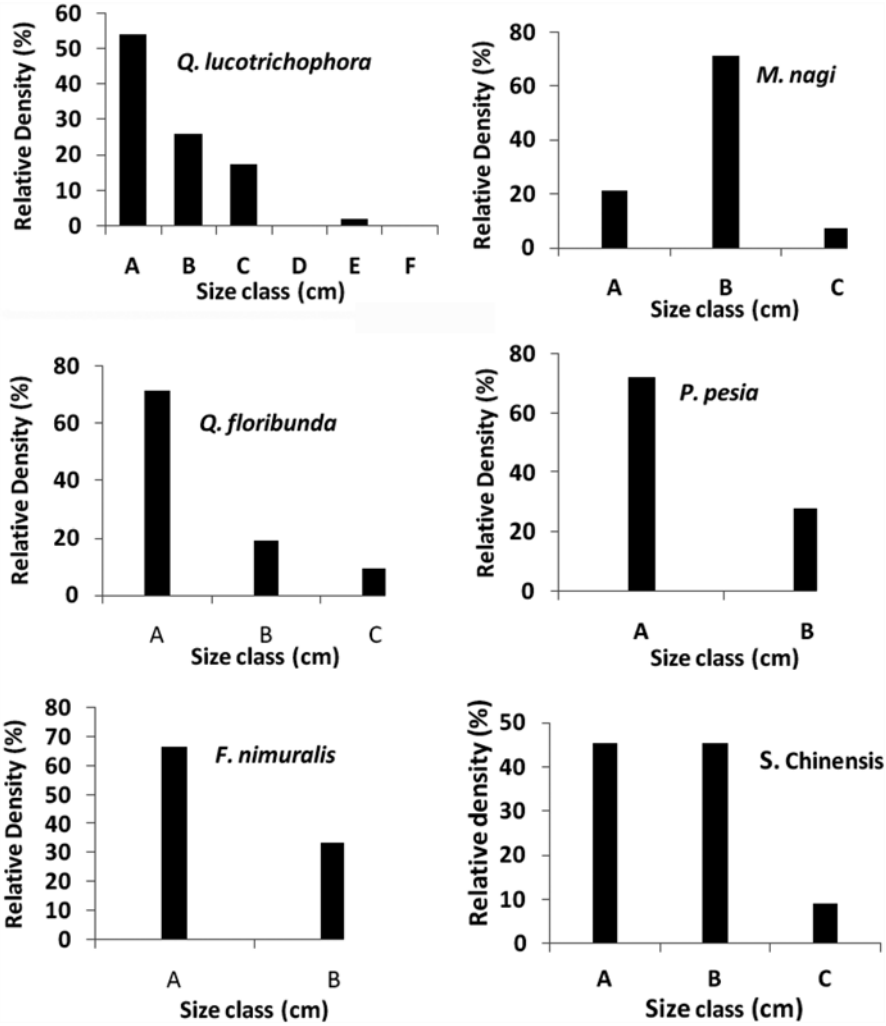

Fig. 1 White oak regenerating forest site I in Indian central Himalaya. *A*–*H* represent girth classes of individuals of the species in cm. *A*: seedlings, *B*: 10–30, *C*: 30.5–60, *D*: 60.5–90, *E*: 90.5–120, *F*: 120–150, *G*: 150.5–180 and *H*: >180

According to Singh et al. (1984) pine has greater nutrient conserving ability than oak and it creates N shortage in the soil that makes it difficult for oak to reinvade pine encroached sites. Present study addressed the question what conditions favour oak to reestablish in these sites. Present study observes that after the fire removes the pine, oak is able to reoccupy the sites in moist valley areas only with some degree of shade. The mountain ridge areas with higher light conditions remain under pine. It seems that nutrient required by oak would be flowing down to valley sites from the mountain slopes through surface and subsurface runoff during rainy seasons. Once the oak gets established it further

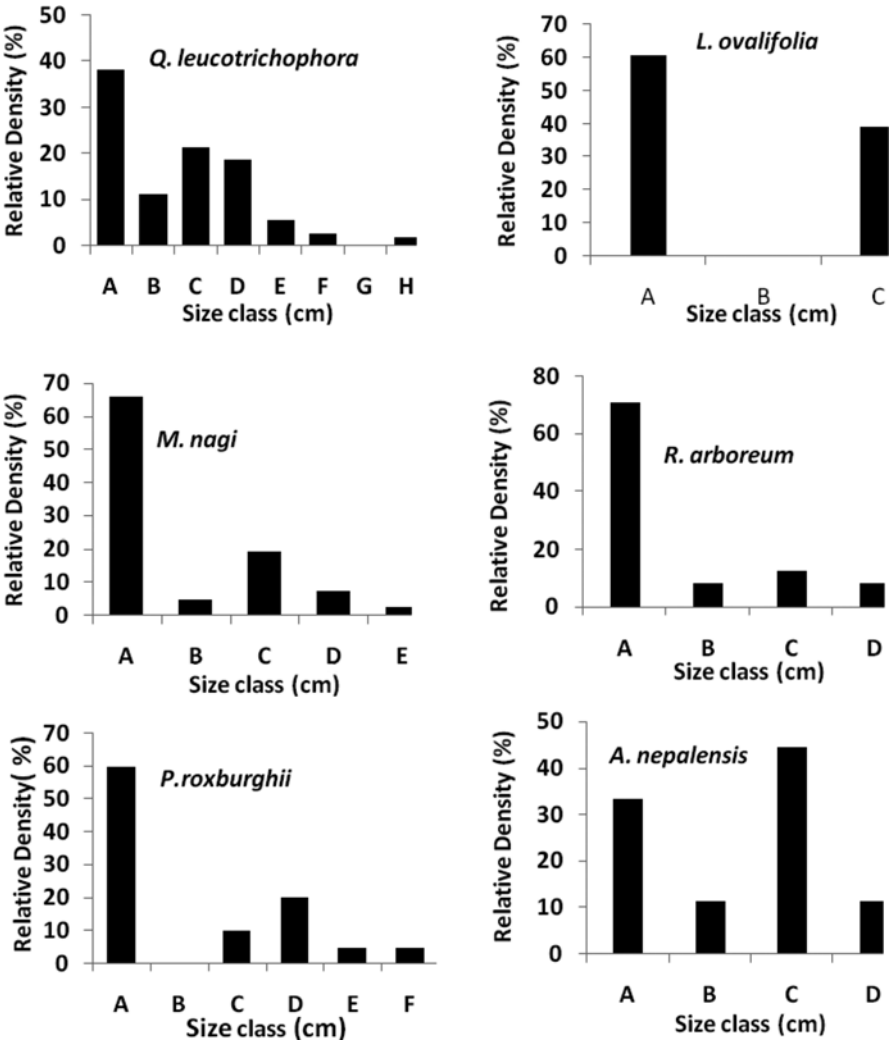

Fig. 2 White oak regenerating forest site II in Indian central Himalaya. *A*–*H* represent girth classes of individuals of the species in cm. *A*: seedlings, *B*: 10–30, *C*: 30.5–60, *D*: 60.5–90, *E*: 90.5–120, *F*: 120–150, *G*: 150.5–180 and *H*: >180

improves nutrient status of the habitat and makes gradual opening for its associates from the adjacent forests.

Oak has comparatively higher demand for N than the pine (Singh and Singh 1992). In ridge area that was occupied by pine, the dynamic available N pool in the soil at any point of time is very low and N immobilization by microbes in decomposing pine litter further increases the N shortage in the soil (Singh et al. 1984). Because of this reason oak in general is not able to reoccupy the habitats in ridge areas. However, the wash off of nutrients from the slopes that brings soil and nutrients improves the moisture as well as nutrient status in valley areas. Once established,

white oak is able to maintain high soil fertility, through return of nutrient rich litter and rapid mineralization of nutrients (Singh and Singh 1992). Total soil N was 0.48 and 0.41 % in valley areas, and 0.38 and 0.39 % in ridge areas (at 0–10 and 10–20 cm soil depths, respectively). If fire occurs at the time when other environmental factors are in favour of oak it regenerates vigorously (Negi 2002) and paradoxically out competes pine from the site.

Q. leucotrichophora has an expanding population structure. As the disturbance in the form of forest fire and lopping has been excluded for some time in the past the oak was able to reestablish and expand. A few years after the oak establishment several of its associates like *Q. floribunda*, *Pyrus pashia*, *Ficus* sp. *L. ovalifolia* have joined the sites. Most of these species were absent in adjacent pine forest (Garkoti pers. Communication). It seems that return of white oak ameliorates the habitat conditions (e.g., N and moisture) which allows these associates to occupy the available niches in the community.

The establishment of oak after fire damages the pine poses a question as to how or what conditions make a climax species (oak) to replace a successional species (pine) after the disturbance (ecological knowledge so far reflects the opposite). Severe fire in the pine forests removes individuals of all the species present. In the dry and sunny mountain ridges pine always reoccupies the area after the fire damages. On dry slopes especially once the area comes under pine it reduces the available N pool in the soil through immobilization properties of its decomposing litter (Singh et al. 1984). As white oak has comparatively higher demand for N and other nutrients than pine, it is not able to reinvade the areas from where it is displaced by the pine. However, in certain years, after the fire that removes pine, oak is paradoxically able to occupy the sites in moist valley areas. It seems that nutrients required by oak would be flowing down to valley sites from the mountain slopes through surface and subsurface runoff during rainy seasons and sites remain favourable for oak. If fire occurs at the time when other environmental factors such as high moisture associated with lower temperature are in favour of white oak, it regenerates vigorously and out competes chir pine in those sites. Once the oak gets established it further improves nutrient status of the habitat and makes habitat favourable for its associates from the adjacent forests. The wash off of nutrients from the slopes that brings soil and nutrients improves the moisture as well as nutrient status in valley areas. Once established, white oak is able to maintain high soil fertility, through return of nutrient rich litter and rapid mineralization of nutrients (Singh and Singh 1992).

Conclusion

In both the sites of the present study, white oak has expanding population structure indicating natural regeneration of oak and restoration of the habitat. It seems that establishment of white oak results in improvement of soil nutrient capital (as evidenced from the soil N) which in turn facilitates the arrival of its several associates in the community and results in increase in stand diversity. Disturbances are now

considered integral part and also the driving force in ecosystem dynamics in most of the regions in the Himalaya and elsewhere. Present study indicates that even a short period of protection (e.g. 5–8 years) is sufficient to permit the oak to reestablish and regenerate and to check the invasion of pine in valley areas in central Himalaya. It is important to identify such sites in the region. Conservation of such areas not only would help people directly by supplying the ecosystem goods and but also indirectly through increase in biodiversity and conservation of soil, nutrients and moisture and various other ecological services.

References

Hargreaves AL, Harder LD, Johnson SD (2010) Native pollen thieves reduce the reproductive success of a hermaphroditic plant, *Aloe maculata*. Ecology 91:1693–1703

Joshi G, Negi GCS (2011) Quantification and valuation of forest ecosystem services in the western Himalayan region of India. Int J Biodivers Sci Ecosyst Serv Manag 7:2–11

Misra R (1968) Ecology work book. Oxford/IBH, Calcutta

Negi GCS (2002) Hydrological research in the Indian Himalayan mountains: soil and water conservation. Curr Sci 83:974–980

Negi GCS, Semwal RL (2010) Valuing the services provided by forests and agroecosystems in the Central Himalaya. Mt Forum Bull 10(1):44–47

Negi AS, Negi GCS, Singh SP (1996) Establishment and growth of Quercus floribunda after a mast year. J Veg Sci 7:550–564

Semwal RL, Mehta JP (1996) Ecology of forest fires in chir pine (*Pinus roxburghii* Sarg.) forests of Garhwal Himalaya. Curr Sci 70:426–427

Singh SP (1998) Chronic disturbance, a principal cause of environmental degradation in developing count. Environ Conserv 25:1–2

Singh SP (2002) Balancing the approaches of environmental conservation by considering ecosystem services as well as biodiversity. Curr Sci 82:1331–1335

Singh JS, Singh SP (1992) Forests of Himalaya: structure, functioning and impact of man. Gyanodaya Prakashan, Nainital

Singh JS, Rawat YS, Chaturvedi OP (1984) Replacement of oak with pine in the Himalaya affects the nitrogen cycle. Nature 311:54–56

Singh SP, Rawat YS, Garkoti SC (1997) Failure of brown oak (*Quercus semecarpifolia*) to regenerate in Central Himalaya: a case of environmental semisurprise. Curr Sci 73:371–374

Singh SP, Singh V, Skutsch M (2010) Rapid warming in the Himalayas: ecosystem responses and development options. Clim Dev 2:1–13

Tewari JC (1982) Vegetation analysis along altitudinal gradients around Nainital. PhD thesis, Kumaun University, Nainital, India

Thadani R, Ashton PMS (1995) Regeneration of banj oak (*Quercus leucotrichophora* A. Camus) in the central Himalaya. For Ecol Manag 78:217–224

Troup RS (1921) The silviculture of Indian trees, vols I–III. Clerandon Press, Oxford

Vishnu-Mittre (1974) Late quaternary paleobotany and palynology in India: an appraisement. In: Vishnu-Mittre (ed) Late quaternary vegetation development in extra European areas. Birbal Sahani Institute of Paleobotany, Lucknow

Part III
Environmental Pollution: Issues and Strategies

Human Health Risk Assessment of Heavy Metals from Bhalaswa Landfill, New Delhi, India

Balsher Singh Sidhu, Dikshant Sharma, Tushar Tuteja, Smit Gupta, and Arun Kumar

Introduction

A landfill is the most common method of organized waste disposal, and in developing countries like India, landfills continue to be the most commonly practised form of municipal solid waste (MSW) disposal due to their economic advantages. Bhalaswa landfill site, located in north-eastern part of Delhi, came into operation in 1993. It has an area of 21.06 acres; this land was once used for sugar cane plantation. About 6 ha is devoted to a composting facility. This is an unlined landfill, and only has a layer of waste construction material topped with soil instead of a layer of plastic required for a secure landfill. Approximately, 2,200 tonnes of MSW is buried in the landfill every day. The landfill has already reached about 22 m of height, and is past its closure date of November 2009. A very pertinent danger to human health from landfills such as Bhalaswa is the domestic use of groundwater that has been contaminated by leachate. Contaminants are leached from the solid waste as water percolates through the landfill and mixes with ground water. The heavy metals usually pose a threat in a landfill when they enter the leachate. The motivation for this study was the fact that the health risk posed by heavy metals is serious, and requires immediate remedial measures.

Methodology

The risk assessment study was done using a five-step approach. First, the hazard was identified by defining the harmful contaminants and their corresponding health effects. Next, exposure assessment was done in which the concentration of the

B.S. Sidhu • D. Sharma • T. Tuteja • S. Gupta • A. Kumar (✉)
Department of Civil Engineering, Indian Institute of Technology Delhi, New Delhi, India
e-mail: arunku@civil.iitd.ac.in

© Capital Publishing Company 2015

N.J. Raju et al. (eds.), *Management of Natural Resources in a Changing Environment*, DOI 10.1007/978-3-319-12559-6_16

contaminants in the environment and their rate of intake was studied. The third step was dose-response assessment to find the relation between the amount of exposure and the risk involved. It was followed by risk characterization, which estimated the potential impact of the hazard based on the severity of its effects and amount of exposure. The last part of the study curtailed risk management and communication, wherein suggestions to divide the region into successive risk-zones were made.

Hazard Identification

Lead: Lead is a highly toxic substance, exposure to which can produce a wide range of adverse health effects. Lead poisoning has been known to affect the health of children more than that of the adults. Over the years, tens of millions of children have suffered its health effects. Children under the age of six are especially vulnerable to its harmful effects, because their brains and central nervous system are still being formed. Even very low levels of exposure can result in reduced IQ, learning disabilities, attention deficit disorders, behavioural problems, stunted growth, impaired hearing, and kidney damage. At high exposures, it can even result in death (Guidotti and Ragain 2007).

Among the adults, lead can increase blood pressure and cause fertility problems, nerve disorders, muscle and joint pain, irritability, and memory or concentration problems (Schwartz et al. 1990; Staudinger and Roth 1998). However, the adverse health effects require very high concentrations of lead as compared to children. Apart from these health effects, lead poisoning has also been known to cause gastrointestinal tract disorders, nausea, diarrhoea, weight loss, muscular weakness, bone degradation, among other things. In pregnant women, high levels of lead can easily be transferred to the foetus. This is a very serious problem, which can have adverse effects on the unborn child for the rest of its life.

Several studies have tried to find a link between exposure to lead and an increase in cancer rates among the general population. Some of these studies have found a small increase in lung cancer risk. Some studies have also found an increased risk of stomach cancer with higher lead exposure. However, the link between lead exposure and cancer is not clear, and more studies are needed to better define the possible link between lead exposure and cancer risk.

Zinc: Zinc in general is an essential requirement for a healthy body; it is critical in supporting the immune system, which protects us from pathogens, infections, and disease. However, it can be very harmful if it is present in excess amounts. Zinc poisoning is a potentially life-threatening emergency. Excessive absorption of zinc in the body can cause copper retention in the cells along the intestine, which prevents the body from properly absorbing copper. This copper deficiency can cause anaemia symptoms, such as fatigue, weakness and pale skin. Apart from copper deficiency, excessive zinc consumption may also irritate the intestinal tract, causing

nausea, vomiting and diarrhoea. Diarrhoea may be accompanied by appetite loss and abdominal cramping, bloating and discomfort. Zinc poisoning may also cause flu-like symptoms, including fever, headache, dizziness, chills, lethargy, and body or muscle aches. More severe side effects include convulsions, severely low blood pressure and loss of consciousness (Fosmire 1990).

Exposure Assessment

Exposure assessment involves measuring or estimating the intensity, frequency, and duration of exposure to heavy metal in leachate from landfill. The evaluation of the exposure assessment has been based on previous studies and experience. The first step involved in exposure assessment is to obtain heavy metal concentration in the leachate. The data was acquired from the report by Bhalaswa Lok Shakti Manch, wherein random sampling of groundwater from hand pumps and bore wells was done to analyze the metal concentrations. The metals that were predominantly present were lead (Pb) and zinc (Zn) with highest concentration of 0.053 mg/L and 0.516 mg/L respectively. The permissible limits according to WHO guidelines on safe drinking water are 0.01 mg/L and 15 mg/L for lead and zinc respectively. The concentration of zinc in the water samples was within the acceptable limits. However, lead concentrations were higher than the permissible concentration and hence included in the exposure assessment. The potential pathways by which humans could be exposed to lead from leachate are shown in Fig. 1.

The second step was to identify the possible sources of lead which can be lead batteries, e-waste, construction waste (having lead-based paint) and chemicals for photograph processing. All these waste materials reach the landfill when they are dumped as a part of the municipal solid waste.

The next step was to determine exposure rates (magnitude, frequency, duration). Average Daily Dose (ADD) and Chronic Daily Intake (CDI) have been calculated using the default exposure parameters.

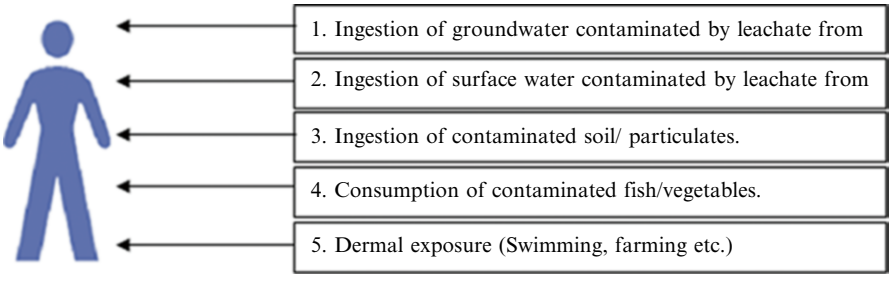

Fig. 1 Potential pathways for lead exposure

Average Daily Dose (ADD)

The ADD is the assumed average maintenance dose per day for a drug used for its main indication in adults.

$$\mathrm{ADD} = \frac{\mathrm{CW} \times \mathrm{DI}}{\mathrm{BW}} \tag{1}$$

where CW is contaminant concentration in water; DI = average daily intake and BW = average body weight.

Chronic Daily Intake (CDI)

Exposure expressed as mass of a substance contacted per unit body weight per unit time, averaged over a long period of time (usually 70 years, as in this study).

$$\mathrm{CDI} = \frac{\mathrm{CW} \times \mathrm{IR} \times \mathrm{EF} \times \mathrm{ED}}{\mathrm{BW} \times \mathrm{AT}} \tag{2}$$

where CDI is chronic daily intake by ingestion (mg/kg-day); CW = concentration in water (mg/L); IR = ingestion rate (L/day); EF = exposure frequency (days/year); ED = exposure duration (years); BW = average body weight (=70 kg) and AT = averaging time (=70 years).

Exposure rate for ingestion of water is calculated. For that, we have to first determine the average daily consumption of contaminated water which in turn depends significantly on various factors as age, gender, body weight, and climate. But for convenience, conservative "default exposure" parameters as suggested by USEPA (1997) are used for exposure quantification (ingestion rate = 2 L/day; annual exposure frequency = 350 day/year).

For Lead:

$$\mathrm{ADD} = \frac{\left(0.053\,\frac{\mathrm{mg}}{\mathrm{L}}\right) \times \left(2\,\frac{\mathrm{L}}{\mathrm{Day}}\right)}{(70\ \mathrm{kg})} = 1.51 \times 10^{-3}\,\mathrm{mg\,kg^{-1}day^{-1}}$$

$$\mathrm{CDI} = \frac{\left(0.053\,\frac{\mathrm{mg}}{\mathrm{L}}\right) \times \left(2\,\frac{\mathrm{L}}{\mathrm{Day}}\right) \times \left(350\,\frac{\mathrm{days}}{\mathrm{year}}\right) \times (30\ \mathrm{years})}{(70\ \mathrm{kg}) \times \left(70\ \mathrm{years} \times 365\,\frac{\mathrm{days}}{\mathrm{year}}\right)}$$

$$= 6.22 \times 10^{-4}\,\mathrm{mg}/(\mathrm{kg\text{-}day})$$

Food supply pathway is another important exposure route. Lead is often bio-accumulated or concentrated in plants or fishes, thereby exposing those humans who are ingesting it. But this study is limited to calculations of exposure through ingestion of groundwater only. The exposure rates for other pathways such as ingestion of soil, consumption of fish/vegetables, and dermal exposure are out of scope of this study.

Dose-Response Assessment

Dose-response relationship is a quantitative relationship that indicates the agent's degree of toxicity to exposed species. The method involves derivation of occupational, clinical and epidemiological studies of the risk of that agent. Dose is normalized as milligrams of substance or pathogen ingested, inhaled, or absorbed (in the case of chemicals) through the skin per kilogram of body weight per day (mg/kg-day). The goal of this exercise is to have a mathematical relationship between the amount of a toxicant (lead in this case) to which a human being is exposed and the risk of a hazardous outcome from that toxicant.

Lead is both a non-carcinogen, and a potential carcinogen, as explained in the earlier part of this study. So, there will be two parts of this study.

Non-carcinogenic Effects

Lead is only slowly excreted by the body. Small amounts of lead ingested over a long time can slowly accumulate to reach harmful levels. Harmful effects may therefore develop gradually without warning. Short-term exposure to high levels of lead may also cause harm.

The dose-response effects for non-carcinogens follows an existence of a level after which certain observable level of effects take place. The threshold value is represented by Reference Dose, or RfD which is an assumed dose below which there is no appreciable risk to humans. The U.S. EPA has not established a Reference Concentration (RfC) or an oral Reference Dose (RfD) for lead. However, WHO guidelines state the upper limit for lead concentration in drinking water to be 0.01 mg/L. ADD is divided by RfD to get the Hazard Quotient (HQ). If HQ is greater than 1, the exposed population is assumed to be at risk, else not.

Carcinogenic Effects

There are several inconclusive epidemiological studies of exposed workers which provided limited evidence of cancers of the kidney, stomach, and respiratory tract. The U.S. EPA has classified lead in Group B2: Probable human carcinogen (USEPA 2006).

The International Agency for Research on Cancer has classified lead and inorganic lead compounds in Group 2B: Possibly carcinogenic to humans, and organic lead in Group 3: Not classifiable (IARC 1987).

The carcinogenic potential of lead salts (primarily phosphates and acetates) administered via the oral route or by injection has been demonstrated in rats and mice by more than 10 investigators (Sanchez-Chardi et al. 2007). The most characteristic cancer response is bilateral renal carcinoma. Rats given lead acetate or subacetate orally developed gliomas disease, and lead subacetate also produced lung adenomas in mice. Most of these investigations found a carcinogenic response only at the highest dose. The lead compounds tested in animals are almost all soluble salts. Studies of inhalation exposure have not been located in the literature.

Missoun et al. (2010) conducted lab experiments on 14 male Wistar rats and investigated the effects of lead acetate exposure on kidney function. The results showed an increase in renal deficiency in lead exposed rats. Hamadouche et al. (2009) investigated reproductive toxicity of lead acetate in adult rat males. Results showed significant decrease in weight of sex glands and pituitary along with significant reduction in sperm production.

There have been lot of controversy regarding the mathematical model for carcinogenic studies. The authors have chosen linear multistage model which is EPA's model of choice for carcinogens. At low doses, the slope of the dose-response curve is called potency factor (PF) or slope factor (SF) which is further used to calculate lifetime incremental risk in the risk characterization section.

Risk Characterization

It is the final phase of risk assessment process where exposure and dose-response studies are combined to yield probabilities of effects occurring in humans under specific exposure conditions. Quantitative risk are calculated using the default exposure parameters as discussed in exposure assessment study and the slope factors or reference dose value obtained from dose-response study. This integrated framework can be used by the risk managers to develop guidelines for safety or for categorization of the study area on basis of acceptability of risk.

Cancer Risk

The model used is linear multi-stage model assuming dose-response curve to be linear at low concentration of lead. The incremental lifetime risk of cancer can be calculated using the following formulae:

$$\text{Incremental lifetime risk of cancer} = \text{CDI} \times \text{PF} = \left(6.22 \times 10^{-4}\right) \times (0.28)$$
$$= 1.742 \times 10^{-4} \left(\text{lead acetate}\right)$$

$$\text{Incremental lifetime risk of cancer} = \left(6.22 \times 10^{-4}\right) \times (0.038)$$
$$= 2.364 \times 10^{-5} \left(\text{lead sub-acetate}\right)$$

The oral potency factor that has been used is based on a study in California which was 2.8×10^{-1} (milligram per kilogram per day) for lead acetate and 3.8×10^{-2} (milligram per kilogram per day) for lead sub acetate (OEHHA 1992). Therefore from a cancer risk standpoint, the risk over this period of exposure is greater than acceptable goal of 10^{-6}. Hence the people living in the vicinity are at cancer risk from lead exposure.

Non-cancer Risk

Non-cancer risk as discussed in previous section is represented in terms of Hazard Quotient (HQ).

$$\text{Hazard Quotient} = \frac{\overset{\text{Average}}{\text{Daily Dose}}\ (\text{ADD})}{\text{Reference Dose}\ (\text{RfD})} = \frac{0.053 \text{mgL}^{-1}}{0.01 \text{mgL}^{-1}} = 5.3$$

Since the hazard quotient is greater than 1, the water is unfit for drinking and poses high risk of getting infection from its consumption. HQ does not depend on the time period of exposure as evident from the equation above. The area around the landfill is divided into different zones (Fig. 2) based on the mean distance from the landfill,

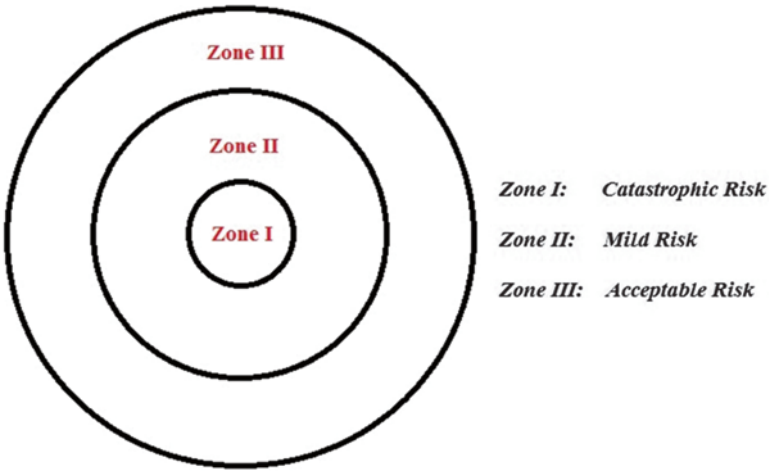

Fig. 2 Risk zones on basis of risk obtained

Table 1 Zoning of the landfill area

Zones	Radial distance (in metres)	Pb maximum concentration (mg/L)
Zone I	0–2,520 m	0.053
Zone II	2,520–3,740 m	0.027
Zone III	Beyond 3,740 m	ND

Table 2 Risks for the zones

Zones	Non-carcinogenic risk (HQ)	Carcinogenic risk		Decision
		Lead acetate	Lead sub-acetate	
Zone I	5.3	1.742×10^{-4}	2.364×10^{-5}	Risk
Zone II	2.7	8.874×10^{-5}	1.204×10^{-5}	Risk
Zone III	NA	NA	NA	No Risk

HQ Hazard quotient, *NA* Not applicable

as shown in Table 1. These risks are calculated for each stated zone as discussed for Zone I above and are presented in Table 2.

Risk Management and Communication

After completing the risk characterization process, various regulatory options need to be evaluated in a process called risk management which includes consideration of social, economic and political issues. One important step of risk management is risk communication which is interactive process of information and opinion exchange at personal, group and institutional level. Main focus should be transfer of the valuable information from experts to non-experts i.e. local residents in the vicinity of the landfill in a balanced nature. This would help in minimizing the impact of the risk in an effective manner, thus completing the risk assessment study successfully.

Limitations and Recommendations

This study is indicative, and there is a need to carry out a more detailed study, with a larger number of samples being taken. There are currently no linings in the landfill. It is a major cause for leaching of heavy metals into the groundwater. Steps have to be taken to ensure a clean water supply to the residents, and also to ensure that the landfill does not lead to further contamination of the groundwater. Regular monitoring of groundwater for heavy metals needs to be implemented.

Conclusions

This study conducted qualitative and quantitative assessments of probable health risks from the heavy metals to residents near the Bhalaswa landfill. Human exposure to two metals (lead and zinc) through drinking subsurface water was considered and published data were used to estimate risks during exposures of lead and zinc metals. Initial estimation showed that zinc concentration was within the acceptable limits and thus it was not included in the systematic risk assessment. However, lead concentrations were higher than the permissible limits and hence included in the exposure assessment. Cancer risks for lead acetate and lead sub-acetate were found to be 1.742×10^{-4} and 2.364×10^{-5}, respectively, exceeding the USEPA guideline for annual incremental risk of cancer (i.e., 10^{-6}). The hazard quotient for non-carcinogenic risk was found to be 5.3, indicating potential risks to residential population. Using this information, zoning of area in these incremental risk-zones was proposed for risk management and public communication. It is important to note here that findings of this preliminary study depends on data reported in the Bhalaswa Lok Shakti Manch and thus further more data are required to reach conclusive results.

Acknowledgements The authors would like to thank the Indian Institute of Technology Delhi for supporting this study.

References

Fosmire GJ (1990) Zinc toxicity. Am J Clin Nutr 2:225–227

Guidotti TL, Ragain L (2007) Protecting children from toxic exposure: three strategies. Paediatr Clin North Am 2:227–235

Hamadouche AN, Slimani M, Merad-Boudia B, Zaoui C (2009) Reproductive toxicity of Lead acetate in adult male rats. Am J Sci Res 3:38–50

IARC (1987) IARA monographs on the evaluation of carcinogenic risks to humans. http://monographs.iarc.fr/ENG/Classification/ClassificationsAlphaOrder.pdf. Accessed 12 Nov 2013

Missoun F, Slimani M, Aoues A (2010) Toxic effect of lead on kidney function in rat Wistar. Afr J Biochem Res 4(2):21–27

OEHHA (Office of Environmental Health Hazard Assessment) (1992) Expedited cancer potency values and proposed regulatory levels for certain proposition 65 carcinogens

Sanchez-Chardi A, Peñarroja-Matutano C, Ribeiro CA, Nadal J (2007) Bioaccumulation of metals and effects of landfill pollution in small mammals. Part II: The wood mouse, *Apodemus sylavaticus*. Chemosphere 70:101–109

Schwartz J, Landigran PJ, Baker EL, Orenstein WA, von Lindern IH (1990) Lead-induced anaemia: dose-response relationships and evidence of threshold. Am J Public Health 80:165–168

Staudinger KC, Roth VS (1998) Occupational lead poisoning. Am Fam Physician 57(4):719–726, 731–732

USEPA (1997) Exposures factors handbook, EPA/600/P 95/002Fa. ORD/NCEA, Cincinnati

USEPA (2006) Air quality criteria for Lead final report. U.S. Environmental Protection Agency, Washington, DC

Transport of Trace Metals by the Rainwater Runoff in the Urban Catchment of Guwahati, India

Upama Devi and Krishna G. Bhattacharyya

Introduction

Rapid urbanization and the consequent changes to urban traffic characteristics such as increased volume and congestion affect pollutant build-up on road surfaces as well as the top layer of soil (Zhao et al. 2010). In such cases, surface runoff accounts for quite a considerable contribution to the total runoff from land, and carries with it various contaminants from the road surfaces, built-up areas and other settlements to the receiving waters. The runoff quality is also important in identifying the nature of biogeochemical weathering processes (Skidmore et al. 2004) and in characterizing the evolution of the drainage system (Tranter et al. 1996). This has necessitated the study of basic qualities and characteristics of organic or inorganic contaminants in the rainwater runoff all over the world (Monticelli et al. 2004; Wei et al. 2010). Metals in water and soil are involved in various sorption/desorption interactions, redox reactions and chemical complexation with inorganic and organic ligands (Li et al. 2000; Violante et al. 2010). The mobility and reactivity of metals in water and soil affect their bioavailability, toxicity and distribution in the environment (Xue and Yong 2007). The solubility during precipitation and the redistribution into water can alleviate their immobilisation by adsorption or complexing (Misra and Chaturvedi 2007).

Surface runoff is a significant source of contaminants having tremendous impact on the receiving aquatic environment and significantly threatening nearby aquatic habitats. The present study aims at the determination of diurnal changes in the physical and chemical properties of the runoff in the city of Guwahati including the trace metal composition (Cd, Co, Cu, Mn, Ni, Pb and Zn) of the runoff in rainy seasons, hence to correlate the metal concentrations with pH of the runoff measurements.

U. Devi • K.G. Bhattacharyya (✉)
Department of Chemistry, Gauhati University, Guwahati 781014, Assam, India
e-mail: kgbhattacharyya@gmail.com

© Capital Publishing Company 2015

N.J. Raju et al. (eds.), *Management of Natural Resources in a Changing Environment*, DOI 10.1007/978-3-319-12559-6_17

The sources of pollutants in urban runoff may depend considerably on location and it is important to compare different types of land use in urban areas. The study area is confined to Guwahati which is now the largest city of the entire north-east India and has undergone rapid expansion with a consequent increase in population. As per the 2011 census, population of Guwahati is 963,429 with a total area of 340 km^2. The city is the main corridor for passage to the states of Assam, Meghalaya, Mizoram, Tripura, Manipur, Nagaland and Arunachal Pradesh and all the roads, including the two highways, NH31 and NH37, passing through the city, are busy with vehicular traffic day and night. The climate is homogenous over the city. Summer temperatures range from a minimum of 22° to a maximum of 38° C. Winter temperatures range from a minimum of 10° to a maximum of 25° C. The average annual rainfall is 180 cm during the months of May to September.

The city of Guwahati is situated between the southern bank of the Brahmaputra river and the foothills of the Shillong plateau and is located approximately along 26° 10′ N latitude and 92° 49′ E longitude. The city is situated on undulating plain with varying altitudes of 49.5–55.5 m above mean sea level (MSL). The central part of the city is interspersed with small hillocks like Sarania hill (193 m), Nabagraha Hill (217 m), Nilachal hill (193 m), and Chunsali hill (293 m). Structurally, this region is situated on the 50 m thick alluvium of the middle Brahmaputra valley. The topography of the city is non-uniform with a preponderance of high and low areas. Guwahati city straddles the valley of the river Bharalu, except where it is discharged to the Brahmaputra. The Nilachal hill with a maximum height of 303 m in the middle of the city is said to be the home of Goddess Kamakhya. There is Nabagraha temple on the top of Chitrachall hill. The Narakasur hill was named after the legendary king of ancient Assam, Fatashil hill and Japarigog hills are having approximately same height. The western periphery of the city contains the Deepar Beel, a huge natural water reservoir and the adjoining wetland areas. Three other major reservoirs viz., Sorusola Beel, Borsola Beel, Silsako Beel also exist in the city.

Methodology

The rainfall runoff was collected at seven selected locations (Fig. 1) along the major road systems in the city during and immediately after major rain events of April to October at 5–20 min intervals between two adjacent samples. Plastic containers of 1 L capacity, detergent cleaned, acid rinsed, washed with de-ionized water several times, and dried, were used for sampling. A description of the sampling details is given in Table 1.

The water samples were immediately filtered through Whatmann 42 micron filter paper, stored and analysed as per standard procedure (APHA 1995). The pH of each sample was measured immediately after collection of the runoff samples with a digital pH-meter (Elico pH-Meter Model LI 127) using standard buffers of pH 4 and 9 (for calibration purposes).

For analysis of the trace metals, nitric acid digestion technique (APHA 1995) was used for the runoff samples. The trace metals, namely, Cd, Co, Cu, Mn, Ni, Pb

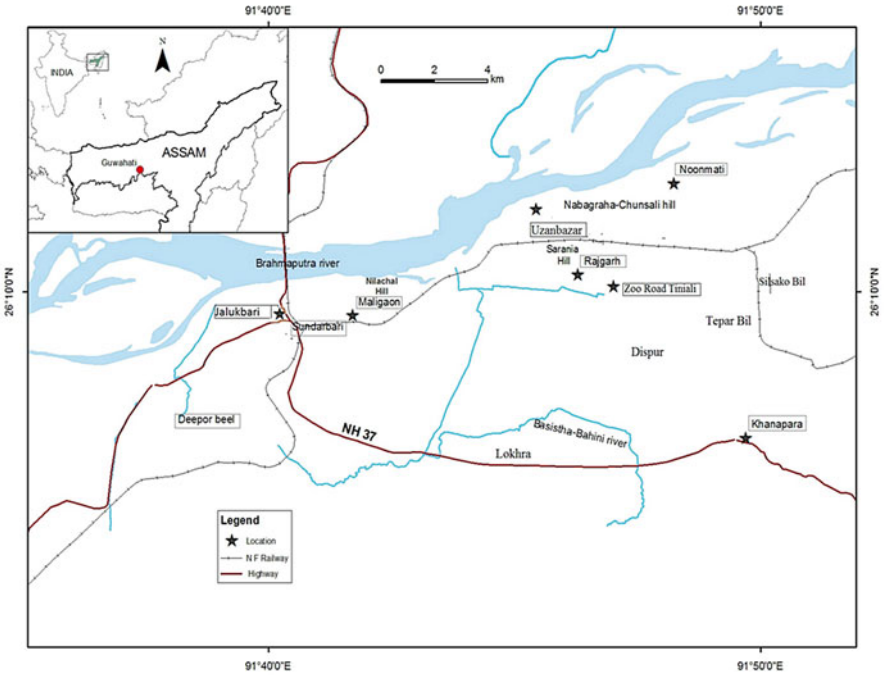

Fig. 1 Sampling location of Guwahati

and Zn were analysed by Atomic Absorption Spectrometer (PerkinElmer AAnalyst 200) using three standards calibration curve.

Results and Discussion

Acidity-Basicity of the Runoff

The pH of the runoff samples ranges from 4.6 to 7.9, where J19 sample showed the minimum and Z5 showed the maximum values. The variation patterns of the pH were different for each of the seven locations and these are presented in Fig. 2.

pH had different diurnal trends from one event to another. In location J, the pH was in the range of 4.6–7.6 with a mean value 6.5. The pH decreased diurnally in four of the seven events namely I, III, IV and VI, but in two of the events, II and V, there was an increasing trend and lastly in the event VII no specific trend was observed. Three of the runoff samples (J3, J19 and J20) had pH less than the pH of natural rainwater (i.e. 5.6) and this might be due to contamination from the soil over which the runoff was flowing. Intrusion of nitrates and sulphates from the soil in the form of acids was possible. The rest of the runoff samples possessed pH greater than

Table 1 Details of locations and sampling frequency for the runoff

S. N.	Site location		Site	Event	Samples (5–20 min interval)					
	Latitude (N)	Longitude (E)								
1	26°09′05″	91°40′21″	Jalukbari	I	J1	J2				
				II	J3	J4				
				III	J5	J6				
				IV	J7	J8	J9	J10		
				V	J11	J12				
				VI	J13	J14	J15	J16		
				VII	J17	J18	J19	J20		
2	26°12′04″	91°48′14″	Noonmati	I	N1	N2				
				II	N3	N4	N5	N6		
				III	N7	N8	N9	N10	N11	N12
3	26°07′13″	91°49′42″	Khanapara	I	K1	K2				
				II	K3	K4	K5	K6		
				III	K7	K8	K9	K10	K11	K12
4	26°09′33″	91°41′42″	Maligaon	I	M1	M2	M3			
				II	M4	M5	M6			
				III	M7	M8	M9	M10	M11	M12
5	26°10′20″	91°46′17″	Rajgarh	I	R1	R2	R3	R4	R5	R6
				II	R7	R8				
				III	R9	R10	R11	R12	R13	R14
6	26°11′29″	91°45′25″	Ujanbazar	I	U1	U2	U3			
				II	U4	U5	U6			
				III	U7	U8	U9	U10	U11	U12
7	26°10′30″	91°46′35″	Zoo Road	I	Z1	Z2	Z3			
				II	Z4	Z5	Z6	Z7	Z8	

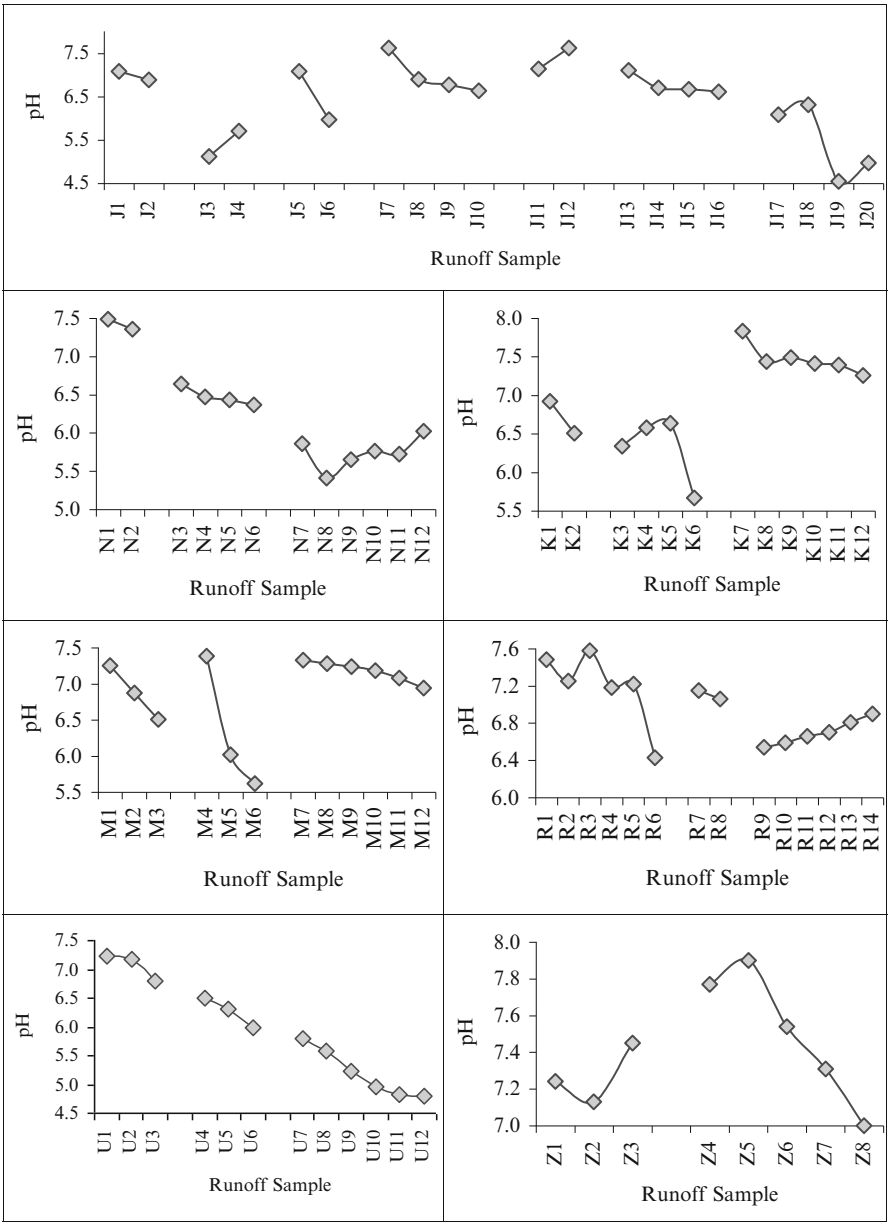

Fig. 2 Variation of pH in seven runoff locations

that of the natural rainwater that may be attributed to the presence of calcium and magnesium carbonate/bicarbonate and other alkaline components from soil which neutralise and compensate the acidity of sulphuric acid and nitric acid (Demirak et al. 2006; Salve et al. 2008).

In location N, the pH spread from 5.4 to 7.5 with a mean value of 6.3. The first two events at this location showed decreasing diurnal trend while the third event showed no distinct trend. All the runoff samples, excepting N8, had pH >5.6 i.e. pH of natural rainwater. It indicates that the rainwater after falling on soil received some alkaline contamination from the soil.

Similar unpredictable behaviour in diurnal variations in pH was also seen in the location K where the values were in the range of 5.7–7.8 with a mean 6.95. All the samples had pH greater than that of natural rainwater (5.6).

Location R had pH from 6.4–7.6 with a mean value 6.98. The pH showed a continuous increase with time in the third event, the first event showed no specific trend and the second event showed a decreasing trend. All the events in this location had alkaline contamination after the rainwater flowed over the land surfaces. This area is covered with high traffic volume and the alkaline contaminants might be related to vehicular emissions and other traffic wastes that might contain calcium or magnesium (positive correlation) carbonate/bicarbonate.

For the location M and U, all the events showed decreasing diurnal trend in pH. The decrease in pH of the runoff with time might be due to leaching of acidic elements such as Al and Fe from the soil that replaced Ca and Mg in the runoff.

Location Z had the pH value spread in a small range from 7.0 to 7.9. Here the two events showed no general trend for pH values. This location had the highest mean pH (7.4) attributable to the alkaline contamination from vehicular emission, human wastes and other anthropogenic activities.

The basic statistics of pH for the seven locations are shown in Fig. 3. The pH of water affects the solubility of many toxic and nutritive chemicals and the availability

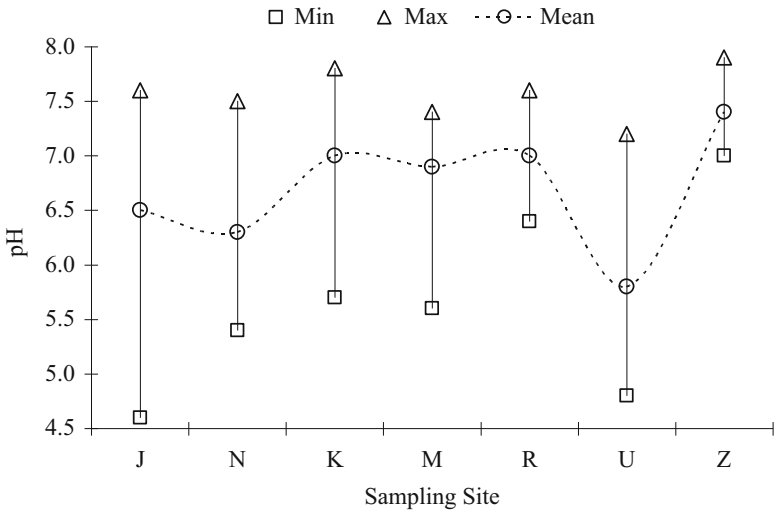

Fig. 3 Basic statistics in pH of the seven runoff locations

Table 2 Basic statistics of the metals (in mg/L) along with pH for the seven locations

Parameter	Sampling sites							
		J	N	K	M	R	U	Z
Cadmium	Min	0	0	0	0	0	0	0
	Max	0.018	0.024	0.021	0.015	0.021	0.017	0.003
	Mean	0.007	0.006	0.009	0.006	0.009	0.009	0.0005
Cobalt	Min	0.032	0.02	0.029	0.033	0.054	0.02	0.113
	Max	0.895	0.67	0.643	0.693	0.797	0.155	0.495
	Mean	0.385	0.300	0.284	0.309	0.259	0.093	0.353
Copper	Min	0	0.022	0	0	0	0.007	0.004
	Max	0.446	0.614	0.258	0.283	0.019	0.078	0.043
	Mean	0.127	0.190	0.094	0.121	0.002	0.028	0.018
Manganese	Min	0	0	0.089	0	0	0.438	0.018
	Max	1.022	0.54	0.765	0.599	0.642	0.672	0.082
	Mean	0.313	0.232	0.359	0.281	0.317	0.558	0.043
Nickel	Min	0	0.002	0.004	0.004	0.004	0.005	0.011
	Max	0.178	0.185	0.08	0.107	0.17	0.032	0.208
	Mean	0.038	0.059	0.027	0.030	0.066	0.018	0.088
Lead	Min	0	0	0	0	0	0	0.079
	Max	0.283	0.08	0.405	0.079	0.032	0.018	0.122
	Mean	0.061	0.014	0.155	0.021	0.005	0.007	0.100
Zinc	Min	0.007	0.014	0.024	0	0.031	0.107	0.079
	Max	0.408	0.325	0.288	0.152	0.287	0.286	0.174
	Mean	0.134	0.169	0.117	0.064	0.132	0.208	0.129

of the same to aquatic organisms. As acidity increases, most metals become water soluble and thus, the runoff becomes more toxic (Wondie 2009).

Trace Metals

Urban soils and road-side soils are huge sink for the heavy elements and other pollutants. The heavy metals as well as the inorganic and organic pollutants accumulate in the top layer of soil. This may be contaminated to the runoff by heavy rainfall. Mobility of the metals from sediment to runoff depends on the pH of the sediment (Biljana and Natasa 2013). The basic statistics of the trace metals in the present study are shown in Table 2.

Significant levels of trace metals are found in urban and highway runoffs from many investigations. Among a variety of metals present in storm water, cadmium, copper and lead are the most hazardous ones (Edwards et al. 1997) which appear to be directly correlated to traffic intensity on surfaces such as highways, streets, and parking lots (Davis and Shokouhian 2001).

The trace metal contents in the present study are as follows:

Cadmium

Cd in the runoff could be found from below detection level (BDL) to 0.024 mg/L (N5) with a mean value 0.007. In total, 37 of the samples (41 %) had values below detection level. Cadmium was the least abundant metal found in the surface runoff. The site-wise variation in seven runoff locations for Cd for the different events is shown in Fig. 4. The values showed different diurnal trends from one event to another.

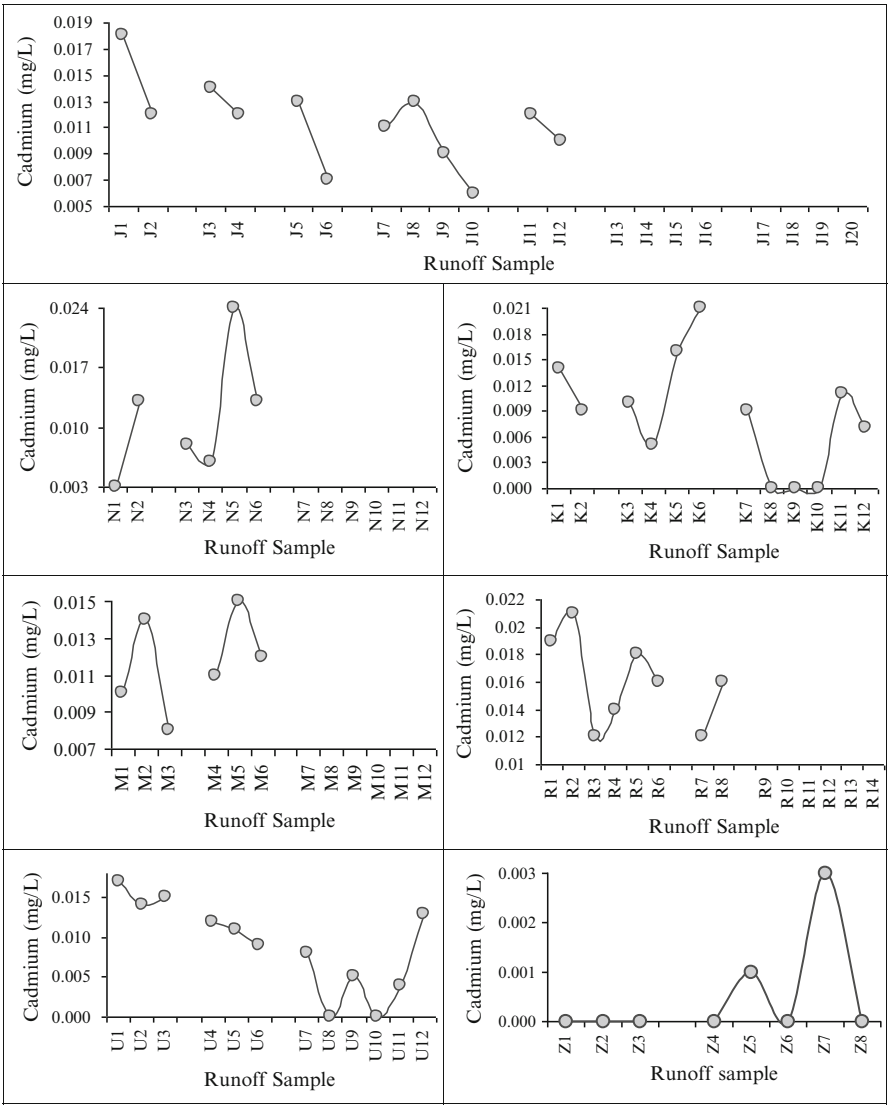

Fig. 4 Cadmium variations for seven runoff locations

In case of the location J, the Cd content was distributed from 0 to 0.018 mg/L in the runoff samples with a mean value 0.007. The values showed decreasing diurnal trend for five events namely I, II, III, IV (except sample J7) and V while no Cd could be detected in the rest events, VI and VII. Here the concentration of cadmium showed positive correlation with pH i.e. cadmium is leached to the runoff more with increasing pH.

For location N, the range of Cd content was 0–0.024 mg/L with a mean value 0.006. Event I had an increasing trend, event II had no distinct trends and no Cd could be detected in event III. The cadmium concentration increased with increasing pH values i.e. more cadmium mobility from soil to rainfall runoff was observed with higher pH values.

Location K showed Cd content from 0 to 0.021 mg/L with a mean value 0.009. There was a decreasing trend in event I and no distinct trend was seen in case of events II and III. The Cd values showed an inverse correlation with the corresponding pH values.

For the location M, Cd content was found from 0 to 0.015 mg/L with mean value 0.006. In such cases, an increasing trend was followed by a decreasing one for two of the events, I and II. The cadmium content showed inverse correlation with the pH of the location.

In case of location R, the range of Cd was 0–0.021 mg/L with a mean value 0.009. The diurnal variation for each event was different. Event I showed no specific trend whereas event II showed increasing trend and in the last event no cadmium could be detected. The location showed cadmium mobility to the runoff at lower pH conditions.

In case of location U, Cd content distributed from 0.001 to 0.017 mg/L with a mean value 0.013. The three events showed different diurnal variation where no distinct trend could be seen in any of the three events.

The location Z had a Cd content in the range of 0–0.003 mg/L with a mean 0.0005 where there is no Cd detected in the event I and no specific trend could be observed in the event II.

The cadmium content showed an inverse correlation with pH which was found by Manning et al. (2011) in his work on spring runoff water at Colorado. This could be attributed by the findings by McDowell (2010) that since cadmium sorbs to and accumulates to the top layer i.e. 0–2 cm depth of soil (Jalali and Arfania 2011), there is possibilities for the cadmium loss via surface runoff in particulate associated and dissolved phase, hence erosion becomes significant form of Cd loss (Edwards and Withers 2008).

Cadmium may be contributed to the runoff via leaching of soil which occurs through soil-plant systems (McDowell 2010). Cadmium may enter into water from industrial processes such as the smelting and refining of ore minerals, electroplating and paint manufacturing, combustion of fossil fuels, and also from the application of phosphate fertilizers (Selles et al. 2003), leaching from contaminated landfill or from soil having sewage sludge dumping. The concentration in unpolluted water is <1 μg/L.

Cadmium is considered as a very toxic metal due to its high mobility and at a low concentration, it can affect the living organism (Benavides et al. 2005). A set of

experiments (McDowell 2010) using simulated rainfall to generate surface runoff indicated that the major form of Cd lost was dissolved (average 65 %, <0.45 μm) and could be predicted by water extraction of the soil. Cadmium in soil tends to be more available when the soil pH is low (acidic) (Elinder 1992). It has been found that cadmium concentration in water is inversely related to the pH and the concentration of organic material in the water.

Cobalt

Co in the rainwater runoff was distributed from 0.020 mg/L (N5 and U1) to 0.895 mg/L (J13). The minimum, maximum and mean Co contents are shown in Fig. 5. Location J possessed the maximum value of cobalt (0.895 mg/L) as well as the highest mean value (0.385) and location N and U had the minimum value (0.020 mg/L).

The location J had decreasing diurnal trends of Co in I and III events, increasing trend in II and V events and the other three events had no distinct trends. For location N, increasing trend was found for event I, decreasing trend for event II and no specific diurnal trend for event III.

For location K, Co increased diurnally for event I, while the event II had both increasing and decreasing trends and no specific trend for the event III. In location M, event I had a decreasing trend while no specific diurnal trend could be observed for the events II and III. In location R decreasing trend was found for the event II and the events I and III had no specific trend. In the location U, increasing trend was shown by event I in straight line and the event II showed the decreasing trend and the rest event showed no distinct trend. In the location Z, increasing trend was seen in event I and no distinct trend were seen in the event II.

The cobalt concentration in the runoff was found to be inversely correlated to the pH for the locations J, N, R, U and Z. Such type of result was also obtained by Moore (1991).

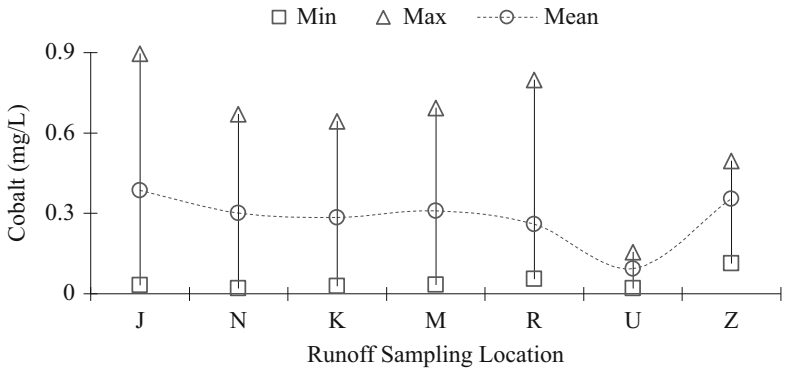

Fig. 5 Basic statistics of cobalt for seven runoff locations

Co is present in trace amounts naturally in rock, soil, water, plants, animals and air. Co occupies 0.0025 % of the earth's crust. Co occurs in mineral form as arsenides, sulfides and oxides, such as linnaeite (Co_3S_4), carrolite ($CuCo_2S_4$), safflorite ($CoAs_2$), skutterudite ($CoAs_3$), erythrite ($Co_3(AsO_4)_2.8H_2O$), and glaucodot (CoAsS). Co anthropogenic sources are exhaust from vehicles, coal-fired power plants and incinerators. Co mining and processing activities, the production of alloys and chemicals containing cobalt, sewage effluents and agricultural run-off are major anthropogenic contributors of cobalt to the aquatic environment (Nagpal 2004).

In higher concentrations cobalt is toxic to humans and to terrestrial and aquatic animals and plants. Acute exposure to cobalt may lead to a depression in iodine uptake, anorexia, nausea, vomiting and diarrhoea (Nagpal 2004).

Copper

Its concentration was from below detection level (BDL) to 0.614 mg/L in the runoff. The sample N9 had the maximum Cu content. 33 of the samples (37 %) had Cu below detection level.

For location J, Cu was distributed from 0 to 0.446 mg/L with a mean value 0.127. Cu could not be detected for the events I, II, III, and three samples of the event IV. Event V had decreasing trend while event VI had increasing trend and for the event VII, Cu content showed no distinct trend.

In location N, the range of Cu was from 0.022 to 0.614 mg/L with a mean of 0.190. The event I showed decreasing trend while the events II and III showed no specific trend. For location K, Cu content was from 0 to 0.258 mg/L with a mean 0.094. Cu could not be detected in the events I and II. Event III showed no specific diurnal trend. For location M, Cu content was distributed from 0 to 0.283 mg/L with a mean value 0.121. The behaviour of the events is same as in case of location K.

In location R, Cu was distributed from 0 to 0.019 mg/L with a mean value 0.002. No Cu could be detected except only two samples from event III. Location U showed the range of Cu 0.007–0.078 mg/L with a mean value 0.028. No distinct diurnal variation of Cu could be detected for the events present. Location Z showed a range of Cu from 0.004 to 0.043 mg/L with a mean value 0.018. Like location U, here also no specific trend could be detected for the two events.

Cu contents of locations J, N, R and Z showed negative correlation with pH as was also found by He et al. (2001). This is attributed to the leaching of more Cu from soil to runoff water in lower pH. Dortwegt and Maughan (2001) has reported that Cu at pH <7.0 becomes more stable in solution. This metal has moderate mobility under slightly acid soil conditions (Zhang et al. 2003).

Copper is consistently added to soils in the form of fertilizers, pesticides, livestock manures, sewage sludge, and industrial emissions such as vehicle production, electrical wires, batteries, and electrical apparatus (Li et al. 2009). It was found earlier that Cu concentration in the runoff water from a field was as high as 0.7 mg/L following long-term application of poultry litter (Edwards et al. 1997).

Manganese

The runoff had manganese in the range of 0–1.022 mg/L. The sample J1 had the maximum Mn content. It was observed that 23 samples (26 %) of the five locations had values below detection level.

For the location J, the values decreased for two events, I and II; increased for three events III, IV and V; and Mn could not be detected for event VI and lastly no specific trend was seen for the event VII. In the location N, manganese showed increasing trend for the event I, and no specific trend for the events II and III. For the location K, increasing trend was observed for the event I, decreasing trend for the event II and no specific trend for the event III. In the location M, the values first decreased and then increased for the two events I and II, and no manganese was detected for the event III.

In the location R, there was no specific trend seen in the event I while event II had decreasing trend and no distinct trend could be detected in event III. For location U, the range of Mn was from 0.438 to 0.672 mg/L with a mean 0.558. No distinct trend could be found in any of the three events. Location Z had Mn content from 0.018 to 0.082 mg/L with a mean 0.048.

Mn concentration showed an increase in the runoff water with decrease in pH for the locations J, K, M, U and Z. This may be attributed to the fact that at lower pH the mobility of Mn increases (Heal 2002) from soil to the runoff which enhances the concentration of Mn.

Naturally, manganese oxides are found in various forms of discrete particles, coatings, nodules, micro-nodular deposits, thin layers on mineral surfaces, or interspersed in clay minerals (Koljonen et al. 1976). These oxides tend to be deposited at the redox front which may occur near the water table and also at places along the ground-water flow path owing to changes in vertical and horizontal permeability. Under favourable conditions of water circulation pattern and/or chemical composition, these salts can be redissolved (Lind et al. 1987) and leached into the runoff.

Nickel

Its contents of the runoff were in the range of 0–0.208 mg/L with the maximum value at Z4. For two of the samples (2.2 %) Ni could not be detected. The values showed different diurnal trends for the events of seven runoff locations.

For the location J, increasing trend was observed for events II, III and V and event I showed decreasing trend, but such distinct trend was missing in the rest three events. Also the events VI and VII recorded very high Ni contents. For the location N, decreasing trend was seen for the event I; no specific diurnal trend for the events II and III could be observed. The same was observed for the location K that increasing trend was observed in event I and no general trend could be seen in the rest two events. For the location M, decreasing trend was seen for the events I and II, and no specific trend for the event III. For location R, decreasing trend was seen for the event II and no specific trend for the events I and III. For the location U and Z no specific trend could be detected for any of the events.

Nickel showed a negative correlation with pH values in the runoff locations J, N, R, U and Z may be due to the leaching of Ni from the soil at lower pH. Most of the dissolved Ni in surface runoff is likely to occur in complexed form. Moderately strong metal-complexing ligands in the form of humic substances are responsible for the complexation of about 20 % of Ni and the remaining Ni is complexed by ligands with apparent stability constants comparable to those of synthetic chelating agents (Sedlak et al. 1997).

Lead

It occurred in the runoff from 0 to 0.405 mg/L, the highest value being found at the location, K12. BDL values were recorded by 38 of the samples (42 %).

For the location J, lead could not be detected for the first four events I, II, III and IV; for the event V there was decreasing trend and for the events VI and VII, no specific trend was observed. For the locations N, K, R and M, Pb was found below detection level for the first two events while no particular trend in Pb content in the runoff could be seen for the event III. Also no distinct trend was observed in any events of the locations U and Z.

The concentration of Pb was in a positive correlation with pH of the corresponding samples. The main source of lead in the atmosphere was tetraethyl lead used earlier in fuel to improve its octane number. Many soils contain appreciable amount of Pb from natural sources. Being mostly insoluble, the runoff can remove a small part of Pb in the soil. In this context, Pb-content of the runoff at some of the locations can be described as substantial. Long-term exposure to lead or its salts can affect adversely the nervous system and kidneys (Tebbutt 1983; Bloutsos and Yannopoulos 2011).

Zinc

The runoff had zinc from 0.024 to 0.0.408 mg/L with a mean value 0.136. The sample J7 had the maximum value and M11 and M12 did not show any Zn content. For the location J, decreasing trend was seen for the three events I, IV and VI, increasing trend for the three events II, III and V and the rest events did not possess any distinct trend.

For location N and M, Zn was found in increasing trend for the event I; no general trend for the events II and III. In the location K, decreasing trend was seen for the two events I and II and no specific trend for the event III. In the location R, Zn showed an irregular trend for the event I, decreasing trend for the event II and increasing trend for the event III. For the location U, the event I showed an increasing diurnal trend while no specific trend was seen in II and III events. Location Z showed no general trend in any of the events.

According to Budai and Clement (2011), zinc is produced mainly from tyre and brake wear and the corrosion of galvanized steel. It is likely that the runoff leached some of Zn in the soil deposited from these sources.

Conclusions

The present work has yielded a comprehensive database on the quality of the surface runoff of Guwahati city. The observed pH of the runoff varied from 4.6 to 7.8. The results indicated that the pH might be controlled by leaching of acidic elements such as Al and Fe from the soil that replace Ca and Mg. The average pH of the runoff samples was 6.69, probably due to neutralization. Most of the samples had pH > 5.6. This may be an indication of alkaline contamination of the rainwater as the pH of natural rain water is ~5.6. Cadmium and lead are positively correlated with pH of the runoff for three sites J, N and R, suggesting the entry of the metal into the runoff from the surrounding topsoil. In contrast, Co, Cu, Mn and Ni are inversely correlated with pH in most of the locations. Thus, more and more metals leach into the runoff from the topsoil as pH goes down. The concentration of the trace metals is found to depend on the traffic intensities in the sampling sites. Location J, which has high traffic density, has the maximum content of the metals, namely Co (0.895 mg/L), Mn (1.022 mg/L) and Zn (0.408 mg/L). The location N has the maximum content of Cd (0.024 mg/L) possibly due to contribution from nearby industries. Considerable amount of Cu (0.614 mg/L) at this site may be due to both vehicular and industrial inputs. Location Z has the highest content of Ni (0.208 mg/L) and a large part may have come from anthropogenic activities including vehicular exhausts and atmospheric deposition. Mn is the most abundant and Cd the least abundant metals in the surface runoff. The average concentrations of the metals are in the order of Mn (0.313 mg/L) > Co (0.289 mg/L) > Zn (0.136 mg/L) > Cu (0.088 mg/L) > Pb (0.050 mg/L) > Ni (0.044 mg/L) > Cd (0.005 mg/L). It is possible that the runoff is contaminated due to leaching from the top layers of soil which has served as a receptor for various wastes generated by anthropogenic activities in the rapidly urbanized city. Increase in traffic volume, congestion, growing fuel use etc., might have contributed significantly to runoff contamination.

References

APHA (American Public Health Association) (1995) Standard methods for the examination of water and wastewater, 19th edn. APHA, Washington, DC

Benavides MP, Gallego SM, Tomaro ML (2005) Cadmium toxicity in plants. Braz J Plant Physiol 17(1):21–34

Biljana S, Natasa DM (2013) Distribution of heavy elements in urban and rural surface soils: the Novi Sad city and the surrounding settlements, Serbia. Environ Monit Assess 185(1):457–471

Bloutsos AA, Yannopoulos PC (2011) Concentration of Selected Toxic Elements in Airborne Particulates of Patras, Greece. Global Nest J 10(10):20–30

Budai P, Clement A (2011) Refinement of national-scale heavy metal load estimations in road runoff based on field measurements. Transp Res D 16:244–250

Davis AP, Shokouhian M (2001) Loading estimates of lead, copper, cadmium, and zinc in urban runoff from specific sources. Chemosphere 44(5):997–1009

Demirak A, Balci A, Karaoglu H, Tosmur B (2006) Chemical characteristics of rainwater at an urban site of south western Turkey. Environ Monit Assess 123:271–283
Dortwegt R, Maughan EV (2001) The chemistry of copper in water and related studies planned at the advanced photon source. In: Proceedings of the 2001 particle accelerator conference, Chicago
Edwards AC, Withers PJA (2008) Transport and delivery of suspended solids, nitrogen and phosphorus from various sources to freshwaters in the UK. J Hydrol 350:144–153
Edwards DR, Moore PA, Daniel TC, Srivastava P, Nichols DJ (1997) Vegetative filter strip removal of metals in runoff from poultry litter—amended fescuegrass sites. Trans ASAE 40:121–127
Elinder CG (1992) Cadmium as an environmental hazard. IARC Sci Publ 118:123–132
He W, Wallinder IO, Leygraf C (2001) A laboratory study of copper and zinc runoff during first flush and steady state conditions. Corros Sci 43:127–146
Heal KV (2002) Manganese in runoff from upland catchments: temporal patterns and controls on mobilization. Hydrol Sci J des Sciences Hydrologiques 47(5):769–780
Jalali M, Arfania H (2011) Distribution and fractionation of cadmium, copper, lead, nickel, and zinc in a calcareous sandy soil receiving municipal solid waste. Environ Monit Assess 173:241–250
Koljonen T, Lahermo P, Garlson L (1976) Origin mineralogy and geochemistry of manganese rocks and ferruginous precipitates found in sand gravel deposits in Finland. Bull Geol Soc 48:111–135
Li X, Shen Z, Wai OWH, Li YS (2000) Chemical partitioning of heavy metal contaminants in sediments of the Pearl River Estuary. Chem Speciat Bioavailab 12(1):17–25
Li F, Fan Z, Xiao P, Oh K, Ma X, Hou W (2009) Contamination, chemical speciation and vertical distribution of heavy metals in soils of an old and large industrial zone in Northeast China. Environ Geol 57:1815–1823
Lind C, Hem J, Roberson C (1987) Reaction products of manganese-bearing waters. In: Averett RC, McKnight DM (eds) Chemical quality of water and the hydrologic cycle. Lewis Publishers Inc., Chelsea
Manning AH, Verplanck PL, Mast MA, Marsik J, McCleskey RB (2011) Spring runoff water-chemistry data from the Standard Mine and Elk Creek, Gunnison County, Colorado, 2010, U.S. Geological Survey open-file report 2011–1159, 20
McDowell RW (2010) Is cadmium loss in surface runoff significant for soil and surface water quality: a study of flood-irrigated pastures? Water Air Soil Pollut 209:133–142
Misra V, Chaturvedi PK (2007) Plant uptake/bioavailability of heavy metals from the contaminated soil after treatment with humus soil and hydroxyapatite. Environ Monit Assess 133:169–176
Monticelli D, Van den Berg CMG, Pozzi A, Dossi C (2004) Copper speciation in glacial stream waters of Rutor Glacier (Aosta Valley, Italy). Aust J Chem 57(10):945–949
Moore JW (1991) Inorganic contaminants of surface water—research and monitoring priorities. Springer, New York
Nagpal NK (2004) Technical report—water quality guidelines for cobalt. ISBN 0-7726-5229-5
Salve PR, Maurya A, Wate SR, Devotta S (2008) Chemical composition of major ions in rainwater. Bull Environ Contam Toxicol 80:242–246
Sedlak DL, Phinney JN, Bedsworth W (1997) Strongly complexed Cu and Ni in wastewater effluents and surface runoff. Environ Sci Technol 31:3010–3016
Selles F, Clarke JM, Zentner RP, Campbell CA (2003) Effects of source and placement of phosphorus on concentration of cadmium in the grain of two durum wheat cultivars. Can J Plant Sci 83:475–482
Skidmore M, Sharp M, Tranter M (2004) Kinetic isotopic fractionation during carbonate dissolution in laboratory experiments: implications for detection of microbial CO_2 signatures using d13C-DIC. Geochimica Cosmochimica Acta 68(21):4309–4317
Tebbutt THY (1983) Relation between natural water quality and health. UNESCO, Paris

Tranter M, Brown GH, Hodson A, Gurnell AM (1996) Hydrochemistry as an indicator of the nature of subglacial drainage system structure: a comparison of Arctic and Alpine environments. Hydrol Process 10:541–556

Violante A, Cozzolino V, Perelomov L, Caporale AG, Pigna M (2010) Mobility and bioavailability of heavy metals and metalloids in soil environments. J Soil Sci Plant Nutr 10(3):268–292

Wei Q, Zhu G, Wu P, Cui L, Zhang K, Zhou J, Zhang W (2010) Distributions of typical contaminant species in urban short-term storm runoff and their fates during rain events: a case of Xiamen City. J Environ Sci 22(4):533–539

Wondie TA (2009) The impact of urban storm water runoff and domestic waste effluent on water quality of lake Tana and local groundwater near the city of Bahir Dar, Ethiopia. Master thesis, Cornell University

Xue SW, Yong Q (2007) Leaching characteristics of heavy metals and As from two urban roadside soils. Environ Monit Assess 132:83–92

Zhang M, He Z, Calvert DV, Stoffellab PJ, Yanga X (2003) Surface runoff losses of copper and zinc in sandy soils. J Environ Qual 32:909–915

Zhao H, Li X, Wang X, Tian D (2010) Grain size distribution of road-deposited sediment and its contribution to heavy metal pollution in urban runoff in Beijing, China. J Hazard Mater 183(1–3):203–210

Analysis of Leachate Characteristics to Study Coal Ash Usability

Pooja Vishnoi and M. Shambhavi Kamath

Introduction

The combustion of coal in coal-fired power plants produces several materials, including: fly ash, bottom ash, boiler slag, and flue gas desulfurization material. Together, these materials represent what is generally referred to as coal ash, or sometimes as CCBs. About 750 metric tonnes (MT) of total coal ash is produced per year globally, but less than 50 % of world production is utilized (Izquierdo 2012).

Disposal of this huge amount of coal ash is of great environmental concern as it has various harmful effects like air pollution, contamination of ground water, surface water etc. There is a common misconception deeply rooted in the minds of general public that the coal ashes are simply the waste by-products of thermal power generation industry and that they are harmful and hazardous to the social life. In order to eliminate such misconceptions and bring in more clarity, many Government sponsored projects have been initiated and are being motivated. The quality of coal depends upon its rank and grade. Anthracite is of highest grade and peat is of lowest grade. Indian coal is mostly sub-bituminous rank followed by bituminous and lignite (brown coal). The ash content in Indian coal ranges from 35 to 50 %. Many researchers and organisations, in India and abroad as well, have studied the characteristics of coal ashes in detail (Sridharan and Prakash 2007).

The results from such continued and collaborative efforts have proved that coal ash possess many physical, chemical and engineering properties that are beneficial to the society (Pandian et al. 2001; Prakash and Sridharan 2009; Sridharan and Prakash 2008). These beneficial properties of coal ashes make possible their bulk utilization in the field of geotechnical engineering, contributing to an effective and efficient sustainable development of the region/country. Various research on properties of coal ash

P. Vishnoi (✉) • M.S. Kamath
Department of Civil Engineering, Manipal Institute of Technology, Manipal 576104, India
e-mail: pooja16193@gmail.com

© Capital Publishing Company 2015

N.J. Raju et al. (eds.), *Management of Natural Resources in a Changing Environment*, DOI 10.1007/978-3-319-12559-6_18

shows it can be utilized as a construction material, in waste treatment, soil stabilization, stowing material, liner for landfills, embankments, etc. which may allow it to be used for environmental benefit rather than being disposed of as a waste.

Ashes contain various potential hazardous chemical compounds. Therefore precautions must be taken to avoid leaching of harmful substances both in its disposal and its utilization. Major problem among these coal ashes are of pond ash and fly ash, therefore in this paper mixture of fly ash and pond ash have been taken and its leachate properties are studied. The leaching tests performed in this study indicate that the major environmental challenge for the management of coal fly. This paper focuses on some chemical properties and leachability of various coal ash samples collected from five different thermal power plants across India. Extraction and leaching of various metals like Fe, Pb, Cu, Ni, Cd and Cr, and soluble salts like potassium, calcium, sodium and phosphate and sulphate ions were studied.

Materials and Methods

Coal Ash Samples

Coal ash samples were collected from five different thermal power plants shown in Table 1. Fly ash was collected from the silos and pond ash was collected from the ash disposal pond. Fly ash and pond ash were mixed together. Coal ash (fly ash and pond ash mixture) samples were oven dried for 24 h. to carry out the experiments.

Coal Ash Characterization and Chemical Compositions

The chemical composition of coal ash samples were determined by IS 1355-1984 method. Loss on ignition was carried by ASTM D7348-08 method to know the amount of unburnt carbon. SEM and EDXA analysis was done to understand its particles in closer view and to find the presence of various elements respectively.

Table 1 Sample names and location

Sample No.	Power plants	Sample names	Location
1	Bokaro Thermal Power Station	BTPS	Bokaro district, Jharkhand
2	Chandrapura Thermal Power Station	CTPS	Bokaro district, Jharkhand
3	Durgapur Thermal Power Station	DTPS	Durluvpur, Mejia, Bankura, West Bengal
4	Mejia Thermal Power Station	MTPS	Durluvpur, Mejia, Bankura, West Bengal
5	Maithon Power Limited	MPL	Dhanbad, Jharkhand

Measurement of pH

Sub-bituminous and lignite coal ashes typically contain relatively high concentrations of calcium, with concentrations exceeding 15 % (expressed as CaO), and produce alkaline solutions (pH 11–12) on contact with water. Bituminous coal ashes generally contain much less calcium and yield slightly acidic to slightly alkaline solutions (pH 5–10) on contact with water (Izquierdo 2012). To calculate pH 5 g of sample was taken and was mixed with 5 ml of distilled water and then stirred for 10 s and allowed to stand for 5 min; then pH was measured using pHmeter.

Batch Leaching Test

The leaching test at liquid to solid (L/S) ratio 1:20 was carried out. Leaching was performed at the natural pH of the samples (i.e. about pH 7–8.1), for 17 h (ASTM 1992). After the extraction, the extracts were separated from the solid residue by filtration through Whatman filter paper no. 42 followed by glass fibre filter of 0.7 µm. Few drops of 1 N nitric acid were added and extracts were stored in a refrigerator (4 °C) until the element determination. Leachate was analysed using AAS, Flame Photometry and other methods.

Leachate Analysis

The pH of extracted leachate was determined using pHmeter. Various elements like Fe, Pb, Cu, Ni, Cd and Cr were analysed by using AAS to understand the leaching potential of the coal ash samples. Various salts like potassium, calcium and sodium salts were determined using flame photometry. Phosphate and sulphate ions were determined using molybdate method and turbidity method respectively.

Result and Discussion

Coal Ash Characterization

The major element composition of the respective coal ashes are shown in Table 2. The result indicates that samples contain mostly SiO_2, Al_2O_3, Fe_2O_3, CaO and MgO. Silica oxide is the major content found in all the samples i.e. 85–90 %. CaO content varied from 0.6 to 1.3 % depending upon the parent coal. EDXA analysis indicated the presence of the following elements: Ca, Mg, Al, Na, K, Ti, Fe, C, O and Si in the coal ash samples (shown in Fig. 1). Results show the high content of oxygen which indicates presence of elements in their oxide form. SEM was used to

Table 2 Chemical composition of coal ash samples (%)

Sample no.	SiO_2	R_2O_3	Fe_2O_3	Al_2O_3	CaO	MgO	LOI
1	85.8	6	0.3	5.7	1.1	0.7	0.11
2	84	5.5	1.5	4	0.9	0.6	0.12
3	87.6	5.9	0.1	5.8	0.7	0.9	0.10
4	90	6.7	0.2	6.5	1.3	0.6	0.03
5	88.3	3.5	1	2.4	0.6	0.6	0.04

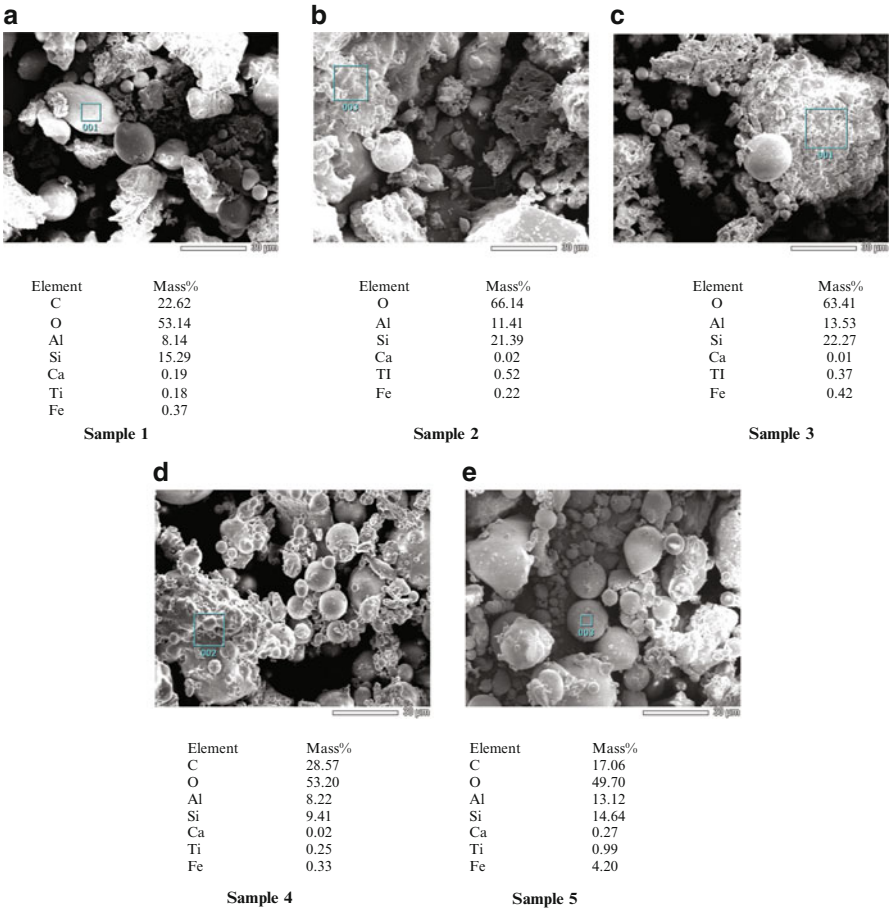

Fig. 1 SEM and EDXA analysis

analyse the closer particle view of the coal ash samples shown in Fig. 1. SEM studies carried out shows that fly ashes are fine particles compared to bottom ashes (Powell et al. 1991). Pond ashes consist of both finer and coarser particles. Investigations show that the coal ash particles are generally cenospheres. They also confirm that fly ash particles are finer compared to bottom ash particles and the pond ash

particles are sized in between fly and bottom ashes (Pandian et al. 1998). The SEM microphotograph shows the presence of solid spherical cenospheres in the samples and also reveals that it is a mixture of spherical particles of different sizes between fly ash and bottom ash. The Loss on Ignition is an indirect parameter to indicate the presence of unburnt carbon. Fly ash also contains a variable amount of unburned carbon, depending on the combustion conditions (Palo 2006). The result indicates that LOI is in the range of 0.03–0.12 % (Table 2), which is very less and indicate the high temperature combustion (Palo 2006).

pH of Coal Ash

pH of the coal ash samples were analysed and results are shown in Table 3. Result of pH varied from 7 to 8.1 and indicates that coal ash samples are slightly alkaline.

Leachate Analysis

The leaching test such as the batch test may provide a reasonable approximation of environmental leaching behaviour of CCPs. After batch leaching test the leachate of coal ash samples were collected and analysed.

pH of Leachate

Table 3 shows the pH values of leachate from coal ash samples after batch leaching test. The pH of leachate was found to be in the range of 6.2–6.5. The pH was found to be less when compared to the pH of the initial coal ash samples. This could be attributed to the consumption of hydroxyl ion by precipitation of secondary minerals over time (Izquierdo 2012).

Trace Elements Analysis

The mode of occurrence of trace elements in coal plays a primary role in the distribution of elements within ash particles. The elements enriched in the core of fly ash particles are not directly exposed to leaching, whilst surface associated elements are

Table 3 pH of coal ash samples and its leachate

Sample No.	pH of sample	pH of leachate
1	7.0	6.24
2	7.5	6.22
3	7.6	6.46
4	8.1	6.64
5	7.6	6.50

Table 4 Trace elements analysis of leachate

Element name	Sample 1 (mg/L)	Sample 2 (mg/L)	Sample 3 (mg/L)	Sample 4 (mg/L)	Sample 5 (mg/L)
Fe	0.10	0.03	0.02	0.06	0.03
Mn	0.04	0.04	0.05	0.04	0.05
Pb	ND	ND	ND	ND	ND
Cu	0.09	0.06	0.12	0.13	0.12
Ni	ND	ND	ND	ND	ND
Cd	ND	ND	ND	ND	ND
Cr	0.01	0.01	0.01	0.01	0.01

ND not detected

more accessible to leaching in an aqueous environment. Therefore, the mode of occurrence in the parent coal controls to a large extent whether a given element will be immobile or will be easily released to the environment (Izquierdo 2012). During these studies, leaching behaviours of various heavy metals like Fe, Mn, Pb, Cu, Ni, Cd and Cr from coal ash samples was studied. The concentrations of the heavy metals that were leached out with deionised water as a result of the batch leaching test are shown in Table 4.

Ni, Pb and Cd did not leach from the coal ash samples. Cu concentrations were low (0.06–0.13 mg/L); this is probably because Cu gets precipitated as their insoluble hydroxides. Mn and Cr are leached in samples but shows very low concentration i.e. 0.04–0.05 mg/L and 0.01 mg/L respectively. Fe leached from ash is probably precipitated as hydroxides due to the alkaline nature of ash, hence found in low amount i.e. 0.02–0.1 mg/L.

Research shows that elements in the ash particles were mainly associated with the surface, and these surface-associated fractions might dominate the leachate chemistry at the early stages of fly-ash disposal in contact with water. However, the elements incorporated within the interior of the fly ash dissolved at a slower rate compared with the readily leachable surface associated elements (Choi et al. 2002).

Calcium, Potassium and Sodium Salts Analysis

Soluble salts like Ca, K and Na leached from coal ash samples are shown in Table 5. Low values of calcium leached in samples, i.e. 1.8–3.9 mg/L, indicate that low amount of Ca was present as free lime.

Calcium is not regarded as an element of concern, but it does play a primary role in the environmental quality of the ash. The amount of Ca states the pH of the ash–water system, and most trace elements display a pH-dependent solubility (Izquierdo 2012). Potassium and sodium are tightly bound within the glassy matrix, and therefore less than 2 % is available for leaching (Ward et al. 2003; Moreno et al. 2005). Result shows potassium and sodium were leached in very less amount i.e. 3.2–4.9 mg/L and 2.2–4.7 mg/L respectively.

Table 5 Calcium, potassium, sodium, sulphate and phosphate analysis of leachate

Sample no.	Na^+ (mg/L)	K^+ (mg/L)	Ca^{2+} (mg/L)	Sulphate (mg/L)	Phosphate (mg/L)
1	3.3	3.2	2.4	5.57	0.002
2	2.2	3.4	1.8	4.66	0.002
3	4.6	4.3	3.3	28.9	0.002
4	3.2	3.8	2.6	6.15	ND
5	4.7	4.9	3.9	3.38	0.001

ND not detected

Table 6 Indian standards for discharge of effluents into surface water and public sewers

Parameter and unit	Into surface water (IS 2490-1974)	Into public sewers (IS 3306-1974)
pH	5.5–9.0	5.5–9.0
Sulphates (mg/L)	1,000	1,000
Phosphates (mg/L)	5	–
Copper (mg/L)	3	3
Iron (mg/L)	3	3
Manganese (mg/L)	2	2
Lead (mg/L)	0.1	1
Cadmium (mg/L)	2	1
Chromium (mg/L)	2	2
Sodium (%)	–	60
Nickel (mg/L)	3	3

Source: Garg (2010)

Sulphate and Phosphate Ions Analysis

Due to dominant surface association in fly ash and the marked solubility of most sulphate-bearing compounds, sulphur is the major soluble element in fly ash. In environmental conditions, reduced S species are generally present in negligible quantities and sulphate is the dominant species (Fruchter et al. 1990). The leachability in terms of absolute levels varies over one order of magnitude, depending upon the nature (i.e. pH) of the ash. Result in Table 5 shows that in samples 1, 2, 4 and 5 sulphates leached in very low amount i.e. 3.38–6.15 mg/L and in sample 3 sulphates leached in high amount that is 28.9 mg/L, indicating the presence of high sulphur in the ash sample. Research shows that P remained immobile over 2 years-long column leaching test and concluded that this element occurs within the silicate matrix or as adsorbed constituents (Dudas 1981).

However, this evidence comes from very limited data available in the literature (Moreno et al. 2005). Results shows very low amount of phosphorus has been leached from all the samples i.e. 0.001–0.002 mg/L.

Table 6 shows the Indian standards for discharge of effluents. The concentrations of all the metals, salts and ions under this study of the leachate when compared with the Indian standards for discharge of effluents were found to be within the limit.

Conclusions

The main chemical compositions of coal ash are SiO_2, Al_2O_3, Fe_2O_3, CaO and MgO, in which SiO_2 content is high showing high pozzolanic property. EDXA analysis indicated the presence of the following elements: Ca, Mg, Al, Na, Si, K, Ti, Fe, C and O in the coal ash samples. The SEM microphotograph of ash reveals that it is a mixture of spherical particles of different sizes indicating less surface area. The concentrations of all the metals, salts and ions under this study of the leachate were invariably well below the permissible limits for discharge of effluents as per the Indian standards. Mixture of fly ash and pond ash can be utilized as the potential material as leachability of elements was found to be very low. Long term leaching tests are required to be studied to understand long term leachate behaviour.

References

ASTM (1992) Standard test method for shake extraction solid waste with water. ASTM D3987, West Conshohocken

Choi SK, Lee S, Song YK, Moon HS (2002) Leaching characteristics of selected Korean fly ashes and its implications for the groundwater composition near the ash mound. Fuel 81:1080

Dudas MJ (1981) Long-term leachability of selected elements from fly ash. Environ Sci Technol 15:840–843

Fruchter JS, Rai D, Zachara JM (1990) Identification of solubility-controlling solid phases in a large fly ash field lysimeter. Environ Sci Technol 24:1173–1179

Garg SK (2010) Sewage disposal and air pollution engineering. Khanna Publishers, New Delhi

Izquierdo M (2012) Leaching behaviour of elements from coal combustion fly ash: an overview. Int J Coal Geol 94:54–66

Moreno QN, Andrés X, Stanton JM, Towler M, Nugteren H (2005) Physico-chemical characteristics of European pulverized coal combustion fly ashes. Fuel 84:1351–1363

Palo A (2006) Potential health effects of crystalline silica exposures from coal fly ash: a literature review. EPRI, Palo Alto, 1012821

Pandian NS, Rajasekhar C, Sridharan A (1998) Studies on the specific gravity of some Indian coal ashes. J Test Eval ASTM 26, 177–186

Pandian NS, Sridharan A, Rajasekhar C (2001) Heavy metal retention behaviour of clayey soils. J Test Eval ASTM 29(4):361–371

Powell MA, Hart BR, Fyfe WS, Sahu KC, Tripathy S, Samuel C (1991) Geochemistry of Indian coal and fly ash. Environmental considerations. In: Sahu KC (ed) Proceedings of the international conference on environmental impact of coal utilization from raw materials to waste resources, Indian Institute of Technology Bombay

Prakash K, Sridharan A (2009) Beneficial properties of coal ashes and effective solid waste management. Pract Period Hazar Toxic Radioact Waste Manag ASCE 13(4):239–248

Sridharan A, Prakash K (2007) Geotechnical engineering characterisation of coal ashes. C.B.S. Publishers and Distributors, New Delhi

Sridharan A, Prakash K (2008) Beneficiary aspects of coal ashes in geotechnical engineering practice. In: Proceedings of the International conference on civil engineering in the new millennium, opportunities and challenges, 150-year anniversary conference at Bengal Engineering and Science University, Shibpur, India, vol 3, pp 361–368

Ward CR, French D, Jankowski J (2003) Comparative evaluation of leachability test methods and element mobility for selected Australian fly ash samples. Cooperative Research Centre for Coal in Sustainable Development Technical

Air Pollution Mapping and Quality Assessment Study at an Urban Area Tirupati Using GIS

M. Praveen Kumar, S. Venkata Mohan, and S. Jayarama Reddy

Introduction

The study of particulate air pollution is interesting for a number of reasons; they involve radiation budget, chemical deposition budget, effects on human health, effects on terrestrial and aquatic ecosystems (Bodhaine 1983; Nriagu and Davidson 1986; Fenger 1999; Riga-Karandinos and Saitanis 2005). Particulate air pollution is a complex mixture of small and large particles of varying size and chemical composition (Stanier et al. 2004). Health and environmental effects of particulate air pollution strongly depend on their size and chemical composition (Wichmann and Peters 2000; Cakmak et al. 2007; Kappos et al. 2004). Many processes like solar radiation, cloud-aerosol interaction and biosphere impacts are determined by size resolved chemical composition (Meszaros et al. 1997). The characteristics and distribution of particulate air pollution are highly variable, changing spatially, temporally and with altitude and source (Ulrich 2005). Particulate matter is introduced into the atmosphere through a variety of processes including sea-salt aerosol generation, structural weathering, biologically or physically mediated volatilization, volcanism, biomass burning, fossil fuel combustion, industrial activity and incineration (Nriagu 1989). Particulate air pollution presents a formidable challenge to theoretical as well as experimental chemists and physicists (Kvetoslav 2000) and they consist of both inorganic and organic components. The inorganic part of ambient aerosols consists of sulfates, ammonium, nitrates, chlorides, iodides, crustal elements,

M.P. Kumar (✉) • S.J. Reddy
Department of Chemistry, Sri Venkateswara University, Tirupati 517502, India
e-mail: praveen.mallupattu@gmail.com

S.V. Mohan
Bioengineering and Environmental Center, Indian Institute of Chemical Technology, Hyderabad 500007, India

© Capital Publishing Company 2015

N.J. Raju et al. (eds.), *Management of Natural Resources in a Changing Environment*, DOI 10.1007/978-3-319-12559-6_19

trace metals etc. (Murphy et al. 1998). The organic component of ambient particles in both polluted and remote areas is a complex mixture of hundreds of organic compounds (Reilly et al. 1998). Since rapid urbanization and increase in population in recent years, several researchers have focused on assessment of air pollution (Praveen Kumar et al. 2005; Chandra Mouli et al. 2006).

Conventional methods of chemical analysis are not sufficient for monitoring networks or policy makers to assess the impact of urban air pollution. There is growing need to assess air pollution using new technologies like Geographical Information System (GIS). GIS technologies provide capabilities to combine multiple data sources and that allows better understanding to researchers (Kaminska et al. 2004). The development of spatial data management using GIS has created a new era of environmental modelling (Matejicek 2005). The main objective of this paper is determination of ions in particulate air pollution as well as to study spatial distribution of these pollutants using GIS, assess the quality of air using National Ambient Air Quality Standards (NAAQS) and to provide valuable data for epidemiological studies, health risk assessment and monitoring networks to improve air quality.

Data Collection and Processing

The study area, Tirupati region (Fig. 1) is located nearby the metropolitan city, Chennai at a distance of about 145 km in southern peninsular India. Tirupati, a world famous holy pilgrim place for devotees of Lord Sri Venkateswara is situated in Chittoor district of Andhra Pradesh (AP) state at an altitude of 182.9 m (13.050 N latitude and 79.050 E longitude). Six locations, Shetti Palle (SP), Bhavani Nagar (BN), Thummalagunta (TG), SVU Campus (SVUC), Gandhi Road (GR) and Ramanuja Circle (RC), were selected for the collection of total suspended particulate matter (TSP). Detail description about sample locations are given in Table 1. TSP samples ($n=24$) were collected in summer of May 2006 on a glass fiber filter

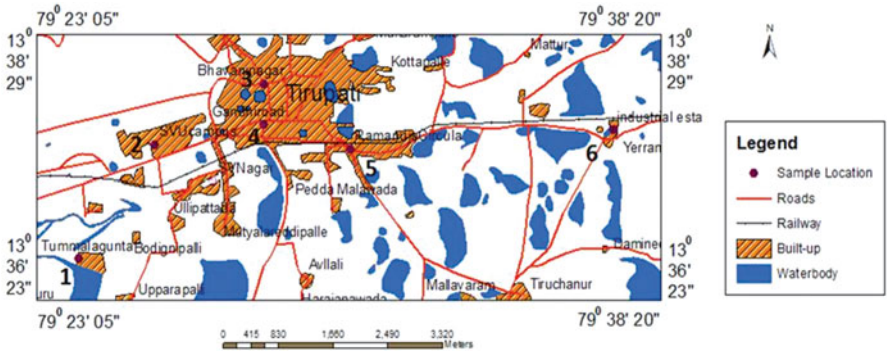

Fig. 1 Location map of study area

Table 1 Sampling points of the study area

S. No.	Location name	Description
1	Thummalagunta (TG)	Rural
2	SVU Campus (SVUC)	Educational
3	Bhavani Nagar (BN)	Residential
4	Gandhi Road (GR)	Traffic
5	Ramanuja Circle (RC)	Traffic
6	Shetti Palle (SP)	Industrial

with a frequency, once in a week for 24-h monitoring using High Volume Sampler (Envirotech, APM 415). Ion chromatography was employed to analyze anions and cations. Spatial distribution maps were prepared for air quality parameters (F, Cl, NO_3, SO_4, Na, K, Ca, Mg, NH_4) and for TSP classified map by doing interpolation technique of inverse distance weighted (IDW) method in Arc-GIS spatial analyst tools.

Results and Discussion

Spatial Distribution of Ions

The mean ionic concentrations of TSP are presented in Table 2. The obtained mass of TSP is between 69.34 ± 14.02 (SVUC) and 178.31 ± 13.14 μg/m^3 (SP). Highest mass loading of TSP is due to the presence of small scale industries at sampling point SP. In areas such as TG, GR, RC and BN the mass of TSP observed were 97.25 ± 7.94, 110.16 ± 13.86, 120.23 ± 18.49 and 134.42 ± 10.06 μg/m^3 respectively. Among all ions SO_4 reported maximum concentration, whereas lowest is F. The ionic concentrations of TSP are in the following order SO_4 > Na > NO_3 > Cl > Ca > K > NH_4 > Mg > F (Table 2). Spatial distribution of SO_4 is shown in Fig. 2. The concentration of SO_4 varies from east to the west direction. Lowest concentration is seen in the centre of the map (RC), whereas highest concentration pocket is seen in the western area of SVUC. Highest concentrations may be soil derived from the cultivated land near the SVUC and also gas-phase SO_2 on the wet surface of basic soil particles. Figure 3 shows the spatial distribution of NO_3, and is found to be distributed over the east to the western region of the study area. Small pocket of high concentration is seen in the northwest region (BN). Similarly, high concentrations are seen in the western regions, SVUC and TG. Higher concentrations may be attributed to soil dust from cultivated lands and also NO_3 may be formed by the absorption and subsequent reaction of NO_2 on the soil aerosol droplet or by the dissolution of gaseous HNO_3. Dairy farm with livestock of around 500 herds of cattle, located near the western region of the study area, this may act as major source of ammonia gas and would be favoured for the formation of NH_4NO_3.

Spatial distribution of NH_4 is shown in Fig. 4. The concentration of NH_4 is consistence throughout the study area. However, low concentration pockets are located

Table 2 Mean concentrations (ng/m^3) of ionic composition in TSP

Ions	Thummalagunta	SVU Campus	Gandhi Road	Ramanuja Circle	Bhavani Nagar	Shetti Palle
Na	304.23 ± 33.58	1047.27 ± 61.14	1297.36 ± 144.54	1052.54 ± 98.95	1051.35 ± 109.56	973.68 ± 125.90
NH_4	90.26 ± 12.13	14.21 ± 3.17	119.82 ± 16.16	103.53 ± 14.42	237.49 ± 26.95	91.24 ± 4.52
K	162.31 ± 14.65	293.72 ± 40.12	338.21 ± 33.61	453.26 ± 43.97	447.65 ± 45.38	158.12 ± 14.00
Mg	73.53 ± 8.90	62.18 ± 5.87	98.28 ± 13.05	151.54 ± 8.57	113.42 ± 11.0	86.39 ± 5.34
Ca	968.21 ± 60.56	465.67 ± 32.78	582.54 ± 15.95	632.57 ± 33.50	810.73 ± 23.20	893.52 ± 94.84
F	24.86 ± 5.89	15.23 ± 2.99	31.84 ± 3.12	33.84 ± 5.67	29.57 ± 3.79	61.58 ± 5.48
Cl	692.17 ± 61.60	273.54 ± 29.59	1257.26 ± 151.23	1314.56 ± 96.31	917.95 ± 36.93	962.74 ± 47.59
NO_3	1155.13 ± 53.55	1326.25 ± 42.60	538.82 ± 54.25	638.72 ± 36.72	1673.87 ± 75.30	327.38 ± 17.03
SO_4	2268.54 ± 87.81	3568.27 ± 127.07	2863.73 ± 105.98	1537.34 ± 38.46	2379.78 ± 84.40	2074.13 ± 88.46
TSP (μg/m^3)	97.25 ± 7.94	69.34 ± 14.02	110.16 ± 13.86	120.23 ± 18.49	134.42 ± 10.06	178.31 ± 13.14

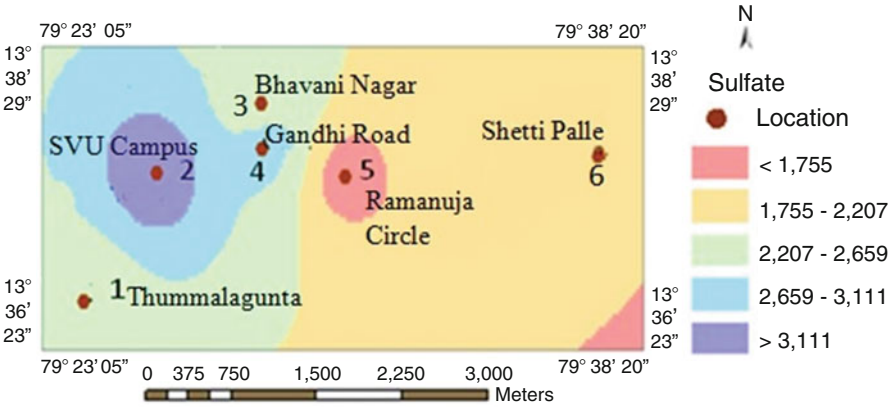

Fig. 2 Spatial distribution of sulphate

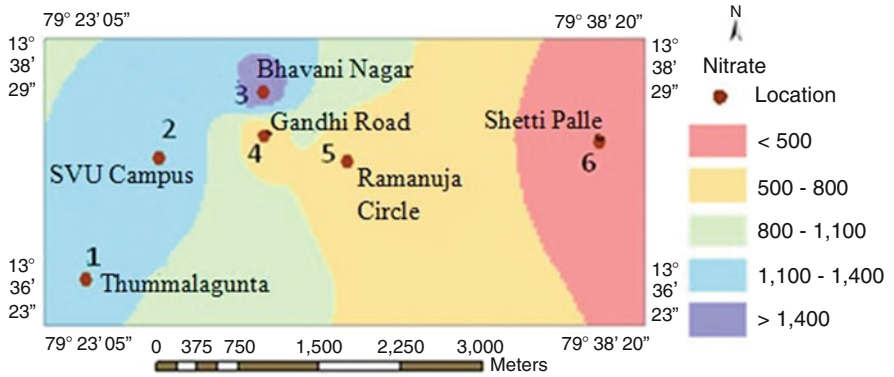

Fig. 3 Spatial distribution of nitrate

in the western region of the study area (SVUC), whereas small pocket of higher concentration is seen in northwestern region (BN). Refuse dumps could emit large amount of HCl and HF when being smashed or incinerated. NH_4 particles are formed when these acidic gases may react with NH_3 vapour or condense on an acidic particle surface of anthropogenic origin. Spatial distribution of Na is shown in Fig. 5 and is found to be consistent all over the map, except some low concentration pockets seen in the southwest corner region (TG) and a higher pocket is seen in the centre (GR) of the study area. Figure 6 shows the spatial distribution of Cl in the study area. It can be seen from Fig. 6 that the high concentrations were observed in the centre of the map (GR and RC), whereas, lower concentration pockets are seen at western parts of the study area (SVUC). These higher concentrations may be due to waste incinerations. As the study area is far away from sea coast the main sources

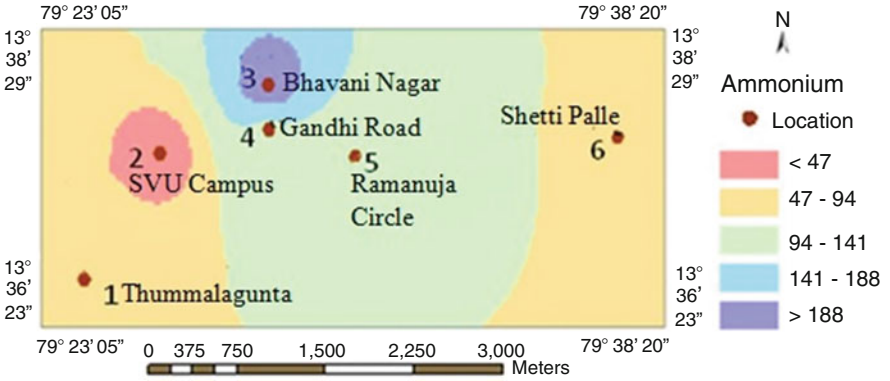

Fig. 4 Spatial distribution of ammonium

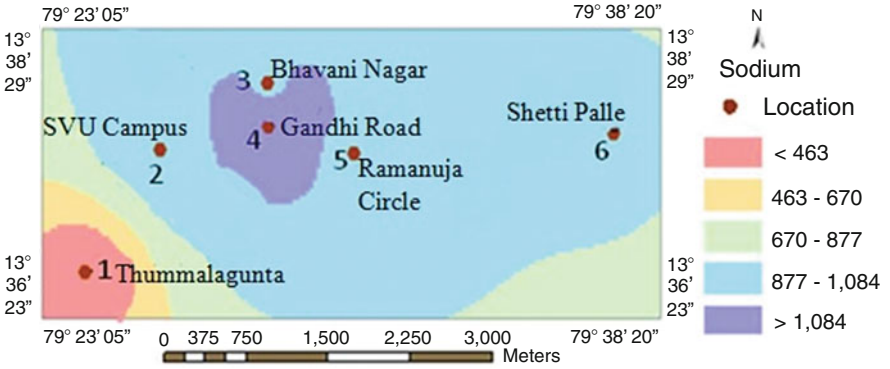

Fig. 5 Spatial distribution of sodium

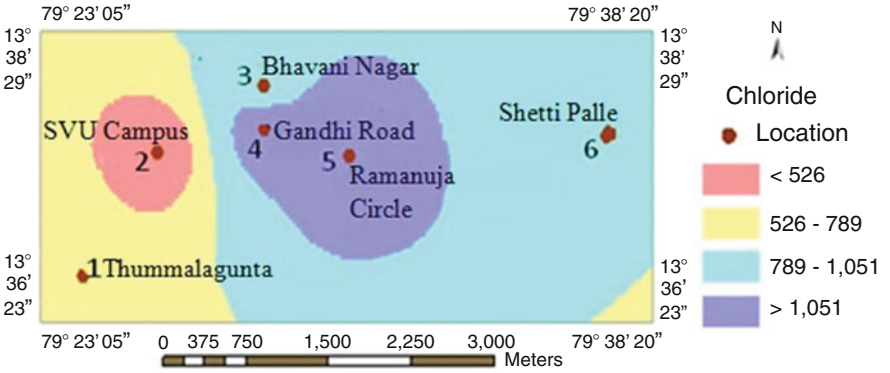

Fig. 6 Spatial distribution of chloride

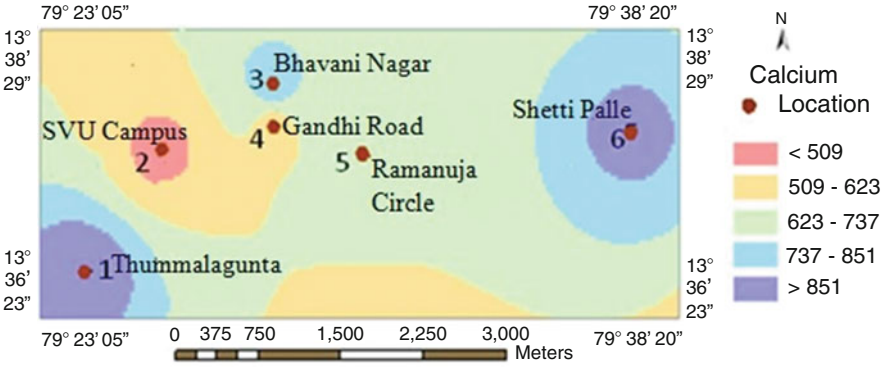

Fig. 7 Spatial distribution of calcium

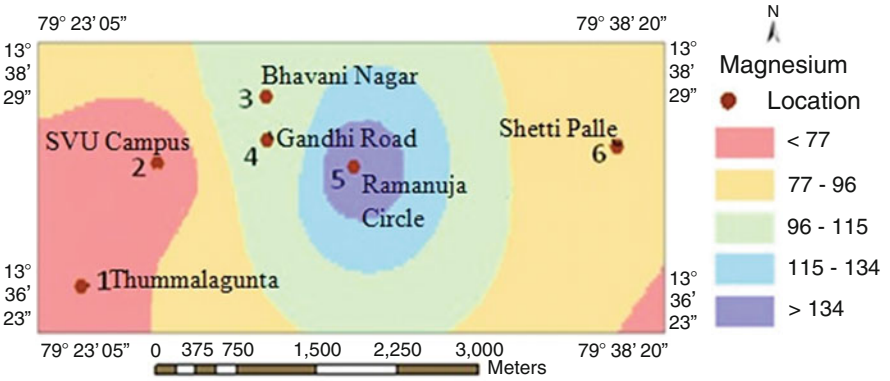

Fig. 8 Spatial distribution of magnesium

to Na and Cl may be attributed to terrestrial sources. Ca and Mg are considered to be crustal elements, and main sources are soil dust and windblown rock-derived minerals. Spatial distribution of Ca in the study area is shown in Fig. 7 and found to be distributed over the west to the east region. Some higher concentration pockets are seen at eastern region area, SP and southwest corner area, TG. This is attributed to the soil dust which was due to cultivated land present near these areas. Figure 8 shows the spatial distribution of Mg and is found to be lowest in the southwest region (TG and SVUC). Higher concentration pockets are seen in the centre of the map (RC). Higher concentrations are attributed to traffic dust, because these regions are located at high traffic centre. Soil dust may be considered to be main source for both Mg and Ca in the study area. Figure 9 shows the spatial variation of K in the study area. As seen from Fig. 9, the low concentrations are seen in the southwest corner (TG) and eastern region (SP), whereas higher concentrations are seen in the

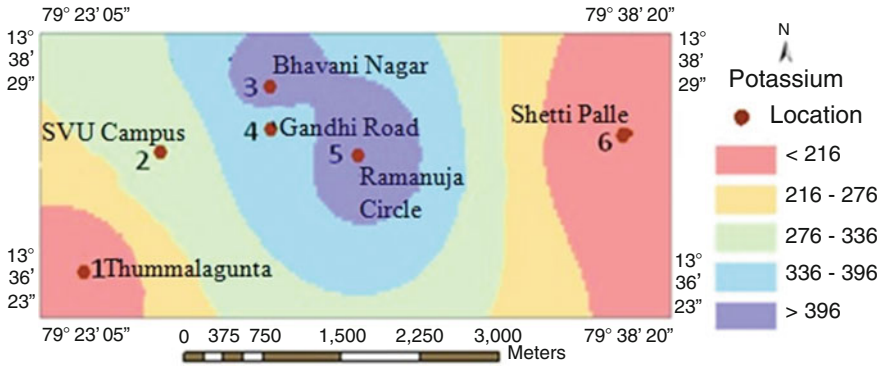

Fig. 9 Spatial distribution of potassium

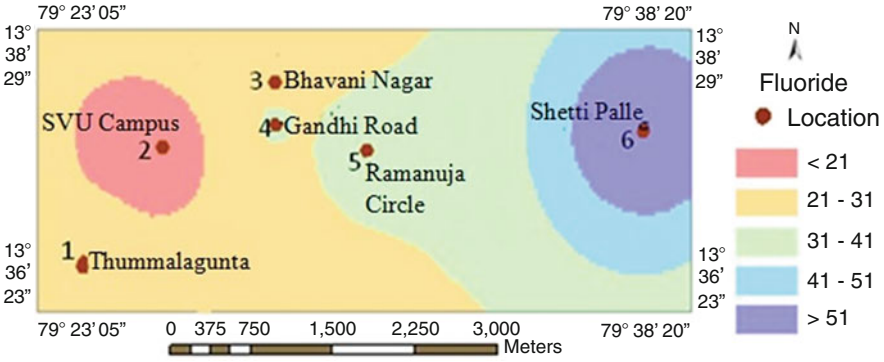

Fig. 10 Spatial distribution of fluoride

centre of the map. Higher concentrations may be attributed to traffic dust and combustion process. Figure 10 shows spatial distribution of F in the study area and found to be distributed over the west to the eastern region. Higher concentrations may be due to the presence of small scale industries in the eastern region. Fluoride may be contributed by emission from industrial activities like brick kilns and lime pulverization units situated in and around the study area.

Air Quality Assessment

Only TSP has been taken for further classification, because, there are no standards established for ionic composition studied by any agency. TSP was classified into four categories according to NAAQS i.e. excellent (0–100), good (100–200), moderate (200–300) and poor (>300). The classified map of TSP is shown in Fig. 11. It can be seen

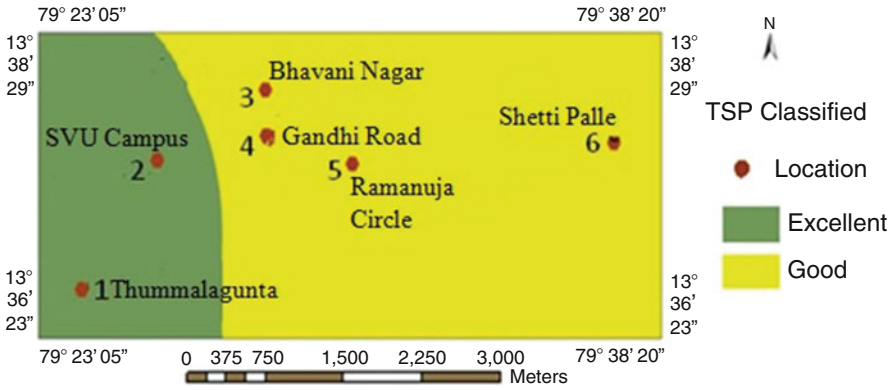

Fig. 11 Classified map of TSP

Table 3 Statistical results for TSP classified map

Class	Area (km^2)
Excellent	9.87
Good	26.56
Grand total	36.44

from Fig. 11, the quality of air is well below the standards proposed by NAAQS (1994). The locations such as SVUC and TG lie under the 'excellent' category. These locations are away from traffic and also industrial activities, whereas, other sampling locations BN, GR, SP and RC are under the 'good' category. Even though these sampling points are located nearby traffic and small scale industries, the overall quality of air is not affected much. The statistical results of the classified map are given in Table 3. It is evident from Table 3 that out of 36.44 km^2 study area 9.87 km^2 is found to be excellent quality, whereas 26.56 km^2 area is found to be good quality.

Conclusions

Continuous increase of urban air pollution now becomes a bigger challenge to urban planners, policy makers and health officials. There is a need for continuous monitoring of air pollution levels and also make the information obtained available to public. Present study provides data instantly in a comprehensive form and also it is easy to analyze the impact of pollutant on particular geographical area. Our results show that the study area does not exceed the standards suggested by NAAQS. TSP classified map shows that the overall quality of air fall under two categories i.e. excellent and good. Since present study is first in its kind in the study region Tirupati, the obtained results provides base for future researcher and planning officials.

Acknowledgements One of the authors Mr. M. Praveen Kumar is highly grateful to Council of Scientific and Industrial Research (CSIR), Government of India, New Delhi, India for providing financial assistance.

References

Bodhaine BA (1983) Aerosol measurements at four background sites. J Geophys Res 88:10753–10768

Cakmak S, Dales RE, Vidal CB (2007) Air pollution and mortality in Chile: susceptibility among the elderly. Environ Health Perspect 115:524–527

Chandra Mouli P, Venkata Mohan S, Balaram V, Praveen Kumar M, Jayarama Reddy S (2006) A study on trace elemental composition of atmospheric aerosol (PM_{10}) at a semi-arid urban site—modelling approach. Atmos Environ 40:136–146

Fenger J (1999) Urban air quality. Atmos Environ 33:4877–4900

Kaminska IA, Oldak A, Turski WA (2004) Geographical information system (GIS) as tool for monitoring and analysing pesticide pollution and its impact on public health. Ann Agric Environ Med 11:181–184

Kappos AD, Bruckmann P, Eikmann T, Englert N, Heinrich U, Hoppe P (2004) Health effects of particles in ambient air. Int J Hyg Environ Health 207:399–407

Kvetoslav RS (2000) Aerosol chemical processes in the environment. CRC Press, Schmallenberg

Matejicek L (2005) Spatial modelling of air pollution in urban areas with GIS: a case study on integrated database development. Adv Geosci 4:63–68

Meszaros E, Barcza T, Gelencser A, Hlavay J, Kiss G, Krivácsy Z, Molnar A, Polyak K (1997) Size distributions of inorganic and organic species in the atmospheric aerosol in Hungary. J Aerosol Sci 28:1163–1175

Murphy DM, Thomson DS, Mahoney MT (1998) In situ measurements of organics, meteoritic material, mercury, and other elements in aerosols at 5 to 19 kilometers. Science 282:1664–1669

NAAQS (1994) National Ambient Air Quality Standards

Nriagu JO (1989) A global assessment of natural sources of atmospheric trace metals. Nature 338:47–49

Nriagu J, Davidson C (eds) (1986) Toxic metals in the atmosphere. Wiley Intersciences, New York

Praveen Kumar M, Chandra Mouli P, Venkata Mohan S, Jayarama Reddy S (2005) Differential pulse anodic stripping voltammetric determination of Pb, Cd, Cu, and Zn in air, diet, and blood samples: exposure assessment. Anal Lett 38:463–475

Reilly PTA, Gieray RA, Whitten WB, Ramsey JM (1998) Real-time characterization of the organic composition and size of individual diesel engine smoke particles. Environ Sci Technol 32:2672–2679

Riga-Karandinos AN, Saitanis C (2005) Comparative assessment of ambient air quality in two typical Mediterranean coastal cities in Greece. Chemosphere 59:1125–1136

Stanier CO, Andrey YK, Spyros NP (2004) Ambient aerosol size distributions and number concentrations measured during the Pittsburgh Air Quality Study (PAQS). Atmos Environ 38:3275–3284

Ulrich P (2005) Atmospheric aerosols: composition, transformation, climate and health effects. Angew Chem Int Ed 44:7520–7540

Wichmann HE, Peters A (2000) Epidemiological evidence of the effects of ultrafine particle exposure. Philos Trans R Soc A Math Phys Eng Sci 358:2751–2769

Environmental Hazards and Conservation Approach to the Biodiversity and Ecosystem of the St. Martin's Island in Bangladesh

Nurul Hoque Upal

Introduction

St. Martin's Island, a unique island of Bangladesh, is of high ecological significance as it is the only island in Bangladesh that has coral colonies in the shallows including large areas of sand dunes and mangrove formations (Tomascik 1997). It is recognized as one of the richest biodiversity hotspot in terms of marine biotic resources, unparallel in the country. The island is endowed with vast marine and land resources having global biodiversity significance. The island is a good example of co-occurrence of corals, algae, sea weeds, grasses and mangroves (UNDP 2010). Besides the ecological importance St Martin's is one of the most attractive tourist spots in Bangladesh because of its panoramic landscapes, clear sea water, and natural treasures of coral colonies.

The attractive coral island in the Bay of Bengal is now threatened by environmental collapse due to several natural and anthropogenic factors ingrained which are directly or indirectly affecting the sustainability of biodiversity and ecosystem of the island. All the native species of flora and fauna of St. Martin's Island are under significant environmental impact. The deep-seated threats such as global climate change, deforestation, over exploitation of natural resources, and uncontrolled tourism make the ecological sustainability of the island vulnerable. Furthermore, other supplementary issues such as over population, poor agricultural custom, water pollution, construction activities, and harmful boat anchoring practices are demanding strict conservation practices inevitable to protect the marine and land resources of the island.

N.H. Upal (✉)
Institute of Water and Flood Management (IWFM), Bangladesh University of Engineering and Technology, Dhaka 1000, Bangladesh
e-mail: upalhoque@yahoo.com

© Capital Publishing Company 2015

N.J. Raju et al. (eds.), *Management of Natural Resources in a Changing Environment*, DOI 10.1007/978-3-319-12559-6_20

Physical Features

St. Martin's is located about 9 km south of the Cox's Bazar-Teknaf peninsular tip and about 8 km west of the northwest coast of Myanmar at the mouth of the river Naf. The island lies between 92°18′ and 92°21′E longitudes and 20°34′ and 20°39′N latitudes and forms the southernmost part of Bangladesh. It is almost flat and is 3.6 m above the mean sea level. The island has an area of only about 8 km^2 and is aligned NNW and SSE. The main island is dumbbell in shape and is divided in five different physiographic areas—Uttar Para, Golachipa, Madhya Para, Dakhin Para, and Cheradia (UNDP 2010).

While within the tropical belt, the weather of the St. Martin's Island is heavily influenced by the subtropical monsoonal climate that prevails over Bangladesh. Lying in a north-south direction, the island has a wider northern section and a narrower elongated southern section with a constriction between where the sand dunes of the western and eastern shores have almost joined. This narrow neck is gradually being eroded from both sides. The site is a sedimentary continental island consisting of continental base rocks which coral communities have colonised. The base rock is Girujan Clay shale (Pliocene), and grey to bluish grey inter-bedded with subordinate sandstone (UNDP 2010). The soil type of the island consists mainly of alluvial sands mixed with marine calcareous deposits. The surface water temperature around St. Martin's ranges between 18 and 31 °C, while coastal water salinity fluctuates between 26 and 35 ppt (Tomascik 1997). The turbidity of inshore water ranges from 1.5 to 8.0 m depending on the sea condition and tide cycle (UNDP 2010) (Fig. 1).

Ecosystem Assortments

Rocky Land Habitat

The rocky land area covers about 1 km^2 and is the last remaining habitat for rare species such as the water monitor (*Varanus salvator*), Bengal cobra (*Naja kaouthia*), bush birds, water birds and garden lizards, as well as native herbs, shrubs and climbers (Kamal 2008). The rocky ground and shallow water pools provide an excellent terrestrial microhabitat, especially during winter.

Sand Dunes and Beaches

The main shoreline habitats are sandy beaches and dunes, with the main sediments being alluvial sands. The sandy beaches of the site are supposedly the best nesting sites in Bangladesh for globally threatened marine turtles (Kamal 2008).

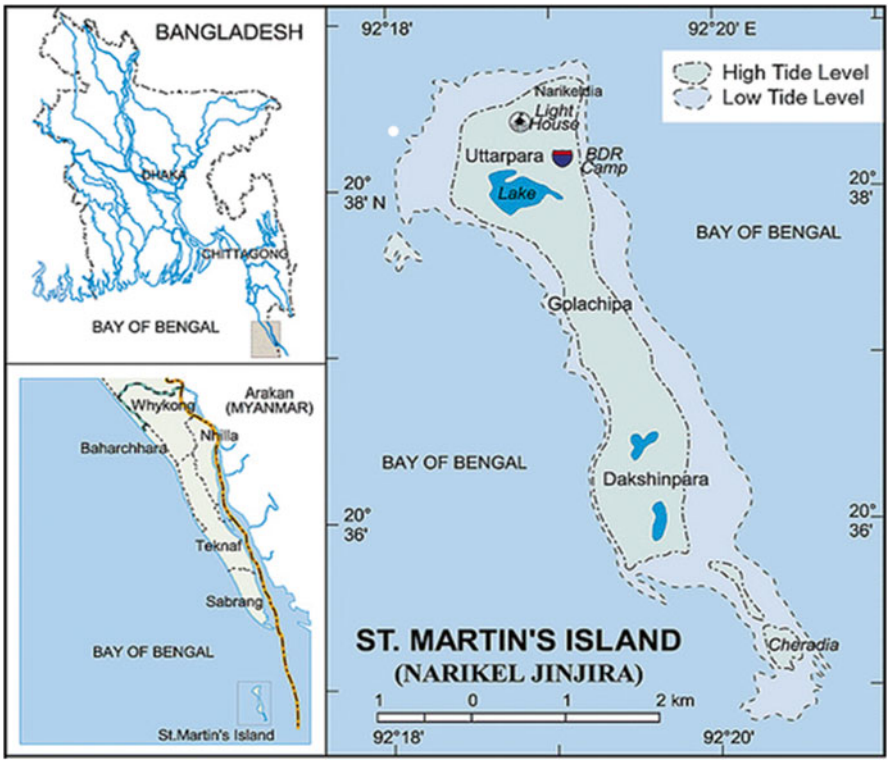

Fig. 1 Location map of the St. Martin's Island (*Source*: Banglapedia 2013)

Lagoons and Wetlands

Several lagoons and wetlands associated with mangrove and floodplain areas occur on the island, probably providing important habitats for birds. There is a lagoon at Uttar Para, a freshwater wetland at Dakhin Para and sizeable floodplain areas scattered throughout the island (UNDP 2010).

Mangrove

At one time the island probably had a significant area of mangrove vegetation, but most of this has been degraded with the passage of time. The top canopy was dominated by *Lumnitzera racemosa*, a total of 29 mangrove species were recorded (Tomascik 1997). There is a very small remaining mangrove patch at the site nowadays.

Mudflats

Within the inter-tidal zone there is a small mudflat area (known as Gaitta Banya) located at the southern end of the western beach. The mudflat is also the only habitat on the island for the yellow-lipped Sea Krait or Colubrine Amphibious Sea Snake (*Laticauda colubrine*) and also supports mud crabs and a large population of fiddler crabs (UNDP 2010).

Marine Habitats

The shallow water marine habitats include rocky and sandy intertidal habitats, offshore lagoons, rocky sub-tidal habitats, coral aggregations, seagrass beds, soft coral habitats and offshore soft-bottom habitats (Quader 2010). The extensive algal and seagrass beds in the island's coastal waters are highly productive and diverse and may be important spawning and/or nursery grounds for a number of economically important fish and shell fish species (Kamal 2008). There are only a few examples worldwide where coral communities dominate rock reefs; St Martin's Island provides a unique set of environmental conditions (biotic and abiotic) not found elsewhere in Bangladesh and perhaps not in the world.

Resourceful Biodiversity

Floral Diversity

Though many species of flora have disappeared, St. Martin's Island still has quite diverse vegetation because the remaining native species have been supplemented by a considerable number of cultivated and introduced species. Recent floral surveys have recorded 150 herbs, 32 climbers, 25 shrubs and 53 trees, belonging to 58 families (Quader 2010; UNDP 2010).

Coconut Palm *Cocos nucifera* (locally called Narikel) is abundantly cultivated on the island and is given the Bangla name of St. Martin's—Narikel Jhinjira. *Streblus asper* (locally called shaora) is considered to be the most abundant tree on the island (Tomascik 1997). Among the naturally occurring trees, two species of *Pandanus* (locally called keya) and one species of Streblus are predominant (UNDP 2010).

Areas of shrubs are dominated by the abundant *Vitex trifolea* (locally known as Nil-nishinda) and *Vitex negundo*, both belonging to the Amiacea family, and by some species of Leguminosae (Tomascik 1997). The main herb of note is the *Ipomoea pescaprae* (locally called Shagor lota). A small-bulbed variety of onion *Allium* sp. (Family Alliaceae) is indigenous to the island and is cultivated nowhere else in Bangladesh.

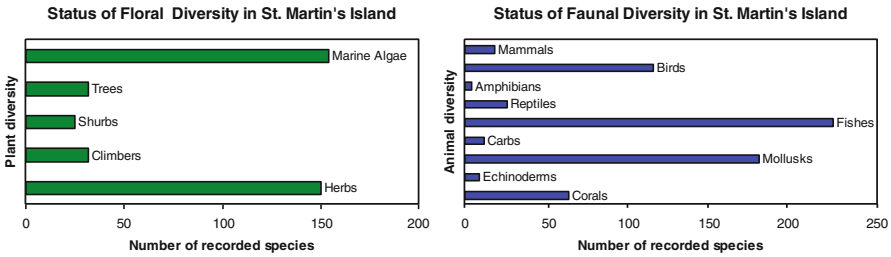

Fig. 2 Number of recorded species of floras and faunas in St. Martin's Island (*Source*: Tomascik 1997; Quader 2010; UNDP 2010)

The following mangrove species are found in the leftover scrap of mangrove forest: *Acanthus ilicifolius*, *Hibiscus tiliceous*, *Sonneratia apetala, Excoecaria agallocha*, *Avicennia marina* and *Clerodendrum inerme* (Tomascik 1997). *Aegialitis rotundifolia*, an early coloniser, has disappeared from the island (UNDP 2010).

So far 154 species of marine algae have been identified, largely from the island's inter-tidal and littoral zone (Tomascik 1997). Marine algae form an important source of nutrients for the myriads of animal life in the sea (Fig. 2).

Faunal Diversity

A total of only nine species belonging to eight genera in four classes of the phylum Echinodermata have been identified to species level from the island, these comprise four species of sea urchin, one species of sea star, three species of nudibranchs, and one species of sea cucumber (Tomascik 1997).

Due to its suitable environment, St. Martin is the only spot in Bangladesh where coral colonies are found. Coral communities extend to about 200 m offshore of the island (Islam and Islam 2008). A total of 66 coral species were recorded, of which 19 are fossil corals, 36 living corals and the rest are under six families of subclass Octocorallia (soft corals) (Tomascik 1997). The genera *Porites, Favites, Goniopora, Cyphastrea* and *Goniastrea* are the most abundant. The soft coral community off the east coast of St. Martin's Island is a unique feature of the subtidal zone (Islam and Islam 2008).

A total of 187 species of mollusks have been recorded from the island, among which 44 species are gastropods and the rest are bivalves. Tomascik (1997) reported the presence of some economically important gastropods which at that time were abundant, e.g. *Conus striatus*, *Conus textile* and *Conus geogrphes*, and also two economically important gastropods, *Trochus niloticus* and *Turbo marmoratus* that are heavily depleted worldwide.

About 12 species of crab have been recorded from the island, including commercially important crab species such as the mangrove crab *Scylla olivacea*,

which is widely distributed in the Bay of Bengal (Tomascik 1997). Some of the other crab species recorded are *Atergatis integerrimus, Matuta lunaris*, *Matuta planipes*, *Charybdis feriatus*, *Portunus pelagicus*, *Portunus sanguinolentus*, *Scylla serrata*, *Thalamita crenata*, *Dotilla myctiroides*, *Ocypode ceratophthalma* and *Carcinoscorpius rotundicanda* (UNDP 2010).

The fish and fisheries resource of the St. Martin's Island of Bangladesh is undoubtedly very rich in terms of species diversity. A total of 234 species of fish have been identified from the waters around the island, 89 of which are coral associated species, and only 16 of which are freshwater fish (UNDP 2010). The most abundant coral or reef associated fish are Damsel, Parrot, Surgeon, Groupers, Snappers, Emperors and Butterfly fish (Feeroz 2009).

A total of 27 reptile species from 11 families of three orders have been recorded from the island; of them 11 species are locally threatened (Tomascik 1997). Three species of marine turtles, *Lepidochelys olivacea, Eretmochelys imbricate,* and *Chelonia mydas*, are known to nest on the island. The island supports four amphibian species: the Common Asian Toad (*Bufo melanostictus*), and three frog species: *Euphlyctis cyanophlyctis*, *Hoplobatrachus tigerinus* and *Polypedates maculatus*.

The site lies on the boundary or overlap zone of the East Asia-Australasian Flyway and the Central Asian Flyway and provides a stepping stone for a number of migratory wader or shorebird species. A total of 120 species of birds have been recorded from the island (77 resident species and 43 migratory species) of which 18 species may be classified as locally threatened (Tomascik 1997; Moudud 2009).

A total of 19 species of mammals were reported from the St. Martin's, of which dogs are the only land-based carnivorous animal living in the island. The waters around St. Martin's Island are considered likely to be visited by six species of marine mammals or cetaceans: *Sousa chinensis, Neophocaena phocaenoides*, *Orcaella brevirostris*, *Tursiops aduncus*, *Stenella attenuate* and *Stenella longirostris* (UNDP 2010).

Environmental Threats to Biodiversity and Ecosystem

Climate Change Impacts

The effects of global climate change pose significant threats to the biodiversity of St. Martin's Island. The most noticeable damage caused by high sea temperature is coral bleaching. Coral bleaching turns into colourless ugly coral. Coral reefs have already suffered major mortalities as a result of high-temperature events. It is also dependent on a species of algae that lives symbiotically in its body and produces additional food by photosynthesis. When the sea temperature rises above 28 °C, the coral expels the algae and consequently it starves (Rahman 2009). Sea-level rise causes erosion of turtle nesting beaches. Higher sand temperature leads to changes in sex ratios or prevent eggs from hatching. Coral reefs are essential feeding habitats

of turtles. Coral bleaching destroys the feeding sources of turtles. Huge rainfall can raise ground water tables, thereby flooding nests of turtles (UNDP 2010).

Deforestation and Coastal Erosion

Deforestation in the St. Martin's Island has increased at an alarming rate during the course of last few decades. There are many forces like agricultural expansion, collection of sand dune vegetations for fodder and fuel wood, population density and natural disasters largely responsible for forest degradation of the island. Another major cause of recent deforestation is the clearing of vegetation including mangroves to make claims on land by local people (Ahmed 2011). Though coastal erosion is a natural process, indiscriminate vegetation losses accelerate the erosion which led to water turbidity and sedimentation, both of which impede the coral development and survival (Islam and Islam 2008). A decrease in vegetation is correlated to the decrease of local and migratory bird species. The decline in wintering shorebirds gulls, terns, plovers, herons, egrets, snipes, curlews etc. can be attributed to the loss of wilderness.

Unregulated Tourism

The St. Martin's Island has been a tourist destination for many years, but with recent developments in tourism infrastructure it has become one of Bangladesh's most popular tourist destinations. The existing tourism industry is making a big impact on the ecological sustainability of the area. More than 3,000 tourists arrive everyday during peak seasons (November to February) and tend to stay overnight in such a small island. But the fragile ecosystem on the island is not well-equipped to handle it. Reckless construction of buildings for tourist accommodation such as hotels, motels and restaurants has increased at a very rapid rate as a result of intensive development in certain areas, largely trembling to the ecological balance of the area.

Corals and sea turtles are the main biodiversity of St. Martin's Island and these are threatened due to tourism. Sea turtles come to nest on the beaches of the island between 10.00 pm and 02.00 am. It is noted that generators of the hotels and motels are run till midnight for tourists which is another reason for disturbing as well decreasing the number of nesting turtles there. Snorkeling and scuba diving are the most popular activities that tourists engaged in during their visit. These activities have been noted to pose significant threat to corals in shallow water as inexperienced snorkelers and scuba divers tend to either crush or stand on the reefs (Moudud 2010). Tourists purchase or collect large quantities of coral, different species of shells, and star fish which has resulted in the severe depletion of these species. The main season for migration of wintering birds coincides with the peak tourist season of the year, during which time large areas of preferred shoreline habitat are inundated with tourists,

which hamper the normal existence of the birds. There are regular big ship services and engine boat, used for carrying of tourist, to the island and for this reason, a huge amount of rough oil, plastic and other non-biodegradable waste are discharged in the marine water adjacent to the island, which ultimately cause depletion of fishes and other marine species.

Indiscriminate Extraction of Natural Resources

The large scale removal of keystone species and other marine resources (e.g. seaweeds, mollusks, lobsters) for food or as ornamental souvenirs is an on-going threat to the biodiversity of the inter-tidal, sub-tidal and coastal habitats of St. Martin's Island and its adjacent coastal waters. While seaweeds play an important role in protecting soil erosion as well as beach protection and improvement, they are harvested in large quantities by the local community for trading to Myanmar (Kamal 2008). Endless over-exploitation has brought the nesting turtles near to extinction. Major consumers of the turtle eggs are the ethnic communities of the country and the biggest business zone are the three hill tract districts of Khagrachari, Rangamati and Bandarban.

Commercial coral collection began in the 1960s and is now the professional activity of a few families (Islam and Islam 2008). The main threat to future viability of coral communities comes from direct extraction of coral colonies. As shells and live mollusks are extracted from the beach, they are now overexploited. The *Holothuria atra*, a species of sea cucumber, occurs in very low numbers due to over-exploitation and sea urchins are collected for sale to curious traders and tourists. In addition, a number of fish species are being over-fished, resulted alarming reduction of the fish and fisheries diversity in the present days (Feeroz 2009).

Other Negative Environmental Factors

Human settlement has started on the island around 150 years ago when only six families migrated from Myanmar to live on the island permanently (UNDP 2010). At present, however, this island abodes more than 6,000 people (Feeroz 2009). Over population is a further major threat for the ecological diversity of the island. Expectedly, the local community heavily depends on the natural resources of the island for their livelihood as they don't have alternative living options. Agriculture, one of the major occupations of the local people, is causing the ongoing destruction of habitats, especially the clearing of rocky land for cultivation and the filling in of lagoons. Additional problems are the cultivation of exotic and hybrid plants and the use of chemical pesticides and fertilizers (Feeroz 2009). Floods and heavy runoff during the rainy season introduce high quantities of sediments, nutrients and pesticides from poorly managed agricultural lands to inshore waters, and this has a

negative impact on coastal ecosystems. In addition, cyclones, storm surges, harmful boat anchoring practices, uses of destructive fishing gear, and other anthropogenic activities have taken the island's flora and fauna in danger.

Conservation Status

At past, several NGOs and organizations like Centre for Advanced Research in Natural Resources and Management (CARINAM), Centre for Natural Resource Studies (CNRS), Marine Life Alliance (MLA), and POUSH have implemented activities related to biodiversity conservation on the island, contributing greatly to increasing awareness among the local community about the need to conserve resources on the island, particularly turtle conservation (Molony et al. 2006). An assessment of the status of St Martin's Island according to criteria used by The World Conservation Union (IUCN) to determine the suitability of a site for protected area status was undertaken by Tomascik in 1997. According to the assessment, St Martin's Island was considered to satisfy the requirements for IUCN Protected Area Category II or Marine Park (Tomascik 1997). A zoning plan was subsequently developed as part of a management plan to manage the island as a marine protected area. The management plan was never implemented and the IUCN protected area category never applied.

As per section 5 of the Bangladesh Environment Conservation Act, 1995, the Government of Bangladesh by the Department of Environment (DoE) is empowered to declare any area as an Ecologically Critical Area (ECA) if such an area is threatened to be environmentally critical. Considering its rich natural biodiversity, the Department of Environment (DoE) in a gazette notification declared St Martin's as an ECA on 19 April 1999 (Islam 2001). Extraction of coral, seashell and conch, felling of trees and building structures were declared restricted in the gazette. In addition, building of any structure and carrying out any activity that might pollute the environment or harm the flora and fauna in an ECA is strictly prohibited. Despite that, nearly 100 privately owned hotels and restaurants are currently doing business in the small island, and surprisingly most of these business houses have established themselves in last 14 years (Moudud 2010). However, the unauthorized structures developed on St Martin's over the years with law enforcers and government agencies turning a blind eye to the violation.

The Ministry of Environment and Forests (MoEF) later undertook a "Conservation of Biodiversity, Marine Park Establishment & Eco-tourism Development at St Martin's Island Project" spanning from 2001 to 2007, mainly to conserve island's biodiversity, protect environment and halting indiscriminate housing by private companies and individuals (Moudud 2010). After years of irregularities, absence of proper monitoring and spending a staggering Tk 1.3 million, the project turned out to be a failure without making any headway. The MoEF has prepared a second phase of the project now to achieve the project goals and preserve natural resources of the island.

Conclusions

St. Martin's Island is gifted with extraterrestrial oceanic and land resources having global biodiversity significance. The island has an important ecological value as it contains a variety of unique habitats and a number of rare and endangered species. However, the island has now been identified as one of the environmentally sensitive areas of Bangladesh because of suffering from severe environmental degradation. The unique flora and fauna of this island have experienced tragic changes over the last two decades. Regretfully there is not much data or information available on the present status of corals and other associated flora and fauna in St. Martin's.

Though the Government of Bangladesh (GoB) and other international and non-governmental organizations have taken several initiatives to protect the biodiversity and ecosystem of the island, those were not enough due to lack of proper implementation efforts. Just by declaring the island as an ecologically sensitive zone is not enough. Proper implementation of the rules and regulations for 'Ecologically Critical Areas (ECAs)', control of pollution, sustainable and controlled tourism, alternative livelihood for the local people, and further research should be immediately undertaken to safeguard the rich biological resources of this important island. It is also imperative that a synchronized management with proper implementation plan should be formulated based on intergovernmental co-ordination and cooperation. All the stakeholders including government policy makers should come forward to protect the unique biodiversity of this critical island. Though the ecological damage has already been made up to a great extent, still there may be time to save the leftovers; otherwise it may be too late to conserve the only coral island of Bangladesh.

References

Ahmed A (2011) Some of the major environmental problems relating to land use changes in the coastal areas of Bangladesh: a review. J Geogr Reg Plan 4(1):1–8

Banglapedia (2013) St Martin's Island. www.banglapedia.org/HT/S_0537.HTM. Accessed 3 Jan 2013

Feeroz MM (2009) Effects of environmental degradation on food security in the St. Martin's Island of Bangladesh. National Food Policy Capacity Strengthening Programme, Dhaka

Islam MZ (2001) Draft final report, St Martin pilot project, national conservation strategy implementation project-1. Ministry of Environment and Forests, Dhaka

Islam MZ, Islam MS (2008) Threats to coral habitat in St. Martin's Island, Bangladesh. In: 11th international coral reef symposium, 7–11 July 2008, Florida

Kamal AHM (2008) Biodiversity and ecological aspects of Saint Martin's Coral Island, Bangladesh. In: 11th international coral reef symposium, 7–11 July 2008, Florida

Molony LA, National Project Professional Personnel (2006) St. Martin's Island ECA conservation management plan, coastal and wetland biodiversity management project. Department of Environment, Dhaka

Moudud HJ (2010) St. Martin's Island and its unique biodiversity face serious threats. http://www.iucn.org/about/union/secretariat/offices/asia/working_together/asia_members/?4887/St-Martins-Island-and-its-unique-biodiversity-face-serious-threats. Accessed 28 Dec 2012

Quader O (2010) Coastal and marine biodiversity of Bangladesh (Bay of Bengal). In: International conference on environmental aspects of Bangladesh, Sept 2010, Fukuoka, Japan

Rahman M (2009) Impact of climate change on St. Martin's Island. The Daily Star [Internet] 23 December 2009. Available at http://www.thedailystar.net/newDesign/news-details.php?nid=120032. Accessed 6 Jan 2013

Tomascik T (1997) Management plan for coral resources of Narikel Jinjira (St. Martin's Island). Final Report: National Conservation Strategy Implementation Project–1, Dhaka

UNDP (2010) Environmental profile of St. Martin's Island. Coastal and Wetlands Biodiversity Management Project, United Nations Development Programme, Dhaka

Uranium Toxicity in the State of Punjab in North-Western India

Alok Srivastava, Friedhart Knolle, Frieder Hoyler, Ulrich W. Scherer, and Ewald Schnug

Introduction

Lately there has been an increasing concern about uranium toxicity in some districts of Punjab State located in the North Western part of India after the publication of a report (Blaurock-Busch et al. 2010) which showed that the concentration of uranium in hair and urine of children suffering from physical deformities, neurological and mental disorder from Malwa region (Fig. 1) of Punjab State was manifold higher than the reference ranges. A train which connects the affected region with the nearby city of Bikaner which has a Cancer Hospital has been nicknamed as Cancer Express due to the frenzy generated on account of uranium related toxicity.

A detailed study of ground water samples in Malwa (Kumar et al. 2011) using fluorescence spectrometry showed that concentration of uranium in subsurface water samples from Malwa region ranged from 2 to 644 ppb with a mean of 73.1 ppb: more than five times higher than the permissible limit of 15 ppb prescribed by the World Health Organization (WHO 2011). A study (Rohit 2012) carried out using Total X-Ray Reflection Spectrometry too reported that the concentration of uranium in ground water samples obtained from Bathinda District in Malwa region varied

A. Srivastava (✉)
Chemistry Department, Panjab University, Chandigarh 160014, India
e-mail: alok@pu.ac.in

F. Knolle
GeoPark Harz, Braunschweiger Land, Ostfalen Network,
Grummetwiese 16, D-38640 Goslar, Germany

F. Hoyler • U.W. Scherer
Technical College Aachen, Heinrich Mussmann-Strasse 1, D-52428 Jülich, Germany

E. Schnug
Department of Life Sciences, Technical University,
Pockelsstraße 14, D-38106 Braunschweig, Germany

© Capital Publishing Company 2015

N.J. Raju et al. (eds.), *Management of Natural Resources in a Changing Environment*, DOI 10.1007/978-3-319-12559-6_21

Fig. 1 Districts in Malwa region of Punjab state where the concentration of uranium in ground water was observed beyond WHO permissible limit are encircled

between 139 and 295 ppb. The fly ash from two coal-fired power plants located in this region was presumed to be one of the causes of the uranium related toxicity but a recent study (Alrakabi et al. 2012) which corroborated the observation of high concentration of uranium in ground water in Malwa region ruled out the possibility of fly ash being the cause of ground water contamination. The uranium concentration in water from Nawanshahr region of Punjab has been reported (Bajaj et al. 2011) to be slightly higher than 15 ppb, the threshold of permissible limit prescribed by WHO.

The State of Punjab being the home to the Green Revolution in India as well as being one of the most prosperous states has seen excessive use of chemical fertilizers in the past couple of decades. It has been shown (De Kok and Schnug 2008) that the uranium in phosphate fertilizers can contribute significantly to the uranium load in the soils and this could perhaps lead to contamination of subsurface ground water sources. Therefore a humble attempt was made to evaluate the actual significance of fertilizer as possible source leading to the extremely elevated uranium concentration in the ground water.

Methodology

Eight samples of top soil from different locations in Punjab State lying between 29.5° N and 32.5° N latitude and between 73.8° E and 76.9° E longitude representing region having threshold and above threshold uranium concentration in ground water besides those from where no uranium toxicity has so far been reported were collected using standard auger method. Two additional top soil samples were obtained for comparing purpose from sites nearly 1,000 km away known to be normally fertilized and located in the State of Uttar Pradesh (22.4° N and 88.4° E) which too like the State of Punjab lies in the Indo-Gangetic plain to act as comparator. The only parameter common to all the samples was that they all had common geologic origin i.e. the Indo-Ganges Alluvion.

The samples were dried for a day in an oven at 60 °C until moisture was driven out and then further pulverized and homogenized. 50 g of the dried, pulverized and homogenized soil samples were then packed in leak proof PET containers. The sealed containers were kept aside for 4 weeks for attainment of secular equilibrium between radium, thorium and their daughter products before carrying out measurements using direct gamma spectrometry.

The uranium concentration (^{238}U) was determined by high resolution low level gamma ray spectrometry following the 186.2 keV gamma line of the daughter ^{226}Ra which is in secular equilibrium with its precursor namely ^{238}U. The samples were measured using a 40 % high purity germanium detector shielded by 10 cm of lead and coupled to a 16 K multi channel analyzer. The resolution of the detector was found to be 1.7 keV at 1,332 keV gamma peak of ^{60}Co. The spectral analysis was carried out using the GENIE 2000 software program (Canberra Co., USA).

Results and Discussion

Table 1 shows the concentration of the elements of interest expressed in terms of disintegration of ^{238}U per gram of soil as well as in mg/kg (ppm). Samples PUH1, PUH2 and PUH3 are from locations from the region showing high level of uranium in ground water, samples PUT1, PUT2 and PUT3 are from locations from the region where threshold concentration of uranium in ground water was observed and samples PUN1, PUN2, UPN1 and UPN2 are from locations from the region where so far no report related to uranium toxicity has been published.

It can be clearly observed from the obtained experimental data that the mean concentration of uranium based on three measurements in top soil irrespective of the locations from where they were collected seems to be not only low and comparable but even lie within the mean natural abundance of 3 ppm (Kabata-Pendias 2011). Therefore it becomes rather difficult to conclude that uranium from fertilizers in top soils could be the main cause for the observation of extremely high levels of uranium in water in the Malwa region of Punjab.

Table 1 Uranium concentrations in top soil samples from different locations

Sample	U (Bq/kg)	Standard deviation	U (ppm)	Standard deviation
PUH1	27.2	1.3	2.20	0.11
PUH2	17.4	0.8	1.41	0.07
PUH3	27.3	1.7	2.21	0.14
PUT1	21.1	1.0	1.71	0.08
PUT2	20.0	1.0	1.62	0.08
PUT3	25.9	1.7	2.10	0.14
PUN1	12.8	0.9	1.04	0.08
PUN2	11.1	0.7	0.91	0.06
UPN1	32.9	1.7	2.66	0.14
UPN2	7.9	1.0	0.64	0.08

Origin of samples: PUH1-3: Punjab regions with low level of uranium in ground water; PUT1-3: Punjab regions with around 15 ppb U in ground water; PUN1-3: Punjab regions and UPN1-2: Uttar Pradesh regions without reported U toxicity so far

This leads us to assume that uranium toxicity in Punjab could be related to the geogenic factors of the region. A geological view on the Indo Gangetic Plain situated between the two rivers Indus and Ganges shows that the soil in this region is mainly derived from new and old alluvial sediments. The affected Malwa region of Punjab in the catchment area of River Indus lies in the proximity (200–300 km) of the Shivalik Hills (younger Himalayas) whereas the comparator region is located in the catchment area of River Ganges nearly 1,000 km away. The Shivalik sediment group, namely their sandstones have been shown (Swarnkar et al. 2002) to host uranium mineralizations. Several locations in the Shivaliks (Una 31.48° N and 76.28° E and Kulu 31.96° N and 77.15° E) have been reported to have elevated level (Srivastava 2004) of indoor radon. The Shivalik sedimentary group crops out north of the Indo-Ganges Plains, dips in to the south and underlies parts of the alluvion complex. It is probable that there are hydrogeological links transporting geogenic uranium from the deep-lying Shivalik sediments up to the shallow groundwater horizon. This would be a sound explanation of the linear or scattered uranium hot spots in the ground water reported by several authors.

Conclusions

It can be concluded from the present work that fertilizer derived uranium may perhaps not be the cause for contamination of the ground water of this region. It is quite likely that geogenic sources may be playing a more significant role. The body of data is still small so it would be interesting to carry out further studies to make definitive conclusion.

Acknowledgement One of the authors (Alok Srivastava) would like to place on record his special thanks to Alexander von Humboldt Foundation, Bonn, Germany for providing financial support to carry out the experimental work in Germany.

References

Alrakabi M, Singh G, Bhalla A, Kumar S, Kumar S, Srivastava A, Rai B, Singh N, Shahi JS, Mehta D (2012) Study of uranium contamination of ground water in Punjab state in India using X-ray fluorescence technique. J Radioanal Nucl Chem 294:221–227. doi:10.1007/s10967-011-1585-x

Bajaj M, Eiche E, Neumann T, Winter J, Gallert C (2011) Hazardous concentrations of selenium in soil and groundwater in North-West India. J Hazard Mater 189:640–646

Blaurock-Busch E, Friedle A, Godfrey M, Schulte-Uebbing CEE, Smit C (2010) Metal exposure in the children of Punjab, India. Clin Med Insights: Ther 2:655–661. doi:10.4137/CMT.S5154 Chandigarh

De Kok LJ, Schnug E (eds) (2008) Loads and fate of fertilizer-derived uranium. Backhuys Publishers, Leiden

Kabata-Pendias A (2011) Trace elements in soils and plants, 4th edn. CRC Press, Boca Raton

Kumar A, Usha N, Sawant PD, Tripathi RM, Raj SS, Mishra M, Rout S, Supreeta P, Singh J, Kumar S, Kushwaha HS (2011) Risk assessment for natural uranium in subsurface water of Punjab State, India. Hum Ecol Risk Assess 17:381–393. doi:10.1080/10807039.2011.552395

Rohit K (2012) M.Sc thesis, Chemistry Department, Panjab University

Srivastava A (2004) An overview of an indoor radon study carried out in dwellings in India and Bangladesh during the last decade using solid state nuclear track detectors. J Environ Radioact 78:113–121

Swarnkar BM, Umamaheshwar K, Srinivasan S, Kothari PK (2002) Exploration for sandstone type uranium mineralisation in the northern Himalaya, India. Explor Res Atomic Miner 14:1–27

WHO (2011) Guidelines for drinking-water quality, 4th edn. WHO, Geneva

Fluoride Toxicity in the Fluoride Endemic Villages of Gaya District, Bihar, India

Shahla Yasmin and Suneet Ranjan

Introduction

High level of fluoride (F) in drinking water has been recognized as a potential health hazard all over the world. In India, 17 out of 32 states have been identified as 'endemic' areas for fluorosis, with an estimated 25 million people impacted, and another 66.62 million people (including six million children below the age of 14) 'at risk' of facing health hazards due to high water-borne fluoride concentrations. After ingestion of fluoridated water, majority of the fluoride is absorbed from the stomach and small intestine into the blood stream (Whitford 1996). Approximately, 50 % of the fluoride absorbed each day by young or middle-aged adults becomes associated with hard tissues (teeth and bones) within 24 h while virtually all of the remainder is excreted (Whitford 1996). More fluoride is retained in young bones than in the bones of older adults (Whitford 1996; Horowitz 1996). Fluoride toxicity at high levels has also been associated with thyroid changes, growth retardation, kidney changes, and even urolithiasis (Dhar and Bhatnagar 2009). According to Strunecka et al. (2007), fluoride in excess amounts causes several ailments viz, metabolic disturbances, endocrine dysfunctions and physiological alterations in the body. F exposure also disrupts the synthesis of collagen and leads to the breakdown of collagen in bones (Susheela and Jha 1981). Its excessive intake may result in slow, progressive crippling condition known as fluorosis. This paper reports about the groundwater quality of certain regions of Gaya district of Bihar, with special emphasis on fluoride contamination and its impact on human health.

S. Yasmin (✉) • S. Ranjan
Department of Zoology, Patna Women's College, Patna University, Patna 800001, India
e-mail: shahla_apex@yahoo.co.in

© Capital Publishing Company 2015

N.J. Raju et al. (eds.), *Management of Natural Resources in a Changing Environment*, DOI 10.1007/978-3-319-12559-6_22

Geology of the Study Area

Gaya district is located at 84.4° E to 85.5° E Longitude and 24.5° N to 25.1° N Latitude and has total area of 487,607.83 km^2. Greater part of Gaya district is occupied by the Gangetic alluvium, but older rocks rise above its level, chiefly in the south and east. These rocks are mostly composed of foliated gneiss, a subdivision of the Archean system which contains the oldest rocks of the earth's crust (O'malley 2007). The Gidhour hills lie across the southern boundary of Gaya, composed of Dharwars, including micaceous and ferruginous schist so highly metamorphosed by intrusive coarse pegmetitic granites that they yield mica. The north eastern part of district is mainly quartzite and slate, and very barren because of lack of forests. The south east corner of district is situated in the middle of rich mica belt.

Methodology

A total of 31 villages of Bodh Gaya, Manpur, Wazirganj, Belaganj, Amas and Bankebazar blocks in Gaya district of Bihar were included in this study. Twenty samples of drinking water were collected from each block, except Bankebazaar, from where 23 samples were collected. Likewise 123 samples were collected and analyzed for fluoride and other physico-chemical parameters. The samples were collected during the pre-and post-monsoon in pre-cleaned high density polypropylene sample (1 L) bottles and stored at 4 °C before analysis. Fluoride (F) level was measured by using Fluoride Ion selective electrode Orion 9690 BNWP with PCD 650 cyber scan portable meter. Commercially available ion strength adjusting buffer i.e. ISA I was added to the samples before the estimation of fluoride. Other physico-chemical parameters were estimated according to APHA-AWWA-WPCF (1995). Hardness and calcium were estimated with EDTA titrimetric methods. pH, conductivity, TDS and turbidity were measured by portable PCD 650 multi tester. Iron was estimated with the Phenanthroline method. Moreover, 93 urine and blood samples from different age groups including adult males, adult females and children (with confirmed dental fluorosis) from F affected areas were also analyzed. Fifty-two samples from Bodh Gaya block were also collected as controls for hematological and biochemical analysis. The blood was collected in heparinized vials. The hematological analysis was done with the help of Automatic Hematolyzer (Sysmex KX-21). Further plasma was separated for biochemical analysis. The reagents kits of ERBA make were used for blood analysis. The levels of glucose and calcium were estimated by using Blood Chemistry analyzer (Biotech BT-260 plus). The TT3, TT4, and TSH levels were estimated by ELISA reader (ERBA Lisa scan EM). The health survey was conducted with a pre-designed questionnaire. The F exposure dose was calculated by the equation as was done by Viswanathan et al. (2009):

$$\text{Exposure dose} = C \times WI / BW$$

where C = F concentration (mg/L), WI = water intake (l/day) and BW = body weight (kg).

The water intake was estimated from the information collected during the health survey. The average water intake for children was 2 l/day and that for adults was 4 l/day. Average body weight of children was taken as 20 kg and that of adults was taken as 60 kg. Statistical analysis was performed with t-test.

Results and Discussion

Fluoride concentration in the groundwater of different blocks is presented in Table 1. None of the samples of Bodh Gaya and Belaganj blocks had F above the desirable limit of 1.0 mg/L as suggested by BIS 2003. In Manpur block, Mayapur village had F level of 1.1 mg/L. In Wazirganj block, Bharaiti (1.7 mg/L) and Karhauna (1.6 mg/L) villages recorded higher fluoride concentration (i.e. above the WHO permissible limit). Amas and Bankebazar blocks were endemic with respect to fluoride contamination of groundwater, with F level ranging 0.47–6.3 mg/L. The mean pre-monsoon F level in groundwater (1.05 ± 0.09, N = 123) was insignificantly different from mean post-monsoon F level (1.02 ± 0.08, N = 123).

A positive correlation was found between pH and fluoride which indicates that alkaline nature of the water promotes leaching of fluoride from rocks (Table 2). The alkaline water can mobilize fluoride from rocks with precipitation of calcium carbonate because the solubility of fluorite (CaF_2) increases with an increase in $NaHCO_3$ rather than with other salts (Handa 1975; Saxena and Ahmed 2001; Sunitha et al. 2012). A negative correlation was found between the Ca (r = –0.4), Fe (r = –0.2) as well as Mg (r = –0.2) and F levels in the water samples. This indicates low solubility of F with these ions (Das et al. 2003).

The F level in serum and urine were significantly higher in the fluorotic individuals as compared to control (Table 3). According to Susheela et al. (2005), normal upper limit of fluoride in serum and urine should be 0.02 mg/L and 0.1 mg/L respectively. Residents of Amas (Bhoop Nagar, Masooribaar) and Bankebazar block (Dhaneta, Bhaktauri) were found to suffer with skeletal fluorosis (children 80 %, adult males 52 % and adult females 33 %) and dental fluorosis (children 87.6 %, adult males 79 % and adult females 59.7 %) (Table 4, Fig. 1). Residents of F endemic areas also complained of gastro-intestinal and neurological problems (i.e. headache and insomnia). In Dhaneta village of Bankebazar block, 55 % adult males, 63 % adult females and 35 % of children suffered with neurological problems, while in Bhaktauri village of Bankebazar block, 71 % adult males and 75 % adult females suffered with headache and insomnia. In Bhupnagar village of Amas block, 88 % of adult males, 76.3 % of adult females and 50 % of children were found to have neurological problems. It has been found that F can reduce levels of melatonin, the sleep hormone, in the body, causing chronic insomnia (Hileman 1988). Spittle (1994) also recorded cases of severe headache in adult subjects exposed to F in their drinking water. Sharma et al. (2009) found an increase in the severity of neurological

Table 1 Fluoride concentration in water samples of different blocks of Gaya district, Bihar

Blocks	Villages	No. of samples	Mean ± S.E. (pre-monsoon)	Mean ± S.E. (post-monsoon)	Range of fluoride (mg/L)	No. of samples exceeding the desirable limit of 1 mg/L
Bodh Gaya	Shillonja, Chotki Basadhi, Bakraur, Tekuna, Kharanti, Bagdaha	20	0.49 ± 0.04	0.64 ± 0.02	0.55–1.0	0
Manpur	Alipur, Gangti, Manpur pehani, Lakhanpur, Rasalpur, Rampur, Budhgere, Mayapur	20	0.46 ± 0.04	0.44 ± 0.05	0.24–1.1	1
Wazirganj	Karhauna, Dhuriyawa, Singhaura, Motibigha, Bharaiti, Aarsh Gali	20	0.82 ± 0.09	0.69 ± 0.1	0.32–1.7	3
Amas	Bhoop Nagar, Rampur, Masooribaar	20	1.8 ± 0.23	1.7 ± 0.19	0.89–3.2	13
Belaganj	Beladih, Paranpur, Siyaram Colony, Korma, Yadavpur	20	0.42 ± 0.01	0.35 ± 0.01	0.3–0.46	0
Bankebazar	Dhaneta, Bhaktauri, Kamalpur	23	2.0 ± 0.28	2.01 ± 0.3	0.71–6.2	15

Table 2 Correlation of different parameters in pre-monsoon (a) and post-monsoon (b) groundwater samples

	Turbidity	pH	EC	TDS	Fluoride	Total Hardness (TH)	Calcium	Iron	Mg
(a)									
Turbidity		0.08	−0.02	−0.01	−0.005	−0.15	−0.11	0.64	−0.105
pH	0.08		0.07	0.06	0.54	−0.15	−0.35	−0.17	−0.09
EC	−0.02	0.07		0.99	0.02	0.71	0.53	−0.13	0.64
TDS	−0.01	0.06	0.99		0.01	0.71	0.53	−0.12	0.64
Fluoride	−0.005	0.54	0.02	0.01		−0.33	−0.42	−0.25	−0.22
TH	−0.15	−0.15	0.71	0.71	−0.33		0.78	−0.11	0.74
Calcium	−0.11	−0.35	0.53	0.53	−0.42	0.78		0.04	0.67
Iron	0.64	−0.17	−0.13	−0.12	−0.25	−0.11	0.04		−0.08
Mg	−0.10	−0.09	0.64	0.64	−0.22	0.74	0.67	−0.08	
(b)									
Turbidity		0.12	−0.03	−0.04	−0.05	−0.17	−0.21	0.56	−0.09
pH	0.12		0.15	0.16	0.24	−0.02	−0.24	−0.13	−0.04
EC	−0.03	0.15		0.99	0.01	0.71	0.49	−0.13	0.63
TDS	−0.04	0.16	0.99		0.02	0.71	0.48	−0.13	0.62
Fluoride	−0.05	0.24	0.01	0.02		−0.34	−0.42	−0.27	−0.25
TH	−0.17	−0.02	0.71	0.71	−0.34		0.77	−0.11	0.73
Calcium	−0.21	−0.24	0.49	0.48	−0.42	0.77		−0.05	0.68
Iron	0.56	−0.13	−0.13	−0.13	−0.27	−0.11	−0.05		−0.05
Mg	−0.09	−0.04	0.63	0.62	−0.25	0.73	0.68	−0.05	

ailments with the increase in F concentration in drinking water. The occurrence of gastro-intestinal complaints is considered to be the early warning signs of F toxicity (Susheela et al. 1992). F causes serious damage to the gastrointestinal (GI) mucosa by destroying the microvilli resulting in non-absorption of nutrients from the diet (Susheela et al. 1992; Das et al. 1994).

Biochemical analysis showed elevated TT3 in all the age/sex groups and elevated TT4 and TSH level in children of F endemic areas as compared to control subjects (Table 5). This suggests that F can induce thyroid dysfunction. Previous studies indicated that excessive F, with or without adequate iodine (I) intake, was a significant risk factor for the development of thyroid dysfunction (Liu et al. 2002; Ge et al. 2005a, b). Hypocalcemia was found in the adults of F endemic area, while hypoglycemia was found in both adults and children of F endemic areas. Hypocalcemia could be due to a decrease in the intestinal absorption of calcium since fluoride is known to produce insoluble complexes with calcium. Similar findings were also reported by Michael et al. (1996) and Barot (1998). Fluoride toxicity leads to a number of adverse effects including hypoglycemia (Bălan 2012).

The haematological analysis of residents of F endemic villages showed lowered Hgb level in all the adult residents (Table 6). F may cause the erythrocyte membranes

Table 3 Age and fluoride exposure of study subjects of control and F endemic areas

	Control area				F endemic area			
	Age in years	F* exposure dose (mg/kg/day)	F in serum (mg/L)	F in urine (mg/L)	Age in years	F** exposure dose (mg/kg/day)	F in serum (mg/L)	F in urine (mg/L)
Adult males	42.10 ± 2.37 (N = 21)	0.039	0.05 ± 0.002	0.32 ± 0.04	43.52 ± 2.31 (N = 33)	0.16	0.09 ± 0.006***	0.70 ± 0.02***
Adult females	38.78 ± 2.02 (N = 18)		0.04 ± 0.002	0.28 ± 0.04	43.90 ± 2.85 (N = 30)		0.07 ± 0.001***	0.69 ± 0.01***
Children	7.462 ± 0.46 (N = 13)	0.059	0.035 ± 0.004	0.16 ± 0.02	8.66 ± 0.50 (N = 30)	0.23	0.06 ± 0.001***	0.55 ± 0.02***

Values are Mean ± S.E.

***$p < 0.0001$ for comparison with control

Table 4 Certain health problems observed during survey

	F non-endemic area			F endemic area		
	Adult males (N = 858)	Adult females (N = 850)	Children (N = 374)	Adult males (N = 186)	Adult females (N = 179)	Children (N = 81)
Dental fluorosis (Mottled teeth)	0	0	0	147 (79 %)	107 (59.7 %)	71 (87.6 %)
Skeletal fluorosis	0	0	0	93 (52 %)	59 (33 %)	65 (80 %)
Joint pain	41 (4.7 %)	227 (26.7 %)	0	141 (75.8 %)	151 (84.3 %)	61 (75.3 %)
Gastro-intestinal problems	197 (22.9 %)	193 (22.7 %)	95 (25.4 %)	92 (49 %)	90 (50 %)	40 (49 %)
Headache	81(9.4 %)	120 (14 %)	14 (3.7 %)	72 (38.7 %)	65 (36 %)	18 (22 %)
Insomnia	28 (3 %)	67 (7.8 %)	0	38 (20 %)	36 (20 %)	0

Fig. 1 Skeletal fluorosis [(**a**) and (**b**)] and dental fluorosis [(**c**) and (**d**)] cases in the F affected areas of Gaya region

Table 5 Comparison of certain biochemical parameters of study subjects of F non-endemic and F endemic areas of Gaya region

	Adult males		Adult females		Children	
	Control area	F endemic area	Control area	F endemic area	Control area	F endemic area
Parameter	N = 21	N = 33	N = 18	N = 30	N = 13	N = 30
T3 (pg/dL)	1.12 ± 0.08	1.85 ± 0.12***	1.14 ± 0.09	1.94 ± 0.12***	9.25 ± 0.63	13.93 ± 0.92*
T4 (μg/L)	9.59 ± 0.45	10.53 ± 0.78	10.44 ± 0.8	10.41 ± 0.82	0.65 ± 0.05	2.65 ± 0.22***
TSH (mIU/L)	2.75 ± 0.47	2.42 ± 0.29	2.58 ± 0.29	2.64 ± 0.28	0.47 ± 0.08	3.63 ± 0.28***
Serum Ca (mg/L)	9.96 ± 0.14	7.49 ± 0.34***	9.85 ± 0.16	7.06 ± 0.26***	9.04 ± 0.06	8.01 ± 0.33
Serum Glucose (mg/dl)	96.78 ± 2.56	77.51 ± 5.76*	92.80 ± 3.31	72.83 ± 4.45*	97.16 ± 2.28	62.93 ± 8.82*

Values are Mean ± S.E.

*$p < 0.01$; ***$p < 0.0001$ for comparison with control

Table 6 Haematology of study subjects in control (F non-endemic) and F endemic areas of Gaya region

	Adult males		Adult females		Children	
	Control area	F endemic area	Control area	F endemic area	Control area	F endemic area
Parameter	N = 21	N = 33	N = 18	N = 30	N = 13	N = 30
WBC ($\times 10^3$ µL)	7.27 ± 0.29	6.83 ± 0.50	5.61 ± 0.44	6.88 ± 0.56	4.97 ± 0.45	9.00 ± 0.73*
RBC ($\times 10^6$ µL)	4.58 ± 0.12	4.52 ± 0.11	4.61 ± 0.17	4.26 ± 0.14	5.04 ± 0.14	4.87 ± 0.16
HGB (g/dL)	14.32 ± 0.08	11.26 ± 0.47***	13.04 ± 0.38	10.02 ± 0.2***	11.63 ± 0.15	10.95 ± 0.25
HCT (%)	42.25 ± 0.36	35.99 ± 0.94***	37.81 ± 0.69	31.94 ± 0.7***	35.93 ± 1.01	34.65 ± 0.70
MCV (fL)	88.36 ± 1.12	79.89 ± 1.53**	87.22 ± 1.00	75.94 ± 1.4***	81.81 ± 2.20	70.65 ± 1.62**
MCH (pg)	30.36 ± 0.40	25.63 ± 0.65***	28.82 ± 0.39	23.94 ± 0.5***	29.15 ± 0.26	22.4 ± 0.66***
MCHC (g/dL)	33.71 ± 0.20	31.95 ± 0.25***	32.49 ± 0.17	31.43 ± 0.22*	32.88 ± 0.10	31.58 ± 0.26*
LYM (%)	31.34 ± 0.87	31.67 ± 1.72	32.13 ± 1.42	37.38 ± 2.00	26.91 ± 0.98	45.03 ± 2.72**
LYM ($\times 10^3$ µL)	2.38 ± 0.10	2.04 ± 0.16	2.13 ± 0.10	2.45 ± 0.19	1.46 ± 0.07	4.26 ± 0.62*

Values are Mean ± S.E.

*$p < 0.01$; **$p < 0.001$; ***$p < 0.0001$ for comparison with control

to lose calcium (Susheela and Jain 1983), leading to deformed RBCs, called echinocytes. Echinocytes are eliminated from the body leading to fall in haemoglobin content in people facing chronic fluoride toxicity. The fall in MCV, MCH and MCHC suggests iron depletion or deficiency. According to Susheela et al. (2010), fluoride ingestion may arrest the absorption of nutrients including orally administered iron and folic acid and thus cause anaemia. Significantly higher lymphocyte counts were found in the children of F endemic area as compared to control. Higher lymphocyte count in the peripheral blood has been reported in hyperthyroid animals (Fowles et al. 1997) and humans (Jafarzadeh et al. 2010) suggesting that thyroid hormones may have profound effects on the lymphopoiesis.

Conclusion

It was found that F contamination in the groundwater of Gaya region was due to geogenic contamination. Consumption of F-rich water has resulted in the development of dental, skeletal and non-skeletal fluorosis. Although, water filters have been installed by the Government, necessary action has to be taken to ensure the supply of fluoride-free water.

Acknowledgements We are grateful to UGC for the financial support under the Major Project Scheme and to Dr. Sister Doris D'Souza, Principal, Patna Women's College for providing the necessary facilities.

References

APHA (1995) Standard methods for the examination of water and wastewater, 19th edn. American Public Health Association, Washington, DC

Bălan H (2012) Fluoride – the danger that we must avoid. J Intern Med 50(1):61–69

Barot VV (1998) Occurrence of endemic fluorosis in human population of North Gujarat, India: human health risk. Bull Environ Contam Toxicol 61:303–310

Das TK, Susheela AK, Gupta IP, Dasarathy S, Tandon RK (1994) Toxic effects of chronic fluoride ingestion on upper gastro-intestinal tract. J Clin Gastroenterol 18:194–199

Das B, Talukdar J, Sarma S, Gohain B, Dutta RK, Dutta HB, Das SC (2003) Fluoride and other inorganic constituents in groundwater of Guwahati, Assam, India. Curr Sci 85(5):657–661

Dhar V, Bhatnagar M (2009) Physiology and toxicity of fluoride. Indian J Dent Res 20(3):350–355

Fowles JR, Fairbrother A, Kerkvliet NI (1997) Effect of induced hypo- and hyperthyroidism on immune function and plasma biochemistry in mallards. Comp Biochem Physiol 118:213–220

Ge YM, Ning HM, Wang SL, Wang JD (2005a) Comet assay of DNA damage in brain cells of adult rats exposed to high fluoride and low iodine. Fluoride 38:209–214

Ge YM, Ning HM, Wang SL, Wang JD (2005b) DNA damage in thyroid gland cells of rats exposed to long term intake of high fluoride and low iodine. Fluoride 38:318–323

Handa BK (1975) Geochemistry and genesis of fluoride containing groundwater in India. Ground Water 13:275–281

Hileman B (1988) Fluoridation of water: questions about health risks and benefits remain after more than 40 years. Chem Eng News 26–42

Horowitz HS (1996) The effectiveness of community water fluoridation in the United States. J Public Health Dent 56:253–258

Jafarzadeh A, Poorholami M, Izadi N, Nemati M, Rezayati M (2010) Immunological and haematological changes in patients with hyperthyroidism or hypothyroidism. Clin Invest Med 33(5):E271–E279

Liu GY, Chai CY, Kang SL (2002) Effects of fluoride on ultrastructure of thyroid in chicks. Chin J Vet Sci 22:512–514 (in Chinese)

Michael M, Barot VV, Chinoy NJ (1996) Investigations of soft tissue functions in fluorotic individuals of North Gujarat. Fluoride 29(2):63–71

O'malley LSS (2007) Bengal district gazetteer: Gaya. Concept Publishing Company

Saxena VK, Ahmed S (2001) Dissolution of fluoride in groundwaters: a water-rock interaction study. Environ Geol 40:1084–1087

Sharma JD, Sohu D, Jain P (2009) Prevalence of neurological manifestations in a human population exposed to fluoride in drinking water. Fluoride 42(2):127–132

Spittle B (1994) Psychopharmacology of fluoride: a review. Int Clin Psychopharmacol 9:79–82

Strunecka A, Patocka J, Blaylock RL, Chinoy NJ (2007) Fluoride interactions: from molecules to disease. Curr Signal Transduct Ther 2:190–213

Sunitha V, Muralidhara Reddy B, Ramakrishna Reddy M (2012) Variation of fluoride and correlation with alkalinity in groundwater of shallow and deep aquifers—a case study in and around Anantapur district, Andhra Pradesh. Int J Appl Sci Eng Res 1(4):569–575

Susheela AK, Jain SK (1983) Fluoride-induced hematological changes in rabbits. Bull Environ Contam Toxicol 30:388–393

Susheela AK, Jha M (1981) Effect of Fluoride on cortical and cancellous bone composition. IRCS Med Sci: Library Compend 9(11):1021–1022

Susheela AK, Das TK, Gupta IP, Tandon RK, Kacker SK, Ghosh P, Deka RC (1992) Fluoride ingestion and its correlation with gastro-intestinal discomfort. Fluoride 25:5–22

Susheela AK, Bhatnagar M, Vig K, Mondal NK (2005) Excess fluoride ingestion and thyroid hormone derangements in children living in Delhi, India. Fluoride 38:98–108

Susheela AK, Mondal NK, Gupta R, Ganesh K, Brahmankar S, Bhasin S, Gupta G (2010) Effective interventional approach to control anaemia in pregnant women. Curr Sci 98(10):1320–1330

Viswanathan G, Jaswanth A, Gopalakrishnan S, Siva Ilango S (2009) Mapping of fluoride endemic areas and assessment of fluoride exposure. Sci Total Environ 407(5):1579–1587

Whitford GM (1996) The metabolism and toxicity of fluoride, 2nd revised edn, Monographs in oral science, vol 16. Karger, Basel

Index

% Na, 9, 22, 23
16S rDNA, 157, 159
16S rRNA, 157
$^{18}O/^{16}O$, 30
δD, 30, 31, 35
$\delta^{18}O$, 30, 31, 35, 37
^{238}U, 273

A
AARE, 96, 98
Absolute relief, 85
Absorbed, 277
Absorption, 139, 216, 281
Abundant, 232
Accumulation, 167
Acid activation, 178
Acidification, 100
Acidity, 229
Activated carbon, 168
ADD, 217, 218
Adsorbed, 22
Adsorbents, 168, 169, 173, 174, 178
Adsorption, 118, 122, 123, 140, 144, 167, 170, 172, 225
Adsorption coefficient, 178
Aeration tank, 132
Aerobic reactor, 132
Aerosol, 251
Agriculture, 3, 7, 22, 65, 75, 85, 89, 90, 266
Air pollution, 241, 249, 257
Algal and Seagrass beds, 262
Alkalies, 14
Alkaline, 229, 230, 238, 245
Alkaline Earths, 14
Alkaline solutions, 243
Alluvial sediments, 274
Alluvium, 62, 226
Ambient, 249
Ambient temperature, 143
Ammonia gas, 200, 251
Amorphous nanoparticle, 122
Amplitude, 81
Anaerobic digestion, 125, 135, 138
Anaerobic reactor, 130, 131
Analyzed, 67
Anantapur, 61
Andhra Pradesh, 39, 61, 62
Animal waste, 136
Anion, 10
Anion resins, 126
ANN, 93, 94, 98
Annual groundwater extraction, 93
Annual rainfall, 226
Anthracite, 241
Anthropogenic, 4, 7, 10
Anthropogenic activities, 230, 238
Antibiotics, 159
Apparent resistance, 41
Aquatic diversity, 99
Aquatic ecosystems, 249
Aquatic environment, 106, 195, 235
Aquatic habitat, 107
Aquifer, 39, 45, 65
Arabian Sea, 30
Aravali, 4, 5
Arc GIS, 65
Archean, 62, 63
Archean system, 278
Arsenic, 155, 157, 168

© Capital Publishing Company 2015

N.J. Raju et al. (eds.), *Management of Natural Resources in a Changing Environment*, DOI 10.1007/978-3-319-12559-6

Arsenite, 167, 170, 176
Artificial, 29
Artificial barriers, 108
Asbestos, 181
Ash, 241, 243, 248
Ash–water system, 246
Anion Exchange Capacity (AEC), 170, 178
Assessment, 249
Atlantic, 31
Atmosphere, 237
Atmospheric cycle, 37
Atomic absorption spectrometer, 227
Atomic absorption spectroscopy, 156, 170
Auger method, 273
Augmented, 4, 75
Ausgram block, 75, 79, 80, 84, 87, 89
Average body weight, 218
Average water temperature, 105

B
Bacteria, 117, 125, 155, 163
Bacterial viability, 116
Bamboo dust, 167–169, 172, 178
Bangladesh, 168, 259, 262, 265
Base Exchange, 7
Base Exchange indices, 18, 24
Baseline, 110
Basin, 83
Batch, 118
Batch leaching test, 243, 245
Bay of Bengal, 40, 259
Brevibacillus sp., 156, 159
BDL, 232, 235, 237
Bed rock, 61
Behavioural problems, 216
Bench marks, 79
Benthic, 100
Bhagirathi, 100, 106
Bhalaswa, 215, 217
Bihar, 277
Bilateral renal carcinoma, 220
Bioaccumulated, 219
Bioavailability, 225
Biochemical, 278, 281
Bio-compatibility, 116, 184
Biodegradable, 135
Biodegradable fraction, 125
Biodegradation, 125
Biodiversity, 211, 259, 262, 265, 267
Biogas, 135, 136, 138, 139, 143, 151
Biogas digester, 151
Biogas fertilizer plants, 145, 148
Biogeochemical, 225
Biomass, 158, 162, 193–195, 200
Biomass resources, 135
Biomethanation, 136
Biomethane, 143
Biomimetic, 190
Bioremediation, 155, 156, 163
Biotic and abiotic, 75
Black Soil, 94
BOD, 128, 195
Bore wells, 6, 7, 63
Bottling technology, 135, 138
Brackish, 21
Brahmaputra flood plain, 168
Brahmaputra River, 226
Braided river, 109
Breeding, 99
Bronchiolitis, 182
Burdwan, 75
Bureau of Indian Standards, 146

C
Ca^{2+}/Mg^{2+} ratio, 14
Cadmium (Cd), 232, 233
Calcification, 68
Calcite, 17
Calcium carbonate, 279
Calibrated model, 96
Caliche concretion, 77
Cancer, 216, 220, 271
Carbon, 242
Carbon nanotubes, 181, 183, 185
Carbonate weathering, 14
Carcinogen, 219
Carcinogenic, 115
Cardiopulmonary, 185
Catchment, 94, 225, 274
Catfishes, 108
Cation, 10
Cation resins, 126
CDI, 217, 218
Cell-free supernatant, 158
Cenosphere, 245
Central Himalaya, 205, 206, 211
Centrifugal pump, 126
Characterization, 128, 243
Chattarpur, 4
Check dams, 90
Chemical fertilizers, 272
Chittoor, 39
Chloride, 9, 21
Chlorine (Cl), 54, 58
Chromium (VI), 116, 118, 120, 123
Clay, 22, 168

Clay minerals, 236
Clean energy, 132
Climate, 65, 206, 260
Climate change, 135
Climate change impacts, 264
CNG, 142–145, 151
CNT, 182, 183, 185, 187
CO_2, 10, 138–140, 143
Coagulate, 21
Coal, 241, 243, 248
Coastal, 45
Coastal erosion, 265
Coastal water salinity, 260
Cobalt, 234
COD, 127, 128, 130, 195
Coefficient correlation, 96
Cold environment, 37
Collagen, 277
Column, 125
Columnar joints, 94
Combustion, 241, 245, 256
Combustion engines, 139
Commercial LPG cylinders, 151
Compost, 136
Compressed biogas, 146
Concentration, 29, 155, 217, 233, 251
Configuration, 81
Conservation, 259, 267
Conservation practices, 85
Constar, 43, 56–58
Consumption, 141, 216, 218
Contaminants, 215, 225
Contaminated, 155, 163, 168
Contamination, 61, 115, 227, 272
Continental, 30
Copper, 216, 235
Co-precipitation, 116
Coral bleaching, 264
Coral colonies, 259, 263
Correlation, 14, 17, 45, 56, 195, 230, 233, 235
Correlation coefficient, 57, 58
Corrosion, 67, 139, 237
Cost effective, 115
Covalent, 184
Cox's Bazar-Teknaf peninsular tips, 260
Crippling, 69, 277
Crop, 155
Cryogenic separation, 140
Crystalline rocks, 65
Cuddapah super group, 62
Cultivated, 87
Cultivated land, 255
Cultivation, 76, 77
Cylinder, 138, 139, 146
Cytotoxicity, 185, 188

D
Dam, 99, 100, 105, 108
Dar-Zarrouk parameters, 43, 45
Datasets, 71
Deccan traps, 94
Decomposition, 135, 205
Decontamination, 164
Default exposure, 218
Defluoridation, 168
Deforestation, 265
Deformation of ligament, 72
Degradation, 205
Deionised, 246
Delhi, 193
Delta, 76
Dental caries, 69, 167
Dental fluorosis, 67, 279, 286
Denudational hills, 62
De-oxygenation, 100
Depletion, 76, 98, 265
Depressions, 90
Desert, 31
Desirable limit, 279
Development, 93
Dharwars, 62, 278
Diarrhoea, 217
Direct gamma spectrometry, 273
Disease, 4, 182
Disposal, 241
Dissection index, 81
Dissolution, 20, 24, 67
Dissolved oxygen, 103
Dissolved phase, 233
Distilleries, 136
Diurnal trends, 227, 230, 232, 234
DNA, 187
DO, 195
Dolerite rock, 62
Dolomite, 17
Domestic, 9, 21, 65, 75
Dose, 218, 219
Double distilled water, 116
Downstream, 100, 102, 108
Drainage, 22, 64
Drainage density, 76, 83, 89
Drainage frequency, 85
Drilling, 39
Drinking water, 68, 115
Drought, 76
Dry ponds, 90

Dug-cum-borewell, 63
Dugwell, 63
Dust storms, 31
Dyes, 115, 122, 169

E
Earth, 75
Earth crust, 155
EC, 7, 23, 41
Ecological, 200, 206
Ecological diversity, 266
Ecologically critical area, 267, 268
Economic activity, 89
Ecosystem assortments, 260
Ecosystem, 76, 99, 211, 259, 268
EDTA, 6
EDXA, 242, 243, 248
Effect, 193
Efficiency, 143
Effluents, 125, 127, 128, 193, 235, 247, 248
Effluent treatment plant, 132
Eichhornia biomass, 202
Eichhornia crassipes, 193, 194, 200, 202
Electrical resistivity method, 39
Electricity, 132, 150
Elements, 4, 242
Endemic, 277
Endemic species, 100
Energy, 125, 132
Energy production, 135
Energy security, 135
Energy state, 110
Engineering structures, 85
Enrichment, 61
Environment, 72, 155, 159, 163, 225
Environmental concern, 241
Environmental factors, 210
Environmental hazard, 259
Environmental modeling, 250
Environmental pollution, 136
Environmental tracer, 29
Environmental quality, 246
Environmental remediation, 115
Ephemeral, 84, 90
Epidemiological, 219
Equilibrium, 6, 85, 172, 178, 273
Erlenmeyer flask, 118
Erosion, 85, 233
ETP, 130
Eutrophic, 202
Evaluation, 79, 96
Evapo-transpiration, 75, 194
Exhaust, 235
Exotic, 266
Exotic species, 109
Exploration, 39, 45
Exposure, 216–218, 223, 237
Exposure dose, 278
Exposure rate, 218
Extraction structures, 93
Extraction, 242

F
Facies, 10
Farming communities, 205
Faunal diversity, 263
Fine particles, 244
Fires, 206
Fish population, 104
Fishes, 109
Floods, 76, 266
Flora and fauna, 99, 109, 259, 267
Floral diversity, 262
Fluorescence spectroscopy, 271
Fluoride, 61, 65, 167, 170, 174, 256, 277
Fluorine bearing minerals, 61, 65
Fluorine, 167
Fluorosis, 167, 277
Fluvial, 83
Fly ash, 242, 244, 248, 272
Fodder, 205
Foetus, 216
Foliated gneiss, 278
Food chain, 167
Food industry, 115
Forecasting, 93
Forest, 205, 207
Forest degradation, 265
Fossil fuels, 135, 233
Fossil fuel combustion, 249
Fraction, 246
Fractionation, 29
Fragile ecosystem, 265
Fragmentation, 99
Frequency, 87, 228
Frequency of surface water bodies (FSWB), 76, 79, 87, 89
Fresh water, 24, 99
Freundlich isotherm, 178, 179
Fuel wood, 205
Fullerenes, 181, 183, 187, 190
Functionalization, 184, 185, 187, 190

G
Ganges, 78, 99, 106, 110
Gangetic alluvium, 278
Gangetic Plain, 155
Garhwal Himalayan region, 100
Garmin, 64
Gas flow, 139
Gases, 18
Gas-solids-liquids, 125
Gastro-intestinal, 279, 281
Gastrointestinal tract disorder, 216
Gastropods, 263
Gaya district, 277
Genotoxicity, 185
Genus, 105
Geogenic, 61
Geogenic contamination, 286
Geogenic factor, 274
Geographical area, 257
Geometries, 70
Geomorphic, 77, 79
Geomorphic evolution, 82
Geomorphic units, 62, 65
Geophysical, 39, 40, 58
Geospatial, 61
Geotechnical engineering, 241
Germanium detector, 273
GIS, 69, 75, 249
Glassy matrix, 246
Global hotspot, 100
Global Meteoric Water Line (GMWL), 35–37
Global warming, 133
Glutathione, 117, 120
GPS, 6
Graphical plot, 13
Green house gas emissions, 125, 126, 131
Green revolution, 272
Greenhouse gases, 135
Grids, 80
Groundwater, 3, 6, 39, 40, 61, 63, 65, 93, 158, 215, 219, 222, 241, 271, 279
Groundwater level, 93, 96
Groundwater Potential Zone, 40
Groundwater quality, 69
Groundwater table, 98
Guwahati, 225
GWL, 93, 94, 97, 98
Gypsum, 14

H
H_2O^{18}, 29
Habitat, 210, 225
Habitat restoration, 110
Hard tissues, 277
Harmful, 259
Harvesting sites, 75
Hatching, 264
Hazard, 215, 216
Hazard quotient (HQ), 221, 223
Hazardous, 155, 231, 241
Hazardous gases, 130, 133
Hazards, 182
$HD^{16}O$, 29
Health effects, 215
Health hazard, 136, 167, 277
Health risk assessment, 250
Heavy metals, 67, 115, 159, 215, 217, 222, 246
High pressure compressor, 144, 150
High volume sample, 251
Himalayan range, 193
Hindon River, 193, 195
Hotel industry, 151
Human activity, 39
Human cells, 115
Human health, 61, 67, 168, 181, 215, 277
Human settlements, 266
Hybrid model, 94, 96
Hybrid modelling technique, 93
Hydro-electric energy, 99
Hydrogen, 29
Hydrogeochemical, 3, 21, 24, 40
Hydrogeology, 62, 65, 274
Hydrology, 29, 39
Hydrophobic, 122
Hydrospheres, 193
Hydroxides, 246
Hypocalcaemia, 68
Hypoglycemia, 281
Hypo-limnion, 100

I
IAEA, 30
IDW, 69
Immobile, 246, 247
Immobilization, 209, 225
Impact, 75
Incinerated, 253
Incinerators, 235
India, 3, 29, 39, 75, 215, 225, 271, 277
Indo-Gangetic alluvial plains, 4
Indo-Gangetic plain, 273
Indus, 274
Industrial effluents, 193
Infection, 221
Infiltration capacity, 83

Inflammation, 185
Ingestion rate, 218
Inhalation, 220
Inoculation, 126
Input-output mapping, 97
Inselberges, 4
Intolerable levels, 195
Inundated, 109
Ion-exchange, 24
Ion exchange resins, 126, 128
Ion selection electrode, 278
Iran, 29, 30
Iron, 115–117, 119
Irrigation, 21
Island, 262, 263
Isolate, 157
Isolines, 84, 87
Isopleths, 76
Isotherm, 178
Isotope, 29, 30, 37
IUCN, 267

J
Jaggery, 126, 130
JNU, 3, 4
Jurkat cells, 187

K
Kadiri, 62
Kinetic energy, 85
Kinetics, 10, 171, 173
KUMAs1, 156, 157, 159, 160, 163

L
Lagergren plot, 173, 174
Lagoons, 261, 266
Lake, 76
Landfill, 137, 215, 221, 222, 233
Landfill site, 10
Landforms, 81
Landscape, 76
Langmuir isotherm, 169, 179
Laterite, 174
Lateritic soils, 94
LC50, 183
LD50, 183
Leachate, 215, 245, 246, 248
Leaching, 7, 72, 233, 237, 279
Lead, 216, 237
Lentic, 109
Ligaments, 68
Ligands, 225, 237
Lignite, 241
Liquefaction, 138
Litter, 205
Littoral zone, 263
Livestock, 136
LMWL, 35, 36, 37
Load, 272
Longitudinal unit conductance, 40, 41, 44, 45, 58
Long-term data sets, 109
Long-term sustainability, 98
Lotic, 109
LULC, 75
Lymphocyte, 286

M
Madhya Pradesh, 94, 98
Magnetic decantation, 118
Magnetic nanoparticles, 115, 117
Magnitude, 85
Malachite green, 115, 116, 118
Malwa region, 271, 273
Mammals, 264
Management, 75
Maneri-Bhali Phase, 99, 100, 102
Manganese, 236
Mangrove, 259, 261, 263
Manifestation, 68, 72
Mapping, 39, 40, 249
Marine and land resources, 259
Marine calcareous deposits, 260
Marine habitats, 262
Marine speices, 266
Mass displacement, 109
Mass spectrometry, 29–30
Mathematical model, 220
Measurement, 273
Mediterranean, 31
Melatonin, 279
Membrane, 187, 281
Membrane separation, 140
Membrane technology, 128
Metamorphic rocks, 7
Meteoric, 3
Meteoric genesis indices, 18
Meteorological, 31, 37
Methane generation, 132
Methane, 138, 139, 143, 151
Mica, 278
Micacious, 7, 24

Mice, 185
Microorganisms, 125, 129, 130, 156, 161
Microbiological decomposition, 103
Micronutrient, 200
MiliQ water, 117
Mineral, 3, 10, 18, 39
Mineralization, 210
MLSS, 126, 127, 129
MLVSS, 126, 127, 129
Mobility, 231, 233, 235
Moisture removal, 138, 140
Molecular, 133
Molluscs, 108, 109
Monitoring, 30
Monsoon, 206
Mottling of teeth, 72
Mountain, 30
Mountain ridge, 208, 210
MSW, 215
Mudflats, 262
Municipal wastewater, 193
Myanmar, 266

N
N pool, 210
NAAQS, 256, 257
Nanoparticle, 115–117, 119, 182, 183
Natural abundance, 273
Natural disaster, 265
Natural gas, 141, 143
Natural resources, 80
NCT, 4
Nellore, 40
Neurological problem, 279
New Delhi, 3, 29, 215
NH_4, 251
Niche, 99, 207
Nickel, 236
NO_3, 52, 54, 58
Non-linear regression model, 94
Normalized Root Mean Square Error (NRMSE), 96, 98
Nutrient, 194, 208–210, 263
Nutritive chemicals, 230

O
Oceans, 75
Okhla barrage, 193
Organic, 10
Organic carbon, 156
Organic loading rate (OLR), 129, 130, 133
Organic waste, 136
Organic wastewater, 125
Organisms, 195
Osmotic effect, 22
Osteosclerosis, 68
Over-exploitation, 93, 259, 266
Oxygen, 29, 31, 243

P
Packed bed, 144
Paddy cultivation, 76–77
Paleozoic, 62
Paper industry, 168
Parking lots, 231
Particulate matter, 249
Pathogenic, 183
Pathogens, 216
Pathways, 217
pCO2, 8
Pediments, 62
Pediplain, 62
Pegmatite dykes, 62
Percolation, 18
Perennial, 205
Permeability, 22, 236
Permissible limit, 21, 215, 271
Pesticides, 100
Petrochemical industries, 139
Petrol, 142
pH, 193, 195, 198, 200, 226, 230, 279
Phosphate, 195
Phototoxic, 187
Phylum, 263
Physico-chemical, 99
Physiological stress, 68
Phyto-plankton, 102, 105, 107, 110
Phytoremediation, 193
Pilot plant, 128
Pilot scale biogas, 148
Pine, 205, 206, 208, 210
Pipeline network, 141
Piper diagram, 13, 14
Planktonic, 100
Pleural membrane, 185
Poisoning, 16
Pollutant, 115, 225, 231
Polluted waters, 195
Pollution, 61, 167
Pollution control, 136
Polyhouse, 194
Polymers, 184, 190
Polystyrene, 126

Pond, 76
Pond ash, 242, 244, 253
Population, 226
Pore, 194
Post-monsoon, 4, 7, 10, 14, 19, 71, 72, 278
Potable, 39
Power generation, 135
Pozzolanic property, 248
Precambrian, 62
Predator, 107
Premonsoon, 4, 7, 10, 14, 19, 72, 278
Primary porosity, 63
Prism, 44
Productivity, 193
Proteins, 155
Pulverized, 273
Pumping, 64
Punjab, 271, 274

Q
Q Leucotrichophora, 205, 207
Qualitative, 45, 57, 58
Quality, 3, 4, 39, 58, 249
Quantitative, 19, 45, 56, 58
Quartzite ridge, 4

R
Radium, 273
Ruggedness Index, 76, 80, 81, 89
Rainfall, 30, 31, 62, 94, 206
Rainfall frequency, 77
Rainwater, 225
Ratio, 30
Redox potential, 155
Redox reactions, 225
Reducing, 181
Reduction, 158, 163
Reforestation, 85, 132
Refuse dump, 253
Regeneration, 205, 206, 210
Regression coefficient, 96
Regression models, 31
Relationship, 29, 35, 219
Relative relief, 76, 81, 89
Remedial measures, 215
Removal, 115, 122
Replenishable, 93
Replenished, 75
Reservoirs, 75, 100, 109, 226
Resistivity, 44
Resource, 79
Respiratory impairment, 181
Respiratory tract, 219
Rhizosphere, 156, 160, 164
Risk, 155
Risk assessment, 182, 215
Risk characterization, 216, 220
Risk communication, 222
Risk management, 222
Risk-zone, 216, 221
River, 85
River ecology, 109
River eco-system, 107
River Inn, 109
Rotor pump, 144
Rough topography, 88
RSC, 9, 21–23
Runoff, 77, 208, 225, 226, 230, 236
Run-off intensity index, 83
Runoff models, 94

S
Safety, 220
Sagar, 94, 98
Saline intrusion, 17
Saline water aquifer, 45
Salinity, 13, 22
Sampling, 226
Sampling points, 257
Sand dunes, 259
Sand dunes and beaches, 260
Sandstone, 274
SAR, 9, 21–23
Saturation Index, 6, 19, 24
Scanning electron microscopy, 119
Scarcity, 75
Scatter plots, 96
Sea-level rise, 264
Seasonal variation, 7, 72
Sedimentary, 260
Seedling, 207
Seepage, 75
SEM, 242–244, 248
Semi-arid, 10, 65
Semi-confined, 63
Settlement, 85
Sewage, 136, 235
Sex glands, 220
Sharry, 135–136
Shell fish, 262
Shivalik sediment group, 274
Shiwalik, 193
Silicate weathering, 14, 17

Skeletal fluorosis, 68, 72, 279, 286
Slope, 85, 86
Sludge, 125
Sludge recycling, 133
Smelting, 233
Snow clad mountain, 110
Socio-economic, 205
Sodium, 21–22
Sodium dodecyl sulfate, 117
Soil, 21, 155, 157, 158, 227
Soil-plant system, 22, 233
Soil-water interaction, 3
Solubility, 230–231, 279
Sorption, 178
Southwest monsoon, 30
Spatial analysis, 69
Spatial data management, 250
Spatial distribution, 250
Species, 3, 105, 205, 206, 208
Specific conductance, 57
Spectrophotometer, 116, 118
Sperm, 220
St. Martin's Island, 259, 262
Statistical parameters, 65
Statistics, 104
Storage capacity, 75
Storm water, 231
Strong acid, 14
Structural ridges, 4
Subsurface, 39
Subsurface water, 75
Suffering, 271
Super position, 96
Super saturated, 19
Surface modification, 181
Surface water, 75, 76, 79, 241
Surface water bodies, 86–87
Surface water harvesting, 77
Surface water harvesting potential zones, 80, 87, 88, 90
Surface water resources, 86–88
Sustainability, 259
Sustainable development, 241
Sustainable environment, 135
Swarnamukhi River, 40
Symbiotically, 264

T
TDS, 7, 41
Tehran, 29, 30
Temperature, 36, 195, 200, 226, 264
Terrain, 81
Terrain morphology, 85
Terrestrial, 85, 254–255
Terrestrial microhabitat, 260
Thermal power generation, 241
Thickness, 44
Thorium, 273
Threshold, 272, 273
Threshold statistics, 96, 98
Thyroid dysfunction, 281
Tide cycle, 260
Time-series forecasting, 93
Tirupati, 249, 257
Topographic, 64
Topography, 76
Toposheets, 64
Tourism, 265, 268
Toxic, 115, 155, 159, 168, 230–231, 233
Toxicant, 219
Toxicity, 167, 181, 184, 185, 187, 200, 225, 271, 273, 277
Trace metals, 225, 226, 231, 250
Tracer, 29
Traffic dust, 255
Transition zone, 206
Transport, 225
Treatment, 125, 128, 168, 169
Tropical belt, 260
TSP, 250, 251, 256
TSS, 127
t-test, 279
Tubewells, 64, 65
Tunnels, 110
Turbidity, 21, 100, 260
Turbulence, 144
Two-indicators, 99

U
UASBR, 125, 130–132
Ubiquitous, 155
Unburnt carbon, 245
Under saturated, 20
Undulating, 76, 226
Undulating topography, 90
Unit cross sectional area, 44
Unpolluted, 233
Unsaturated, 18
Untreated, 167, 178
Upstream, 101, 108
Uranium, 271, 273
Urban, 225
Urban area, 249
Urbanization, 39, 250
Urine and blood, 278

Uttarakhand, 99
Uttarkashi, 99, 100

V
Vegetation, 262
Vegetation cover, 83
Vehicular and cooking applications, 135
Vehicular emissions, 230
Vehicular fuel, 138, 139
Vertical electrical soundings, 41, 45, 58
Village, 68
Vindhyan quartzite sandstone, 94
Vitro, 185, 188

W
Warm environment, 36–37
Waste, 115
Waste disposal, 215
Waste management, 135
Wastewater, 125, 126, 128, 194, 195, 198
WATEQ4F, 6, 10
Water bearing, 39
Water bodies, 136
Water circulation, 236
Water demand, 77
Water extraction, 234
Water level, 109
Water management, 76
Water quality, 109
Water resistivity (RW), 45
Water resource planning and management, 80
Water scarcity, 89
Water scrubber technology, 139
Water scrubbing, 150, 151
Water storage, 88, 90
Water stress, 75–77
Water table, 61
Watershed, 75, 115
Weak acid, 14
Weathering, 63, 115, 225
West Bengal, 75, 155
Wet lands, 261
Whatmann, 226
White Oak, 205, 208
White patches, 67
WHO, 67, 155, 167, 217, 271, 279
Wilcox, 22
Windblown rock-derived minerals, 255
WMO, 30

Y
Yamuna, 4, 193
Yield, 22

Z
Zinc, 216, 237
Zoo-plank tones, 102, 105, 107, 110